

University of Bradford eThesis

This thesis is hosted in [Bradford Scholars](#) – The University of Bradford Open Access repository. Visit the repository for full metadata or to contact the repository team



© University of Bradford. This work is licenced for reuse under a [Creative Commons Licence](#).

THE ROLE OF MMP10 IN NON-SMALL CELL LUNG CANCER, AND PHARMACOLOGICAL EVALUATION OF ITS POTENTIAL AS A TARGET FOR THERAPEUTIC INTERVENTION

Investigation of the role of MMP10 in the tumour microenvironment of non-small cell lung cancer using gene, protein and mass spectrometry approaches to determine MMP10's potential in drug development strategies

Abdulaziz Saad Abdulaziz BIN SAEEDAN

Submitted for the degree of
Doctor of Philosophy

Institute of Cancer Therapeutics
University of Bradford

2014

Abstract

Abdulaziz Saad Abdulaziz Bin SAEEDAN

The role of MMP10 in non-small cell Lung cancer, and pharmacological evaluation of its potential as a target for therapeutic intervention

Keywords: NSCLC, Matrix metalloproteinase-10 (MMP10), MMP3, histone deacetylase-7, Metabolism, siRNA, Angiogenesis, LC-MS/MS, pharmacology

Non-Small Cell Lung Cancer (NSCLC), which accounts for 80% of all lung cancer cases, is associated with resistance to chemotherapy and poor prognosis. Exploitation of NSCLC-upregulated pathways that can either be targeted by novel therapeutics or used to improve the tumour-delivery of current chemotherapeutics are required. Among the matrix metalloproteinases (MMPs) that are essential for tumour development, MMP10 is a potential candidate as a therapeutic target based on its expression and contribution to NSCLC development. This research aims to explore the expression and functions of MMP10 in the tumour microenvironment of NSCLC and evaluate the potential of MMP10 as a target for therapeutic intervention. Herein, MMP10 expression at gene and protein levels were analysed in a panel of NSCLC cell lines using RT-PCR and Western blotting analysis. To determine MMP10 functional relevance, an *in vitro* angiogenesis assay using cell conditioned media was carried out. To identify specific peptide sequences for the design of prodrugs rationalised to be MMP10 activated, *in vitro* substrate cleavage studies were performed using a mass spectrometry approach to differentiate between MMP10 and the structurally similar MMP3. This study demonstrates that MMP10 is highly expressed in NSCLC and that high levels of MMP10 are associated with induction of angiogenesis, a crucial process supporting tumour growth. In addition to the achievement of having been able to differentiate between closely similar MMP3 and MMP10 through carefully monitoring the hydrolysis rate of compound 444259 (a known MMP substrate), data generated herein provides the basis for further studies to exploit MMP10 as a prodrug-activator.

Acknowledgement

Foremost, I am very much thankful to my supervisors, Dr Steve Shnyder, Prof Paul Loadman and Prof Laurence Patterson as well as the original supervisor, Dr Jason Gill, for their guidance, advice and unequivocal support over the course of this project. Their commitment, as well as their willingness to impart their extensive knowledge and expertise, contributed greatly to my understanding and the success of this project.

I am also thankful to Dr Andriana Margariti and Dr Simon Allison for the valuable information and support they provided. I am grateful for their cooperation during the period of my study. I also take this opportunity to express my appreciation and deep regards to Dr Mark Sutherland for the technical assistance he provided in the laboratory over the course of this thesis. Finally, I thank my beloved wife for her enduring love, inspiration and cheer; my son for his vivacity and my parents and my friends for their constant encouragement. Above all, I thank God Almighty for He has given me the strength to finish this PhD.

Contents

Abstract	i
Acknowledgements	ii
Contents	iii
List of Figures	viii
List of Tables	x
List of Abbreviations	xi
Chapter 1: Introduction	1
1.1 Cancer.....	1
1.1.1 Overview of Lung Cancer	2
1.1.2 Lung Cancer Clinical Incidence and Mortality	3
1.1.3 Current Treatment for Lung Cancer	4
1.1.4. Molecular Signature of NSCLC and Targeted Therapy	6
1.2 Tumour Microenvironment.....	10
1.2.1 Tumour Vasculature and Angiogenesis	13
1.3 Matrix Metalloproteinases (MMPs)	16
1.3.1 Structure of MMPs	18
1.3.2 Regulation of MMP Expression and Activity	20
1.3.2.1 Transcriptional and post- transcriptional regulation	21
1.3.2.2 Post-translational activation of MMPs	22
1.3.2.3 MMP regulation by endogenous MMP inhibitors	23
1.3.3 MMPs and Pathophysiology	24
1.3.3.1 Roles of MMPs in cancer	24
1.3.3.1.1 MMPs and tumour angiogenesis	28
1.4 MMP Inhibition as a Therapeutic Strategy for Cancer	29
1.5 MMP10 in NSCLC	32
1.6 Regulation of MMP10 Gene Expression.....	34
1.6.1 Histone Deacetylases	35
1.6.2. Regulation of MMP10 by HDAC7	36
1.7 Limitations of Classical Chemotherapeutics	37
1.8 The Prodrug Concept	38
1.8.1 Tumour-Activated Prodrugs (TAPs).....	39
1.8.2 MMPs as Target for Tumour Selective Anticancer Drug Delivery	42
1.8.2.1 Tumour-activated prodrugs directed to the matrix metalloproteinases	43
1.9 Aims and Objectives.....	44
Chapter 2: General Materials and Methods	46
2.1 Materials.....	46
2.1.1 Cell culture.....	46
2.1.1.1 Cell lines.....	46
2.1.2 Gene Expression Analysis	47
2.1.3 Protein Expression Analysis	48
2.2 Methods.....	49
2.2.1 Cell Lines Maintenance.....	49
2.2.2 Growth Curve Analysis	50

2.2.3 Animals and Experimental Tumour System	50
2.2.4 Reverse Transcription-Polymerase Chain Reaction (RT-PCR)	51
2.2.4.1 RNA extraction	51
2.2.4.2 RNA quantification analysis.....	52
2.2.4.3 cDNA synthesis using reverse transcriptase enzyme.....	52
2.2.4.4 PCR primers design and selection	53
2.2.4.5 PCR protocol	54
2.2.5.6 Agarose gel electrophoresis to analyse PCR products	56
2.2.5 PCR Optimisation	57
2.2.6 Western Blotting	57
2.2.6.1 Cell sample preparation	57
2.2.6.2 Collection of culture supernatant	58
2.2.6.3 Tissue sample preparation	58
2.2.6.4 Protein concentration assay (Bradford Assay)	59
2.2.6.5 Protein gel electrophoresis	59
2.2.6.6 Immunoblotting.....	60
2.2.6.7 Blocking and antibody incubation	60
2.2.6.8 Protein detection	61
 Chapter 3: Characterisation of Models for the Evaluation of MMP10	
Functionality in NSCLC	63
3.1 Introduction.....	63
3.1.1 Aims and Objectives	66
3.2 Materials.....	67
3.2.1 Cell Lines	67
3.2.2 Proteomics.....	67
3.3 Methods.....	67
3.3.1 NSCLC Cells Growth Analysis	67
3.3.2 RT-PCR Analysis	68
3.3.3 Western Blotting	68
3.3.4 Manual MALDI TOF-MS of Peptides	68
3.3.4.1 Instrumentation.....	68
3.3.4.2 SDS-PAGE.....	69
3.3.4.3 Staining of proteins using Coomassie Brilliant Blue dye.....	69
3.3.4.4 In-gel trypsin digestion and peptides extraction	69
3.3.4.5 Matrix solution preparation.	70
3.3.4.6 Manual analysis of gel digest.	71
3.3.4.7 nHPLC coupled to MALDI-MS/MS for protein identification (LC-MS/MS).	71
3.3.4.7.1 Reverse phase nHPLC fractionation of modified peptides...71	
3.3.4.7.2 nHPLC gradient conditions	72
3.3.4.7.3 Fraction collection and mass spectrum acquisition.....	72
3.4 Results	74
3.4.1 NSCLC Cell Line Growth Kinetics.....	74
3.4.2 Genetic Expression.....	76
3.4.2.1 Optimisation of the PCR conditions.....	76
3.4.3 MMPs mRNA Level in NSCLC Cell Lines	78
3.4.4 MMP10 mRNA in Tumour Xenograft Tissue.....	82
3.4.5 <i>In Vitro</i> and <i>In Vivo</i> MMP10 Protein Expression	84
3.4.5.1 Confirmation of antibody specificity	84

3.4.5.2 MMP10 protein expression in NSCLC cell lines and xenograft tissue.....	85
3.4.6 Detection of Secreted MMP10 Using MALDI-TOF-MS	88
3.4.7 Comparison of Protein and mRNA Expression Detected for MMP10 in the NSCLC Cell Lines	92
3.4 Discussion	93

Chapter 4: Development of <i>In Vitro</i> MMP10 Expressing Models for the Evaluation of the Role of MMP10 in NSCLC	101
4.1 Introduction.....	101
4.1.2 Aims and Objectives	103
4.2. Materials and Methods	104
4.2.1 Materials	104
4.2.2 Methods.....	105
4.2.2.1 Cell line nomenclature	105
4.2.2.2 Cell line maintenance and culture conditions	105
4.2.2.2.1 Culture of HUVEC-Cs	105
4.2.2.3 Evaluation of cytotoxicity using the MTT assay	106
4.2.2.3.1 Validity of the MTT Assay for H460 cells	106
4.2.2.3.2 Optimisation of cell seeding densities for the MTT assay ..	106
4.2.2.3.3 MTT Assay.....	107
4.2.2.4 Generation of stable MMP10 expressing cells	108
4.2.2.4.1 MMP10 expressing clones.....	108
4.2.2.4.2 Stable HDAC7 silencing using shRNA lentiviral particles ..	108
4.2.2.4.3 Optimisation of antibiotic concentration for selection	109
4.2.2.4.4 Selection of stable transfectant.....	110
4.2.2.4.5 Verification of stably transfected H460 cells	110
4.2.2.5 Immunohistochemistry	111
4.2.2.5.1 Semi-quantitative analysis of immunohistochemistry	112
4.2.2.6 <i>In vitro</i> 2-D angiogenesis model	112
4.2.2.6.1 Characterisation of HUVEC growth	113
4.2.2.6.2 Optimisation of HUVEC-Cs seeding density for the tube formation assay.	113
4.2.2.6.3 In vitro angiogenesis assay.....	113
4.2.2.6.4 Quantification of HUVEC tube formation	114
4.2.2.7 siRNA Silencing of HDAC7 in NSCLC cell lines	115
4.2.2.7.1 siRNA-gene knockdown.....	115
4.2.2.7.2 Optimisation of siRNA concentration for transfection.....	116
4.2.2.7.3 Optimisation of Lipofectamine RNAiMAX concentration. ...	116
4.2.2.7.3.1 Evaluation of Lipofectamine toxicity	117
4.2.2.7.4 Optimisation of post-transfection incubation period	117
4.2.2.7.5 Transient HDAC7 Gene Knockdown	117
4.3 Results	118
4.3.1 Optimisation of the MTT Assay for Use with H460 Cells	118
4.3.2 H460-Clone2 as an MMP10 Preclinical Model.....	120
4.3.2.1 Determination of ideal antibiotic concentration for H460-clone2 selection.	121
4.3.2.2 Evaluation of MMP10 in H460-clone2 at mRNA and protein levels.	121
4.3.3 <i>In Vitro</i> Angiogenesis Assay	124

4.3.3.1 HUVEC-C growth curve	124
4.3.4.2 Confirming the presence of secreted MMP10 in concentrated conditioned media of NSCLC.	125
4.3.4.3 Validation of angiogenesis assay	126
4.3.4.4 In vitro angiogenesis assay for H460-clone2.....	130
4.3.4 Confirmation of the Lack of Functional Activity of the H460-clone2 MMP10	130
4.3.5 Lentiviral Transduction Mediates Stable HDAC7 in H460 Cells.....	134
4.3.5.1. Optimisation of puromycin concentration for H460-shHDAC7 cell selection.	134
4.3.5.2 Optimisation of HDAC7 and MMP10 primers for RT-PCR analysis.	135
4.3.5.3 Impact of stable HDAC7 silencing on MMP3 and MMP10 expression in the H460 cells.	137
4.3.6 Transient Transfection Studies	140
4.3.6.1 Optimising of siRNA knockdown conditions using HDAC7 siRNA.	140
4.3.6.2 Optimising appropriate siRNA concentration for the transfection of the H460 cell line.....	140
4.3.6.3 Optimisation of a Lipofectamine RNAiMAX concentration for H460 transfection.	141
4.3.6.3.1 Evaluation of Lipofectamine toxicity on H460 cells.	144
4.3.6.4 Duration of transient HDAC7 knockdown by siRNA transfection.	144
4.3.7 siRNA Mediates Silencing of HDAC7 in H460 Cells	147
4.3.7.1 Impact of HDAC7 silencing on MMPs in H460 cells	147
4.3.7.2 Lack of effects of HDAC7 silencing on MMP3 and MMP10 induction in A549 cells.....	149
4.3.7.3 Impact of HDAC7 silencing on NSCLC cell growth.	151
4.4 Discussion	153

Chapter 5: Identification of MMP Substrates and MMP-Activated Prodrugs Specifically Cleaved by MMP10.....	160
5.1 Introduction.....	160
5.1.1 Aims and Objectives	162
5.2 Materials and Methods	163
5.2.1 Materials	163
5.2.2 Methods.....	163
5.2.2.1 Enzyme activation	163
5.2.2.2 Liquid chromatography (LC)	164
5.2.2.2.1 High performance liquid chromatography coupled with mass spectrometry (LC-MS)	164
5.2.2.2.2 HPLC running conditions	164
5.2.2.3 In vitro MMPs-substrate cleavage study.....	165
5.2.2.3.1 HPLC analysis of substrate cleavage	165
5.2.2.3.2 LC-MS analysis for MMPs-substrate cleavage study	165
5.2.2.4 Activation of MMP Targeted TAPs by MMP10 and MMP3	168
5.2.2.4.1 MMPs targeted TAPs.....	168
5.2.2.4.2 MMP-targeted compounds activation study	168
5.2.2.4.3 HPLC analysis	169

5.2.2.4.4 LC-MS analysis for the activation of MMPs-targeted compounds by MMP3 and MMP10.....	169
5.3 Results	171
5.3.1 Differentiation Between MMP3 and MMP10	171
5.3.1.1 Full length versus activated MMP10.....	171
5.3.1.2 MMPs-substrate cleavage study for peptides selectively cleaved by MMP10	174
5.3.1.3 Structure Activity Relationship Study of 444258 and 444259 Substrates	185
5.3.2 Activation of MMP-Targeted Compounds by MMP10 and MMP3...	187
5.4 Discussion	197
Chapter 6: General Discussion	203
6.1 Overall Summary.....	216
References.....	217
Appendices	244
Appendix 1. TAE Buffer (10X) Recipe	244
Appendix 2. Preparation of 10% Separating and 5% Stacking Gels	245
Appendix 3. Illustration of the Contents of Peptide Calibration Standard Mixture for MALDI/MS	246
Appendix 4. MMP expression in selected NSCLC cell lines	247
Appendix 5. Supplementary Data for MALDI-MS Analysis	248
Appendix 6. HDAC7 detection by Western blotting	250

List of Figures

Chapter 1

1.1	The morphological multistage development of squamous cell lung carcinoma.....	3
1.2	Summary of several cell signalling pathways and potential targets in NSCLC.....	8
1.3	The heterogeneous tumour microenvironment.....	12
1.4	Diagram showing several abnormalities in the tumour vasculature compared to normal tissue	16
1.5	Schematic demonstration of the involvement of MMP in cancer progression.....	27
1.6	Schematic description of proteolysis mechanism by MMP.....	34
1.7	PKD1-dependent phosphorylation of HDAC7 upon VEGF signalling.....	37
1.8	Schematic description of TAPs therapeutic strategy.....	41

Chapter 3

3.1	Growth curves for the NSCLC cell lines, A549, H460 and H661.....	75
3.2	Identification of optimal cDNA concentration for RT-PCR analysis.....	77
3.3	Optimisation of GAPDH primer concentration for RT-PCR analysis.....	78
3.4	MMP10 mRNA expression is elevated in human NSCLC preclinical tumour models.....	81
3.5	High MMP10 expression in NSCLC subcutaneous tissue xenografts compared to mouse normal lung tissue.....	83
3.6	Confirmation of antibody specificity.....	85
3.7	MMP10 protein levels in a panel of NSCLC cell lines using Western blotting.....	87
3.8	Significantly higher MMP10 protein expression observed in NSCLC subcutaneous xenografts compared to normal lung tissue.....	88
3.9	Evaluation of the secreted MMP10 level in the Colo205 and H661 cell lines.....	90
3.10	Mass spectra of blank (negative control), Colo205 and H661 cell conditioned media and recombinant MMP10 (positive control).....	91

Chapter 4

4.1	Relationship between the number of H460 cells and MTT absorbance readings.....	119
4.2	Growth kinetics of the H460 cells cultured in 96-well plates.....	120
4.3	Cytotoxicity profile of G418 antibiotic on wild type and H460-clone2 cells.....	122
4.4	Verification of MMP10 induction in transfected H460-clone2 cells.....	123
4.5	Growth pattern of HUVEC-Cs.....	124
4.6	Confirming the secretion of MMP10 in a panel of NSCLC cell lines.....	126
4.7	Induction of angiogenesis by MMP10 using an <i>in vitro</i> angiogenesis assay.....	128
4.8	Induction of angiogenesis due to MMP10 secretion by NSCLC cells.....	129
4.9	An <i>in vitro</i> angiogenesis functional assay for transfected H460-clone2 cells and their wild type.....	132
4.10	Semi-quantification of microvessel density.....	133
4.11	Optimising appropriate puromycin concentration for selection of lentiviral-HDAC7 transduced cells.....	135
4.12	Optimisation of HDAC7 and MMP10 primers' concentration.....	136
4.13	Confirmation of HDAC7 silencing in H460 cells and evaluation of its impact on MMP3 and MMP10 expressions.....	138
4.14	Verification of HDAC7 silencing at protein level and evaluation of its impact on MMP10... ..	139

4.15	Optimisation of HDAC7 siRNA concentration.....	142
4.16	Identification of optimal lipofectamine concentration for H460 cells transfection.....	143
4.17	Evaluation of lipofectamine toxicity on H460 cells using growth inhibition based MTT assay.....	145
4.18	Duration of transient HDAC7 knockdown in H460 cells.....	146
4.19	Impact of HDAC7 transfection on 22 MMPs mRNA expression using RT-PCR analysis...	148
4.20	No effect upon MMP3 and MM10 mRNA following a significant HDAC7 silencing in A549 cells.....	150
4.21	Impact of HDAC7 silencing on NSCLC cells growth.....	152

Chapter 5

5.1	Validation of recombinant MMP10 using Western blotting.....	172
5.2	Figure demonstrating the comparison between the non-activated and pre-activated recombinant MMP10.....	173
5.3	Figure demonstrating that no metabolite was detected after 18 hours of incubation of substrate (1895) with MMP10 or MMP3.....	175
5.4	Figure demonstrates that substrate 444258 is cleaved in the same position by MMP10 and MMP3.....	176
5.5	Figure demonstrates substrate 444215 is cleaved in the same position by MMP10 and MMP3.....	177
5.6	Figure demonstrates substrate 444220 is cleaved in the same position by MMP10 and MMP3.....	178
5.7	Figure demonstrates substrate 444228 is cleaved in the same position by MMP10 and MMP3.....	179
5.8	Figure to demonstrate substrate 444230 is cleaved in the same position by MMP10 and MMP3.....	180
5.9	Figure demonstrating M-2105 substrate is cleaved in the same position by MMP10 and MMP3.....	181
5.10	Figure demonstrates that ABD1 substrate is cleaved in the same position by MMP10 and MMP3.....	182
5.11	Figure demonstrates substrate 444259 is cleavage after 18 hours of incubation with MMP10 or MMP3.....	183
5.12	Figure demonstrates the half life time evaluation of 444259 substrate within four hours incubation with MMP10 or MMP3.....	186
5.13	Figure demonstrating the comparison between MMP10 and MMP3 to activate the ICT2588 prodrug.....	189
5.14	Figure demonstrating the comparison between MMP10 and MMP3 to activate the ICT3019 prodrug.....	190
5.15	Figure demonstrating the comparison between MMP10 and MMP3 to activate the ICT3115 prodrug.....	191
5.16	Figure demonstrating the comparison between MMP10 and MMP3 to activate the ICT3120 prodrug.....	192
5.17	Figure demonstrating the comparison between MMP10 and MMP3 to activate the ICT3198 prodrug.....	193
5.18	Figure demonstrating the comparison between MMP10 and MMP3 to activate the ICT3146 prodrug.....	194
5.19	Figure to demonstrate that substrate 444228 is cleaved by MMP10 and MMP3 enzymes.....	195
5.20	Amino acid sequence of the N-terminal of human cartilage link protein and cleavage sites by MMP3 and MMP10.....	198

List of Tables

Chapter 1

1.1	Molecular-Targeted Drugs Evaluated in NSCLC.....	9
1.2	Human MMPs.....	17
1.3	Structural Classes of Human MMPs.....	20

Chapter 2

2.1	Cell Line General Information.....	47
2.2	Primers Sequence and Their Optimal Conditions Used for RT-PCR Analysis.....	55
2.3	Primary and Associated Secondary Antibodies with Their Optimal Dilutions.....	62

Chapter 3

3.1	Summary of MMP10 Expressions in the NSCLC Cell Lines Evaluated.....	92
-----	---	----

Chapter 5

5.1	MMP Substrates Used with Full Details of Sequence.....	167
5.2	Illustration of MMPs Targeted Prodrugs Used with Their Sequence.....	169
5.3	SIR for Compounds and Possible Metabolites Used in Mass Spectrometry.....	170
5.4	Illustration of MMP-substrate <i>In Vitro</i> Cleavage Studies.....	184
5.5	Summary of the <i>In Vitro</i> Cleavage Profile of Peptide-Colchicine Conjugates by MMP3 and MMP10.....	196

Chapter 6

6.1	Examples of Significant Overlap in MMP Substrate Specificity.....	215
-----	---	-----

List of Abbreviations

(AP)	Ammonium persulfate
(ADAMs)	Disintegrin and metalloproteinases
(APMA)	4-aminophenylmercuric acetate
(ATCC)	American Type Culture Collection
(bFGF)	Basic fibroblast growth factor
(BLAST)	Basic Local Alignment Search Tool
(bp)	Base pairs
(BSA),	Bovine serum albumin
β-ME	β-mercaptoethanol
(Bz)	Benzyl
(cDNA)	Complementary DNA
(CHAPS)	3-[(3-Cholamidopropyl)dimethylammonio]-1-propanesulfonate
(CHCA)	Matrix α-Cyano-4-hydroxycinnamic acid
(DANSYL)	5-dimethylamino-1-naphthalenesulfonyl.
(DMSO)	Dimethyl sulfoxide
DNP	2,4-Dinitrophenol
(Dpa)	N3-(2,4-dinitrophenyl)-L-2,3-diaminopropionyl
(DTT)	Dithiothreitol
(ECL)	Enhanced chemiluminescence substrate
(ECM)	Extracellular matrix
(EGFR)	Epidermal growth factor receptor
(EGF)	Epidermal growth factor
(EGTA)	Ethylene glycol tetraacetic acid
(EMT)	Mesenchymal transition
(ERK1)	Extracellular signal-regulated kinase
(FASL)	FAS ligand
(FCS)	Foetal Calf Serum
(FITC)	Fluoroisothiocyanate
(GAPDH)	Glyceraldehyde 3-phosphate dehydrogenase
(H460-clone2)	H460 cells engineered to express MMP10
(HB-EGF)	Heparin-binding epidermal growth factor
(HDACs)	Histone deacetylases
(HDAC7)	Histone deacetylase-7
(HPLC)	High performance liquid chromatography
(HRP)	Horseradish peroxidase
HUVEC-Cs	Immortalised human umbilical vein endothelial cells
(ICT)	Institute of Cancer Therapeutics
(IGF-1)	Insulin-like growth factor 1
(IGF-BP)	Insulin-growth-factor-binding protein
(IHC)	Immunohistochemical analysis
(IL)	Interleukin
(LC-MS)	Liquid Chromatography Coupled to Mass Spectrometry
(MALDI)	Matrix-assisted laser desorption/ionization
(MALDI-TOF)	MALDI-Time-of-flight mass spectrometry

(MAPK)	Mitogen-activated protein kinase
(MET)	Hepatocyte growth factor receptor
(MEF2)	Myocyte enhance factor 2
(MMPs)	Matrix metalloproteinases
(MMPIs)	Matrix metalloproteinase inhibitors
(MB2)	Amino colchicine.
(MCA)	(7-methoxycoumarin-4-yl)acetyl
(MPA)	Mobile phase A
(MPB)	Mobile phase B
(MTT)	3-(4,5-dimethylthiazol-2-yl)-2, 5-diphenyltetrazolium bromide
(NaCl)	Sodium chloride
(NMWL)	Nominal molecular weight limit
(NSCLC)	Non-small-cell lung carcinoma
(PBS)	Phosphate buffered saline
(PDGF)	Platelet-derived growth factor
(PDGFR)	Platelet-derived growth factor receptor
(Ph)	2-methoxy-6-nitrophenyl
(PIC)	Protease inhibitor cocktail
(PKD)	Protein kinase D
(p-OMeBz)	S-para-methoxybenzyl.
(Rb)	Retinoblastoma
(RIPA)	Radio Immunoprecipitation Assay buffer
(RAR- γ)	Retinoic acid receptor, gamma
(RET)	Retention time
(RT)	Room temperature
(RT-PCR)	Reverse Transcription-polymerase Chain Reaction
(SAPK/JNK)	Stress-activated protein kinase/Jun N-terminal kinases
(SAR)	Structure activity relationship
(SDS)	Sodium Dodecyl Sulfate
(shHDAC7)	Short Hairpin HDAC7
(shNT)	Short Hairpin non targeting control
(shRNA)	Short Hairpin RNA
(SIR)	Selected ion recording
(STAT)	Transducer and Activator of Transcription
(TAPs)	Tumour-activated prodrugs
(TAE)	Tris-acetate buffer
(TBST)	Tris-buffered saline and tween 20
(TFA)	Trifluoroacetic acid
TGF- β	Transforming growth factor β
(TEMED)	Tetramethylethylenediamine
(TIEs)	TGF inhibitory elements
(TIMPs)	Tissue inhibitors of metalloproteinases
(TNF)	Tumour necrosis factor
(VDAs)	Vascular disrupting agents
(VEGF)	Vascular endothelial growth factor
(VEGFR)	Vascular endothelial growth factor receptors

Chapter 1: Introduction

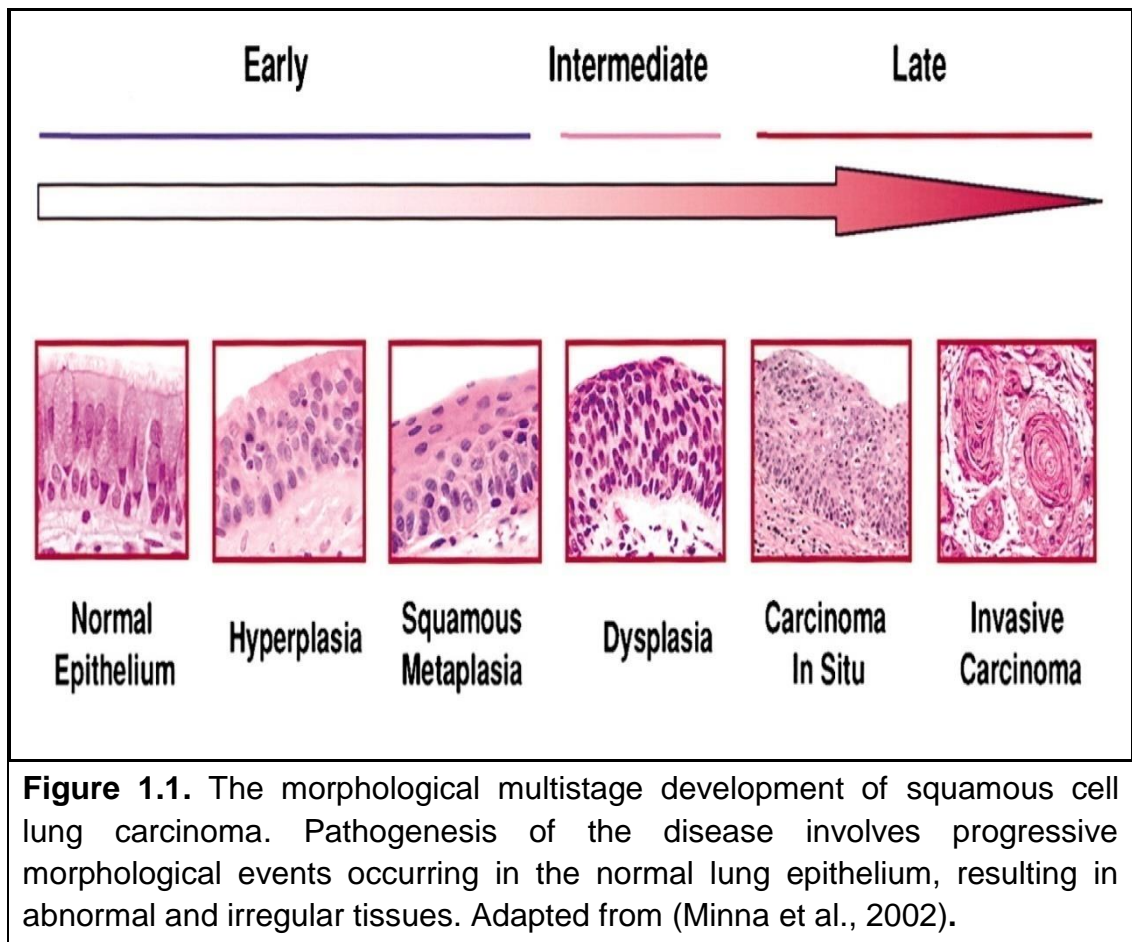
1.1 Cancer

Cancer is a major public health issue with approximately 8.2 million deaths globally in 2012 (CRUK, 2014b). In the UK, a new patient is diagnosed with cancer every two minutes (CRUK, 2014a). Development of cancer begins with the accumulation of genetic and epigenetic alterations in cells, such as reduced expression of tumour suppressor genes and enhanced expression of oncogenes (Podlaha et al., 2012). At the cellular and molecular levels, ten hallmarks have been identified as being essential for cancer growth (Hanahan and Weinberg, 2011). These include self-sufficiency in growth signals, insensitivity to antigrowth signals, enabling of replicative immortality, presence of genome instability and mutation, tissue invasion and metastasis, deregulation of cellular energetics, sustained angiogenesis, inflammation promotion, avoidance of immune destruction and evasion of apoptosis (Hanahan and Weinberg, 2011). Many drugs show limited success for a range of different tumours (with a response rate of almost 100% for testicular cancer to less than 20-35% for NSCLC (Schiller et al., 2002; Verweij and de Jonge), but issues with off-target toxicity and drug resistance limit the overall effectiveness. Therefore, the need arises to acquire better understanding of cancer biology to search for new therapeutic targets that would offer the chance to develop improved cancer therapy.

1.1.1 Overview of Lung Cancer

As the name implies, lung cancer involves the abnormal, uncontrolled proliferation of epithelial cells in the tissue of the lungs. It arises due to serious morphological changes in the normal epithelium as shown in Figure 1.1. Histologically, lung cancer is generally classified according to the size and appearance of malignant cells under the microscope into two major types: small cell lung cancer (SCLC) and NSCLC. Non-small cell lung carcinoma is further classified into three histological subtypes: adenocarcinoma, squamous cell and large cell anaplastic carcinomas. This classification has important implications for the treatment and diagnosis of the disease.

The main cause of NSCLC is cigarette smoking, which is responsible for nearly 85% of all new cases of lung cancer (Mao et al., 1997; Spira et al., 2004). The remaining lung cancer cases are due to other non-smoking related factors (Thun et al., 2008), such as exposure to radon gas (Catelinois et al., 2006), asbestos (O'Reilly et al., 2007) and air pollution (Kabir et al., 2007). These contributing factors interact with the host genetic susceptibility leading to altered protein expression involving genetic and epigenetic changes (Wistuba et al., 2000), consequently resulting in lung cancer development.



1.1.2 Lung Cancer Clinical Incidence and Mortality

There are 1.35 million new cases of lung cancer annually, comprising over 17% of the total new cancer cases worldwide (Jemal et al., 2011). Currently, lung cancer is the 2nd commonest (after breast cancer) in the UK, which accounts for 13% of the total cancer cases (331,487) diagnosed in 2011 (CRUK, 2014a).

Lung cancer is now the leading cause of cancer deaths worldwide (Jemal et al., 2011). The predominant form of lung cancer is NSCLC, which accounts for over 80% of the total lung cancer cases and shows a low survival rate for patients (Wood et al., 2014). Statistics has shown that 85% of patients with

NSCLC die within five years of first diagnosis. This period of time decreases to 18 months for those who were diagnosed at the advanced stages of NSCLC as they suffered from metastatic complications (Langer et al., 2010). Therefore, NSCLC is a serious life threatening disease, and better understanding of the mechanistic basis of its development is essential for improving patients' quality of life and survival.

1.1.3 Current Treatment for Lung Cancer

Currently, there are four approaches available to treat NSCLC. These include surgery, radiation therapy, classical chemotherapy and targeted therapy. Treatment choices depend on the nature and stage of the disease. For NSCLC, surgery is the primary treatment approach; however, only 30% of patients are appropriate for resection (Group, 2010). The majority must receive chemotherapy as part of their curative or palliative treatment. As a consequence, tremendous efforts have been concerned with improving chemotherapy for NSCLC. A major step forward in the treatment of lung cancer is the introduction of platinum-based chemotherapeutics, especially cisplatin and carboplatin. The combination of platinum derivatives with other agents, including gemcitabine, vinorelbine, docetaxel and pemetrexed improved the five-year survival rate from 5% to 14% (Khuri et al., 2001), thereby this approach is commonly used for the first-line treatment of advanced NSCLC (Peters et al., 2012). In the last decade, personalised medicine, which is based on the identification of specific and druggable genetic alterations in the tumour tissue of an individual patient, has been introduced (Crinò and Metro, 2014; Sechler et al., 2013). This means that

patients with NSCLC that have activating mutations in relevant genes should receive a drug that specifically targets the oncoprotein associated with the mutated gene, as exemplified with use of erlotinib against the gain-of-function mutations of the epidermal growth factor receptor (EGFR). Despite the robustness of this strategy, only a minority of patients with the requisite gene mutations can benefit (Crinò and Metro, 2014). However, even with a drug combination strategy being used for a more effective treatment of NSCLC, it soon became obvious that the use of chemotherapy or molecular targeted therapy has reached a limit, in part due to the occurrence of drug resistance (Sechler et al., 2013).

A major issue in the treatment of NSCLC is that most of the patients have reached an advanced stage at the time of diagnosis due to the initial asymptomatic course; hence, poor prognosis is often associated with NSCLC. Patients with an advanced stage of NSCLC are most likely to have metastatic disease, making the treatment options limited to chemotherapy rather than surgery or radiation therapies (Nishio et al., 1999). In addition, NSCLC is well known to be associated with acquired resistance to chemotherapy (Nishio et al., 1999). Several cellular mechanisms have been identified to contribute to the resistance of NSCLC cells to chemotherapy. These include increased efflux of chemotherapeutic drugs, involvement of several alternative DNA-repair pathways, mutations or functional modifications of the drug target and loss of apoptotic functionality (Ambudkar et al., 1999; Eastman and Schulte, 1988; Kavallaris et al., 1997; Sethi et al., 1999; Townsend and Tew, 2003). Thus, there is still an urgent need for research to develop awareness on the emergence and development of

NSCLC, which hopefully will lead to the discovery of new tumour markers and potential targets for therapeutics that can be utilised to improve the diagnosis and management of the disease (Atkinson et al., 2007).

1.1.4. Molecular Signature of NSCLC and Targeted Therapy

Recent advances in our knowledge on the mechanisms of tumourigenesis and on the molecular biology of cancer have recognised key molecular targets involved in several oncogenic pathways that have been proven essential for NSCLC progression. Interfering with these targets can be useful for NSCLC therapy (Reungwetwattana and Dy, 2013). Such important targets include EGFR, vascular endothelial growth factor receptors (VEGFR), hepatocyte growth factor receptor (MET) and insulin-like growth-factor receptors (IGFRs) (Reungwetwattana and Dy, 2013). The majority of the molecular targets with their signalling pathways identified in the context of NSCLC are listed in Figure 1.2. Due to their role in NSCLC progression, extensive work to develop inhibitors for several molecular targets has been made. Several promising molecular-targeted drugs have been tested clinically for NSCLC and their outcome or current status is shown in Table 1.1.

Epidermal growth factor receptor and VEGF were most extensively implicated in NSCLC. This will be explained in more detail. It was reported that 60% of NSCLC cases showed EGFR overexpression and that its presence was associated with poor prognosis (Brabender et al., 2001; Sechler et al., 2013). This tyrosine kinase protein receptor is vital for tumour cell proliferation, angiogenesis migration and survival (Wells, 1999). In

addition, VEGF, a key player in angiogenesis, is revealed in the majority of NSCLCs and its overexpression is linked to poor prognosis (Han et al., 2001). Based on their expression and role in tumour development, EGFR and VEGFR represent attractive therapeutic targets for NSCLC. Despite the development of several inhibitors for EGFR and VEGFR, clinical results with molecularly targeted agents remain modest. This highlights the need to continue screening for other molecular targets for novel therapeutic options.

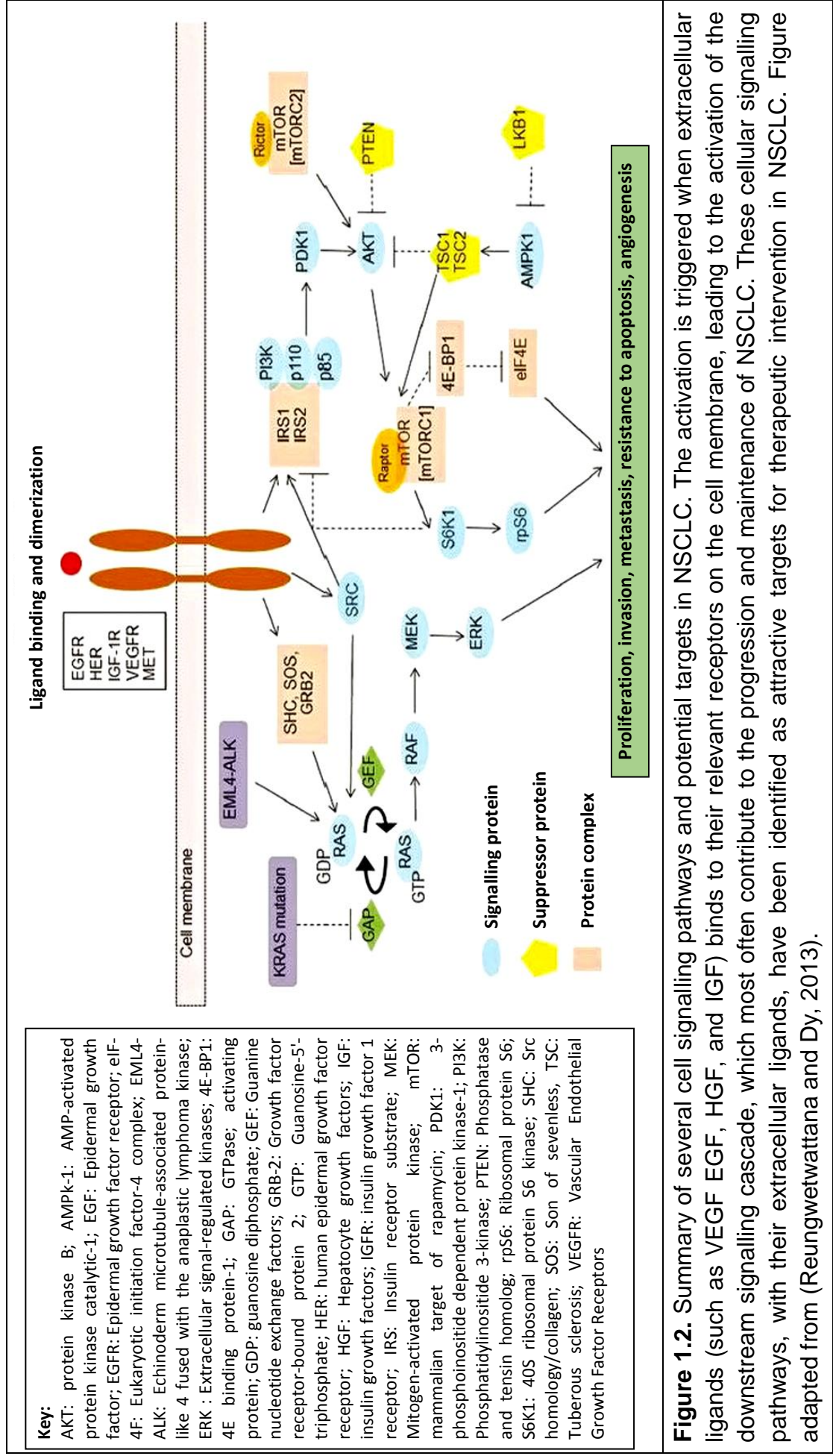


Figure 1.2. Summary of several cell signalling pathways and potential targets in NSCLC. The activation is triggered when extracellular ligands (such as VEGF, EGF, HGF, and IGF) binds to their relevant receptors on the cell membrane, leading to the activation of the downstream signalling cascade, which most often contribute to the progression and maintenance of NSCLC. These cellular signalling pathways, with their extracellular ligands, have been identified as attractive targets for therapeutic intervention in NSCLC. Figure adapted from (Reungwetwattana and Dy, 2013).

Table 1.1. Molecular-Targeted Drugs Evaluated in NSCLC. Abbreviations, EGFR: epidermal growth factor receptor; FGFR: fibroblast growth factor receptors, EML4-ALK: echinoderm microtubule-associated protein-like 4 (EML4) fused to the anaplastic lymphoma kinase (ALK), VEGF: vascular endothelial growth factor, IGF: insulin-like growth factor, FLT4: Fms-related tyrosine kinase 4, C-kit: tyrosine-protein kinase Kit.

Drug	Target	Current status in the development as a drug for NSCLC
Gefitinib, Erlotinib	EGFR	Approved for first, second and third line treatment of advanced stage NSCLC (Fukuoka et al., 2011).
Afatinib		Approved for first line treatment of advanced stage NSCLC and still under evaluation (Sequist et al., 2013)
Cetuximab (mAb)		Reported in clinical phase III trial as useful only in combination with chemotherapy (Pirker et al., 2009).
AZD4547	FGFR	Under evaluation in clinical phase II trial for advanced NSCLC (Reungwetwattana and Dy, 2013).
Crizotinib	EML4-ALK	Approved for advanced ALK-positive NSCLC patients (Camidge et al., 2012).
XL647	EGFR, VEGFR, FLT4, C-kit	Under evaluation in clinical phase III trial compared to erlotinib (Reungwetwattana and Dy, 2013).
Bevacizumab mAb	VEGF	Approved in first line metastatic non-squamous NSCLC (Sandler et al., 2006).
Sorafenib		Failed to improve overall survival in NSCLC patients at advanced stage (Paz-Ares et al., 2012; Scagliotti et al., 2010).
Cixutumumab	IGF-IR	Under evaluation in clinical phase II for advanced NSCLC (Reungwetwattana and Dy, 2013).
Figitumumab (mAb)		No further use in NSCLC based on clinical phase III trial (Jassem et al., 2010).

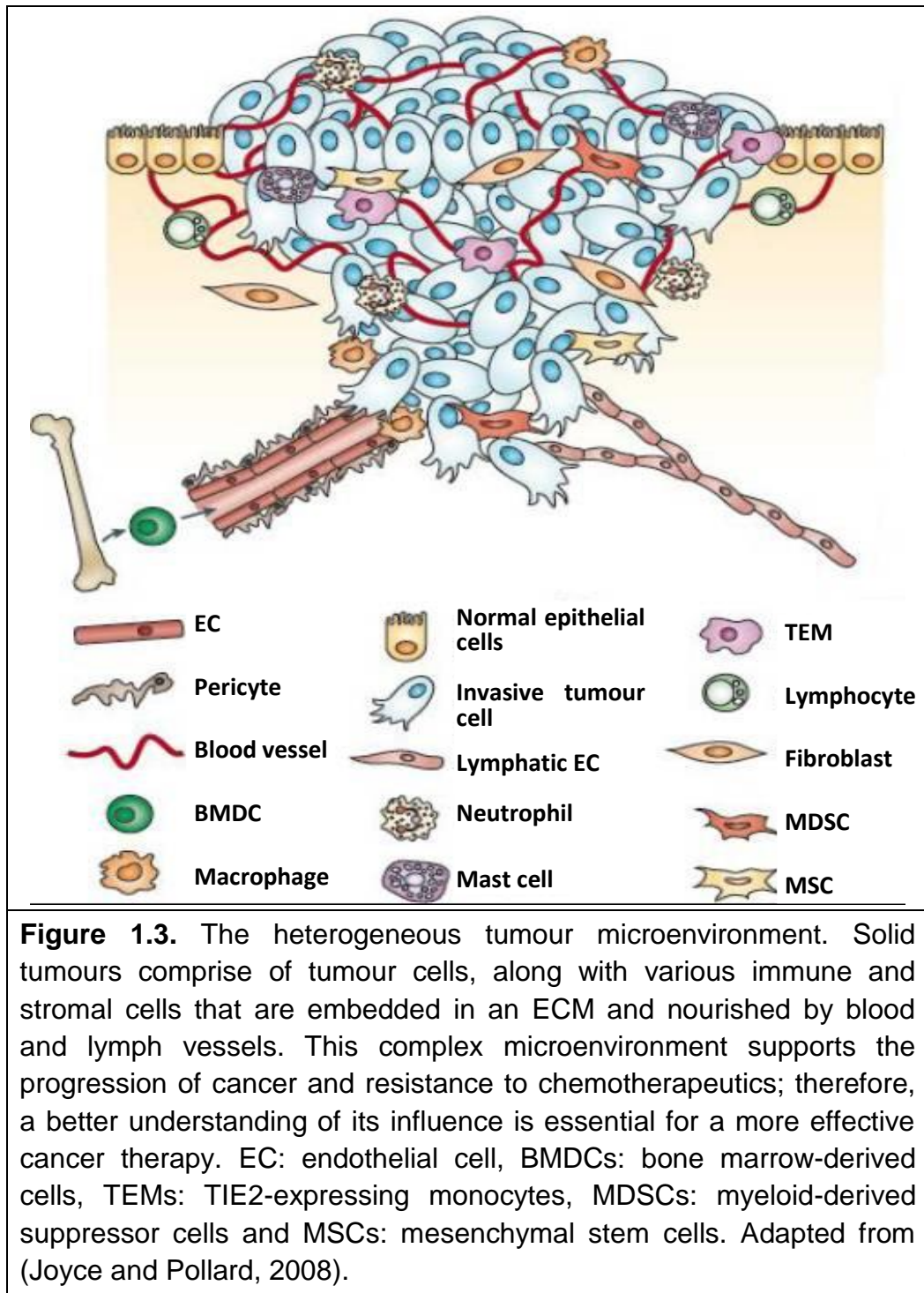
1.2 Tumour Microenvironment

The solid tumour microenvironment encompasses a mixture of tumour cells together with extracellular matrix (ECM), tumour vasculature and immune and stromal cells (Joyce and Pollard, 2008; Junttila and de Sauvage, 2013) (Figure 1.3). This heterogeneous environment has similar characteristics to the initiation of an inflammatory response in a healing wound. In the case of tissue damage, an initiation of several chemokines helps in the healing of the injured tissue and maintains a suitable host response. Immune cells (monocytes and neutrophils) are controlled and recruited by the released chemokines. These cells participate in the repair process (Epstein and Luster, 1998). This inflammatory environment causes the activation of local fibroblasts, leading to the activation and induction of numerous proteolytic enzymes, particularly the matrix metalloproteinases (MMPs), which are involved in angiogenesis and in the remodelling of the extracellular matrix. When there is complete healing of the wound, the inflammatory response, in general, subsides and tissue function returns to normal (Eming et al., 2007; Kalluri and Zeisberg, 2006; Liddiard et al., 2011).

It is known that tumour cells can synthesise and secrete chemokines and cytokines, which help in recruiting endothelial cells, fibroblasts, monocytes, and neutrophils, along with VEGF. Moreover, as evident in healing wounds, the secretion of proteolytic enzymes and cytokines is carried out by the infiltrating inflammatory cells and fibroblasts that are activated at the site of the cancerous tissue. The secretion of cytokines and MMP in the cancer tissue seems dedicated to support cancer progression by recruiting MMPs to

create extracellular space for the further proliferation and metastasis of cancer cells, rather than taking part in the reconstitution of tissues (Coussens et al., 2002; Eming et al., 2007).

Additionally, the low level of oxygen and nutrients in the tumour tissue permits the formation of an aggressive metabolic microenvironment. It was reported that the tumour's metabolic microenvironment might encompass acidosis, high levels of lactate, bicarbonate depletion, high CO₂ levels, low oxygen levels (Vaupel et al., 1989) and low blood sugar, thereby aiding cancer progression and supporting resistance to drugs (Hanahan and Folkman, 1996b; Trédan et al., 2007; Vaupel et al., 1989). Overall, this aggressive inflamed microenvironment represents unique differences between normal and tumour tissue, which can be exploited for novel targeted-tumour therapies.



1.2.1 Tumour Vasculature and Angiogenesis

Angiogenesis is the development of new blood vessels from pre-existing vessels. This dynamic process results from the interaction between endothelial cells, surrounding pericytes, extracellular matrix, angiogenic cytokines/growth factors and smooth muscle cells (Rundhaug, 2003). The molecular mechanism of angiogenesis involves the degradation of the basement membrane surrounding an existing vessel, migration and creation of endothelial cells towards the holes in the basement membrane, forming angiogenic endothelial vessel sprouts. The endothelial cells eventually undergo maturation, differentiation, and adherence to each other, creating a lumen that runs through the capillary sprouts (Lockhart et al., 2003).

Angiogenesis has important functions in several normal physiological processes, such as foetal growth and wound healing (Folkman, 1990). It also has key roles during some pathological conditions, such as tumour growth and atherosclerosis (Carmeliet, 2003; Ferrara et al., 2003; Ha et al., 2008). Under normal circumstances, angiogenesis is highly controlled by the balance between proangiogenic factors and endogenous angiogenesis inhibitors (Harris, 2003). Proangiogenic factors, such as VEGF and platelet-derived growth factor (PDGF), act on endothelial cells by directly stimulating the growth and migration of endothelial cells, or indirectly by influencing other cells involved in angiogenesis (Ferrara, 2000). A series of endogenous antiangiogenic factors, such as arrestin, endorepellin, endostatin, fibulins and thrombospondins, have been reported (Nyberg et al., 2005). These inhibitors

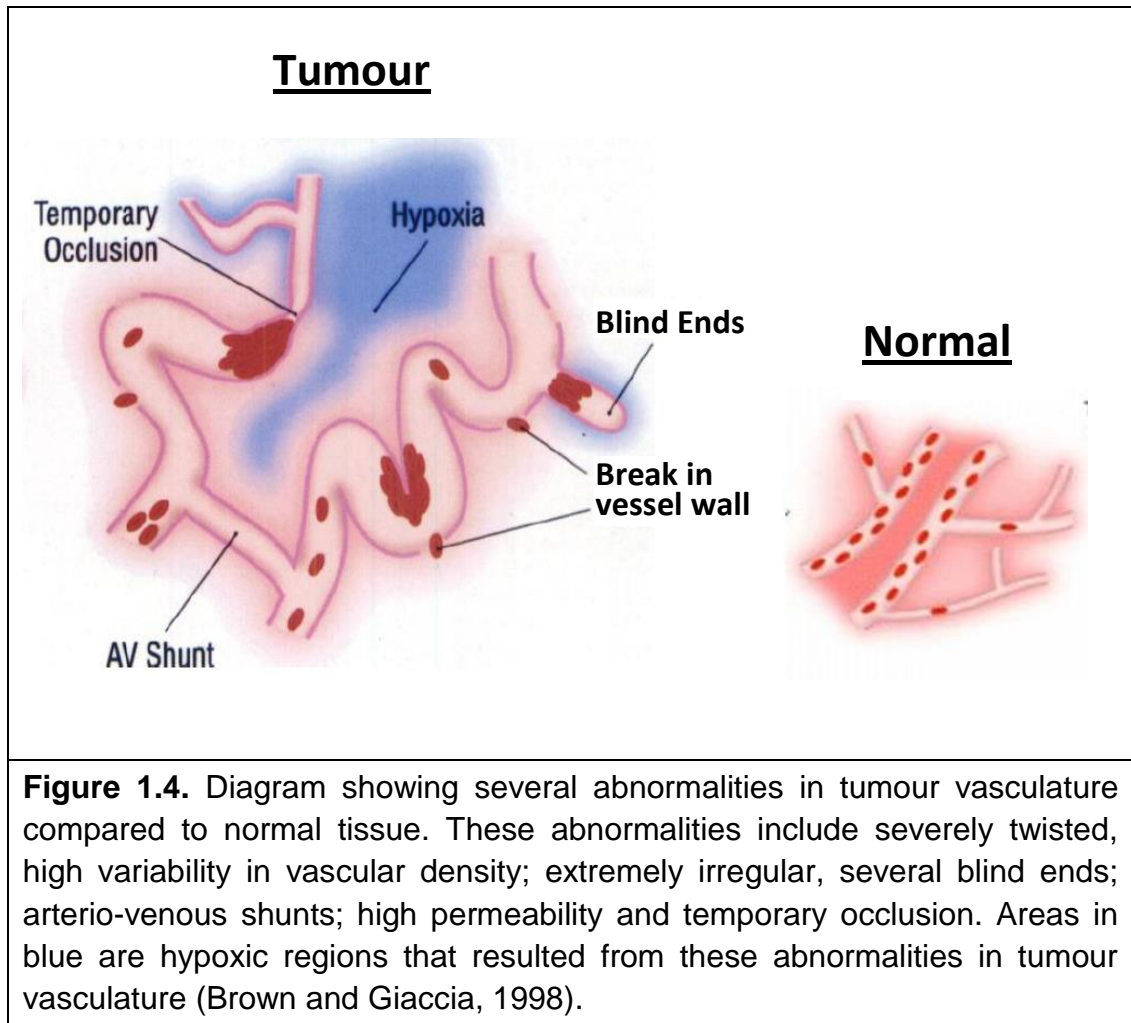
and proangiogenic factors work in concert to generate and sustain the functional vasculature in the body as required.

However, tumours have lost the equilibrium between anti and proangiogenic signals due partially to the influence of the tumour microenvironment (Crinò and Metro, 2014). For example, proangiogenic factors in the tumour tissue were confirmed to be highly expressed as a consequence of hypoxia, especially in NSCLC (De Bock et al., 2011; Ferrara and Kerbel, 2005). The overproduction of proangiogenic factors makes the tumour vasculature vulnerable to various disorders, including high vessel permeability; exceedingly irregular, elevated inconsistency in vascular density; severe tortuous; arterio-venous shunts and deprived or no lymphatic drainage system (Figure 1.4). In addition, the internal structure of the tumour vasculature is weak due to the lack of supporting pericyte cells, perivascular smooth muscle and basement membrane (Benjamin et al., 1999; Grunt et al., 1985). Elevated vascular permeability in tumours allows plasma leakage into the extravascular compartment, adding to the chaotic and inconsistent blood flow (Benjamin et al., 1999; Grunt et al., 1985).

Angiogenesis is essential for tumour growth and metastasis. It constitutes a significant point in the control of cancer development. The suggestion that tumour growth requires the development of the vascular network was first reported by Algir and Chalkley (Algire et al., 1945). In the 1970s, Folkman claimed that the growth of tumours beyond $1\text{-}2\text{mm}^3$ depends on their ability to initiate angiogenesis (Sherwood et al., 1971). Tumours can develop to about 1 mm without angiogenesis by obtaining oxygen and nutrients through

diffusion from adjacent tissues; however, for further growth, they must develop an angiogenic phenotype, which leads to the formation of a functioning blood vessel (Sherwood et al., 1971). Several preclinical models demonstrate that angiogenesis is important for tumour progression and survival and metastasis dissemination (Algire et al., 1945; Folkman, 1990; Nishida et al., 2006). In NSCLC, richly vascularised tumours coupled with high VEGF levels support the angiogenesis process (Crinò and Metro, 2014; Stefanou et al., 2004). Targeting angiogenesis, therefore, would provide a good therapeutic strategy for malignant solid tumours in NSCLC. For example, the inhibition of VEGF in tumours using the anti-VEGF monoclonal antibody bevacizumab results in a significant prolongation of both overall survival and progression-free survival in patients with NSCLC (Sandler et al., 2006).

While the tumour microenvironment has always been associated with the growth and progression of cancer, it is also the basis of the phenotypic difference with normal tissue, a difference that can be exploited for novel therapeutic targeting approaches. For example, banoxantrone (AQ4N) and TH-302 are both hypoxia-activated prodrugs that have a remarkable capacity to specifically target the tumour hypoxic cells, thereby facilitating the sensitivity of solid tumours to therapy (Duan et al., 2008; Meng et al., 2012; Patterson and McKeown, 2000).



1.3 Matrix Metalloproteinases (MMPs)

Matrix metalloproteinases are key players in the tumour microenvironment that have been implicated in the tumour progression in part due to the remodelling of the ECM, thereby promoting angiogenesis and enhancing tumour cell migration (Coussens et al., 2002; Kessenbrock et al., 2010). There are 24 human MMP members of the MMP family that have been described (Puente et al., 2003) and they have been initially classified into two groups based on their cellular localisation (secreted versus membrane bound). Another alternative classification of the MMPs was reported later,

dividing them according to their structure and substrate specificity into collagenases, gelatinases, membrane type, stromelysins and matrilysins (Bourboulia and Stetler-Stevenson, 2010). Table 1.2 illustrates most of these MMPs with their common name and localisation.







Table 1.2 Human MMPs		
MMP Member	Common Name	Localisation
MMP1	Colagenase-1	Secreted (zymogen)
MMP8	Colagenase-2	
MMP13	Colagenase-3	
MMP3	Stromelysin-1	
MMP10	Stromelysin-2	
MMP12	Metalloelastase	
MMP18	Colagenase-4	Secreted
MMP19	RASI-1	
MMP20	Enamelysin	Secreted (zymogen)
MMP27	N/A	
MMP2	Gelatinase A	
MMP9	Gelatinase B	
MMP7	Matrilysin/ Uterine	
MMP26	Matrilysin-2/ Endometase	Secreted (active)
MMP11	Stromelysin-3	
MMP28	Epilysin	Secreted
MMP21	MMP-23A	
MMP14	MT1-MMP	Trans-membrane
MMP15	MT2-MMP	
MMP16	MT3-MMP	
MMP24	MT5-MMP	
MMP17	MT4-MMP	Membrane bound GPI-linked
MMP25	MT6-MMP	
MMP22	NA	membrane-associated

In addition to the MMP, there is a close protease subfamily called a disintegrin and metalloproteinases (ADAMs), has proven to be equally important. This family contains 23 members in human and all are membrane-anchored glycoproteins that involves in a wide variety of biological process including proteolysis, cell adhesion, cell fusion, and intracellular signalling (Blobel, 2005; Schlondorff and Blobel, 1999; Zhong et al., 2008). In cancer pathophysiology, preclinical studies have shown that several ADAM family members (ADAM9, ADAM10, ADAM12, ADAM15 and ADAM17) can play roles in cancer formation and progression (Duffy et al., 2009a; Duffy et al., 2009b; Duffy et al., 2011). This is through an activation of positively-stimulating pathways (e.g. EGFR-PI3K-AKT), inactivation of growth-inhibitory pathways (e.g. mediate shedding of the type 1 TGF- β receptor), shedding of adhesion proteins (e.g. cadherin E), or mediating angiogenesis (Duffy et al., 2011). based on these functions, ADAMS could be one of key players in tumours microenvironment, However, due to the nature of this research, the main focus will be on MMP.

1.3.1 Structure of MMPs

The structure of MMPs consists of the following homologous domains: 1) signal domain essential for directing MMPs to the endoplasmic reticulum prior to secretion; 2) hydrophobic pro-peptide region that protects enzymatic activity by occupying the active site, making the catalytic enzyme inaccessible to substrates or inhibitors until activated; 3) zinc containing catalytic domain responsible for enzymatic activity after pro-peptide removal; 4) hemopexin-like domain at the C-terminus, which is found in all MMPs

except for MMP-7, MMP22 and MMP-26 (Table 1.3) (Bourboulia and Stetler-Stevenson, 2010; Foda and Zucker, 2001; John and Tuszynski, 2001). This domain is linked to the catalytic domain by a flexible hinge region, conferring the specificity of the enzyme and the mediation of the substrate or MMP inhibitors (Bourboulia and Stetler-Stevenson, 2010). In the transmembrane MMP subclass, there is an additional hydrophobic transmembrane binding domain at the C-terminal end of the protein. In type II MT-MMPs (MMP17 and 25), this is a glycosyl-phosphatidyl inositol (GPI) anchor domain. In type I MT-MMPs, this is a transmembrane domain linked to the cytoplasmic tail in MMP14, 15, 16 and 24. The major role of these domains is to allow the MMP to anchor to the cell surface (Table 1.3).

Table 1.3. Structural Classes of Human MMPs. signal peptide (SP); pro-peptide (Pro); catalytic domain (CAT); fibronectin repeats (F); hemopexin-like domain; (PEX); transmembrane domain (TM); glycosyl-phosphatidyl inositol anchor domain (GPI); cytoplasmic domain (C); cysteine array (CA); immunoglobulin-like domain (Ig). The flexible, variable length linker or hinge region is depicted as a wavy black ribbon (Radisky and Radisky, 2010).	
Structural Class	Domain Structure
Simple Hemopexin Domain	 (MMP1, 3, 8, 10, 11, 12, 13, 19, 20, 21, 27, 28)
Gelatin-Binding	 (MMP2, 9)
Minimal Domain	 (MMP7, 22, 26)
Type-I Transmembrane	 (MMP14, 15, 16, 24,)
	 (MMP17, 25)
Type-II Transmembrane cysteine array	 (MMP23)

1.3.2 Regulation of MMP Expression and Activity

Matrix metalloproteinases are tightly regulated at three levels—transcriptional level, post transcriptional level, and the proteolytic level—via activators, inhibitors and cell surface localisation (Sounni et al., 2003).

1.3.2.1 Transcriptional and post- transcriptional regulation

Matrix metalloproteinases are generally not synthesised until required, supporting the theory that the synthesis of MMPs is highly governed and depends on specific stimuli at the transcriptional level (Löffek et al., 2011; Rundhaug, 2003). It is well known that the regulation of gene expression is mediated by transcription factors that bind to specific sites in the gene promoter region (Latchman, 1997; Yan and Boyd, 2007). In terms of MMPs, the most crucial transcription factors involved in the regulation belong to the NF κ B, AP-1, PEA3, and to the signal transducer and activator of transcription (STAT) families (Fanjul-Fernández et al., 2010; Yan and Boyd, 2007), which, in turn, are increased in response to several stimuli, such as cytokines (interleukin [IL]-1, IL-6 and tumour necrosis factor [TNF]), growth factors (epidermal growth factor [EGF] and transforming growth factor β [TGF- β]) and mechanical stress (Fanjul-Fernández et al., 2010; Sorsa et al., 2004; Yan and Boyd, 2007). These extracellular signals mediate the induction of MMP expression in mammals through several mitogen-activated protein kinase (MAPK) signalling pathways, including extracellular signal-regulated kinase (ERK1- 2), stress-activated protein kinase/Jun N-terminal kinases (SAPK/JNK) and p38-MAPK (Kerkelä and Saarialho-Kere, 2003). The basal outcome of activating these pathways might be amplified due to the contribution of other transcriptional pathways in several cancers (Kerkelä and Saarialho-Kere, 2003). In NSCLC, emerging evidence supports the retinoblastoma (Rb)–E2F transcriptional pathway in regulating some MMPs (MMP9, 14, and 15) (Johnson et al., 2012). In contrast to stimulation

pathways, MMP transcription is suppressed when the SMAD family of the transcriptional factors binds to TGF inhibitory elements (TIEs) in the gene promoter regions of several MMPs (MMP-1, MMP-7, MMP-13, and MT1-MMP) (Gorman et al., 2011; Spinale, 2007). Furthermore, epigenetic mechanisms, including histone acetylation and DNA methylation, are also involved in MMP regulation (Fanjul-Fernández et al., 2010). As post-transcriptional modulators of MMP gene expression, mRNA stability, protein translational efficiency and microRNA-based mechanisms have been shown to have been implicated (Fanjul-Fernández et al., 2010).

1.3.2.2 Post-translational activation of MMPs

Matrix metalloproteinases share several common properties, one of which is the requirement of zinc in their catalytic site for activity. It is well known that most MMPs, with the exception of MT-MMPs, are secreted by the cell in a latent form as inactive pro-enzymes owing to the presence of a pro-domain (John and Tuszynski, 2001; Rundhaug, 2003). This domain interacts with the zinc atom at the catalytic site, leading to the inhibition of the enzymatic activity (Rundhaug, 2003). Therefore, MMPs require first to be activated extracellularly to exert their activity. The removal of the pro-domain is usually enough to activate the zymogens (Rundhaug, 2003). This is usually a two-step process, which includes the destabilisation of the protein by an activator protease followed by a final cleavage that is usually catalysed by another MMP; for example, the activation of pro-MMP2 by MT1-MMP/MMP14 or serine proteases, such as plasmin or furin (Rundhaug, 2003). Once the N-terminal pro-domain of the zymogens is cleaved, the enzyme becomes fully

functional. In terms of MT-MMPs, they are activated intracellularly before translocation to the membrane (Overall and López-Otín, 2002).

1.3.2.3 MMP regulation by endogenous MMP inhibitors

A more important regulatory mechanism of the MMP activity is shown through their specific endogenous inhibitors, the Tissue Inhibitors of MetalloProteinases (TIMPs). These low-molecular weight (21-30kDa) secreted proteins form non-covalent complexes with active MMPs through the binding of the N-terminal domain of the TIMP molecule with the active site of the MMP in a stoichiometric ratio of 1:1, inhibiting MMP activity (Brew et al., 2000). At present, homologous mammalian TIMP family members, including TIMP-1, -2, -3 and -4, have been identified (Brew et al., 2000; Curran et al., 2001; Gomez et al., 1997). Other endogenous MMP inhibitors have also been reported, such as the membrane-anchored glycoprotein (RECK) and the plasma protein alpha-2-Macroglobulin (Oh et al., 2001; Sottrup-Jensen, 1989). Under normal conditions, the levels of protease and inhibitor are firmly balanced for controlling net proteolytic activity (John and Tuszynski, 2001). However, this balance between protease and inhibitor is lost in some pathological conditions, such as cancer, wherein MMPs are mainly overexpressed in tissue while TIMPs do not show such a consistent expression pattern (John and Tuszynski, 2001). However, high mRNA expression of TIMP1 and several MMP in NSCLC clinical tissues compared to normal tissue have been reported in several studies (Jumper et al., 2004; Pesta et al., 2011; Safranek et al., 2009), highlighting that TIMP1 was unable to inhibit all MMPs associated with tumourigenesis.

1.3.3 MMPs and Pathophysiology

As has been mentioned, controlling MMP expression and activation is critical for their proteolytic activity (Rundhaug, 2003). Once they become deregulated, serious diseases, such as cardiovascular diseases (atherosclerosis and heart failure), tissue ulceration, rheumatoid arthritis and cancer, may emerge (Rundhaug, 2003; Woessner, 1991).

1.3.3.1 Roles of MMPs in cancer

Despite the role of MMPs in several physiological processes, most attention is placed on their functions during the pathological states where the degradation of the ECM is the main feature. In terms of cancer, MMP proteolytic activity is essential for most cancers, including NSCLC, as it is implicated in various stages of disease development, such as migration, invasion, angiogenesis and metastasis (Rundhaug, 2003). Figure 1.5 summarises the contribution of MMP to the numerous stages of cancer development. Due to the involvement of the MMPs in these functions, they are often highly expressed in the tumour microenvironment of several cancers, especially NSCLC (Atkinson et al., 2010). In addition to the synthesis of MMPs by tumour cells, host cells (e.g. fibroblasts) in the tumour microenvironment are proven to be another source of MMPs in response to a stimulation by several ligands (interleukins and growth factors) that are released by tumour cells (Gialeli et al., 2011; Noël et al., 2008).

This activity of the MMP is not purely due to ECM cleavage (Folgueras et al., 2004), but also to the release of several growth factors that adhered on the

ECM or cell surface. Matrix metalloproteinases make these growth factors more accessible to the cancer cells and the tumour microenvironment, thereby promoting tumour development (Folgueras et al., 2004). For instance, MMPs regulate proliferation through the cleavage of insulin-growth-factor-binding protein (IGF-BP) and release IGF. They also shed growth factors, such as TGF- α and HB-EGF from the cell surface, thereby modifying the ECM, which supports growth indirectly via the interactions between the integrins and the ECM molecules (Egeblad and Werb, 2002).

One major mechanism that shows how MMPs support further tumour growth is the adverse influence on cell apoptosis. Matrix metalloproteinases are reported to cleave the FAS ligand (FASL), a key apoptotic factor, leading to the inhibition of apoptosis (Folgueras et al., 2004). In addition, MMP has been seen to activate the serine/threonine kinase Akt/protein kinase B by indirect activation of EGFR and IGFR (Folgueras et al., 2004), which are both frequently up-regulated in NSCLC (Ludovini et al., 2009), resulting in an anti-apoptotic effect.

Another contribution of MMPs to cancer progression is through the stimulation of cell migration. While the proteolytic activity of the MMPs to degrade physical barriers of ECM is needed during cell migration, the production of ECM-protein fragments also has further extracellular roles, such as cryptic sites from laminin and collagen, which can improve the migration of different cell types (Curran and Murray, 2000; Nagase et al., 2006). Furthermore, MMPs can influence the cell phenotype (epithelial to mesenchymal transition (EMT)) and enhance migration through a role in the

cell-cell and cell-ECM adhesion by processing E-cadherin and integrins, respectively (Gialeli et al., 2011).

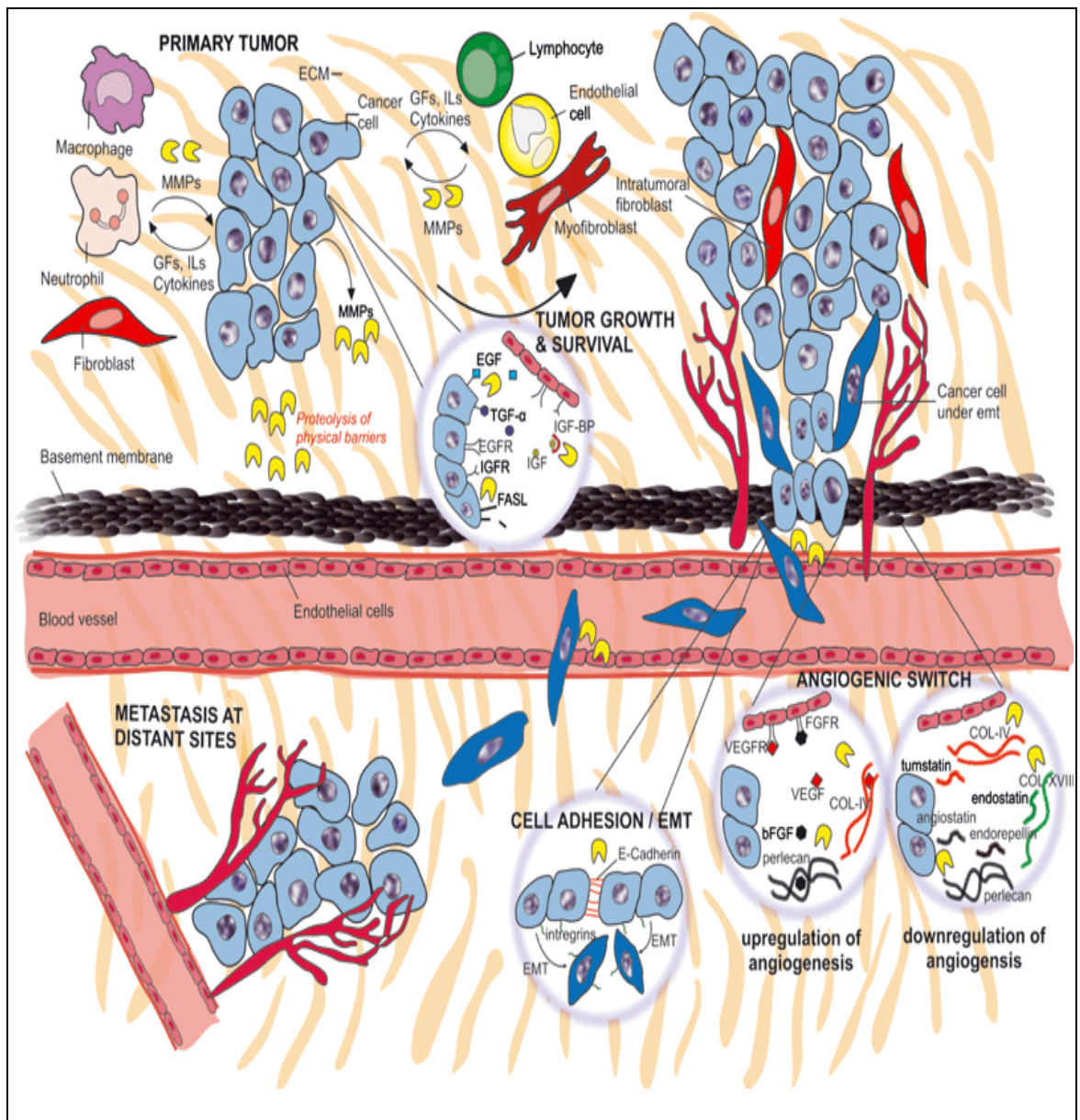


Figure 1.5. Schematic demonstration of the involvement of MMP in cancer progression. MMP modulates four hallmarks of cancer, including tumour growth, invasion, metastasis and angiogenesis. MMP in tumour microenvironment is synthesised and secreted by both tumour and stromal cells. The degradation of ECM by MMP is essential for angiogenesis, tumour cells invasion and metastasis. Improving the availability of several signalling molecules, such as IGF, bFGF and VEGF EGF, TGF- α and the heparin-binding EGF (HB-EGF) due to MMP-ECM degradation is also critical for tumour growth and angiogenesis. The negative regulators of angiogenesis, including angiostatin, tumstatin, endostatin and endorepellin, are also released. MMP can influence the cell phenotype (epithelial to EMT) and enhance migration through a role in the cell-cell and cell-ECM adhesion by processing E-cadherin and integrins, respectively. Adapted from (Gialeli et al., 2011).

1.3.3.1.1 MMPs and tumour angiogenesis

Matrix metalloproteinases play a dual role in tumour vasculature regulation. They can function both as inducers and inhibitors of angiogenesis (Rundhaug, 2005). This is dependent on the time point of their expression during tumour angiogenesis, as well as on the availability of their substrates (Rundhaug, 2003; Rundhaug, 2005).

Proangiogenic factors, MMPs, such as MMP2, MMP3 and MMP9, are heavily implicated in the angiogenesis process, in which they degrade the basement membrane. This allows the detachment of the endothelial cells and the migration of these cells into the surrounding tissues (Bergers et al., 2000; Rundhaug, 2003). Matrix metalloproteinase activity results in a shift in the physiological equilibrium between the pro-angiogenic factors and the angiogenic inhibitor as a consequence of the MMP proteolytic activity (Rundhaug, 2005). Numerous studies have shown that the expression of angiogenic inducers, such as bFGF and VEGF, involve MMP activity in tumour tissue (Hanahan and Folkman, 1996a; Kerbel and Folkman, 2002). Under hypoxic conditions, endothelial progenitor cells secrete MMP9, which also induce angiogenesis by releasing VEGF from the ECM (Du et al., 2008). In contrast, MMP-mediated degradation of the ECM can also release several factors that have an antiangiogenic activity, such as angiostatin, endostatin, neostatin, tumstatin and endorepellin (Chang et al., 2005; Heljasvaara et al., 2005). These small endogenous angiogenesis inhibitors are generated through the cleavage of type IV, XVII collagen, plasminogen and the inactive precursor of serine proteinase plasmin and perlecan (Iozzo et al., 2009;

O'Reilly et al., 1999; Theocharis et al., 2010). Overall, this suggests the opposing effects of MMPs as both positive and negative regulators of angiogenesis as shown in Figure 1.5.

1.4 MMP Inhibition as a Therapeutic Strategy for Cancer

The understanding that MMP expression is enhanced in many cancer types supports the rationale for targeting MMPs in cancer therapy (Egeblad and Werb, 2002). This strategy is strongly supported by *in vitro* and animal model studies that show MMP inhibition as beneficial (Folgueras et al., 2004). More than 50 matrix metalloproteinase inhibitors (MMPis) have been tested as clinical candidates over the last decade (Zucker and Cao, 2009).

Hydroxamates, such as Batimastate and Marimastat, were first generation MMPis that showed a good potential in preclinical studies. They were, however, broad spectrum inhibitors and not available orally. To overcome the latter issue, second generation MMPis were introduced. They entered phase III clinical trials for the treatment of diverse types of advanced cancers (Fingleton, 2003; Overall and Kleinfeld, 2006; Zucker et al., 2000). Unfortunately, broad spectrum MMP inhibitors failed to provide significant anti-tumour effects in the clinic. Instead, they were found to be associated with adverse patient outcomes and a number of serious side effects, such as tendonitis and myalgia (Bissett et al., 2005; Coussens et al., 2002; Nemunaitis et al., 1998; Pavlaki and Zucker, 2003). Many patients who were enrolled into the clinical trial of MMPI declined to participate further because of the decrease in their quality of life (Pavlaki and Zucker, 2003).

The lack of success of the MMP inhibitors in clinical trials was attributed to several reasons, which include the following: Only patients with advanced cancer stage were included in the trial despite some inhibitors demonstrating potential activity at the early stage in animal models. An unrealistic endpoint (reduction in tumour size) was used while time to tumour progression or patient survival benefit was more appropriate. Treatment response could not be monitored as no prognostic marker was available. Toxicity resulted from the poor selectivity of these inhibitors due to the close homology of the catalytic domains of different MMPs, with many MMPs now known to contribute to tumour-inhibition (Sparano et al., 2004).

In summary, the previous trials of MMPI's showed that a general systemic inhibition of a broad spectrum of MMPs as a therapeutic strategy was too simplistic. Such an approach did not consider the physiological and non-ECM-degrading properties affected by the broad spectrum inhibition of MMPs (Szarvas et al., 2011). Fortunately, this time elucidation of the specific roles of MMPs and their complex mechanisms are more complete. It's worth noticing that the discovery of other metalloenzymes such as ADAMS, which were demonstrated to be involved in tumour growth and progression (Duffy et al., 2009a), further supports the inhibition of MMP-associated enzymes as an attractive target for cancer therapy. In this regards, there are other protease families (e.g. cysteine and aspartic) which also provide good targets for therapeutic intervention given their expression and activity in cancer development (Palermo and Joyce, 2008; Ullmann et al., 2004), however the main focus of this research will be restricted to MMPs.

Overall, it is now clear that different MMPs can play opposing roles in cancer. Some MMPs may be beneficial for inhibiting the cancer process, indicating that they should not be targets for inhibition themselves (Rundhaug, 2003). For instance, MMP3-deficient mice demonstrate an increase in pulmonary metastasis compared to wild-type (McCawley et al., 2004). Furthermore, tumours in MMP12-deficient animals demonstrate greater angiogenesis as a result of the reduction of angiostatin synthesis (Acuff et al., 2006). Interestingly, studies have shown that specific MMPs can demonstrate contradictory negative and positive roles during the development of the disease (Rio, 2005). For example, stromelysin-3 (MMP11), demonstrating a collagenolytic activity specifically against collagen VI at normal and tumour tissue (Motrescu et al., 2008), is a stimulator for primary tumour progression, but is also an inhibitor for metastasis (Rio, 2005). Therefore, the complexity of the MMP functions has a serious impact on the possibility of using MMPs as a target for therapy.

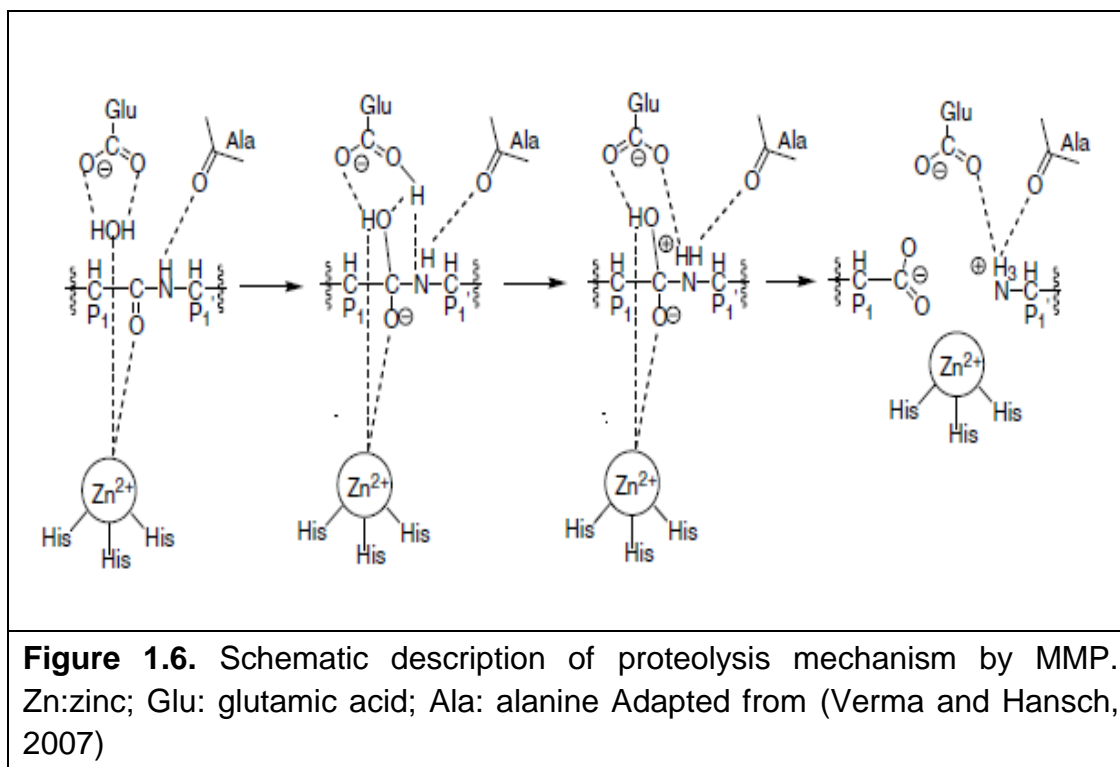
With respect to tumour angiogenesis, although MMPs in general have opposing effects as both positive and negative regulators of angiogenesis, controlling angiogenesis through targeting selected MMPs remains a potential therapeutic approach for cancer (Rundhaug, 2003). It is, therefore, crucial to elucidate the specific role of individual MMPs in tumour evolution and progression with respect to their validity as target or anti-targets for therapeutic exploitation.

1.5 MMP10 in NSCLC

In comparison to other MMPs, little is known about the involvement of MMP10 (stromelysin-2), a secreted endoproteinase, in NSCLC tumour development, although its expression is associated with poor clinical outcomes in NSCLC patients (Frederick et al., 2008). Unlike several other MMPs that are localised predominantly in tumours surrounding the stroma, MMP10 is found to be localised predominantly in tumour cells (Gill et al., 2004; Kerkela et al., 2001). Several studies have shown that MMP10 is extensively expressed by tumour cells (Gill et al., 2004; Impola et al., 2004; Kerkela et al., 2001; Muller et al., 1991; Nakamura et al., 1998). One main feature of MMP10 is the broad substrate specificity. In vitro, it can degrade elastin, nonfibrillar collagens, proteoglycans, gelatin, and casein (Duffy et al., 2000; Egeblad and Werb, 2002; Murphy et al., 1991; Nicholson et al., 1989; Vihinen and Kähäri, 2002). In vivo, it degrades numerous ECM proteins such as collagen type IV, laminin, proteoglycans and fibronectin (Baricos et al., 1988; Bejarano et al., 1988; Nicholson et al., 1989; Saunders et al., 2005). MMP10 participates also to activate several proMMPs, including proMMP 1, 7, 8, 9 and 13 (Nakamura et al., 1998; Ramos-DeSimone et al., 1999). In general, degradation of specific substrates by MMP10 as well as other MMPs might be through an interaction between conserved glutamic acid, zinc ion and water molecule at the cleavage site during the acid-base catalysis reaction. A full description of the mechanism is shown in figure 1.6. High expression levels of MMP10 have been reported in many different tumour types, such as carcinoma of the head and neck, NSCLC, oesophageal and

oral squamous cell carcinoma (SCC) and squamous and basal cell carcinomas of the skin (Gill et al., 2004; Impola et al., 2004; Kerkela et al., 2001; Mathew et al., 2002; Rhys-Evans and Eccles, 2001). In particular, significantly higher levels of proteolytically active MMP10 are detected in NSCLC as compared to corresponding normal lung tissue (Gill et al., 2004). The elevation of MMP10 expression in NSCLC is independent of tumour grade, stage, histological type or lymph node status (Gill et al., 2004).

Interestingly, high levels of MMP10 mRNA are observed in tumour tissues from recurrent human NSCLC patients following surgical resection, supporting MMP10 as a prognostic marker for patients with high risk of recurrence (Cho et al., 2003). In an animal study, a complete knockout of MMP10 results in the development of fewer tumours, indicating the role of MMP10 in tumour initiation (Frederick et al., 2008). In the same study, an overexpression of MMP10 in primary NSCLC tumours was observed and the high MMP10 expression was correlated to poor survival. MMP10 has been also reported to support the autonomous growth of cancer stem cells in lung tumours, resulting in an improvement in tumour-initiating activity, tumour maintenance and metastasis, thereby promoting lung cancer formation (Frederick et al., 2008; Justilien et al., 2012). Together, these findings suggest that MMP10 can also be expressed in the early stages of tumour and that they play a role in the development of human NSCLC rather than just tumour invasion and metastasis (Gill et al., 2004; Kerkela et al., 2001; Seargent et al., 2005). Further investigation of the nature of the role of MMP10 in NSCLC is required.



1.6 Regulation of MMP10 Gene Expression

Like other MMPs, MMP10 gene expression is tightly regulated at the transcriptional level. Its gene is only expressed when transcriptional factors are activated in response to several stimuli, such as cytokines, chemokines, growth factors, matrix protein, adhesion molecules, matrix protein fragments and hormones (Nagase and Woessner, 1999; Sternlicht and Werb, 2001). In addition to the universal transcriptional factors involved in the regulation of MMP gene expression (previously described in section 1.3.2.1), CHF1/Hey2, MEF-2 and STAT3 transcription proteins are reported to have been implicated, specifically in controlling the MMP10 gene expression (Ishikawa et al., 2009; Wu et al., 2011; Zhang et al., 2009). Additionally, the transcriptional regulation of MMP10 is believed to be influenced by epigenetic mechanisms, such as histone acetylation (Chang et al., 2006; Ha et al.,

2008; Ishikawa et al., 2009), as evidenced by histone deacetylase 7 down-regulation in two cellular pathway studies (Chang et al., 2006; Ha et al., 2008). These studies did not address the regulation of the MMP10 gene expression by histone deacetylases (HDACs) in the context of cancer; therefore, this relationship received more focus in the study reported here.

1.6.1 Histone Deacetylases

Histone deacetylases are a class of enzymes that remove acetyl groups from ϵ -N-acetyl lysine amino acid on histones (Sengupta and Seto, 2004). They are generally grouped into two major classes: class I (HDAC1, 2, 3 and 8) and Class II (HDAC4, 5, 6, 7, 9 and 10) (Sengupta and Seto, 2004). In contrast to class I HDACs, which are located predominantly in the nucleus, Class II HDACs, including HDAC7, constantly shuttle between the nucleus and cytoplasm (Harms and Chen, 2007; Kim et al., 2007; Lager et al., 2002). The deacetylation of histone proteins is the initially discovered and best understood enzymatic activity of HDACs. During this process, HDACs can regulate the interaction of positively charged histones with the negatively charged DNA and, as a consequence, control chromatin conformation and transcriptional activity. High levels of histone acetylation (hyperacetylation) are associated with improved transcriptional activity while low levels of acetylation (hypoacetylation) are linked with the suppression of gene expression (Forsberg and Bresnick, 2001; Ito et al., 2000; Wade, 2001). Among other HDACs, HDAC7 is of particular interest to this research as it was reported to specifically regulate MMP10 gene expression (Chang et al., 2006).

1.6.2. Regulation of MMP10 by HDAC7

It has been reported that HDAC7 regulates MMP10 gene expression through the transcriptional factor (myocyte enhance factor 2 [MEF2]) in endothelial cells (Chang et al., 2006). *In vivo* silencing of HDAC7 in the vascular endothelium during early embryogenesis causes a failure in endothelial cell-cell adhesion, dilatation and collapse of blood vessels, leading consequently to embryonic lethality (Chang et al., 2006). Histone deacetylases-7 contains a small N-terminal peptide sequence that linked them to MEF2, resulting in the repression of MEF2 target genes (Verdin et al., 2003). Following the exposure of endothelial cells to VEGF, the phosphorylated protein kinase D (PKD) is translocated from the cytoplasm to the nucleus, leading to HDAC7 phosphorylation at ser178, ser344 and ser479 residues in the N-terminal. This creates docking sites on the HDAC7 for the 14-3-3 chaperone proteins to bind on (Kao et al., 2001), thereby stimulating the shuttling of the HDAC7 from the nucleus to the cytoplasm and resulting in HDAC7 cytoplasmic accumulation. It is well known that HDAC7 suppresses the promoter of the MMP10 gene through interaction with the MEF2, a direct activator of MMP10 transcription and a key regulator of blood vessel development. The low level of HDAC7 in the nucleus leads to free MEF2 and allow p300 to bind with MEF2. This results in the induction of MEF2-dependent transcription of the target gene for MMP10 (Ha et al., 2008) (figure 1.7).

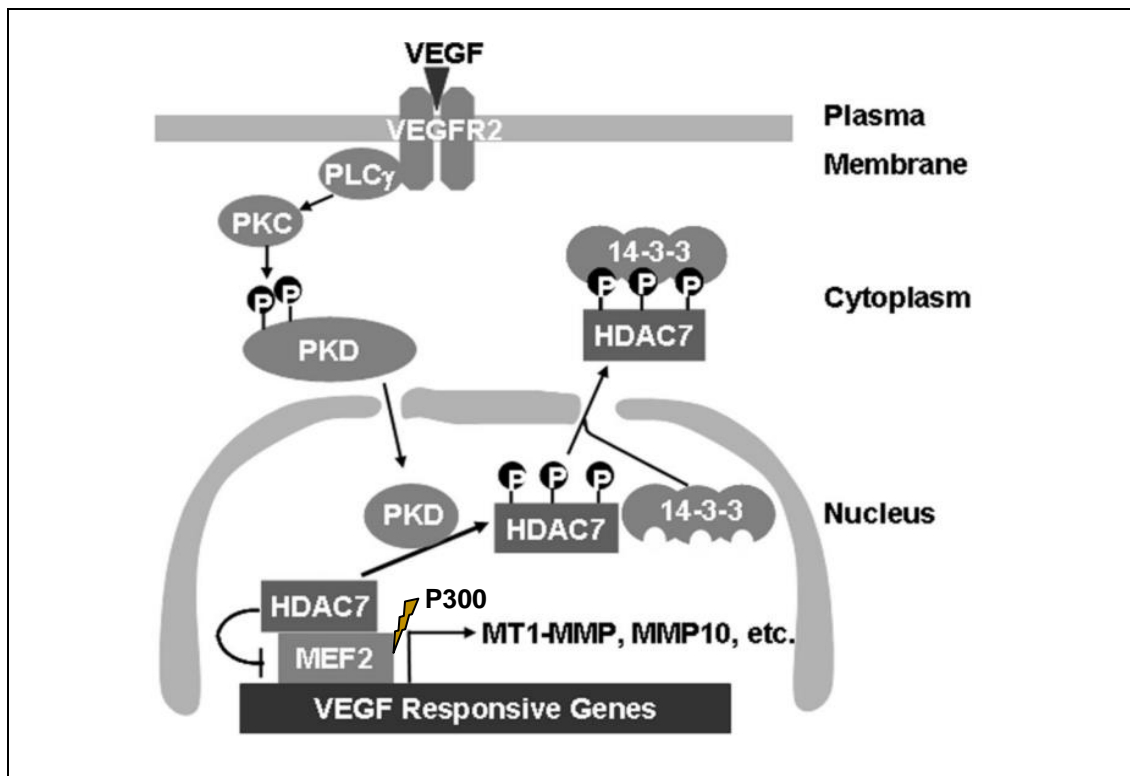


Figure 1.7. PKD1-dependent phosphorylation of HDAC7 upon VEGF signalling. In response to VEGF ligand on the cell membrane, a downstream signalling cascade involving PKD1 is activated, leading to HDAC7 phosphorylation. This allows 14-3-3 chaperon protein to catalyse the shuttling of HDAC7 from the nucleolus to the cytoplasm, resulting in a free MEF2. At this stage, the free MEF2 binds to P300, allowing the stimulation of the MEF2-dependent transcription of the MMP10 gene. Adapted from (Ha et al., 2008) with a slight modification.

1.7 Limitations of Classical Chemotherapeutics

Currently, the efficacy of chemotherapeutics is unquestionable and cancer treatment still highly depends on these cytotoxins. However, there are key disadvantages to the use of conventional chemotherapy, notably narrow therapeutic index and drug resistance. In an attempt to overcome these issues, a molecular targeted approach on the inhibition of pathways that drive the cancer process has been focused on in the last 15 years. This was intended to reduce systemic toxicity associated with cytotoxic drugs, adopting

a more conventional pharmacological approach to cancer treatment. However, this therapeutic approach against malignancies has not been as successful as was predicted. The molecular targeted drugs are not good at debulking tumours and they possess significant normal tissue toxicity on their own (Huang and Oliff, 2001). Subsequently, majority of molecular targeted therapies are frequently used in combination with classical chemotherapeutics. This has led to a resurgence in the interest on developing chemotherapeutics using approaches that address their negative effect on normal tissue. One such approach is the re-emergence of the development of prodrugs.

1.8 The Prodrug Concept

The most significant goals of current cancer drug discovery are to delineate between toxicity to healthy tissue and the tumour. This requires the development of new therapeutics with increased tumour discrimination, lower systemic toxicity and, consequently, a wider therapeutic margin. A possible approach has emerged that meets all these requirements is the use of cancer chemotherapeutic prodrugs. The term prodrug was first described by Adrien Albert in the 1950's (Albert, 1958) as an inactive compound that needs to be enzymatically or chemically converted to the active drug *in vivo* to exhibit a pharmacological effect. The prodrug approach is currently used to improve the biopharmaceutical, physicochemical or pharmacokinetic properties of pharmacological agents. These parameters include chemical instability, poor aqueous solubility, rapid pre-systemic metabolism, deficient oral absorption and local irritation. In terms of drug targeting improvement,

when existing drugs are re-developed as a prodrug, this can prolong the life-cycle of patented drugs (Rautio et al., 2008). Designing new agents as prodrugs is a growing trend worldwide, with up to seven percent of approved drugs categorized as prodrugs (Rautio et al., 2008).

The deep understanding of pharmaceutical concepts alongside tumour biology has enabled the design of pharmaceutically more complex prodrugs with improved targeting (Huttunen et al., 2011). This thesis focuses on exploiting MMP10 expression to improve tumour-targeting for a prodrug development strategy. A prodrug not only improves the pharmacokinetic properties of a compound; it also restricts the pharmacological effect of a drug to its intended tissue. Thus, there is a strong rationale to use this approach to develop smart anticancer drugs.

1.8.1 Tumour-Activated Prodrugs (TAPs)

A number of methods have been employed to develop prodrugs that rely on tumour biology. These include antibody- or gene-directed enzyme prodrug therapy, antigen targeting, and tumour enzyme-activated chemotherapy. The latter approach, in particular, takes advantage of the elevated enzymes that are selectively present in the tumour microenvironment to activate a prodrug. This has demonstrated great promise with the development of bioreductive drug AQ4N, polymer-paclitaxel conjugate (Ct-2103), polymer-doxorubicin conjugates (PK1, FCE28068) and the approved brentuximab vedotin (an antibody- auristatin E conjugate) (Albertella et al., 2008; Atkinson et al., 2010;

Choi et al., 2012; Patterson, 2002; Paz-Ares et al., 2008; Senter, 2009; Seymour et al., 2009).

In the development of tumour-activated prodrugs (TAPs), the effective therapeutic entity is required to be masked until only being activated in the malignant tissue by tumour enzymes, such as endoproteases (Atkinson et al., 2008; Denny, 2001). The structure of a TAP must contain three domains: the trigger, linker and effector. The trigger is linked to the effector. The function of the trigger is to control selectivity and the effector is responsible for the therapeutic effect. The cytotoxic effect of a prodrug is ideally released only when the trigger is activated in the tumour and not in any other tissue (Atkinson et al., 2008; Denny, 2001) (see Figure 1.8).

The selection of enzymes to activate TAPs is the most critical step in the development of these agents. The main features of the tumour enzyme appropriate for targeting TAPs are as follows:

1. Enzyme has relatively high affinity to the prodrug.
2. Overexpression and high activity in the tumour environment.
3. Low or no expression of enzyme in normal tissues.
4. Enzyme can rapidly activate the prodrug (Atkinson et al., 2008).

Proteolytic endoproteases, especially metalloproteases, are now considered to satisfy these criteria for TAP development. Consequently, they have received much attention.

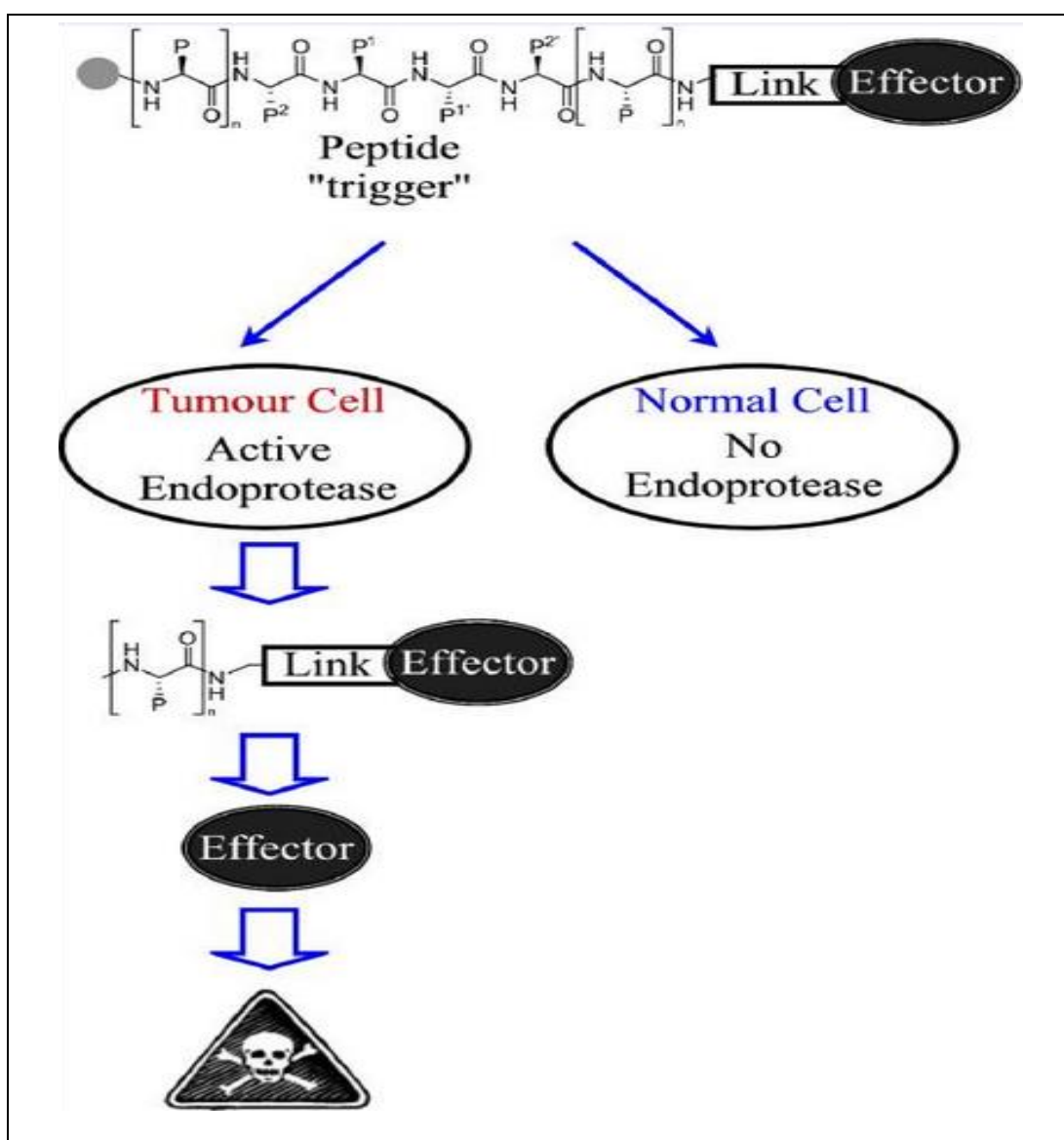


Figure 1.8. Schematic description of TAPs therapeutic strategy. This concept is not exclusive for proteolytic endoproteases, but they were used above to exemplified enzymes that meet the requirement for TAP development. The primary structure of TAPs involves trigger, linker and effector. No cytotoxicity is exhibited until the prodrug is activated by tumour enzymes, such as endoproteases. Adapted from (Atkinson et al., 2008).

1.8.2 MMPs as Target for Tumour Selective Anticancer Drug Delivery

The focus on proteases provides a wide range of opportunities in the process of prodrug development. Proteases account for about 2% of mammalian genes and 5% of all drug targets (Atkinson et al., 2008; Lee et al., 2004; Overall and Blobel, 2007; Overall and Dean, 2006). Several classes of proteases (Cysteine, metalloproteases and serine) have been investigated as prodrug activators (Atkinson et al., 2008; Lee et al., 2004; Lim and Craik, 2009). Given their high and often selective activity in tumours and ability to cleave short peptides, the MMPs are an attractive class of prodrug activating enzymes.

The overexpression of numerous MMPs is linked to poor clinical outcome in several cancers, including gastric (MMP 2 and 9), breast (MMP 11), NSCLC (MMP 3, 10, 11 and 13) (Atkinson et al., 2008; Atkinson et al., 2007; Bodey et al., 2000; Brinckerhoff et al., 2000; Hoekstra et al., 2001; Kamat et al., 2006; Vizoso et al., 2007), oesophageal (MMP-7), SCLC (MMP-3, MMP-11 and MMP-14) (Hoekstra et al., 2001; Vizoso et al., 2007).

The difference in MMP expression and the activity between malignant and normal tissue can be exploited to activate TAPs, in principle leading to a high concentration of active anticancer drug only in the tumour tissue. This was confirmed experimentally when MMPs were shown to activate cytotoxic anthracycline prodrugs into active cytotoxins. *In vivo*, various peptide derivatives of doxorubicin were enzymatically converted into active agents by

MMPs. These peptide derivatives demonstrated a lower systemic toxicity with higher anti-tumour efficacy in comparison to doxorubicin itself (Albright et al., 2005; Lee et al., 2006). Although these results were promising, it has been reported that successful releasing of potent chemotherapeutic in the intended site is highly dependent on the catalytic efficiency of MMPs and their expression (Atkinson et al., 2008). Therefore, the enzymatic competence and appropriateness of individual MMPs must be taken into consideration when designing TAPs.

1.8.2.1 Tumour-activated prodrugs directed to the matrix metalloproteinases

Several structure-activity relationship studies that evaluate the specificity of many MMPs against synthetic peptide substrates have been described. These include MMP1, MMP2, MMP3, MMP7, MMP8, MMP9, MMP13 and MMP14 (Deng et al., 2000; Netzel-Arnett et al., 1991; Turk et al., 2001). This has led to the identification of a structure-activity relationship that can be used to distinguish between the peptide substrate selectivity of different MMPs, a feature useful in designing TAPs selective to specific MMPs. As there is, in particular, a lack of data about the cleavage site specificity of MMP10, further structure-activity relationship studies in this regard are required.

The choice of cytotoxin to be developed as a prodrug is equally important. Colchicine is a plant alkaloid extract that is classified as a mitotic spindle poison or tubulin inhibitor. Colchicine and its derivatives are shown to inhibit

microtubule polymerisation by binding to tubulin, leading to the blocking of the mitosis of cells (Stanton et al., 2011). Due to the potent antimitotic capability of colchicine, it can be rationalised as an effective anticancer therapy. It has also been shown that when colchicine enters the blood supply of solid tumours, it destroys the endothelial cells that constitute the blood vessels, disrupting the tumour blood supply. This results in a reduction of tumour mass due to a starvation of oxygen and nutrients supply (Gaya and Rustin, 2005). Targeting the tumour vasculature by systemically activating tubulin binding inhibitors based on colchicine has been used as a strategy for the development of vascular disrupting agents (VDAs). One problem with this approach is their narrow therapeutic index and recognised cardiac toxicity (Chaplin et al., 1996). On this basis, a TAP approach to improving the therapeutic index of colchicine utilising MMPs is most attractive.

1.9 Aims and Objectives

Despite the development of a number of molecular targeted therapeutics to treat NSCLC, their efficacy is modest, such that the mean five-year survival rate of NSCLC has not greatly improved in the last decade. The use of chemotherapeutics has reached the limit, in part due to toxicity and drug resistance. This highlights the need for the identification of new molecular targets that can be either targeted for novel therapeutics or exploited to improve the tumour delivery of current chemotherapeutics, thereby minimising systemic toxicity. Matrix metalloproteinase 10 is a candidate for TAP developed for NSCLC based on its expression and contribution to NSCLC development. Specifically, the high expression and associated

catalytic activity of MMP10, which is observed in NSCLC compared to normal tissue, indicates its use in the design of NSCLC TAPs.

The overall aim of this project is to further explore the expression profile of MMP10 in the tumour microenvironment of NSCLC and evaluate it as a target for therapeutic intervention.

The specific objectives include:

- Characterisation of preclinical models for the evaluation of MMP10 functionality in NSCLC by screening the MMP10 mRNA and protein levels in a panel of NSCLC cell lines. In addition, mass spectrometric-based proteomics techniques for the detection of secreted MMP10 will be evaluated.
- Development of functionally active high MMP10 expressing in vitro models for the evaluation of the role of MMP10 in NSCLC. Overexpression models will be developed either by direct transfection with MMP10 or by the functional alteration of MMP10 levels due to the knockdown of HDAC7. The functionality of MMP10 will be evaluated using an assay to assess effects on vascularity, the tube formation assay.
- Identification of MMP10-specific cleavable sequences to incorporate into MMP10 targeted TAP. To achieve this, several known commercially available MMP substrates and MMP-targeted compounds developed in-house will be assessed for cleavability by MMP10 using LC-MS techniques.

Chapter 2: General Materials and Methods

2.1 Materials

All chemicals, solutions and media were stored at 4°C unless otherwise specified.

2.1.1 Cell culture

All plasticware were bought from Corning (Amsterdam, The Netherlands). Cell culture medium, supplements and chemicals, including Roswell Park Memorial Institute (RPMI) 1640 culture medium, Hanks' Balanced Salt Solution (HBSS) (stored at room temperature (RT)), Foetal Calf Serum (FCS), L-glutamine, Sodium pyruvate, trypsin/ethylenediaminetetraacetic acid (EDTA) (stored at -20°C) and dimethyl sulfoxide (DMSO) (stored at RT), were all obtained from Sigma-Aldrich (Poole, Dorset, UK). For *in vivo* work, female BALB/c immunodeficient nude mice were purchased from Harlan Laboratories, Inc. (Blackthorne, UK).

2.1.1.1 Cell lines

The human NSCLC cell lines (A549, H460, and H661), human colorectal adenocarcinoma cell line Colo205 and fibrosarcoma cell line HT-1080 were all obtained from the American Type Culture Collection (ATCC) (Middlesex, UK). The three lung cancer cell lines were chosen as they represent two of the most common subtypes of NSCLC, the main focus of this research. The HT-1080 cell line was used because of its known high expression of multiple MMPs, while the Colo205 was due to its overall weak expression of MMPs as

previously reported (Atkinson et al., 2010). Table 2.1 outlines the origin of the human cell lines used in this project.

Table 2.1. Cell Line General Information		
Cell Line	Origin/Source	Reference
A549	Lung carcinomatous tissue from a 58-year-old Caucasian male	(Giard et al., 1973)
H460	Pleural fluid from a male patient with large cell cancer of the lung	(Banks-Schlegel et al., 1985)
H661	Lymph node metastasis from large cell cancer of the lung in a 43-year-old Caucasian male	(Banks-Schlegel et al., 1985)
Colo205	Ascitic fluid from a 70-year-old Caucasian male with carcinoma of the colon	(Semple et al., 1978)
HT-1080	Fibrosarcoma arising adjacent to the acetabulum of a 35 year old Caucasian male	(Rasheed et al., 1974)

2.1.2 Gene Expression Analysis

Chemicals for mRNA analysis, including β -mercaptoethanol (β -ME), phosphate buffered saline (PBS), ethanol, tris base, glacial acetic acid, EDTA, gel loading buffer, agarose and ethidium bromide, were obtained from Sigma-Aldrich and stored at RT. 3-(4,5-dimethylthiazol-2-yl)-2, 5-diphenyltetrazolium bromide (MTT) was also purchased from Sigma-Aldrich. RNeasy Mini Kit, RNase-Free DNase Set and Taq DNA Polymerase PCR Kit were purchased from Qiagen (Crawley, UK) and stored at -20°C. The

RevertAid First Strand cDNA Synthesis Kit was purchased from Thermo (Loughborough, UK) and stored at -20°C. PCR primers and 1KB Plus DNA ladder were obtained from Life Technologies Ltd (Paisley, UK) and stored at -20°C.

2.1.3 Protein Expression Analysis

Tris-HCl (BioRad Laboratories), Sodium Chloride (NaCl), ethylene glycol tetraacetic acid (EGTA), dithiothreitol (DTT), Triton-X-100, protease inhibitor solution, Sodium Dodecyl Sulfate (SDS), Bovine serum albumin (BSA), plastibrand disposable cuvettes, tetramethylethylenediamine (TEMED), Glycine, Ponceau S solution, sodium deoxycholate, urea, thiourea, 3-[(3-Cholamidopropyl)dimethylammonio]-1-propanesulfonate (CHAPS), 4-aminophenylmercuric acetate (APMA) and phosphatase inhibitor cocktail 2 and 3 were purchased from Sigma-Aldrich. Complete Mini EDTA-free protease inhibitor cocktail (PIC) tablets were bought from Roche Diagnostics Limited (Sussex, UK). Bradford dye reagent and acrylamide/bisacrylamide mix were purchased from BioRad Laboratories (Hertfordshire, UK). Ammonium persulfate (AP), full range rainbow marker 10-250kDa, Hybond nitrocellulose membranes (stored at -20°C), blotting papers and hyper X-ray film (both stored at RT) were bought from Amersham Biosciences (Buckinghamshire, UK). High purity methanol was obtained from Fisher Scientific (Loughborough, UK) and stored at RT. Full length recombinant human MMP3 and MMP10 proteins were purchased from R and D system (Abingdon, UK). B-actin primary antibody A1978 was purchased from Sigma-Aldrich and the HDAC7 antibody C-18 was from Santa Cruz Biotechnology

(Heidelberg, Germany). In addition, MMP10 antibody Ab49473 and MMP3 antibody ab38907 were bought from Abcam (Cambridge, UK). All recombinant proteins and primary antibodies were aliquoted upon receipt and stored at -20°C until required. All secondary antibodies, including Polyclonal Goat anti-rabbit and Polyclonal rabbit anti-mouse, were purchased from Dako Cytomation (Cambridgeshire, UK). Western Lightning™ plus-ECL Enhanced Chemiluminescence substrate (ECL) was obtained from PerkinElmer (Cambridge, UK).

2.2 Methods

2.2.1 Cell Lines Maintenance

All epithelial cell lines were routinely maintained as monolayer cultures in RPMI-1640 medium supplemented with 1mM Sodium Pyruvate, 10% FCS and 2mM L-Glutamine. All cells were incubated at 37°C in a humidified atmosphere of 5% CO₂ and 95% air.

Cells were passaged when a confluency of no more than 80% was reached. Cells were washed with HBSS and detached using 0.25% Trypsin-EDTA solution at 37°C. Cells were collected through the addition of complete medium, with the resulting cell suspension centrifuged at 1500g for five minutes and the cell pellet resuspended in fresh complete medium. For studies requiring the calculation of the cell number, 10µl of cell suspension was added to each chamber of the haemocytometer. Under a microscope, cell numbers were counted in five 1mm x 1mm squares of each chamber of

the haemocytometer and the mean value calculated and expressed as number of cells/mL.

2.2.2 Growth Curve Analysis

Growth curve analysis was performed to determine the growth pattern of NSCLC and the endothelial cell lines used in this project. Cells at concentrations of 1×10^4 cells/cm² were seeded in twelve 25cm² flasks in 10mL of complete RPMI medium. On days one, three, five, seven, nine and 11, the number of cells grown in the two flasks was determined using the haemocytometer. The mean density was also calculated. For all the four cell lines, the data obtained was used to plot the growth curves of time versus cell number.

2.2.3 Animals and Experimental Tumour System

All the in vivo work in this research was carried out by experienced ICT staff holding the appropriate Home Office licences. Female Balb/c immunodeficient nude mice were housed according to the guidelines for the welfare of animals of the Institute of Cancer Therapeutics (ICT), which was approved by the Home Office and met all current regulations and standards of the United Kingdom. Mice were fed Teklad 2018 diet (Harlan) and water ad libitum and were accommodated in an air-conditioned room with regular alternating cycles of light and darkness. Mice with ages between six and eight weeks were used in this project. All animal procedures were carried out under a project licence issued by the UK Home Office and following the UK National Cancer Institute guidelines (Workman et al., 2010).

Cultured cells *in vitro* were harvested by trypsinisation and one million cells were injected into each flank of nude mice. Tumours were allowed to grow until they reached ~17 mm in size. When they were removed, they were snap-frozen in liquid nitrogen and stored at -70°C.

2.2.4 Reverse Transcription-Polymerase Chain Reaction (RT-PCR)

Reverse transcription-polymerase chain reaction was used in this project as described below:

2.2.4.1 RNA extraction

Total RNA was extracted from each sample using the RNeasy Mini Kit according to the manufacturer's protocol. All centrifugation steps were carried out at 8,000g at room temperature unless otherwise stated. Initially, cells were grown, harvested and counted as described in section 2.2.1. Cell pellets were directly lysed in 600µL lysis buffer RLT with 1% β-ME. The tube was vortexed and the lysates were transferred into a QIAshredder spin column for complete homogenisation. In the case of tissue samples, 30ug of frozen tissue was immediately ground to a fine powder in liquid nitrogen using a mortar and pestle prior to the addition of the lysis buffer. Following centrifugation of the QIAshredder spin column for two minutes at 10,000g, 600µL of 70% ethanol was added to the homogenised lysate. This was then transferred to a RNeasy spin column. The tube was then centrifuged for 15 seconds and the flow-through discarded. The RNA attached to the RNeasy spin column membrane was subsequently washed with 350µL of Buffer

RW1. The column was then centrifuged and the flow-through carefully discarded. To eliminate genomic DNA contamination, RNA was treated for 15 minutes with DNase I enzyme mix diluted at 1:8 ratio in buffer RDD. RNeasy spin column was washed with 350µL of Buffer RW1 and then centrifuged. The flow-through was carefully discarded. This washing was repeated twice using 500µL buffer RPE. RNA was eluted by the addition of 30µL of RNase-free water directly to the spin column membrane and centrifuged for one minute. The RNA samples were then either directly quantified and subjected to RT-PCR analysis or simply stored at -70°C until required for further use.

2.2.4.2 RNA quantification analysis

For the determination of the RNA concentration, 2µL of the RNA was analysed using a Thermo Scientific NanoDrop™ 1000 Spectrophotometer. Concentration was calculated based on one absorbance unit at 260nm, equivalent to 40µg of RNA per mL. The ratio between the absorbance at 260nm and 280nm was used to evaluate RNA quality, such that RNA samples that have values located in the range of 1.9–2.1 were of high enough quality for complementary DNA (cDNA) synthesis.

2.2.4.3 cDNA synthesis using reverse transcriptase enzyme

Reverse transcription of mRNA to cDNA was carried out using the RevertAid First Strand cDNA Synthesis Kit according to manufacturer's instructions. All reagents were thawed and kept on ice before and during the procedure. For each RNA sample to be reverse transcribed, a control reaction without reverse transcriptase was also performed to examine genomic DNA

contamination. A total of 1µg of RNA sample template was added to 1µL of oligo (dT)18 primer and then adjusted to a final volume of 12µL with nuclease-free water. Samples were denatured at 65°C for five minutes and then quenched promptly on ice to ensure primer annealing. Around 4µL of 5X Reaction Buffer, 1µL of RiboLock RNase Inhibitor (20u/µL) and 1µL of 10mM dNTP mix were then added to each sample. For positive samples only, 1µL of RevertAid M-MuLV Reverse Transcriptase enzyme (200u/µl) was then added to the reaction mixture. In parallel, 1uL of nuclease-free water was added to the negative controls. All samples had a final volume of 20µL. cDNA was synthesised via the incubation of samples at 42°C for one hour to allow the RNA to be reverse transcribed, followed by the inactivation of the enzyme at 70°C for five minutes. cDNA was diluted at a 1:5 ratio with nuclease-free water before being subjected to PCR application or stored at -70°C until required.

2.2.4.4 PCR primers design and selection

The PCR primers for HDAC7 and MMP10 genes were designed in-house according to the human sequence obtained from Genbank. Primer sequences for other MMPs, including MMP1, 2, 7, 8, 11, 12, 13, 14, 15, 16, 17, 19, 20, 21, 23, 24, 25, 26 and 28, were chosen based on the findings of (Köhrmann et al., 2009). The primers used for MMP3 and MMP9 were based on those designed by Konttinen et al. (Konttinen et al., 1999; Yao et al., 2001), respectively. One set of primers for Glyceraldehyde 3-phosphate dehydrogenase (GAPDH), a house keeping gene, were also used based on those designed by Daja et al.(Daja et al., 2003). The primer Basic Local

Alignment Search Tool (primer -BLAST) was used to ensure that every primer's nucleotide sequence was specific and related to the human DNA sequence. All primers were custom-made. When received, they were reconstituted and adjusted with nuclease-free water to give a final concentration of 100 μ M prior to being aliquoted and stored at -20°C. Primer sequences are summarized in Table 2.2.

2.2.4.5 PCR protocol

PCR reactions were carried out using the Taq DNA Polymerase PCR Kit. All kit components were thawed and kept on ice during the procedure. Approximately 20 μ L of reaction mixture containing 5ng template DNA, 2.5 units Taq polymerase, 10% standard reaction buffer, 20% of 5x Q-Solution, 200 μ M dNTPs and 0.5 μ M of both forward and reverse primers was prepared. In the PCR tube, the reaction mixture was thoroughly mixed and centrifuged to ensure that all the liquid were collected at the bottom of the tube. PCR for the gene of interest was performed using an MJ PTC-200 thermal cycler and consisted of the optimal condition for each primer pair as described in Table 2.2. For each cDNA sample, a negative control (sample produced in absence of reverse transcriptase) was used to detect any genomic DNA contamination or non-specific amplification in the reaction. In addition, cDNA samples amplified in the presence of GAPDH primers were used as positive controls to verify the success of cDNA synthesis and PCR functionality.

Table 2.2. Human Primers' Sequence and Their Optimal Conditions Used for RT-PCR Analysis. Length of PCR products are listed in base pairs (bp). F refers to forward while R is for reverse primer.

Gene	Primer Sequences	PCR Conditions	cDNA Size (bp)
MMP1	F: 5'-AAGGCCAGTATGCACAGCTT-3' R:5'-TGCTTGACCCTCAGAGACCT-3'	5 min at 95°C – (30 sec at 94°C, 30 sec at 58°C, 60 sec at 72°C) 32 cycles–10 min at 72°C	480
MMP2	F: 5'-TTTCCATTCCGCTTCCAGGGCAC-3' R:5'-TCGCACACCACATCTTCCGTCAC-3'	5 min at 95°C – (30 sec at 94°C, 30 sec at 60°C, 40 sec at 72°C) 36 cycles–10 min at 72°C	253
MMP3	F: 5'-CTCACAGACCTGACTCGGTT -3' R:5'-CACGCCTGAAGGAAGAGATG -3'	5 min at 95°C – (1 min at 94°C, 1 min at 58°C, 1 min at 72°C) 40 cycles–10 min at 72°C	294
MMP7	F: 5'-TCCAACCTATGGAAATGGAGA-3' R: 5'-GGAGTGGAGGAACAGTGCTT-3'	5 min at 95°C – (30 sec at 94°C, 30 sec at 58°C, 30 sec at 72°C) 34 cycles–10 min at 72°C	196
MMP8	F: 5'-TCTGCAAGGTTATCCCAAGG-3' R:5'- ACCTGGCTCCATGAATTGTC-3'	5 min at 95°C – (30 sec at 94°C, 30 sec at 52°C, 30 sec at 72°C) 45 cycles–10 min at 72°C	154
MMP9	F: 5'-CTCCTCCCTTTCTCCAGAACAGAA-3' R:5'-GGAGCCGCTCTCCAAGAAGCTT-3'	4 min at 94°C – (1 min at 94°C, 30 sec at 58°C, 45 sec at 72°C) 35 cycles–10 min at 72°C	522
MMP10	F: 5'-GTCCTTCGATGCCATCAGCA-3' R:5'- CTTGCTCCATGGACTGGCTA-3'	5 min at 95°C – (30 sec at 94°C, 30 sec at 60°C, 40 sec at 72°C) 37 cycles–10 min at 72°C	380
MMP11	F: 5'-GGGGATGTCCACTTCGACTA-3' R:5'-CAGTGGGTAGCGAAAGGTGT-3'	5 min at 95°C – (30 sec at 94°C, 30 sec at 56°C, 30 sec at 72°C) 32 cycles–10 min at 72°C	165
MMP12	F: 5'-ACAGATGATGGACCCTGGTT-3' R:5'-AGAGTCAAGCAAGAATGGACAA-3'	5 min at 95°C – (30 sec at 94°C, 30 sec at 52°C, 30 sec at 72°C) 36 cycles–10 min at 72°C	392
MMP13	F: 5'-AACATCCAAAAACGCCAGAC-3' R:5'-GGAAGTTCTGGCCAAAATGA-3'	5 min at 95°C – (30 sec at 94°C, 30 sec at 50°C, 30 sec at 72°C) 36 cycles–10 min at 72°C	166
MMP14	F: 5'-GAGCTCAGGGCAGTGGATAG-3' R:5'-AGCAGATGACCCCATTTGAC-3'	5 min at 95°C – (30 sec at 94°C, 30 sec at 52°C, 1 min at 72°C) 33 cycles–10 min at 72°C	798
MMP15	F: 5'-AGGAGACACAGCGTGGAGAC-3' R:5'-TTGCAGTAAAGCAGGACACG-3'	5 min at 95°C – (30 sec at 94°C, 30 sec at 56°C, 1 min at 72°C) 32 cycles–10 min at 72°C	514
MMP16	F: 5'-GACATGCTCTGGGATTGGAG -3' R:5'-TCATTTTTCCTTGGGTGAGC -3'	5 min at 95°C – (30 sec at 94°C, 30 sec at 54°C, 30 sec at 72°C) 32 cycles–10 min at 72°C	217
MMP17	F: 5'-GGAGCTGTCTAAGGCCATCA-3' R:5'-CGACAGGTTCTCTTGTTCC-3'	5 min at 95°C – (30 sec at 94°C, 30 sec at 58°C, 30 sec at 72°C) 28 cycles–10 min at 72°C	190
MMP19	F: 5'-CAGCCTCGTTGTGGCCTAGA-3' R: 5'-ACCAGCCTGCACCTCTTGGA-3'	5 min at 95°C – (30 sec at 94°C, 30 sec at 60°C, 30 sec at 72°C) 32 cycles–10 min at 72°C	207
MMP20	F: 5'-CGACAATGCTGAGAAGTGGA-3' R:5'-ATCTTTGGGGAGGTGGAATC-3'	5 min at 95°C – (30 sec at 94°C, 30 sec at 54°C, 30 sec at 72°C) 40 cycles–10 min at 72°C	169
MMP21	F: 5'-GACGACGACGAGCACTTCAC-3' R:5'-TTTCCTGTCTGACCAGTCCA-3'	5 min at 95°C – (30 sec at 94°C, 30 sec at 52°C, 30 sec at 72°C) 36 cycles–10 min at 72°C	180

MMP23	F: 5'-TGGGACCACTTCAACCTCAC-3' R: 5'-CGTGTTGTGAGTGCATCAGG-3'	5 min at 95°C – (30 sec at 94°C, 30 sec at 58°C, 40 sec at 72°C) 32 cycles–10 min at 72°C	412
MMP24	F: 5'-GAACCTGTGGGCAAGACCTA-3' R: 5'-TGACAACCAGAACTGAGCG-3'	5 min at 95°C – (30 sec at 94°C, 30 sec at 51°C, 30 sec at 72°C) 45 cycles–10 min at 72°C	214
MMP25	F: 5'-CCATTATGAGGCCCTTCTACC-3' R: 5'-TAGGTCTTCCCGTTCTGTGG-3'	5 min at 95°C – (30 sec at 94°C, 30 sec at 60°C, 40 sec at 72°C) 38 cycles–10 min at 72°C	541
MMP26	F: 5'-GATATGAAGCCATCCGCAGT-3' R: 5'-GCTGGAAGGTTCTAGGGTCG-3'	5 min at 95°C – (30 sec at 94°C, 30 sec at 49°C, 30 sec at 72°C) 43 cycles–10 min at 72°C	378
MMP28	F: 5'-CACCTCCACTCGATTACGCG-3' R: 5'-AAAGCGTTTCTTACGCCTCA-3'	5 min at 95°C – (30 sec at 94°C, 30 sec at 55°C, 30 sec at 72°C) 32 cycles–10 min at 72°C	208
HDAC7	F: 5'- AGGCCAGCAAGATCCTCATTG -3' R: 5'-ACAGATGGCTGTGAGGTCATG -3'	5 min at 94°C – (30 sec at 94°C, 30 sec at 58°C, 30 sec at 72°C) 30 cycles–10 min at 72°C	458
GAPDH	F: 5'-CCACCCATGGCAAATTCCATGGCA-3' R: 5'-TCTAGACGGCAGGTCAGGTCCACC-3'	3 min at 95°C – (30 sec at 95°C, 30 sec at 60°C, 90 sec at 72°C) 25 cycles–10 min at 72°C	561

2.2.5.6 Agarose gel electrophoresis to analyse PCR products

RT-PCR products were separated using 1% Agarose gel dissolved in Tris-acetate buffer (TAE) (Appendix 1) and containing 0.01% Ethidium bromide. Gel loading solution was mixed with a sample at 1:4 ratio prior to loading. 1kb Plus DNA ladder was also loaded in parallel, allowing for the later verification of PCR product size. Electrophoresis was carried out at 100 volts for 90 minutes. The amplified cDNA was visualised under UV light and scanned using the BioRad Molecular Imager FX[®]. Expression analysis was performed by densitometry using Quantity One software (Bio-Rad Laboratories Ltd, UK). All genes of interest were normalised to the corresponding GAPDH band density. Consequently, the relative expression of each target gene was determined.

2.2.5 PCR Optimisation

To establish a suitable cDNA amount to use for PCR, a range of cDNA amounts (1ng, 5ng, 10ng and 20ng) from different samples were analysed for GAPDH amplification. In addition, since the concentration of primers influences the specificity and efficiency of the PCR, final concentration of the primer per 20 μ L PCR reactions were also optimised. A range of primer concentrations (0.5 μ M, 1 μ M, 2.5 μ M and 5 μ M) were tested under the same PCR protocol as described above.

2.2.6 Western Blotting

2.2.6.1 Cell sample preparation

Cells were grown, harvested and counted as described in section 2.2.1. The resulting cell pellet was washed twice with PBS then lysed or immediately stored at -20°C for further use. For cell lysis, cell pellets were resuspended in four volumes of lysate buffer containing 50mM Tris-HCl pH7.5, 165mM NaCl, 2.5mM EDTA, 2.5mM EGTA, 1mM DTT, 1% Triton-X-100, 0.5% protease inhibitor solution and 0.5% phosphatase inhibitor cocktails 2 and 3. The mixture was incubated for 30 minutes on ice to ensure complete lysis. Samples were then sonicated three times for 10 seconds and centrifuged for 10 minutes at 4°C and the supernatant was collected. Cell lysates were either immediately transferred to -70°C in small aliquots for storage or subjected to Bradford protein assay.

2.2.6.2 Collection of culture supernatant

A549, H460, H661, HT-1080 and Colo205 cells were grown in T75 flasks to 70-80% confluence before incubation overnight in serum-free RPMI media containing 2mM L-glutamine and 1mM sodium pyruvate. The next day cells culture medium was collected and centrifuged to remove dead cells and the supernatant was collected. If diluted sample was an issue, condition media were then concentrated at 4000g for 15minutes at 4°C using Amicon Ultra-15 centrifuged filter device with nominal molecular weight limit (NMWL) of 30,000. Samples that did not pass through the filter were collected, aliquoted and stored at -70 °C for later use.

2.2.6.3 Tissue sample preparation

Proteins were extracted from tissue xenograft samples using the binary lysis buffer approach according to Lambert et al. (Ngoka, 2008). This involves combining the solubilisation capability of Radio Immunoprecipitation Assay (RIPA) and urea lysis buffers, which was reported to improve protein yields. Tissue samples were incubated with RIPA buffer (containing 0.1% w/v SDS, and 0.25% w/v sodium deoxycholate in PBS, pH 7.4) for 30 minutes with constant vortexing. This was followed by sonication using a Status US70 sonicating probe for 20 seconds on ice and centrifugation at 13400 rpm for 20 minutes. Then, protein supernatants was collected. The remaining tissue pellets were subjected to further lysis using urea buffer (containing 7 M urea, 2M thiourea, 4% w/v CHAPS, and 50mM DTT in PBS pH 7.4) under the same conditions described above. The resulting supernatant was combined

with the initial protein supernatant extracted by the RIPA buffer. Collected total protein was either transferred to -70°C in small aliquots for storage or subjected to the Bradford protein assay.

2.2.6.4 Protein concentration assay (Bradford Assay)

Total protein concentration was determined using the Bradford protein assay. Serial dilutions of BSA, including 1.0, 0.5, 0.25, 0.125 and 0.0625mg/ml, were prepared to generate a standard curve of absorbance. A blank control without BSA was also included for instrument calibration. The 100ul blank and standards were mixed with 3ml Bradford reagent then incubated for 15 minutes at room temperature. The absorbance of BSA standards were read at a wavelength of 595nm using a Cary 50 Bio ultra-violet (UV)-visible spectrometer (Varian Inc.CA, USA). In parallel, samples of unknown concentration were treated in the same manner and results were collected. Total protein concentration of samples were determined using the BSA standard curve created. In case samples fall outside the linear regression, further appropriate sample dilution was carried out and the assay was repeated. Microsoft Office Excel®2010 was used for data analysis.

2.2.6.5 Protein gel electrophoresis

Proteins were separated using 10% polyacrylamide SDS gels (appendix 2.). Freshly made gels were immersed in electrophoresis running buffer containing 25mM Tris Base, 192mM Glycine and 0.1% SDS. Samples equivalent to 50µg of protein were diluted in 2X Laemmli buffer before denaturing at 95°C for seven minutes. The denatured samples were then

loaded into wells at a volume of 20 μ l. One lane was also loaded with prestained full range Amersham rainbow markers (12 to 225 KDa) to allow for later mass identification. The electrophoresis was run at 50 volts all the way through the stacking gel, then at 125V for another hour to separate the proteins.

2.2.6.6 Immunoblotting

Protein was transferred from the acrylamide gel onto the Hybond-P nitrocellulose membrane using a BioRad transfer kit. The gel and membrane were immersed in a transfer buffer containing 0.25M Tris-Base, 1.92M Glycine and 20% methanol. Proteins were transferred on ice at 300mA for 60 minutes. Once completed, membranes were stained with Ponceau S solution to confirm successful transfer.

2.2.6.7 Blocking and antibody incubation

Non-specific protein binding on the membrane was blocked through the incubation of the membrane for one hour at room temperature with 5% dried skimmed milk in Tris buffer solution (pH 7.4) containing 0.1% Tween20 (TBST).

Before use, all primary antibodies were initially tested and their optimal concentrations were determined (Table 2.3) using a human cell lysate prepared as described in section 2.2.6.1. To proceed with Western blotting, primary antibodies were made up to their relevant concentrations in 5% skimmed milk in TBST and incubated with membranes overnight at 4°C with

constant agitation. Following a brief wash with TBST to remove the excess primary antibody, the blot was incubated for 60 minutes with the appropriate horseradish peroxidase (HRP) conjugated in a secondary antibody at a 1:2000 dilution in 5% skimmed milk in TBST. This was followed by further washes with TBST to ensure the removal of the residual secondary antibodies.

2.2.6.8 Protein detection

Probed proteins were revealed using Western Lightning™ plus-ECL according to manufacturer's protocol. Western blots were exposed to ECL reagents for one minute at room temperature before being wrapped in Saran™ wrap. The blot was then exposed to the Amersham hyperfilm™ ECL in a dark room. Exposure times varied from 15 seconds to one hour, depending on the antibody. Films were developed in Multigrade Paper Developer Solution (Ilford) for up to two minutes, then rinsed in distilled water before being fixed in Rapid Film and Paper Fixer Solution (Ilford) for three minutes. The films were finally rinsed under running tap water then left to dry at RT.

Table 2.3. Primary and Associated Secondary Antibodies Used: Optimal Dilutions Used for Each Primary Antibody are Also Described. All antibodies used in this research have human cross-reactivity.

Primary Antibody	Type	Protein Targeted	Diluted as	Secondary Antibody	Bands' Molecular Weight Predicted
C-18 (Santa Cruz)	Goat polyclonal	HDAC7 isoform a	1:500	Polyclonal rabbit anti-Goat (Dako Cytomation)	105 KDa
Ab49473 (Abcam)	Mouse monoclonal	MMP10	1:1000	Polyclonal rabbit anti-mouse (Dako Cytomation)	54 KDa
A1978 (Sigma)	Mouse monoclonal	Actin isoform B	1:10000	Polyclonal rabbit anti-mouse (Dako Cytomation)	42 KDa
ab38907 (Abcam)	Mouse monoclonal	MMP3	1:1000	Polyclonal rabbit anti-mouse (Dako Cytomation)	54 KDa

Chapter 3: Characterisation of Models for the Evaluation of MMP10 Functionality in NSCLC

3.1 Introduction

Human tumour-derived cell lines represent an unlimited, self-replicating source of tumour cells that are free of contaminating stromal cells. Subsequently, they have been commonly used as *in vitro* tumour models to investigate the biology and genetics of cancers, including NSCLC (Prieels et al., 2006; Wistuba et al., 1999). Herein, three lung cancer cell lines (A549, H460 and H661) were chosen to represent two of the most common subtypes of NSCLC, adenocarcinomas (A549) and large cell carcinomas (H460 and H661).

Matrix metalloproteinases are essential for the development of NSCLC tumours. They play a role in the tumours' growth, angiogenesis, migration, and invasion. Since the vast majority of MMPs are implicated in cellular processes that are related to cancer progression, the evaluation of their expression and activity in NSCLC is important in terms of the diagnosis, prognosis and therapy of this disease.

The high expression of several MMPs in NSCLC has been linked either with aggressive disease or poor therapeutic response. These include MMP9 (Jumper et al., 2004), MMP7 (Liu et al., 2007; Roy et al., 2009), MMP1 (Schütz et al., 2002; Su et al., 2005) and membrane-type MMPs, (MMP14, 15 and 17) (Atkinson et al., 2007). By focusing only on one or a few MMPs,

the authors did not account for the complex interactions that took place between different MMPs. Data regarding the whole range of MMP expression in NSCLC would greatly assist in defining the exact roles of these MMPs in this disease.

The tumour microenvironment is a highly complex mixture of tumour—endothelial, stromal, and fibroblastic cells—signalling molecules and ECM (Hanahan and Weinberg, 2011; Visvader and Lindeman, 2008). The interaction between these components contributes to cancer progression as it allows for a diversity of regulatory cascades, resulting in the stimulation of various MMPs (Clark et al., 2008). It is important, therefore, to assess whether the expression patterns seen in the 2D cultures for MMP10 are maintained once cells are subjected to the microenvironment of the *in vivo* situation in the tumour xenografts.

It is known that the gene expression of most secreted enzymes does not necessarily reflect the expression pattern of the corresponding protein due in part to the effects of post-translational regulation (de Sousa Abreu et al., 2009; Lichtinghagen et al., 2002; Zhang et al., 2007). Results of genetic analysis need to be confirmed at the protein level using detection methods, such as Western blotting, ELISA and immunocytochemistry. All these methods, however, depend on antibody specificity, which has raised a considerable amount of debate recently (Mann, 2008). There are concerns that antibody companies do not sufficiently pre-evaluate their antibodies and, as a consequence, the market is full of invalidated antibodies and extra time needs to be taken for troubleshooting during method development (Mann,

2008; Marx, 2013). Another technology that can evaluate protein expression without using antibodies would be valuable. The use of proteomics mass spectrometry provides such a technique.

The term proteomics refers to the large-scale study of proteins, mainly their structure and function (Chandramouli and Qian, 2009). Proteomics is the link between genes, proteins and disease. It has been extensively used in areas, such as drug discovery, diagnostics and molecular medicine. With many advantages offered by this analysis system, including quantitative measurement and the ability to detect the modification status of proteins (Mann, 2008), it has been increasingly used for determining the unique patterns of protein expression or of biomarkers associated with specific diseases. In general, there are two approaches for proteomic analysis that are currently in use. These include bottom-up and top-down (Bogdanov and Smith, 2005). The bottom-up approach, which is used in this research, involves breaking up chemically or enzymatically the parent protein into peptide fragments that are sufficiently small for the available instrumentation (Breuker et al., 2008). When peptide fragments that are unique to each protein are formed, they are usually analysed by peptide mass fingerprinting or by tandem mass spectrometry for peptide sequence tags to allow for protein recognition (Liu et al., 2011). In top-down proteomics, on the other hand, intact proteins are directly analysed into the mass spectrometer where it is subjected to gas-phase fragmentation (Breuker et al., 2008; Wehr, 2006).

Since conventional protein detection techniques suffer from issues concerning antibody selectivity and cost and are time consuming, the

proteomics technique has recently emerged as highly valuable, especially for the rapid identification and quantitation of proteins in complex biological mixtures (Breuker et al., 2008). In particular, MMP10 is secreted from cells in low abundance and subsequently diluted even further in the cell culture medium or body fluid. It is difficult, therefore, to detect and analyse in the majority of biological samples and a highly accurate and sensitive methodology is important. The proteomics approach was employed in this research to attempt to detect secreted MMP10.

3.1.1 Aims and Objectives

The main aim of this chapter is to characterise MMP10 expression at the mRNA and protein levels in a panel of human NSCLC cell lines in order to assess their suitability as models for investigating MMP10 functionality.

The specific objectives include the following:

- Evaluation of the mRNA expression of a large panel of known MMPs in three human NSCLC cell lines (A549, H460 and H661) using semi-quantitative PCR.
- Investigation of MMP10 expression at both genetic and protein levels in a panel of NSCLC cell lines grown *in vitro* and as transplanted xenografts *in vivo* using semi-quantitative PCR and Western blotting.
- Evaluate the mass spectrometric-based proteomics methodology for the detection of secreted MMP10 in cell-conditioned media.

3.2 Materials

3.2.1 Cell Lines

A549, H460, H661, Colo205 and HT-1080 cell lines were used in this chapter. Their origin and culturing details are described in section 2.1.1.1 and 2.2.1, respectively.

3.2.2 Proteomics

All chemicals and solutions were stored at room temperature unless otherwise specified. High performance liquid chromatography (HPLC) grade acetonitrile, ammonium bicarbonate, water and trifluoroacetic acid (TFA) were bought from Sigma-Aldrich (Gillingham, UK). For proteolysis, 99.9% trypsin enzyme was purchased from Roche diagnostics GmbH (Mannheim, Germany). The LC Packings UltiMate 3000 capillary HPLC system used for the protein fractionation was obtained from Dionex (Surrey, U.K.). The matrix α -Cyano-4-hydroxycinnamic acid (CHCA), MTP AnchorChip 800/384 target plate and Peptide Standard II were all purchased from Bruker Daltonik (Bremen, Germany).

3.3 Methods

3.3.1 NSCLC Cells Growth Analysis

The growth curve analysis of the NSCLC cell lines was performed as previously described in section 2.2.2.

3.3.2 RT-PCR Analysis

Cells were screened for their expression of 22 MMPs (MMP1, 2, 3, 7, 8, 9, 10, 11, 12, 13, 14, 15, 16, 17, 19, 20, 21, 23, 24, 25, 26 and 28) using RT-PCR analysis as previously described in section 2.2.4. For normal mouse lung tissues, mouse MMP10 primers (F:5-AGGGACCAACTTATTCCTGG-3; R:5-AGAGTGGGCCAAAATGCTGA-3) and GAPDH primers (F:5-CGGTGCTGAGTATGTCGTGG-3; R:5-GTGTAGCCCAAGATGCCCTTC-3) were used.

3.3.3 Western Blotting

Samples were probed for MMP10 protein using the mouse monoclonal MMP10 antibody (ab49473, Abcam) and following the Western blotting procedure as described in section 2.2.6.

3.3.4 Manual MALDI TOF-MS of Peptides

3.3.4.1 Instrumentation

Mass spectrometric analysis was performed using an UltraflexTM II Matrix-assisted laser desorption/ionization time-of-flight mass spectrometer (MALDI-TOF/TOF) (Bruker Daltonics, Bremen, Germany). This automated MS and MS/MS detection system with a 200Hz pulsed 337nm nitrogen laser is a high throughput identification tool for proteins and peptides. In this work, the mass spectra of all peptides were acquired following the trypsin digestion of proteins as described below.

3.3.4.2 SDS-PAGE.

Cell culture supernatants from Colo205 and H661 cell lines were collected as previously described in section 2.2.6.2. This was followed by protein concentration determination as previously described in section 2.2.6.4. In addition, a recombinant human MMP10 was included to serve as positive control. These samples were then separated electrophoretically in a 10% polyacrylamide gel as described in section 2.2.6.5

3.3.4.3 Staining of proteins using Coomassie Brilliant Blue dye

Following gel electrophoresis, the proteins in the gel were visualised using Coomassie Brilliant Blue dye as follows: The gel was incubated with 50ml of the Coomassie Blue Reagent for one hour at room temperature with gentle agitation. The excess stain was then removed using a destaining solution containing 50% (v/v) methanol, 10% (v/v) acetic acid and 40% (v/v) water. The gel was then scanned and the image was kept for future reference.

3.3.4.4 In-gel trypsin digestion and peptides extraction

After visualization, bands in the stained gel corresponding to the molecular weight of MMP10 (54kDa) were excised, treated and subjected to digestion with trypsin according to the procedure of (Shevchenko et al., 1996). In 1.7ml microcentrifuge tubes, each gel piece was dehydrated in 100µl of acetonitrile for 15 minutes, with solvent removed. Then, the gel piece was rehydrated in 10µl of 25mM ammonium bicarbonate for 15 minutes. These dehydration and

hydration steps were repeated three times before the gel was allowed to dry for 30 minutes at RT. For tryptic protein digestion, the dried gel piece was then resuspended in 20µl of 10ng/µl trypsin in 25mM ammonium bicarbonate and left at 28°C in a water bath for 18 hours. Upon completion of digestion, samples were centrifuged at 8500 g for 20 seconds and supernatants were collected. For full peptide extraction, gel pieces were covered with 100% acetonitrile for 15 minutes and were centrifuged and the supernatants were collected. The gel pieces were further extracted with 5ul of 25mM ammonium bicarbonate and 50ul of 100% acetonitrile for 10 and 15 min, respectively. These extractions with 25mM ammonium bicarbonate and 100% acetonitrile were repeated twice and supernatants were combined with the corresponding initial supernatants. Finally, supernatants containing peptides were lyophilised and stored at -20°C until MS analysis.

3.3.4.5 Matrix solution preparation.

A saturated matrix stock solution was prepared by dissolving 10mg of CHCA in 1ml of 30% acetonitrile and 0.1% trifluoroacetic acid. This mixture was vortexed for two minutes then sonicated for 30 minutes prior to storage at 4°C for future use. Once needed, a fresh CHCA matrix working solution was prepared as the following: 120µl of matrix stock supernatant mixed with 1.056ml ethanol-acetone (2:1), 12ul of 100mM ammonium phosphate and 12µl of 10% TFA.

3.3.4.6 Manual analysis of gel digest.

Following in gel-trypsin digestion, 0.5ul of peptide sample solution was then placed on each spot of an MTP AnchorChip 800/384 target plate previously coated with 1.2µL of 10mg/mL CHCA matrix. Once air-dried, samples were covered with another layer of CHCA matrix (0.5µl). Finally, the peptide-matrix sandwich was allowed to dry before analysis in the mass spectrometer. For the calibration and testing of the MALDI-TOF MS, a Peptide Standard II, which is a mix of seven standard peptides with m/z ranging from 1046 to 3147 (appendix 3), was applied between each group of four samples onto the target plate. Mass spectra were obtained using MALDI-TOF/TOF in reflectron mode in the mass range of 700-4000Da with 50-80% laser power. FlexControl version 3.0 software was used for data acquisition.

3.3.4.7 nHPLC coupled to MALDI-MS/MS for protein identification (LC-MS/MS).

3.3.4.7.1 Reverse phase nHPLC fractionation of modified peptides

Nanoscale RP Liquid Chromatography was carried out for the fractionation of trypsin-digested peptides using an LC Packings UltiMate 3000 capillary HPLC system. Lyophilised peptides that were resuspended in 6.5µl of 10% acetonitrile containing 0.05% TFA were injected onto a (C18, 300µm × 5mm, 5µm diameter, 100 Å PepMap pre-column) then washed with the mobile phase A for 3.5 minutes at a flow rate of 0.3µl/minute. At the same flow rate,

samples were subsequently transferred onto another 100 Å PepMap column with C18, 75µm x 15cm, 3µm diameter.

3.3.4.7.2 nHPLC gradient conditions

After applying the above-mentioned conditions, peptides in the aqueous mobile phase should bind to the stationary phase in the reverse phase nHPLC column. For the elution of peptides, mobile phase B, which contained 80% acetonitrile and 0.05% TFA, was used in a linear gradient manner. Mobile phase B increased by 10% in six minutes followed by a linear increase from 10–40% over the next 75 minutes. Within 81 minutes, 100% of mobile phase B was used for five minutes. Once completed, 100% mobile phase A was used to re-equilibrate the column until the end of the run at 100 minutes. Eluents were measured simultaneously at 280nm and 215nm wavelengths using a deuterium lamp and data was monitored on a computer connected to the system using the Hystar 3.2 software (Bruker Daltonics, GmbH).

3.3.4.7.3 Fraction collection and mass spectrum acquisition

Around 75nL fractions were co-deposited with 1.2µL of saturated CHCA matrix using Proteineer FC fraction collector (Bruker Daltonics, GmbH) onto the MTP AnchorChip 800/384 target plate. This fully automated robot was adjusted to load a well every 15 seconds using the Hystar 3.2 software. For the calibration and testing of the MALDI-TOF MS, a Peptide Standard II covering the mass range between 1046 to 3147 Da (Appendix 3) was applied between each group of four samples onto the target plate. For automated

MALDI-MS/MS analysis, 800 pulse of laser were fired for parent ion and 1200 for the fragment ions in UltraflexTM II MALDI-TOF/TOF instrument.

3.4 Results

3.4.1 NSCLC Cell Line Growth Kinetics

To ensure that cells subjected to analyses in this research were in their log growth phase, growth curves were performed for the A549, H460 and H661 cell lines. Figure 3.1 summarises the growth patterns of the cell lines following the initial seeding density of 1×10^4 cells/cm². Data obtained was also used to calculate the doubling time for cells in their log growth phase. The H661 cell proliferation rate was the slowest amongst all the cell lines used with a doubling time of 25.2 hours. The H661 cells began their log growth phase at day one and entered the stationary phase at day seven. Although the A549 cells took the same time to enter the stationary phase compared to H661, their doubling time was 23 hours, indicating a faster growth rate. The growth rate of the H460 cells was the fastest, with a doubling time of 16.3 hours. Their plateau phase began at day five.

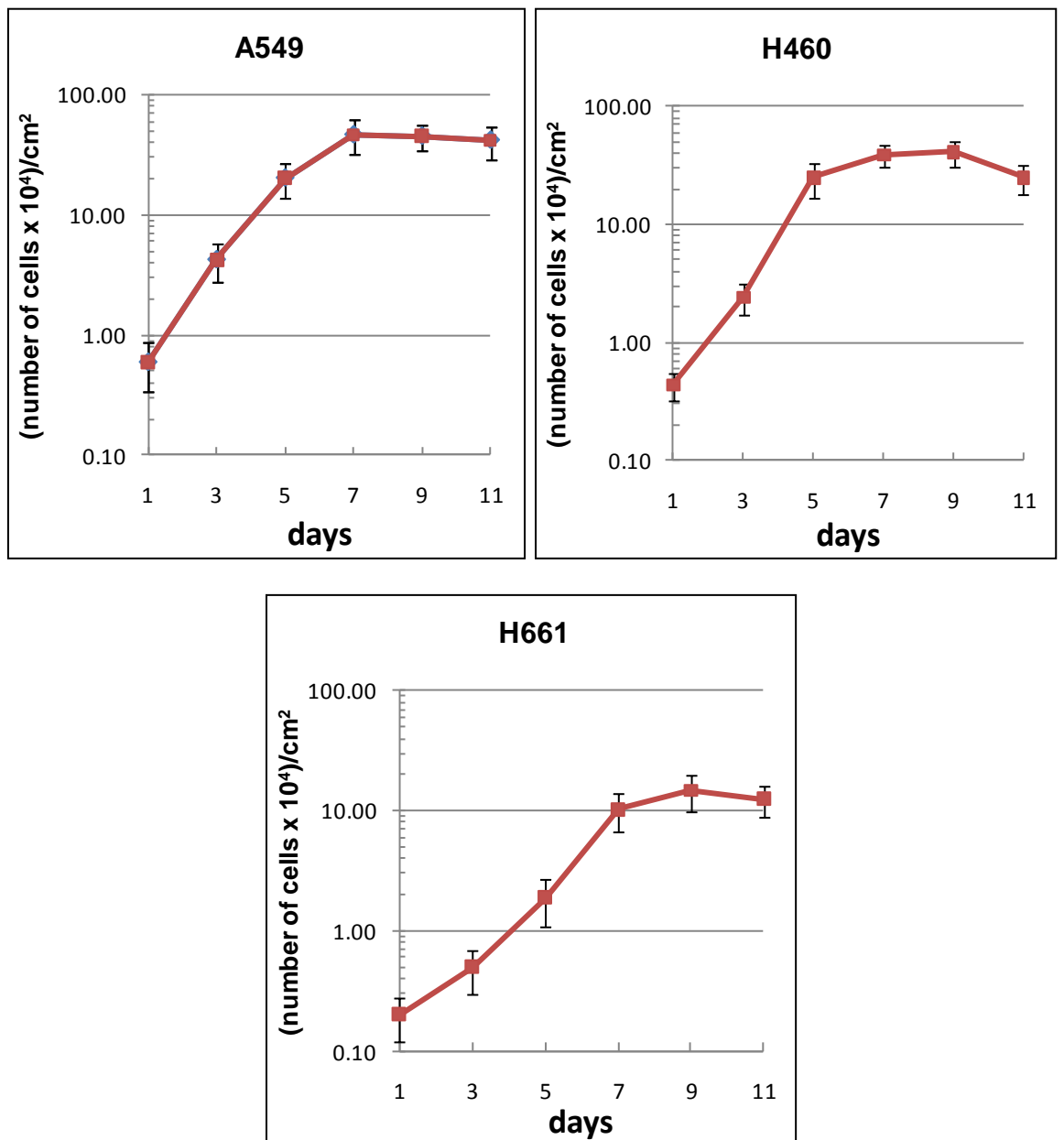


Figure 3.1. Growth curves for the NSCLC cell lines, A549, H460 and H661. Cells were seeded into 25 cm² flasks at seeding concentrations of 1x10⁴ cell/cm². The number of cells was determined every other day for 11 days using a haemocytometer. Presented mean data was obtained from three independent experiments, (+/- S.D).

3.4.2 Genetic Expression

3.4.2.1 Optimisation of the PCR conditions.

The amount of cDNA and final concentration of primers for inclusion in the reaction mixture were optimised to ensure maximum possible efficiency and specificity for the semi-quantitative PCR. For the determination of the optimal cDNA amount, 1ng-20ng of cDNA from the three NSCLC cell lines (A549, H460 and H661) was used and evaluated to amplify the housekeeping GAPDH gene. The optimal cDNA amount was considered as the lowest that could yield consistent GAPDH gene bands from the various cDNA templates within the limits of detection, thus improving reproducibility. Using 5ng cDNA produced the most reproducible bands and was, therefore, chosen as the optimal cDNA amount for further analysis (Figure 3.2). In the same context, a range of primer concentrations (0.5 μ M- 5 μ M) were evaluated to amplify the GAPDH gene. As the lowest primer concentration that produced the maximal PCR product without excess primer was 0.5 μ M per 20 μ l reaction, it was chosen as the optimum primer concentration (Figure 3.3).

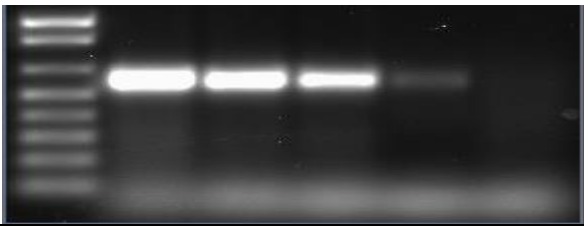
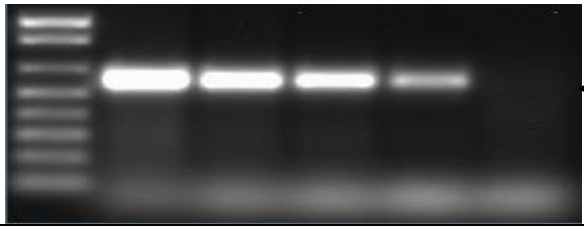
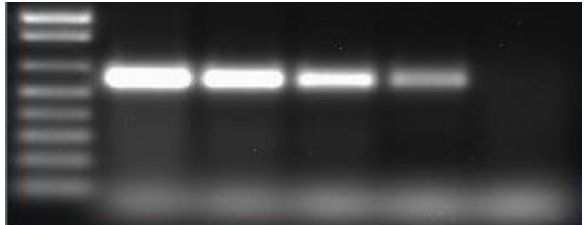
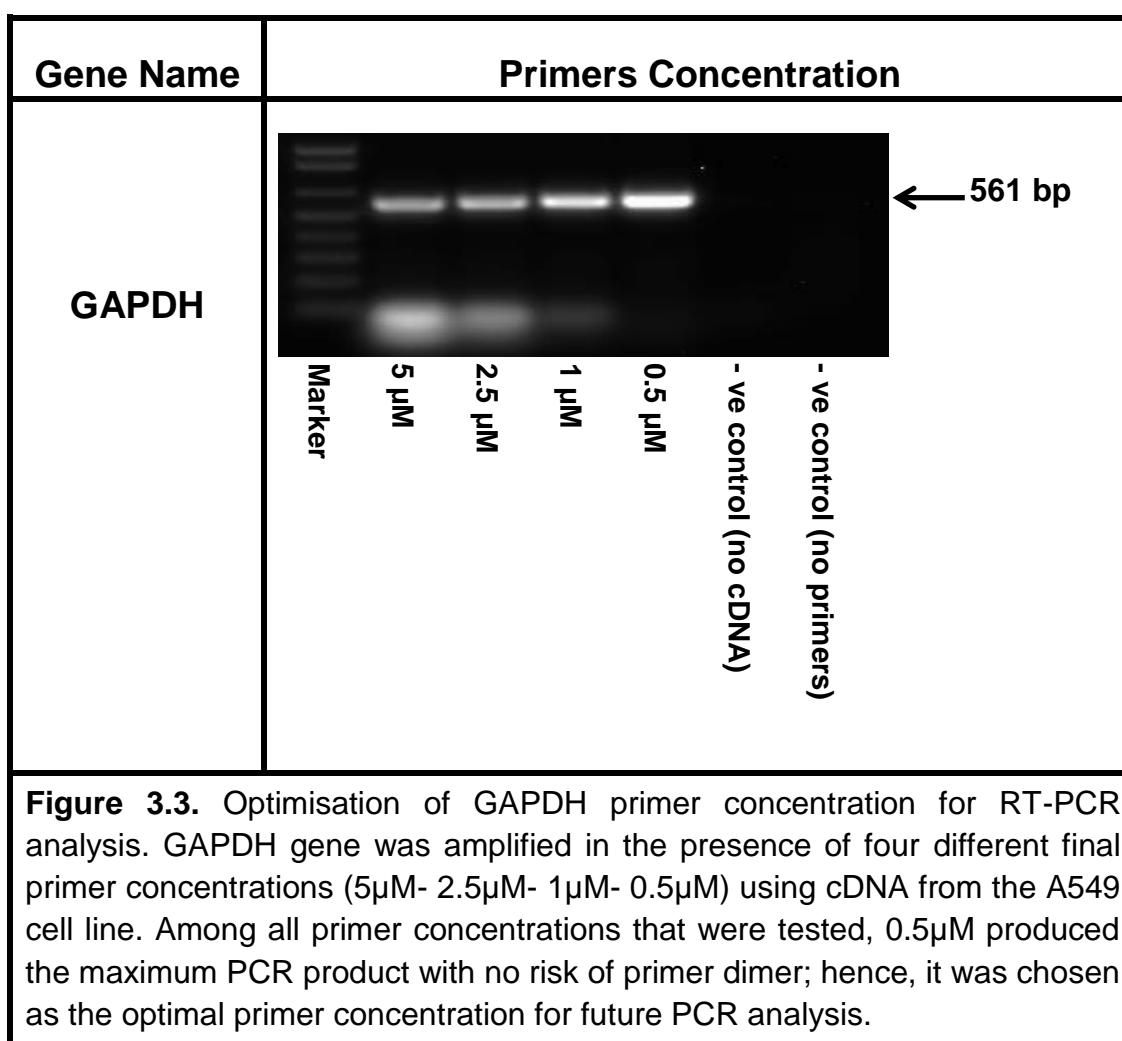
Cell Line	GAPDH Gene				
A549					
H460					
H661					

Figure 3.2. Identification of optimal cDNA concentration for RT-PCR analysis. A range of concentrations of cDNA was tested per 20 μ l reactions to amplify the GAPDH gene in A549, H460 and H661 cell lines. Negative control without cDNA was used to exclude genomic DNA contamination in all samples. Marker used is 1 kb plus DNA ladder from Invitrogen. The 5ng DNA was the minimum amount with the least variation among the different sample intensities, so this was chosen as the optimal DNA amount for PCR reactions.



3.4.3 MMPs mRNA Level in NSCLC Cell Lines

The expression profile of MMPs in human NSCLC reported in the literature is currently incomplete and needs to be further evaluated as previously discussed in the introduction (section 3.1). To fill the gap in our knowledge regarding MMP expression in NSCLC, the expression of 22 human MMPs was evaluated at the genetic level in a panel of NSCLC cell lines (A549, H460 and H661). In parallel, the HT-1080 fibrosarcoma cell line was used as

a universal positive control for MMPs because of its previously well characterised protease profile (Sugiura et al., 1998). The Colo205 colon adenocarcinoma cell line was also used as a negative control due to the overall weak expression of MMPs, which has been previously described (Atkinson et al., 2010). Semi-quantitative RT-PCR analysis was performed as described in section 2.2.4. Results are summarised in Figure 3.4 and appendix 4.

Generally, diverse MMP expression profiles were observed for the NSCLC cell lines. Very high expression pattern was seen in the H661 cells, especially with MMP1, 2, 3, 9, 10, 11, 15, and 25. Lower expression patterns were also seen for the H460 and A549 cell lines, with most of the MMP evaluated as compared to the H661 cell line.

In the three NSCLC cell lines evaluated, the overall high expression of MMP2, 3, 9, 10, 15, and 25 was observed. Matrix metalloproteinase 10 is of particular interest to this research because its expression has been correlated to poor clinical outcome in NSCLC (Frederick et al., 2008). Interestingly, the level of MMP10 mRNA in the H661 cell line was the highest compared to the remaining NSCLC cell lines. The MMP10 mRNA expression levels in the A549 and H460 cell lines were high and moderate, respectively.

Unlike other MMPs, MMP14 was very low in all the cell lines tested, except for the HT-1080. Selected MMPs were as expected; they were highly expressed in the HT-1080 cell line, including MMP 1, 2, 3, 8, 9, 10, 13, 14 and 16. In contrast, the expression levels of the majority of MMPs in Colo205

cells were low, especially MMP2, 9, 12, 14, 16 and 17, which were below the level of detection.

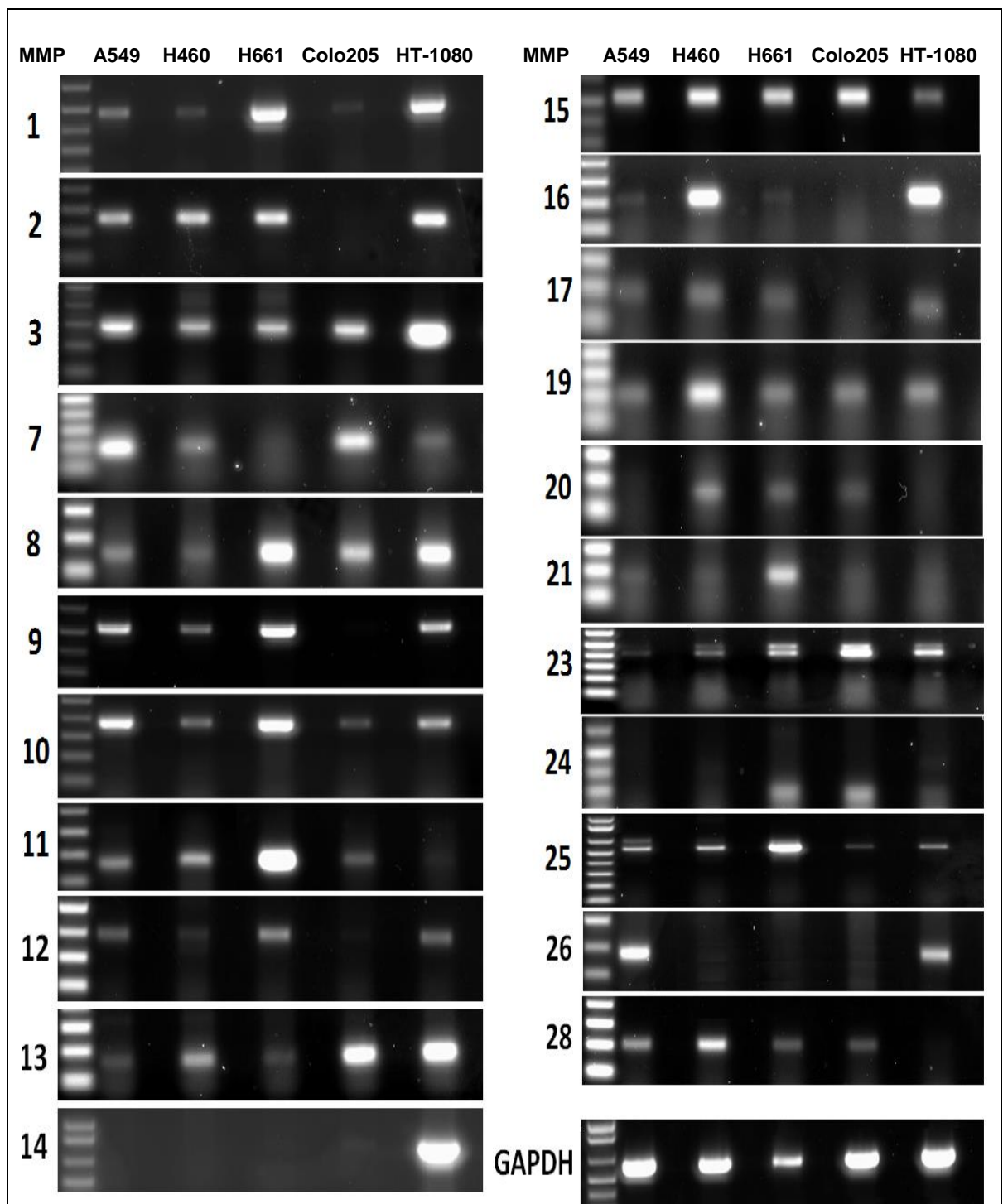
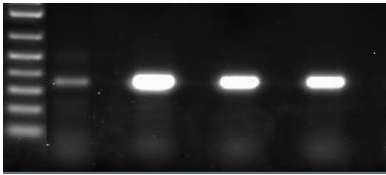



Figure 3.4. MMP10 mRNA expression is elevated in human NSCLC preclinical tumour models as measured by semi-quantitative RT-PCR. Other MMP were also tested to assess any possible interactions that took place between different MMPs. The HT-1080 and Colo205 cell lines were used as positive and negative controls, respectively. GAPDH was also used as a loading control. Results were semi-quantified by densitometry (appendix 4). Although it would be better to use a quantitative PCR for more reliable results, it could not been done within the constraints of this research.

3.4.4 MMP10 mRNA in Tumour Xenograft Tissue

Following the analysis of MMP10 mRNA in a monolayer culture, subcutaneous tumour xenografts of A549 and H460 cells were subjected to semi-quantitative RT-PCR analysis to assess the impact of the tumour microenvironment on MMP10 expression. A mouse normal lung tissue was included in this analysis to give a baseline of the physiological MMP10 expression, and HT-1080 xenografts which are known to highly express several MMPs, were used as a positive control.

The MMP10 mRNA expression from the tissue extracts was significantly higher in the NSCLC xenografts compared to the normal mouse lung tissue (Figure 3.5). The MMP10 expression patterns in the A549 and H460 tissue xenografts were similar to those seen in the 2D cell culture. The elevated MMP10 expression in the A549 cells was the highest in both the 2D culture and tissue xenografts as compared to that of the H460, which showed moderate MMP10 level at both conditions. Collectively, this confirms an elevation in the MMP10 mRNA expression in the NSCLC tumour environment and supports the use of these human cell lines as MMP10 models for future experiments.

Gene Name	RT-PCR
MMP10	
GAPDH	 Normal lung tissue A549 H460 HT-1080

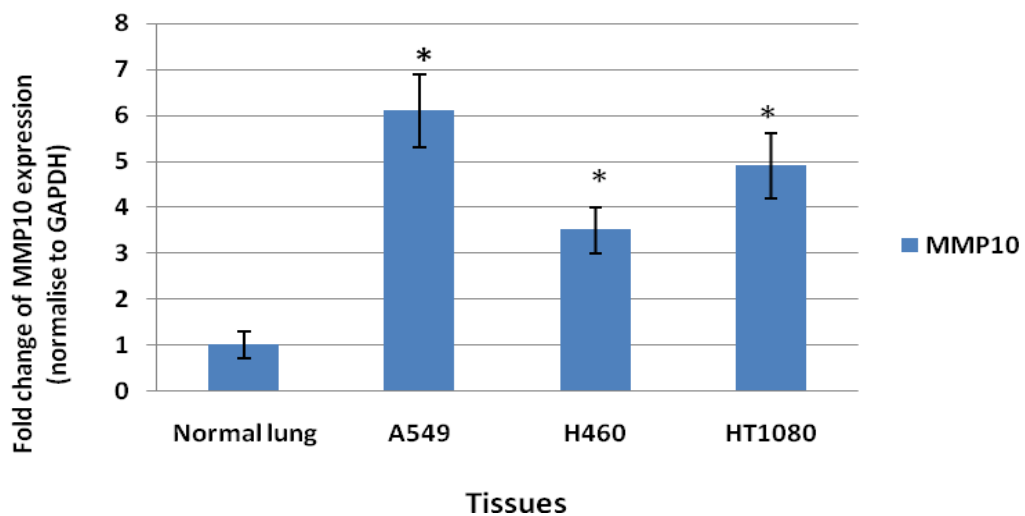


Figure 3.5. High MMP10 expression in NSCLC subcutaneous tissue xenografts compared to mouse normal lung tissue. Data presented as a fold change of MMP10 mRNA expression. HT-1080 tissue xenograft was used as a positive control. Statistically significance was evaluated using student t test. * $p < 0.05$. (n=3). For normal lung tissues, mouse PCR primers were used for MMP10 and GAPDH as described in section (3.3.2). For xenograft tissues, human specific PCR primers were used as described in table 2.2 (section 2.2.4.5)

3.4.5 *In Vitro* and *In Vivo* MMP10 Protein Expression

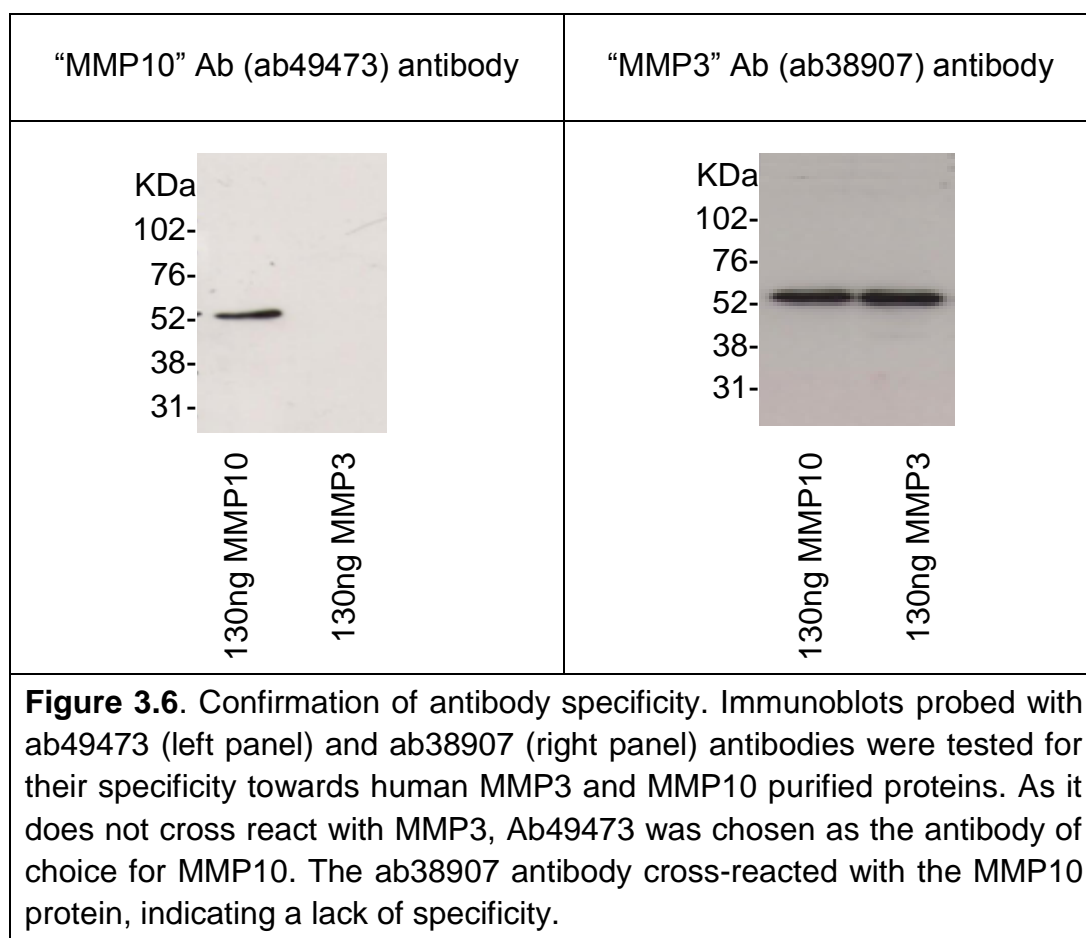
Following the analysis of the MMP10 gene expression at the transcriptional level, MMP10 protein levels were also assessed in the NSCLC cells and xenograft tissues using Western blotting as described in section 2.2.6. For immunoblotting experiments, the specificity of antibodies is critical for accurate results. Thus, all antibodies were initially validated before use in this research.

3.4.5.1 Confirmation of antibody specificity

It is well known that there is a high resemblance between MMP3 and MMP10 in terms of structure and substrate specificity (Murphy and Nagase, 2008). It was essential, therefore, to confirm the specificity of the antibody to MMP10 but not MMP3 protein and vice versa for MMP3. Initially, several commercially available MMP3 and MMP10 antibodies were tested against cell lysates. From this, only two demonstrated potential for specifically detecting their relevant protein. The specificity of both MMP10 (ab49473) and MMP3 (ab38907) antibodies was further evaluated against the recombinant human MMP3 and MMP10 proteins.

Figure 3.6 showed that MMP10 antibody (ab49473) produced a clear band corresponding to MMP10 protein, with no cross reactivity observed against MMP3. In contrast, MMP3 antibody (ab38907) cross-reacted with the MMP10 protein. Despite further testing the MMP3 antibodies, there was a failure to

discriminate between the two proteins tested. Based on these findings, the ab49473 antibody was chosen as the antibody of choice for MMP10 detection, whereas it was not possible within the constraints of the project to identify an MMP3-specific antibody.



3.4.5.2 MMP10 protein expression in NSCLC cell lines and xenograft tissue.

To assess whether the expression results at the protein level match those at the gene level, the expression of MMP10 protein was analysed using the

MMP10 validated antibody (ab49473). For both pro and active forms, MMP10 protein expression analysis was carried out by Western blotting with both cell and tissue extracts.

For NSCLC cells, pro MMP10 protein was highly expressed in both the A549 and H460 cells (Figure 3.7), which was consistent with the expression analysis at the mRNA level. Unexpectedly, a moderate pro MMP10 protein expression was observed in the H661 cells, which differed from what was seen at the gene level. For all cell lines evaluated, active MMP10 protein was below detection levels and could not be observed.

For xenograft tissue, MMP10 proteins were significantly higher in the NSCLC xenografts when compared to mouse normal lung tissue (Figure 3.8). This is consistent with the results seen at the gene level, supporting elevated MMP10 in NSCLC at the transcriptional and translational levels.

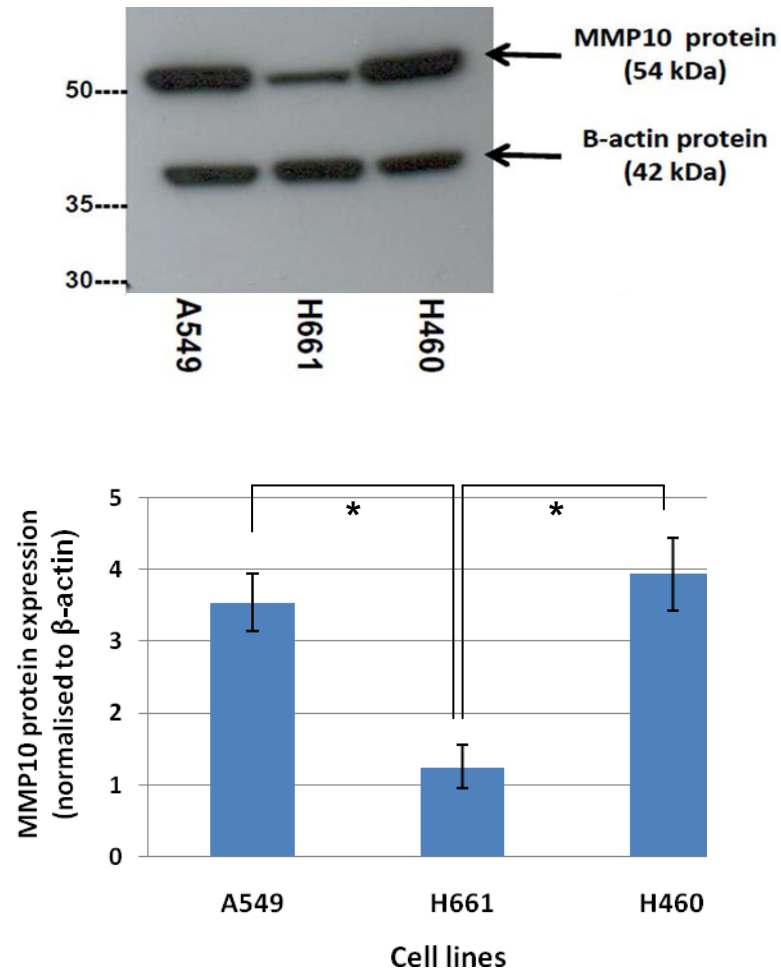


Figure 3.7. MMP10 protein levels in a panel of NSCLC cell lines using Western blotting. Levels of MMP10 protein in the A549 and H460 were high compared to those in the H661 cell line. (β -actin) was used as internal control. Semi-quantification of results was performed using the densitometry tool of Quantity One software. The statistical difference was assessed using Student's t-test. * $p < 0.05$. (n=3).

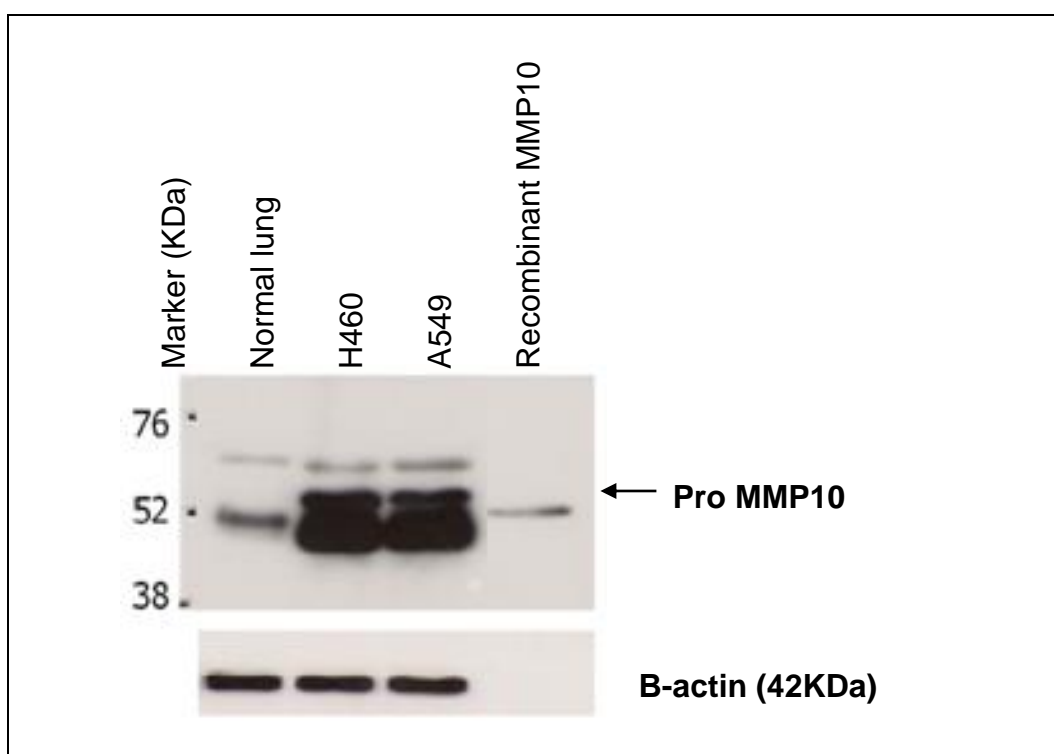


Figure 3.8. Significantly higher MMP10 protein expression observed in NSCLC subcutaneous xenografts compared to normal lung tissue. Although bands at 54 KDa correspond to proMMP10 can be clearly seen, the gel could not differentiate well between pro and active forms of MMP10 protein. Therefore, activation by APMA is required to confirm whether the bands seen at ≈ 44 KDa are the active form of MMP10 or just glycosylated pro MMP10. Recombinant MMP10 with predicted molecular mass for pro and active forms (52 and 43 KDa, respectively) was used as a positive control, but only the pro form evident.

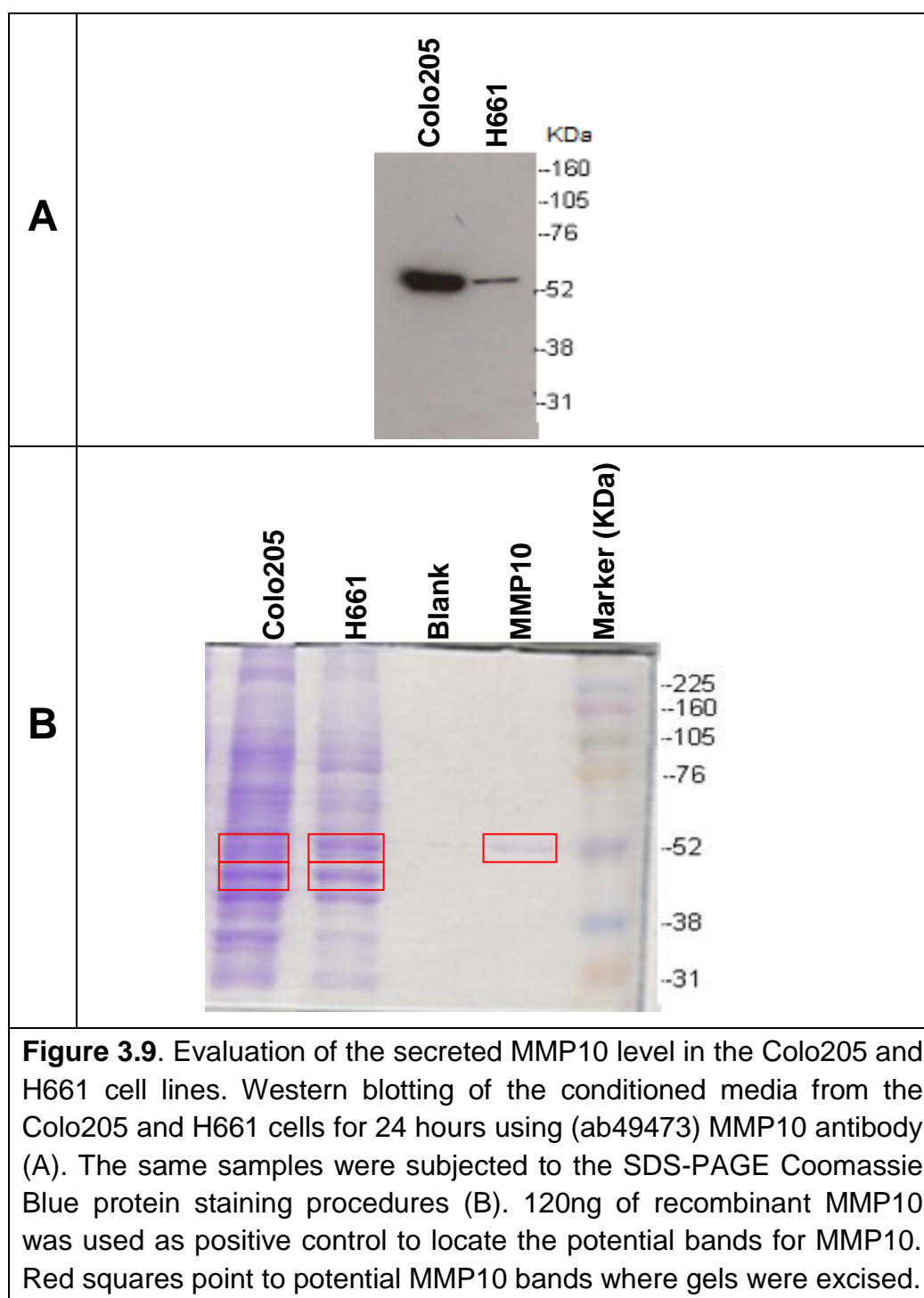
3.4.6 Detection of Secreted MMP10 Using MALDI-TOF-MS

Due to the low level of secreted MMP10 in most tissues, the use of more sensitive methodology than the traditional Western blotting would be essential for secreted MMP10 detection. The MALDI-MS detection system has recently proven to be a powerful procedure. Subsequently, it was used to detect secreted MMP10 protein in this research. The secreted MMP10 was

high in the Colo205 cell line but low in the H661 as suggested by Western blotting (Figure 3.9A). These cell lines therefore were used to evaluate the sensitivity range of the MALDI-MS system. Recombinant MMP10 was also used as a positive control. A blank containing PBS (alone) was run parallel to it as negative control. The protocol involves separating the complex protein mixture using SDS-PAGE followed by Coomassie Blue protein staining (Figure 3.9B). The latter was carried out to locate the protein of interest prior to gel excision. After trypsin digestion, the resulting fragments of all samples were assessed using manual MALDI-MS analysis.

Only two dominant significant signals with m/z of 992.39 and 1463.62 were found in the mass spectra of the peptides generated from the recombinant human MMP10 (Figure 3.10). For the 992.39 signal, a peptide sequence was identified using MS/MS analysis as K.GNEFWAIR.G, which was specifically related to MMP10 (located in hemopexin-like2 domain). Conversely, 1463.62 signal was identified as K.VWEEVTPLTFSR.L, which was related to both the MMP3 and MMP10 (located in catalytic domain in both enzymes). In contrast, MMP10 in conditioned media from both the Colo205 and H661 was below the detection level at this stage as no dominant signals were observed (Figure 3.10). This was attributed to mixture complexity, wherein the signal of interest was suppressed by other strong signals. To overcome this, peptide fragments were further fractionated using Nanoscale RP Liquid Chromatography, then subjected to automated MALDI-MS/MS analysis. Unfortunately, MMP10 was again below the detection level in the conditioned media evaluated (Appendix 5). Given the time and financial constraints, this

methodology was not pursued further. For the remaining studies, secreted MMP10 protein levels were measured using Western blotting.



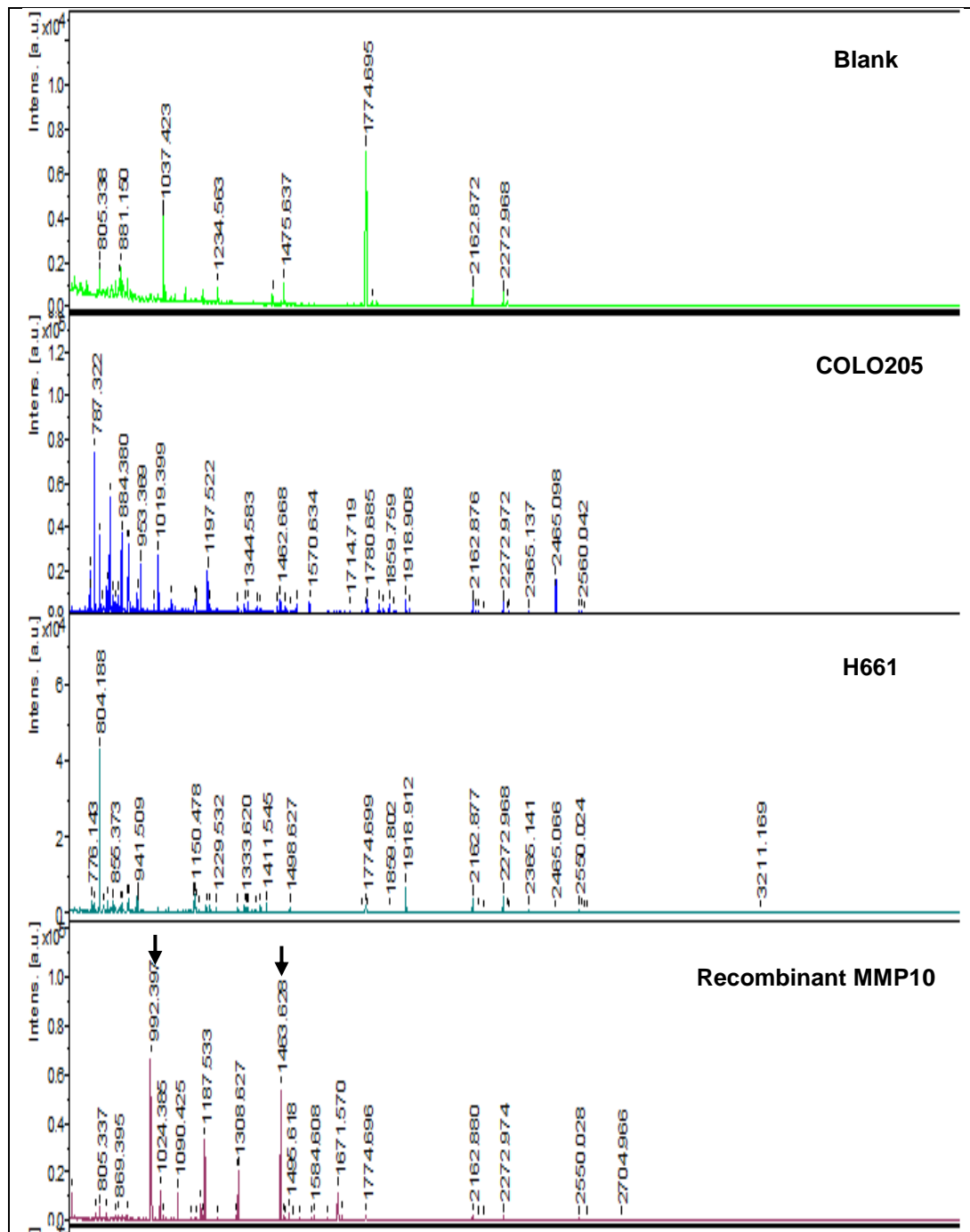


Figure 3.10. Mass spectra of blank (negative control), Colo205 and H661 cell conditioned media and recombinant MMP10 (positive control). Two dominant significant signals with m/z of 992.39 and 1463.62 were generated from the recombinant human MMP10 (arrows). Secreted MMP10 from both Colo205 and H661 was below the detection level with no dominant signals observed. The MMP10 was used as a positive control and the arrows point to dominant peptides signal for MMP10.

3.4.7 Comparison of Protein and mRNA Expression Detected for MMP10 in the NSCLC Cell Lines

Table 3.1 summarises the RT-PCR and Western blotting results for MMP10 expression in both the cell and tissue extracts. As can be seen, for the A549 and H460 cell lines, a consistency between the mRNA and protein levels of MMP10 was observed in both the cells and tissue xenografts. However, high MMP10 mRNA expression in the H661 cell line did not correlate with its protein levels, showing low MMP10 expression. As a consequence, only the A549 and H460 cells were selected for further MMP10 studies.

Table 3.1. Summary of MMP10 Expression in the NSCLC cell lines (A549, H460 and H661) in both the 2D culture and Tissue Xenografts. The mRNA and protein levels of MMP10 were graded from zero to five according to their band intensities. Each + represents approximately 1.3 band intensity as semi-quantified using Quantity One software for RT-PCR and Western blotting results. Levels of active MMP10 protein in cells grown in 2D culture were below the detection level of the Western blotting. ND: not detected, NA: not available. NCA: needs confirmation by APMA.

Cell Lines	MMP10 Expression					
	Cells			Tissue Xenografts		
	mRNA	Protein		mRNA	Protein	
		Pro	Active		Pro	Active
A549	++++	+++	ND	+++++	+++	NCA
H460	+++	+++	ND	+++	+++	NCA
H661	+++++	+	ND	NA	NA	

3.4 Discussion

Matrix metalloproteinase is known to be involved in cancer growth, spread, invasion and angiogenesis. The identification of proteolytic enzyme expression, especially MMPs, in human cancers is critical in understanding the characteristics of individual cancer types (Atkinson et al., 2007; López-Otín and Overall, 2002). The expression profile of MMPs in human NSCLC as reported in the literature is currently incomplete and does not account for the significant interactions between the different MMPs that take place during their involvement in the several processes related to cancer development. The complete profile of MMP expression and activity in NSCLC could increase the understanding about their role in the disease. To achieve this using *in vitro* studies, preclinical models that precisely characterise MMP in the human NSCLC are needed to be established first. Three human tumour NSCLC cell lines (A549, H460 and H661) were chosen as representatives of two of the most common subtypes of NSCLC—adenocarcinomas and large cell carcinomas—and were screened for their expression of 22 MMPs in this chapter using semi-quantitative PCR.

During the screening of MMP mRNA expression in the NSCLC cell lines, the HT-1080 cell line was used as a positive control for MMP expression. Due to the high expression of multiple MMPs, this cell line was previously used in several studies focusing on MMP expression and activity—for example, MMP2, MMP9 and MMP14 (Upadhyay et al., 1999); MMP3 (Kamio et al., 2010) and MMP2, MMP 14 and MMP16 (Atkinson et al., 2010). In agreement with most of these studies, HT-1080 cells demonstrated a high expression of

MMP3, 14, 16, 2, and 9 in this study. However, H661 demonstrated a more diverse and generally higher expression of MMPs than even HT-1080 and thus would itself be a good cell line to select as a positive control in similar studies.

The Colo205 colorectal cancer cell line was used as a negative control for MMP expression. The use of this particular cell line was based on its overall negative expression of MMP that was previously observed (Atkinson et al., 2010). While their result was produced using the more sensitive real-time PCR, a higher expression pattern of MMPs in the Colo205 was detected in the current study using standard PCR. The expression of MMP3, 8, 10, 24, 25, 26 and 28 was below the detection level in the reported research; however, it is observable in this study. The discrepancy between the data may be due to the different reference genes or internal controls used to normalise the results, which can adversely influence the uniformity of the results (Zhang et al., 2007). Other contributing factors might be the variation in cancer cell lines, culture conditions, passages number and cell density, all of which have been reported to influence the *in vitro* expression of several MMPs (Hagemann et al., 2010; Rossi et al., 1995; Trog et al., 2006). Thus, caution should be exercised when relying on MMP expression data from a single source or experiment.

Due to the potential for variation of the MMP expression results, it was necessary to characterise MMP expression in a panel of NSCLC cell lines to assess their suitability for further studies. As was expected, the MMP expression in the NSCLC cell lines evaluated was not consistent with the

only report in the literature using the same three cell lines (Atkinson et al., 2010). Despite this variation, high mRNA expression for MMP2, 3, 9, 10, 15, and 25 were detected in the A549, H460 and H661 cell lines, with extremes observed in the H661 cells in both the reported and current study. It's worth noticing that the reported study used a quantitative real time PCR, whereas the current study used semi-quantitative PCR. Therefore, caution was required when comparing the data due to the variation in detection sensitivity. Overall, this high level of MMP expression in the NSCLC cell lines observed in this and the reported study support the potential roles of these MMPs in NSCLC tumour development. Furthermore, these MMPs may serve as potential therapeutic targets to be exploited in NSCLC.

Matrix metalloproteinase 10 is a specific interest to this study because its expression has been correlated to poor clinical outcome in NSCLC (Frederick et al., 2008). Data in the present study indicated a diverse profile for MMP10 in the panel of the NSCLC cell lines evaluated, with very strong, high and moderate levels of MMP10 expression detected in the H661, A549 and H460 cell lines, respectively. These findings slightly differ from those of Atkinson et al. (2010), which showed high expression of MMP10 mRNA in the H661 cell line and low expression in the A549 and H460 cell lines (Atkinson et al., 2010). In addition, differences were also seen in a study where MMP10 mRNA was evaluated in a glioblastoma cell line (Hagemann et al., 2010). It was seen that MMP10 expression varied with passage in culture. In particular, MMP10 levels were initially high, with a decrease seen by passage five and very low or below levels of detection at passage 15 (Hagemann et

al., 2010). Although in this study no such relationship was observed, all cell lines were only used up to passage eight as a precaution.

In the case of NSCLC xenograft tissues, MMP10 mRNA expression from the A549 and H460 tissue extracts was significantly higher compared to the normal mouse lung tissue. Unfortunately, H661 xenograft tissue could not be included as it had not been grown as a tumour xenograft in these laboratories. Despite this, the data generated from NSCLC xenograft tissues used (A549 and H460) showed a consistent MMP10 mRNA expression in both xenografts and 2D cell culture, confirming the expression of MMP10 in the NSCLC cell lines evaluated.

Although MMP10 mRNA expression levels are detected in the NSCLC cell lines (A549, H460 and H661), RT-PCR analysis alone is insufficient to correctly indicate levels of MMP10 protein due to the effects of the post-translational regulation of the enzymes, such as phosphorylation. Therefore, Western blotting was used to address MMP10 protein expression in these cells. This indicated inconsistencies between gene and protein expression, particularly in the case of the H661 cells. A low to moderate pro-MMP10 protein level was observed in contrast to its mRNA, which showed very high MMP10 expression. There are a few possible reasons for this conflict, including differences in mRNA and protein turnover rates and different posttranslational regulation and modifications (Fu et al., 2007). A potential mechanism by which H661 shows such discrepancies between mRNA and gene expression while the other two cells lines are consistent in both mRNA and protein expression is through their respective p53 statuses. p53 is a key

regulator of the mTOR pathway (Feng, 2010), which is implicated in the MMP10 released in stromal cells (Reikvam et al., 2013). In the published study, the inhibition of the PI3K/mTOR pathway results in an increase in MMP10 release by stromal cells. It is interesting to note there is non-functional P53 in H661 (Stuschke et al., 2002), unlike in the H460 and A549 cells, but more studies would be required to make a link with changes in MMP10 levels observed in the current study. Although conflicting results were seen for the H661, the results for the other NSCLC cell lines evaluated (A549 and H460) for MMP10 expression at the transcriptional and translational levels were consistent and generally supported the elevated MMP10 in these cell lines. Therefore these cell lines were selected for further MMP10 studies in the project. A good candidate for further investigation would be to demonstrate the suggested mechanism of the non-functional p53 that is negatively affecting MMP10 protein expression in the H661 cells.

Following the evaluation of MMP10 protein level at 2D cell culture, selected NSCLC xenograft tissues (A549 and H460) were included to assess the influence of tumour microenvironment on MMP10 expression. Pro MMP10 was successfully detected with bands at the right size (54 KDa). Although bands at the right size of active MMP10 (44 KDa) were seen, caution was taken to consider them active MMP10 as they could be glycosylated pro MMP10. A confirmation step is required that involves an activation by amino-phenyl mercuric acetate (APMA) to ensure these bands corresponding to the active MMP10.

Matrix metalloproteinase 10 is a low abundance secretory protein that is difficult to detect in the majority of the biological samples. Such an obstacle has consequently hampered the elucidation of the roles of MMP10 in cancers, including NSCLC. One procedure that has proven useful in protein detection is the MALDI-MS detection system, which was utilised to detect secreted MMP10 in this research.

In an attempt to evaluate the MALDI-MS detection system to measure secreted MMP10 protein, conditioned media from the Colo205 and H661 cells, as well as recombinant MMP10 protein, were used as sources of MMP10 in the current study. The signature peptide for MMP10 was detected in the recombinant MMP10 digest fragments but not in the Colo205 and H661 conditioned cell media, representing limited success in secreted MMP10 detection in biological samples. This limited success could be explained by the proteomic complexity of biological samples, specifically the dynamic range of proteins (Corthals et al., 2000), with low abundance proteins being masked by high abundance proteins. In addition to this, protein loss at the various stages of the sample processing in MALDI-MS could greatly impact the detection of low abundance protein, such as MMP10.

While the MALDI-MS detection system has been frequently used to detect endogenous MMP substrates (Butler et al., 2010; Starr et al., 2012; Vaisar et al., 2009), the identification of the cellular MMP enzymes themselves in human cells by this method is rare. The few studies that have had success in MMP identification by this method have had to utilise protein enrichment

methods. The MMPs identified include MMP14 (Shuo et al., 2012) and MMP9 (Ries et al., 2007). Based on this, immunoprecipitation of MMP10 in cell conditioned media was attempted in this research using magnetic beads and MMP10 antibody (Ab49473) prior to the proteomics work, but unfortunately this was unsuccessful. The potential for MMP degradation by other proteases present in the biological samples and the need to maintain their structural integrity by an optimised buffer could add to the difficulties encountered in MMP detection by the MALDI approach (Grasso et al., 2006). Overall, the identification of MMP10 by the MALDI-MS system was demonstrated for purified recombinant protein. Detection in complex biological samples remains elusive and is hindered by the factors discussed above, as well as by instrument sensitivity.

In conclusion, screening MMP expression in NSCLC cell lines (A549, H460 and H661) at the genetic level reveals that these cells constitutively express a wide variety of MMPs, including MMP2, 3, 9, 15 and 25, and the focus of this project, MMP10, which has been shown to support tumour development and contribute to poor clinical outcome. In this study, MMP10 demonstrates a stronger expression in the A549 and H460 tissue xenografts compared to mouse normal lung tissue at both the genetic and protein levels. The confirmed high expression of MMP10 in the NSCLC cells, coupled with evidence of selective expression by tumour cells, suggests that MMP10 is a potential target for therapeutic intervention in NSCLC. However, further investigation is needed to elucidate its roles in NSCLC. Based on the mRNA and protein levels of MMP10, the NSCLC cell lines (A549 and H460)

presented themselves as good models for the evaluation of MMP10 functionality in further experiments. The H661 cells were not chosen due to inconsistency in results on MMP10 in the gene and protein levels.

Chapter 4: Development of *In Vitro* MMP10 Expressing Models for the Evaluation of the Role of MMP10 in NSCLC

4.1 Introduction

The use of a relevant preclinical model that precisely characterises the patterns of MMP10 expression in human NSCLC is essential for a better understanding of the roles of MMP10 in the disease. It has previously been reported that MMP10 is up-regulated in NSCLC, where it is strongly linked to poor clinical outcome (Batra et al., 2012; Cho et al., 2003; Frederick et al., 2008; Gill et al., 2004; Zhang et al., 2007). Based on this, well characterised models with a range of expression levels (from high expression to represent the more aggressive NSCLC to little or no expression to act as normal controls) would be useful for the investigation of the involvement of MMP10 in NSCLC.

Two NSCLC cell lines (A549 and H460) have been identified as good potential models based on their mRNA and protein levels of MMP10 in the previous chapter. However, levels are still relatively low in these cell lines compared to those seen clinically; hence, there is a requirement for cell lines that can be engineered to overexpress MMP10 to a more clinically-relevant level.

Several transfection methods have been used to knock down or over express MMP10 in preclinical studies. For MMP10 overexpression, methods involving cloning a sequence-verified human MMP10 cDNA into an expressing vector, which is then inserted into cells by either chemical-based transfection (e.g. lipofection) or non-chemical methods (such as electroporation and viral transduction), have proved to be efficient. It was reported that human MMP10 cloned into pBICEP2 vector and transfected into oral carcinoma cells by lipofection using FuGENE 6HD, resulted in a marked MMP10 expression (Deraz et al., 2011). In another study where pCMV6-Entry vector and electroporation were used to transfect HeLa cells, successful MMP10 overexpression was achieved (Zhang et al., 2014a). On the other hand, silencing MMP10 in the literature is generally achieved by harnessing the endogenous RNA interference (RNAi) mechanisms through introducing into the cell an MMP10 specific short interfering RNA (siRNA) for transient effect or short hairpin RNA for a stable one, followed by the same transfection methods described above (Deraz et al., 2011; Zhang et al., 2014a).

Recently, MMP10 expression has been shown to be repressed *in vivo* by the class II histone deacetylase HDAC7 (Chang et al., 2006) (previously described in general introduction section 1.6.2), with the silencing of HDAC7 leading to an increase in MMP10 expression. This relationship will be investigated here as an alternative strategy to produce MMP10 overexpressing cell lines.

4.1.2 Aims and Objectives

The aim of this chapter is to develop a functionally active MMP10 overexpression model to investigate the consequences of high MMP10 in NSCLC tumour vasculature.

This will be achieved by the following objectives:

1- Development and characterisation of a functionally overexpressing MMP10 cell line either:

a) By MMP10 overexpression in the H460 cells or

b) Using HDAC7 silencing to mediate the induction of MMP10 in the NSCLC cell lines.

2- Evaluation of the effects of functional MMP10 expression on vascular formation using a tube formation assay (Zhang et al., 2014a).

4.2. Materials and Methods

4.2.1 Materials

Opti-MEM[®] Reduced Serum Medium and Lipofectamine[®] RNAiMAX reagent, HDAC7A Pre-designed siRNA (ID:108707) and Silencer[®] Select Negative Control No. 1 siRNA (cat. 4390843) were purchased from Life Technologies Ltd (Paisley, UK). Polybrene was purchased from Sigma-Aldrich (Gillingham, UK). For cell selection, antibiotics, including G418 and puromycin, were also obtained from Sigma-Aldrich (Gillingham, UK). For immunohistochemical analysis, Harris' Haematoxylin and Scott's Tap Water were purchased from Sigma-Aldrich (Gillingham, UK). The CD34 antibody MA1-22646 used for immunostaining was obtained from Fisher Scientific (Loughborough, UK). The Vectashield Kit was purchased from Vector Laboratory Ltd (Peterborough, UK) for slide mounting. For 2D angiogenesis model analysis, the immortalised human umbilical vein endothelial cells (HUVEC-Cs) were obtained from the ATCC (Middlesex, UK) (Hoshi and Mckeehan, 1984; Jaffe et al., 1973). Microvascular endothelial cell growth medium-2 BulletKit EGM[®]-2MV was bought from Lonza (Slough, UK). Amicon Ultra-15 centrifuged filter device, Ilomastat (GM6001) and *In Vitro* Angiogenesis Assay Kit were purchased from Millipore (Watford, UK). The polystyrene eight-well chambered cover glasses (Lab-Tek[™]) were bought from Fisher Scientific (Loughborough, UK). For PCR and Western blotting materials, refer to sections 2.1.2 and 2.1.3, respectively.

4.2.2 Methods

4.2.2.1 Cell line nomenclature

Transduced H460 cells with Short Hairpin HDAC7 (shHDAC7) and non-targeting control (shNT) are termed 'H460-shHDAC7' and 'H460-shNT' respectively, while those genetically modified with mouse MMP10 expressing vector are termed 'H460-clone2'. The H460-clone2 cells were a kind gift from Dr. Jason Gill (Durham University) who transfected them with this vector that was designed as described by (Madlener and Werner, 1997) (see section 4.2.2.4.1). The A549 and H460 cells that have been transiently transfected using HDAC7 siRNA are termed 'A549-siRNA' and 'H460-siRNA', respectively. The immortalised human umbilical vein endothelial cells (HUVEC-Cs) isolated using an enzymatic technique described in (Eccles et al., 2008), were a kind gift from Dr Anne Graham (Bradford University).

4.2.2.2 Cell line maintenance and culture conditions

All cell lines used in this chapter were routinely maintained and cultured in complete RPMI-1640 as described in section 2.2.1 apart from HUVEC-Cs, which were cultured as described below.

4.2.2.2.1 Culture of HUVEC-Cs

The immortalised HUVEC-Cs were grown as monolayer cultures in EGM-2MV medium supplemented with optimal concentrations of EGF, VEGF, IGF-1, bFGF, hydrocortisone, ascorbic acid and 5% FBS. Cells were incubated at 37°C in a humidified atmosphere of 5% CO₂ and 95% air and media was

changed every other day. Before 80% confluence was achieved, cells were detached using 0.25% trypsin-EDTA, as previously described in section 2.2.1. The resulting cells were resuspended in fresh, complete EGM-2MV medium and were either passaged or collected for further experimentation.

4.2.2.3 Evaluation of cytotoxicity using the MTT assay

4.2.2.3.1 Validity of the MTT Assay for H460 cells

To ensure that the cell number correlates with the MTT absorbance readings, the linear relationship between cell viability and absorbance was established for the H460 cells using the MTT assay (Mosmann, 1983). Cells were grown, harvested and counted as described in section 2.2.1. Serial dilutions of cell suspensions (0.5, 1, 1.5, 2, 2.5, 3, 3.5, 4, 4.5, and 5 x10⁴ cells/ well) were prepared and seeded onto 96 well plates. Wells without cells but with media added acted as a blank. The plates were then centrifuged to allow cells to settle onto the bottom and supernatant was removed. Following the addition of the MTT solution, absorbance was read as described below in section 4.2.2.3.3. To demonstrate the linear relationship, the mean absorbance was plotted against the cell number and a trend line was drawn.

4.2.2.3.2 Optimisation of cell seeding densities for the MTT assay

To optimise the H460 cell seeding density for use in the MTT assay, such that the cells would be in the log phase of their growth cycle during the experiments, growth curves of the H460 cells at several different seeding

densities were set up. Five different cell concentrations (one, three, 10, 30, and 100) $\times 10^3$ cells/ml in a final volume of 180 μ l were seeded onto a 96-well plate in hexuplicate, leaving control wells where no cells were added. Plates were then incubated for one, two, three, four or five days. Following the addition of the MTT solution, absorbance representing cells viability was read as described below in section 4.2.2.3.3. Data from three experiments were averaged and plotted against time.

4.2.2.3.3 MTT Assay

The impact of two selection antibiotics, G418 and puromycin, and the transfection reagent lipofectamine RNAiMAX on cell number was measured using the MTT assay. Briefly, cells were seeded at 1.8×10^3 cells per well into 96-well culture plates. Wells without cells but with media added acted as a blank control. All wells received 180 μ l fresh complete medium. The plate was incubated overnight at 37°C in a 5% CO₂ and 95% air humidified atmosphere to allow cells to adhere. The next day, cells were treated with compounds of interest at the required concentration in 200 μ L fresh, complete medium. Control wells that received no drug but contained cells were also included for comparison. The plate was incubated for a further 96 hours in the same conditions described above. The media were then replaced with fresh medium containing 500 μ g/mL MTT and plates were incubated for a further four hours at 37°C. The medium was subsequently removed and the resulting crystals were dissolved in 150 μ L DMSO. Absorbance was measured on a microplate reader at 540nm and were averaged and the mean blank absorbance was subtracted to provide an adjusted absorbance

reading. To assess growth inhibition, the relative proportion of live cells to untreated control was calculated as follows: % cell survival = [adjusted mean treated group absorbance / adjusted mean control group absorbance] x 100. A graph of concentration against percentage cell survival was then plotted. This assay was conducted in triplicate unless otherwise stated.

4.2.2.4 Generation of stable MMP10 expressing cells

4.2.2.4.1 MMP10 expressing clones

The human H460 cells transfected with a mouse MMP10 expressing vector designed as described (Madlener and Werner, 1997) were a kind gift from Dr Jason Gill (Durham University). Since these cells initially were generated for another project to assess *in vivo* the consequences of MMP10 overexpression in tumours on the adjacent normal vasculature, the use of mouse vector in human cells could be justified. The cells were cultured prior to the selection of stable transfectants using G418 antibiotic as described below in section 4.2.2.4.4.

4.2.2.4.2 Stable HDAC7 silencing using shRNA lentiviral particles

Histone deacetylase 7 was silenced in the H460 cells using a Short Hairpin RNA (shRNA) lentiviral transduction system. Lentiviral particles targeting the HDAC7 gene, prepared by MISSION shHDAC7 plasmids DNA (Sigma) according to the manufacturer's protocol, was a kind gift from Dr Andriana Margariti (Queen's University Belfast). A full detail of the procedure is

reported by Margariti et al. (Margariti et al., 2010). A control of the shRNA lentiviral vector that does not target any known genes (shNT) was also prepared in parallel for comparison. For lentiviral infection, H460 cells were seeded in a T75 flask at 60% confluence and allowed to attach overnight. The next day cells were incubated with shHDAC7 or shNT (1x10⁷ transduction units per ml) in RPMI complete media supplemented with 10µg/ml of polybrene for 24 hours. Medium containing lentiviral particles was replaced with fresh medium, then the cells were incubated for another 48 hours before being selected.

4.2.2.4.3 Optimisation of antibiotic concentration for selection

The MMP10 expression and the shRNA lentiviral vectors were designed to encode G418 and puromycin antibiotic resistance genes, respectively. These antibiotics therefore were used to select stable transfectants for this study. To ensure that the optimal antibiotic concentration was used during selection, a growth inhibition assay based MTT for wild type H460 was performed as described in section 4.2.2.3.3. G418 (100, 200, 400, 800, and 1600µg/mL) and puromycin (0.125, 0.25, 0.5, 1, 2, 4, and 8 µg/ml) were tested and cell viability was assessed daily. For G418, H460-clone2 cells were also included to evaluate their resistance as compared to the wild type, consequently confirming the presence and functionality of the vector inside the cells. The minimum concentration of G418 and puromycin that resulted in total cell death within three to four days and one to four days respectively, was considered the optimal antibiotic concentration for generating stable transfectants. The specific time period for the antibiotics was selected

according to their onset mode of action. Experiments were performed in triplicates, then data was averaged and plotted as percentage cell survival against time.

4.2.2.4.4 Selection of stable transfectant

H460-clone2 cells were incubated with complete RPMI media containing the optimal concentration of G418 for 13 days. In the case of lentiviral transduction, H460-shHDAC7 and H460-shNT were incubated with complete RPMI media supplemented with optimal puromycin concentration for seven days. During the incubation period, the medium was replaced every two days and the cells were monitored daily. Surviving cells were subjected to RT-PCR and Western blotting analysis to confirm successful transfection.

4.2.2.4.5 Verification of stably transfected H460 cells

Following cell selection, PCR analysis to confirm the specificity of the vectors was performed as previously described in section 2.2.4. For H460-clone2 cells, mouse MMP10 primers (F:5-AGGGACCAACTTATTCCTGG-3; R:5-CAGTATGTGTGTCACCGTCC-3 according to Van et al (Van Themsche et al., 2004) were used to amplify MMP10 mRNA.

Histone deacetylase 7 and the MMP10 protein levels in transfected cells were evaluated using Western blotting as described in section 2.2.6. The monoclonal MMP10 antibody (ab49473) was confirmed to cross react with murine MMP10 protein before being used for the verification of H460-clone2 cells.

4.2.2.5 Immunohistochemistry

To assess the consequences of MMP10 overexpression on NSCLC tumour vasculature, immunohistochemical (IHC) analysis of CD34 protein was performed using tumour xenografts of wild type H460 and those engineered to express MMP10 (H460-clone2). The CD34 protein is a human hematopoietic and endothelial progenitor cell antigen that is expressed in all types of endothelium (Folkman, 1995), and its antibody has been validated to stain the capillary endothelium (Fina et al., 1990). For immunohistochemistry, formalin-fixed, 5µm thick paraffin-embedded tissue sections were provided by Beryl Cronin of the Institute of Cancer Therapeutics. All incubations were carried out at room temperature unless otherwise stated. Following heating at 60°C for 20 minutes, sections were de-waxed in xylene and rehydrated in distilled water. The dewaxed hydrated sections were then incubated in 1% hydrogen peroxide for 30 minutes to extinguish endogenous peroxidase activity. For antigen retrieval, sections were completely immersed in 0.1mM citrate buffer (pH 6.0) and heated in a microwave for five minutes. Slides were allowed to cool in citrate buffer for 30 minutes before being washed with PBS for 10 minutes. Non-specific binding of primary antibody with sections was blocked through the incubation of the latter with 10% normal rabbit serum (Vector) diluted in PBS for 30 minutes. Sections were subsequently immunostained with 100µl of primary anti-CD34 antibody at 1:2000 ratio in PBS for two hours. A negative control that received no primary antibody treatment was also included. After washing excess antibody with water and PBS for 10 minutes, sections were dried and incubated for one hour with

biotinylated rabbit anti-rat secondary antibody diluted as 1:100 in PBS. Following a further wash with water and PBS, sections were incubated for 30 minutes with ABC reagent (Vector) and developed in DAB. Developed sections were then counterstained in Harris' Haematoxylin solution for 20 minutes before being incubated for two minutes with Scott's Tap water as blueing reagent. Sections were dehydrated and cleared using ascending concentrations of ethanol (70%, 80% and 100%), 50% xylene/ethanol and 100% xylene. Slides were then mounted using DPX mounting medium.

4.2.2.5.1 Semi-quantitative analysis of immunohistochemistry

To assess the microvessel density for microscopic sections, vessels and capillaries identified by positive staining for CD34 and appropriate morphology were manually counted using a grid overlay method. The intersection of visibly interconnected brown-staining endothelial cells with a spot on the grid was counted. Ten representative equal size fields were counted per slide and the mean number was calculated. The values reported herein are averaged of the three independent slides per sample set. The observation was done at 40X objective magnification using a Leica DMLS microscope connected to JVC digital ½ inch CCD video camera.

4.2.2.6 *In vitro* 2-D angiogenesis model

Matrix metalloproteinase 10 protein can exist in both pro and active forms; hence, measuring enzyme activity is essential to ensure the presence of active MMP10. As there is no specific MMP10 activity assay available to date, the well-known angiogenic role of MMP10 can be used as a functional

marker where the amounts of angiogenesis seen should be relative to the amounts of MMP10 present. Thus, an *in vitro* angiogenesis assay was used here to assess the functionality of MMP10 protein in the wild-type and engineered cell lines.

4.2.2.6.1 Characterisation of HUVEC growth

Human umbilical vein endothelial cells cultures were used in the *in vitro* angiogenesis assay for this research to mimic the behaviour of vascular endothelial cells *in vivo* (Boisen et al., 2010; Staton et al., 2009). Growth curves were constructed to characterise their growth pattern as described in section 2.2.2.

4.2.2.6.2 Optimisation of HUVEC-Cs seeding density for the tube formation assay.

As the proper seeding density of endothelial cells is crucial for any tube formation assays, HUVEC-Cs were seeded in an eight-well chamber coated with ECMatrix™ at four different seeding densities: 1×10^4 , 2×10^4 , 3×10^4 and 4×10^4 cells/well as described below. After 24 hours of incubation, tube formation was inspected using the LumaScope 500 at 40x magnification.

4.2.2.6.3 In vitro angiogenesis assay

The *in vitro* angiogenesis assay kit (Millipore) was adopted for use in these studies. The polystyrene eight-chambered cover glasses was used instead of the recommended 96-well culture plate in order to provide sufficient growth space and improve captured image quality. Briefly, ECMatrix™ was thawed

overnight on ice and all the components kept at 4°C before and during the assay to avoid premature solidification of the ECMatrix™. In a cold sterile microcentrifuge tube, ECMatrix™ was diluted in a 1:9 ratio with 10x Diluent Buffer. Approximately 170µL of this mixture was transferred to each well of polystyrene eight-chambered cover glasses. The plate was then incubated at 37°C for at least one hour to allow the matrix solution to solidify. HUVEC-Cs, which were maintained in EGM-2 complete medium, were seeded on the ECMatrix™ polymerised layer at a density of 4×10^4 cells in 210µl EGM-2 complete medium per well. This was followed by the addition of concentrated conditioned media from different samples. For the impact of MMP10 on angiogenesis studies, recombinant MMP10 (equivalent to 0.25, 2.5 and 25nM) was added at this stage. A positive control received no conditioned media and a negative control treated with 25uM broad spectrum MMPs inhibitor (GM6001) was also included. The cells were subsequently incubated in a humidified atmosphere of 5% CO₂ and 95% air at 37°C for 18 hours. Once incubation was completed, tube formation under bright-field illumination was monitored *in situ* using a LumaScope 500 (EtalumaInc, Carlsbad, USA) at 20x or 40x objective lens magnification, with images captured digitally through a CMOS Sensor camera and processed using LumaView 500 software (EtalumaInc, Carlsbad, USA).

4.2.2.6.4 Quantification of HUVEC tube formation

During the complex multistep processes of angiogenesis at the molecular level, activated endothelial cells form capillary tubes sprouting into the

stromal space in a branching pattern. Counting the number of branch points of these tubes should reflect the extent of angiogenesis.

To measure the tube-like structure area following the performance of the angiogenesis assay, the number of branch points formed by HUVEC-Cs after 24 hours incubation per well were counted. All sample values were normalised to the corresponding control (non-treated). Consequently, the relative number of branching points was determined. The values of the three independent experiments were then averaged and presented in a bar graph. Statistical differences were assessed using Student's t test.

4.2.2.7 siRNA Silencing of HDAC7 in NSCLC cell lines

For efficient transient HDAC7 silencing, optimisation was performed as described below.

4.2.2.7.1 siRNA-gene knockdown

Approximately 5×10^5 cells/well were seeded and grown overnight with complete RPMI media in a six-well plate. The next day, media were removed and cells were incubated for four hours with 1mL Optimum media containing the indicated concentration of siRNA and lipofectamine RNAiMAX. A control with non-targeting siRNA and mock transfection was included to assess any potential effect of the transfection reagents on the cells. Cell growth condition was then normalised by the addition of 0.5mL 3X RPMI feed media, supplemented with 30% FCS, 6% L-Glutamine and 3% sodium pyruvate. The cells were then further incubated for 48 hours to recover and their condition

was monitored daily. Once the incubation period was completed, cells were harvested, counted and subjected to RT-PCR analysis as described above in section 2.2.4. For data analysis, HDAC7 mRNA expression level was determined and the ratio of HDAC7 gene knockdown was calculated as residual HDAC7 expression compared to the non-targeting siRNA control.

4.2.2.7.2 Optimisation of siRNA concentration for transfection.

To determine the optimal siRNA concentration for a successful transfection, a titration of HDAC7-siRNA concentrations (25nM, 50nM, 100nM, and 200nM) was tested for HDAC7 silencing in the H460 cell line. This optimisation was performed for 48 hours using 0.5% v/v Lipofectamine and following the protocol described above.

4.2.2.7.3 Optimisation of Lipofectamine RNAiMAX concentration.

To ensure efficient exogenous siRNA uptake by cells during the transfection, concentration of the transfection reagent was optimised. Several concentrations of Lipofectamine RNAiMAX (0.18, 0.26, 0.34, 0.42 and 0.5% v/v) were evaluated for HDAC7 silencing in the H460 cells. This optimisation was performed using the optimal 50nM HDAC7 siRNA and following the protocol described in section 4.2.2.7.1.

4.2.2.7.3.1 Evaluation of Lipofectamine toxicity

Lipofectamine RNAiMAX toxicity on the H460 cells was measured by MTT assay as described in section 4.2.2.3.3. Cells were treated with serial dilutions of Lipofectamine RNAiMAX, including 0.18, 0.26, 0.34, 0.42, 0.5 and 0.58% v/v. Data from the total three separate experiments were then plotted as percentage of cell survival against Lipofectamine RNAiMAX concentrations.

4.2.2.7.4 Optimisation of post-transfection incubation period

The induction and duration of HDAC7 silencing were examined to choose the most suitable post-transfection periods for future experiment. By following the protocol described in section 4.2.2.7.1, the H460 cells were transfected in triplicates with the optimal 50nM HDAC7 siRNA and 0.5% v/v Lipofectamine then incubated for different post transfection periods, including 24, 48, and 72 hours.

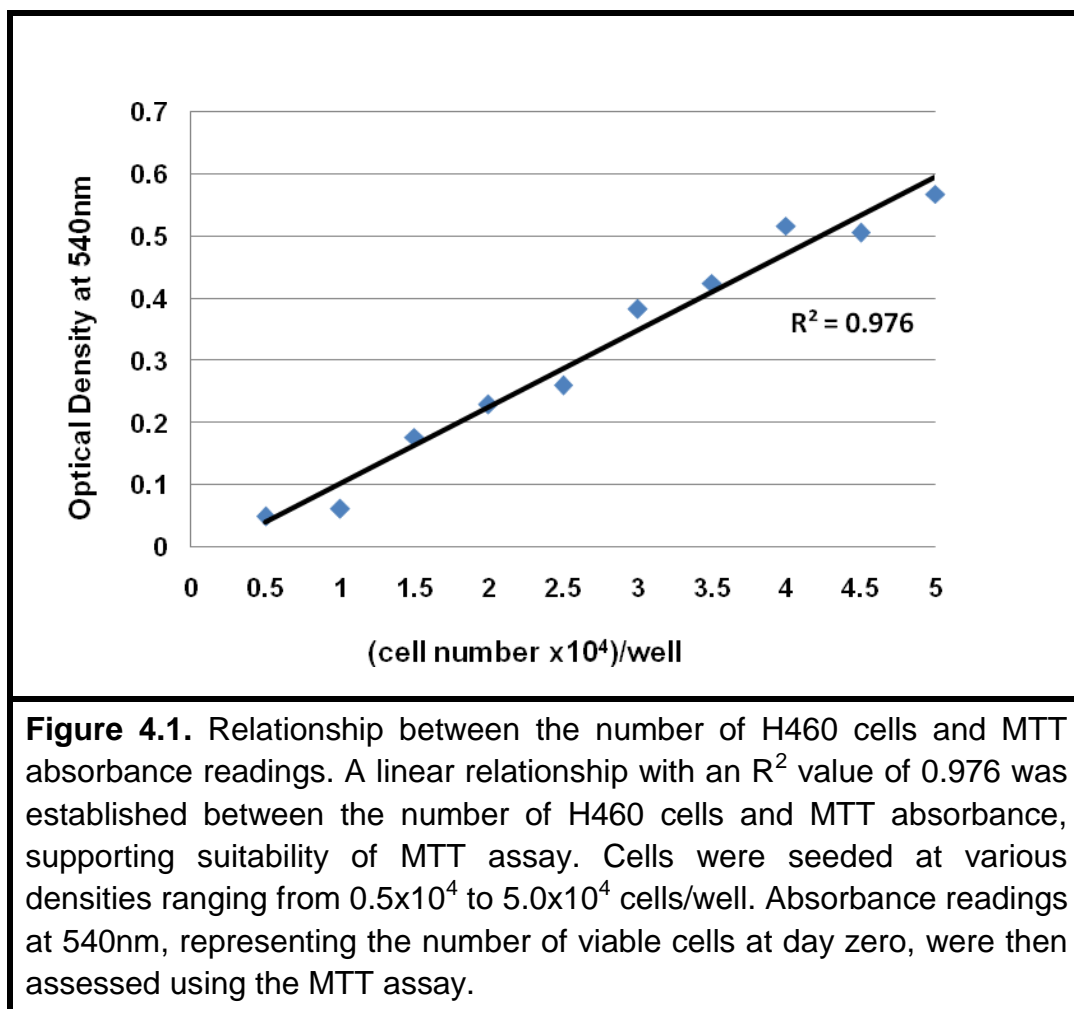
4.2.2.7.5 Transient HDAC7 Gene Knockdown

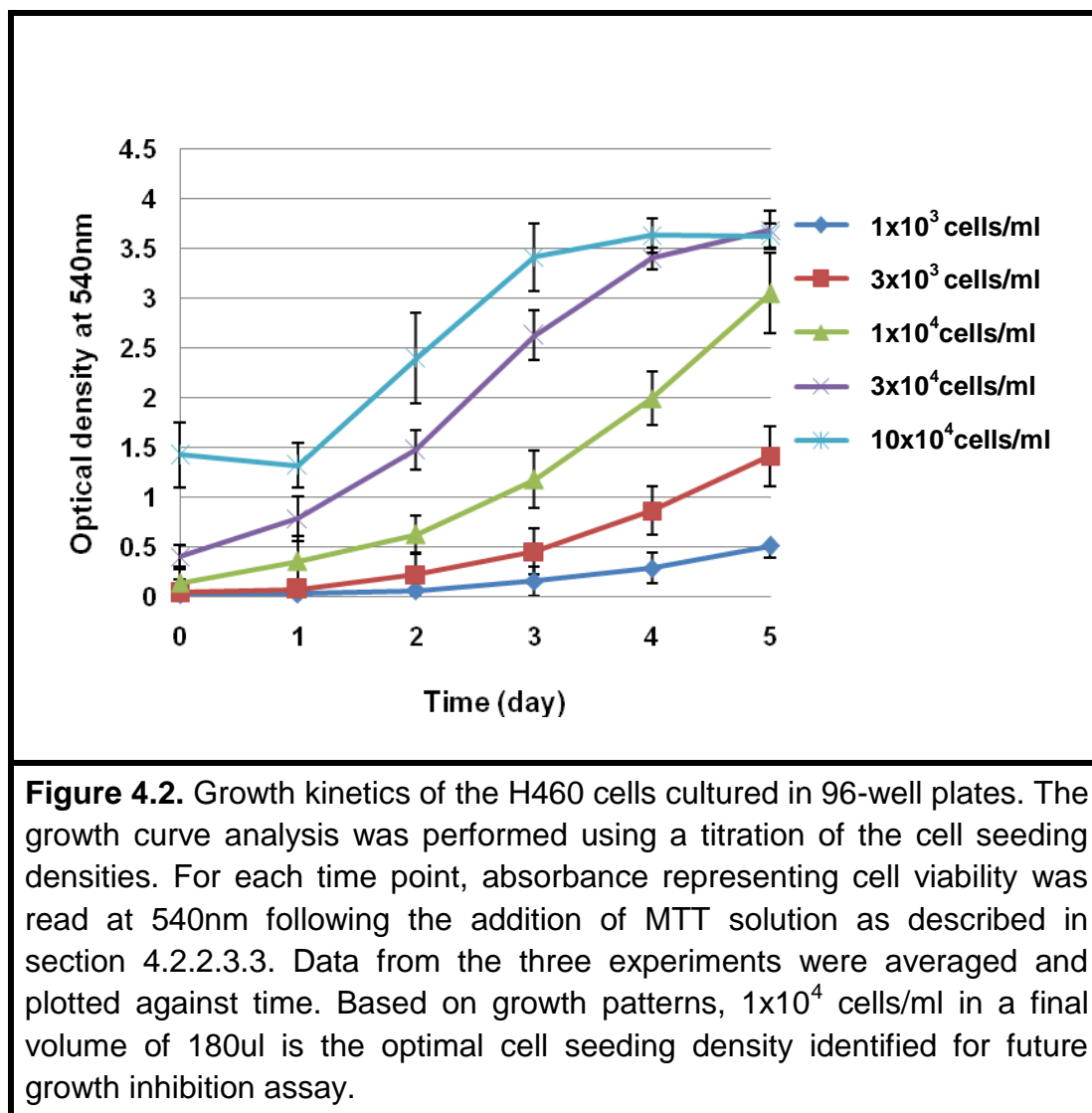
By following the protocol described in section 4.2.2.7.1, transient HDAC7 knockdown was performed in the A549 and H460 cells using the identified optimal siRNA transfection conditions, 50nM HDAC7-siRNA, 0.5% v/v Lipofectamine RNAiMAX, and 24-72 hour post incubation periods.

4.3 Results

4.3.1 Optimisation of the MTT Assay for Use with H460 Cells

Initial day zero studies confirmed the linear relationship between the H460 cell number and absorbance using the MTT assay (Figure 4.1). The growth pattern of the H460 cells generated from five cell seeding densities in a 96-well plate was then evaluated using the MTT assay. Three cell seeding concentrations (1×10^4 , 3×10^4 and 10×10^4 cell/ml) showed a clear exponential phase of growth; however, the stationary phase corresponding to the cell seeding concentrations of 3×10^4 and 10×10^4 cell/ml roughly began at day four and day three, respectively (Figure 4.2). Taking into consideration the fact that incubation periods may extend up to five days, the optimal seeding concentration for the H460 cells to be used in further assays was 1×10^4 cells/ml.





4.3.2 H460-Clone2 as an MMP10 Preclinical Model

To elucidate the exact consequence of the high MMP10 overexpression seen in NSCLC tumour development, engineered models with MMP10 overexpression are a useful tool. One such model has previously been developed in this laboratory by overexpressing MMP10 in the H460 cells (H460-clone2) and it is utilised in these studies.

4.3.2.1 Determination of ideal antibiotic concentration for H460-clone2 selection.

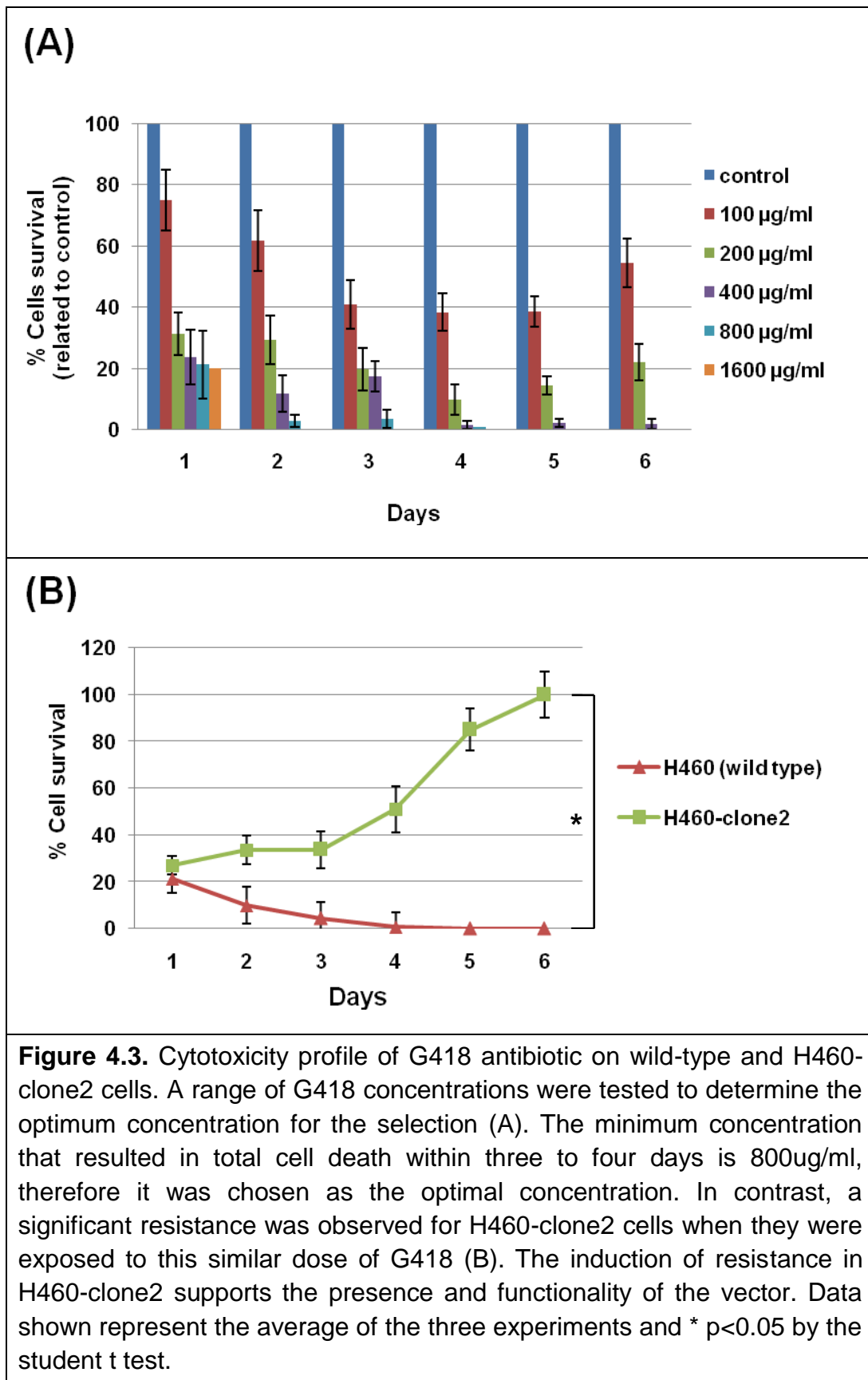
Stable transfectants of H460-clone2 were selected using G418 antibiotic. It was necessary to first optimise the antibiotic concentration to use.

It is clear from the results shown in Figure 4.3A that the minimum concentration of G418 required to kill 100% of the wild-type H460 cells within three to four days is 800ug/ml. This was chosen as the optimum concentration of G418 for selection. When this dose was applied to H460-clone2, significant resistance to G418 was seen (Figure 4.3 B), indicating the presence and functionality of the vector inside the majority of the transfected cells and confirming the suitability of this dose.

4.3.2.2 Evaluation of MMP10 in H460-clone2 at mRNA and protein levels.

Following the H460-clone2 selection, MMP10 induction was assessed at the transcriptional level using RT-PCR analysis. As expected, higher expression of murine MMP10 mRNA was observed in transfectant H460-clone2 as compared to the wild type, confirming the functionality and specificity of the vector. This gave the confidence to proceed to the verification at the protein level using Western blotting.

The Western blotting results showed that the H460-clone2 has significantly higher pro MMP10 protein than the wild-type H460 cells, indicating MMP10 overexpression even at the translational level (Figure 4.4).



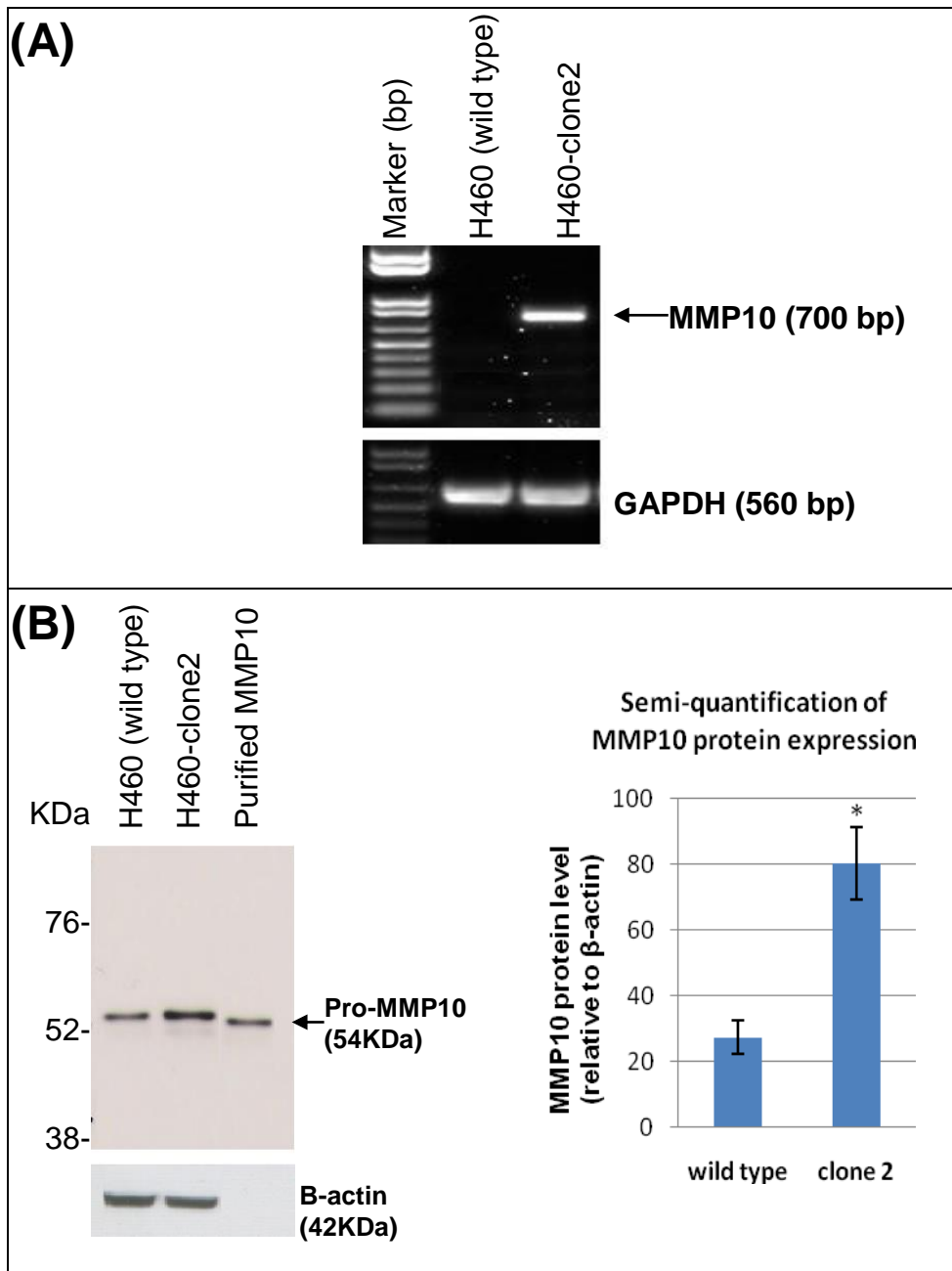
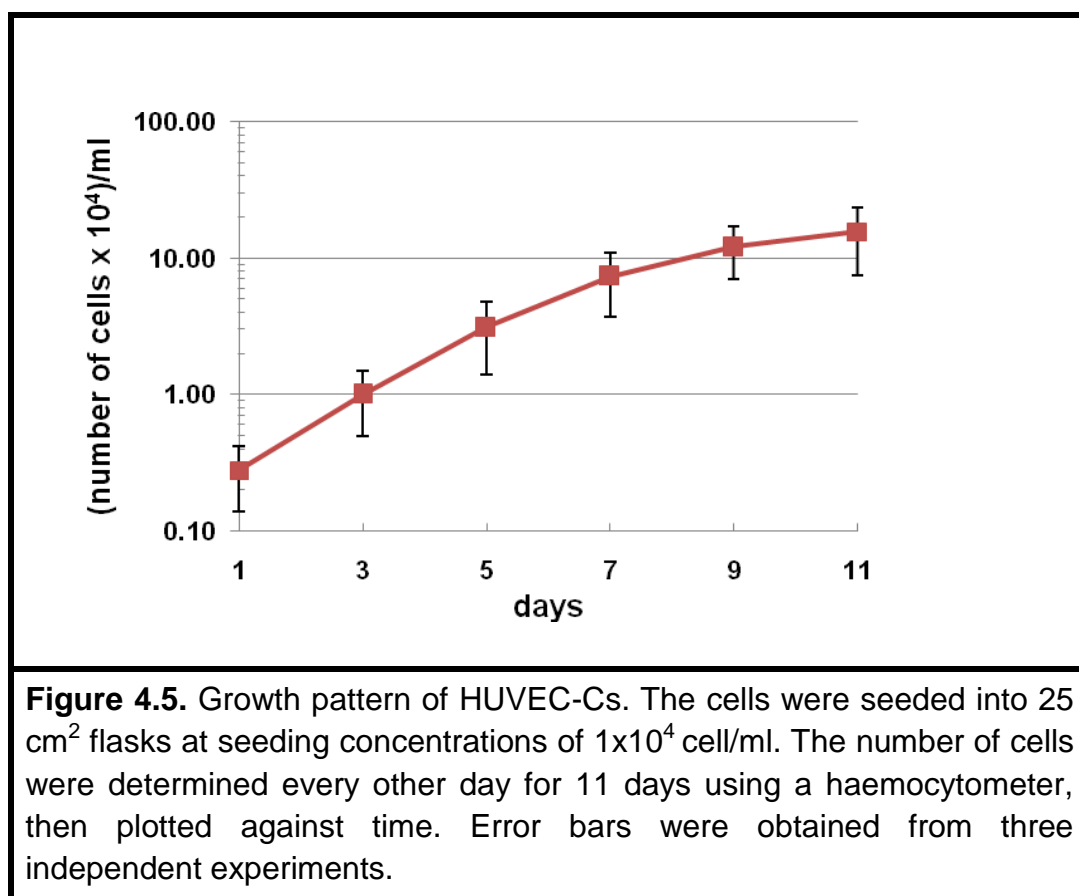


Figure 4.4. Verification of MMP10 induction in transfected H460-clone2 cells. A single band corresponding to mouse MMP10 mRNA was observed with H460-clone2 following RT-PCR analysis (A). MMP10 protein was significantly higher in H460-clone2 compared to the wild type as suggested by Western blotting (B). Recombinant MMP10 with predicted molecular mass for pro MMP10 52 KDa was used as a positive control. * $p < 0.05$.

4.3.3 *In Vitro* Angiogenesis Assay

4.3.3.1 HUVEC-C growth curve

To assess the HUVEC-C growth characteristics for future studies on vasculature, a growth curve analysis was performed as described in section 2.2.2. As shown in Figure 4.5, for the cell concentration applied, HUVEC-Cs log growth phase began at day one with doubling time calculated as 36.6 hours. The log phase lasted for six days, then cells entered the stationary phase approximately at day seven. This data was used to ensure HUVEC-Cs subjected to future analysis were in the log growth phase.



4.3.4.2 Confirming the presence of secreted MMP10 in concentrated conditioned media of NSCLC.

Since MMP10 is a low abundance secreted protein, a centrifuge filtration method for concentrating the conditioned media from cells was utilised prior to Western blotting to confirm the secretion of MMP10 from the NSCLC cell lines in the panel (described in section 2.2.6.2). The Western blotting results in Figure 4.6 generally showed a low level of secreted pro-MMP10 protein (54KDa) in conditioned media from the A549 and H460 cell lines. The secreted pro-MMP10 from the H661 cell line was below the detection level of Western blotting and could not be observed at this stage. However, when conditioned media was concentrated (10-fold concentration) using the centrifuge filtration method to improve the detection level by Western blotting, secreted pro-MMP10 from H661 cells was observed, indicating a very low level in this cell line. Although active MMP10 protein (44 KDa) in all the samples tested was below the detection level of Western blotting and could not be observed, it was assumed that this method successfully concentrated both forms of MMP10 as the membrane cut-off was 30 KDa. Together, data confirmed the secretion of MMP10 from the panel of the NSCLC cell lines evaluated, although at low levels compared to the cellular levels of MMP10.

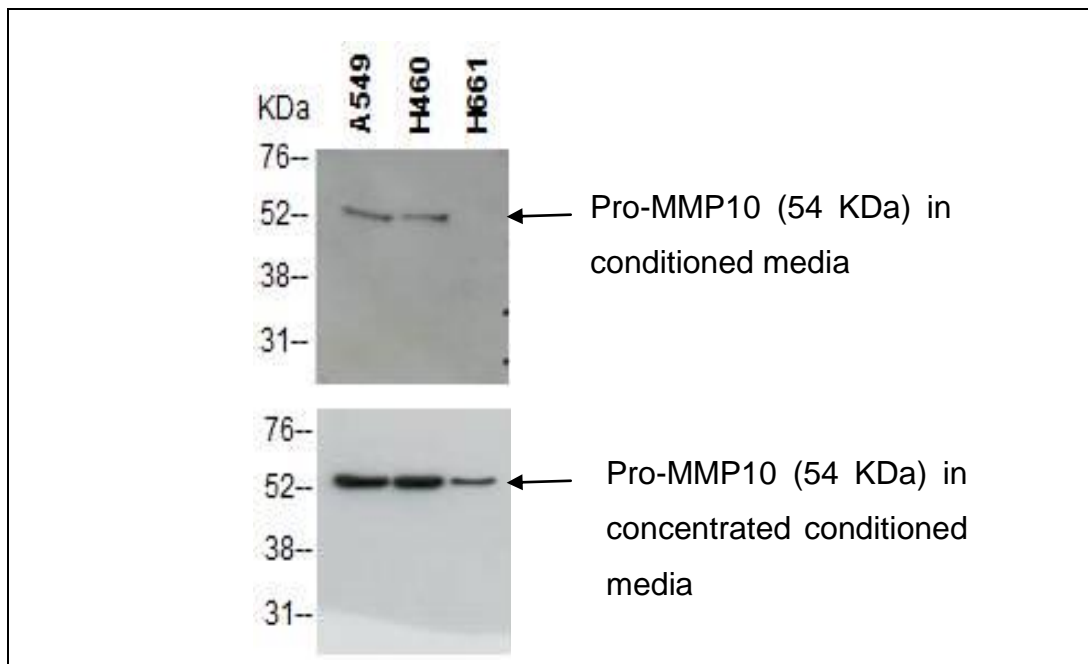


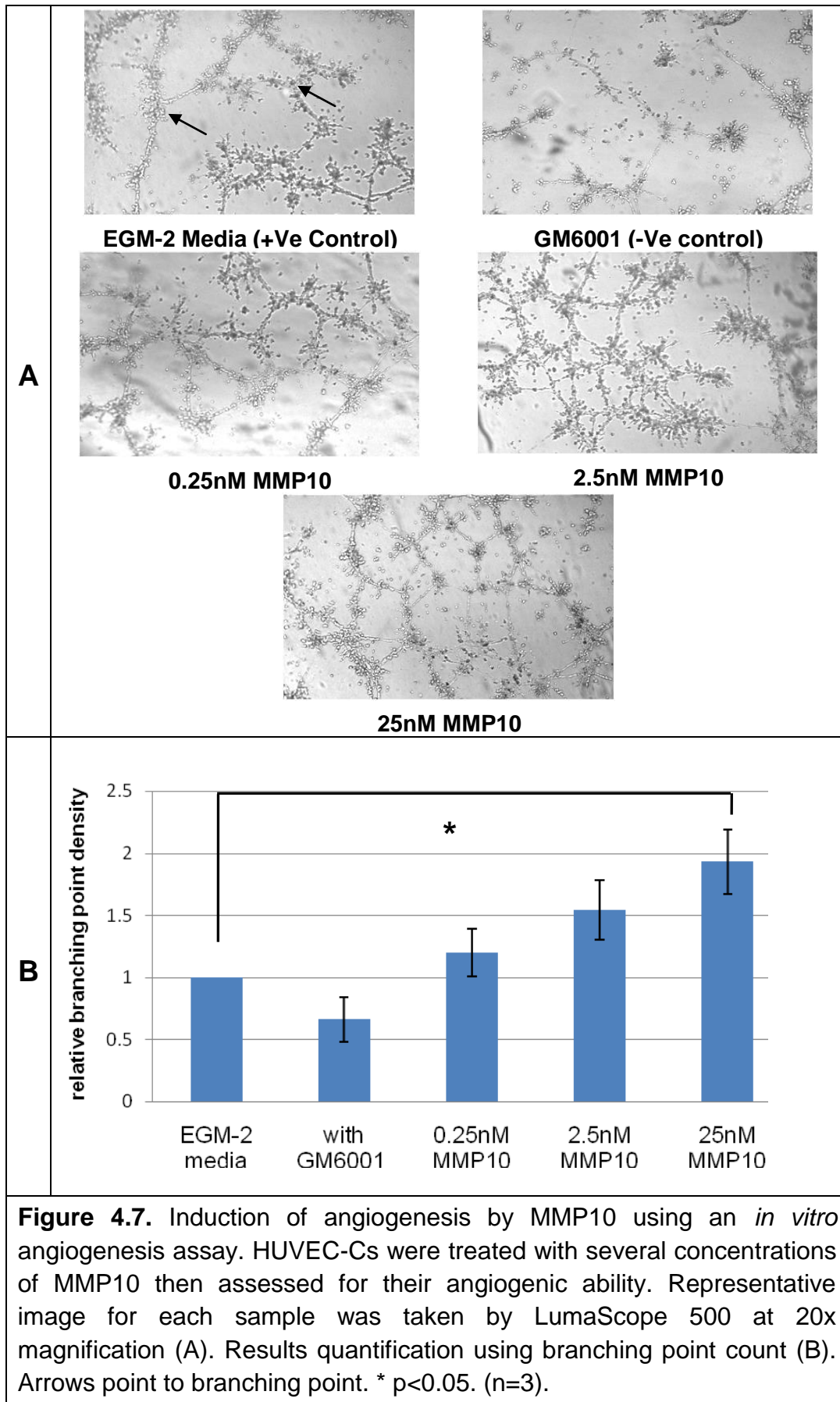
Figure 4.6. Confirming the secretion of MMP10 in a panel of NSCLC cell lines. Evaluation of secreted MMP10 in conditioned medium from A549, H460 and H661 cells by Western blotting showed weak bands corresponding to pro-MMP10 of A549 and H460 cells, whereas no band in the case of the H661 cells. When conditioned media were concentrated, pro-MMP10 in the H661, as well as in other cells, was successfully seen. Despite concentrating the conditioned media, active MMP10 was below the detection level and could not be seen.

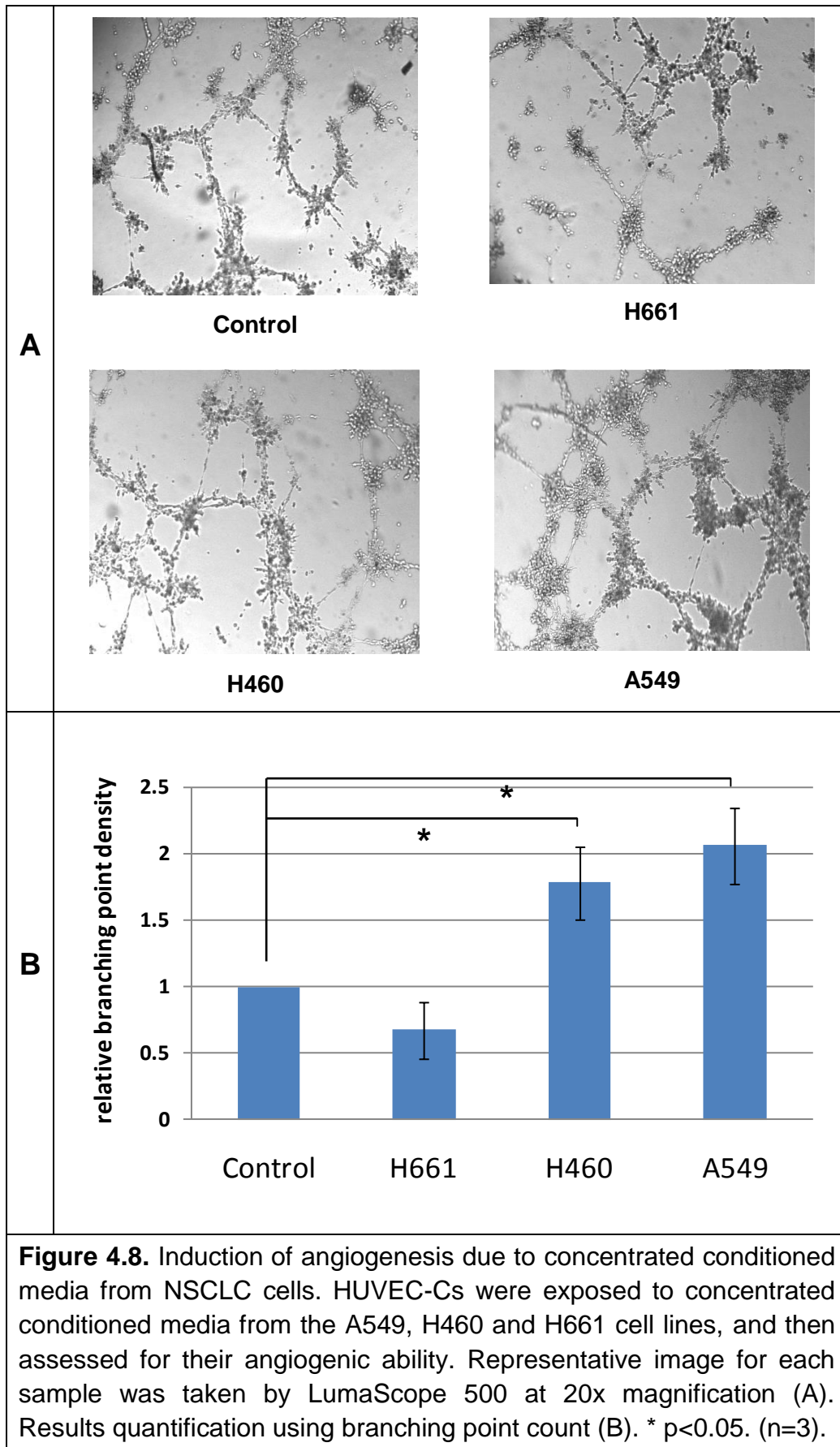
4.3.4.3 Validation of angiogenesis assay

Prior to using the *in vitro* angiogenesis assay for assessing the functionality of MMP10 protein, it was important to validate it first by evaluating the effect of MMP10 addition on the tube formation of HUVEC-Cs. To achieve this, cells were treated with ascending recombinant MMP10 concentrations and assessed for their ability to form tube-like structures using branching point counts. The data show that adding increasing amounts of MMP10 protein resulted in an increase in angiogenesis in a dose dependent manner (Figure 4.7). Significantly higher angiogenesis with 25nM MMP10 was observed

compared to control. Inhibiting the activity of MMP10 clearly reduced the angiogenesis, as demonstrated when GM6001 was used.

In addition, for further validation and evaluation of whether this assay is suitable for assessing the effects of MMP10 in cell-conditioned media, HUVEC-C cells were treated with concentrated conditioned media from the NSCLC cells in the panel and data was compared to the Western blotting results. As would be expected, results in Figure 4.8 showed an induction of angiogenesis due to MMP10 and other potential angiogenic factors secreted by the NSCLC cells with the angiogenesis capacity consistent with the MMP10 levels detected by Western blotting (Chapter 3, Figure 3.7). For the A549 and H460 cells, a marked induction in angiogenesis capacity due to secreted MMP10 was almost identical to the high MMP10 level detected by Western blotting in these cell lines. For the H661, no significant effect on angiogenesis capacity was observed, corresponding to low MMP10 protein by Western blotting. Overall, these data confirm suitability and validate this assay.





4.3.4.4 In vitro angiogenesis assay for H460-clone2.

Since MMP10 overexpression was observed at both the genetic and protein levels for the H460-clone2 cells, it was conceivable that they might have potential as an MMP10 NSCLC preclinical model. This overexpression of MMP10 however was not associated with phenotype changes; therefore, the functionality of the protein being secreted has to be demonstrated.

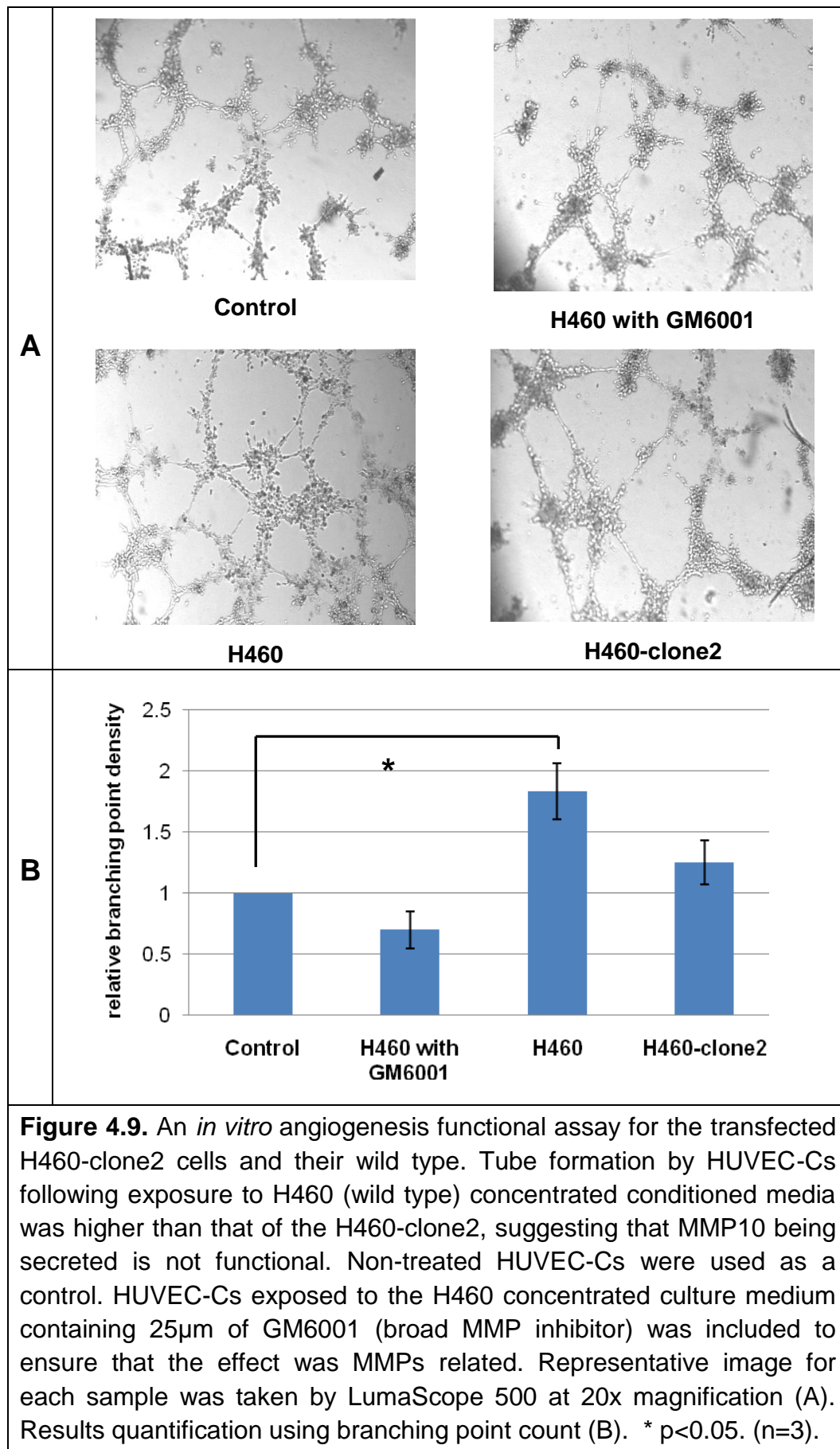
As an increase in the functional secreted MMP10 results in increased angiogenesis, the angiogenic capacity of the H460-clone2 was evaluated using the *in vitro* angiogenesis assay. The wild type H460 was also included for comparison. As would be predicted, the angiogenesis capacity seen for the wild type H460 concentrated conditioned media was significantly higher than for the control. In contrast, no marked increase in angiogenesis was observed for the H460-clone2 cells when compared to the control (Figure 4.9). While high angiogenesis capacity was observed with the H460 concentrated conditioned medium, the addition of 25µm of GM6001 (broad MMP inhibitor) clearly decreased it, indicating that the effect seen was MMP related (Figure 4.9). Overall, this suggests that the MMP10 being overexpressed in the conditioned media of the H460-clone2 cells is inactive, certainly in an *in vitro* setting.

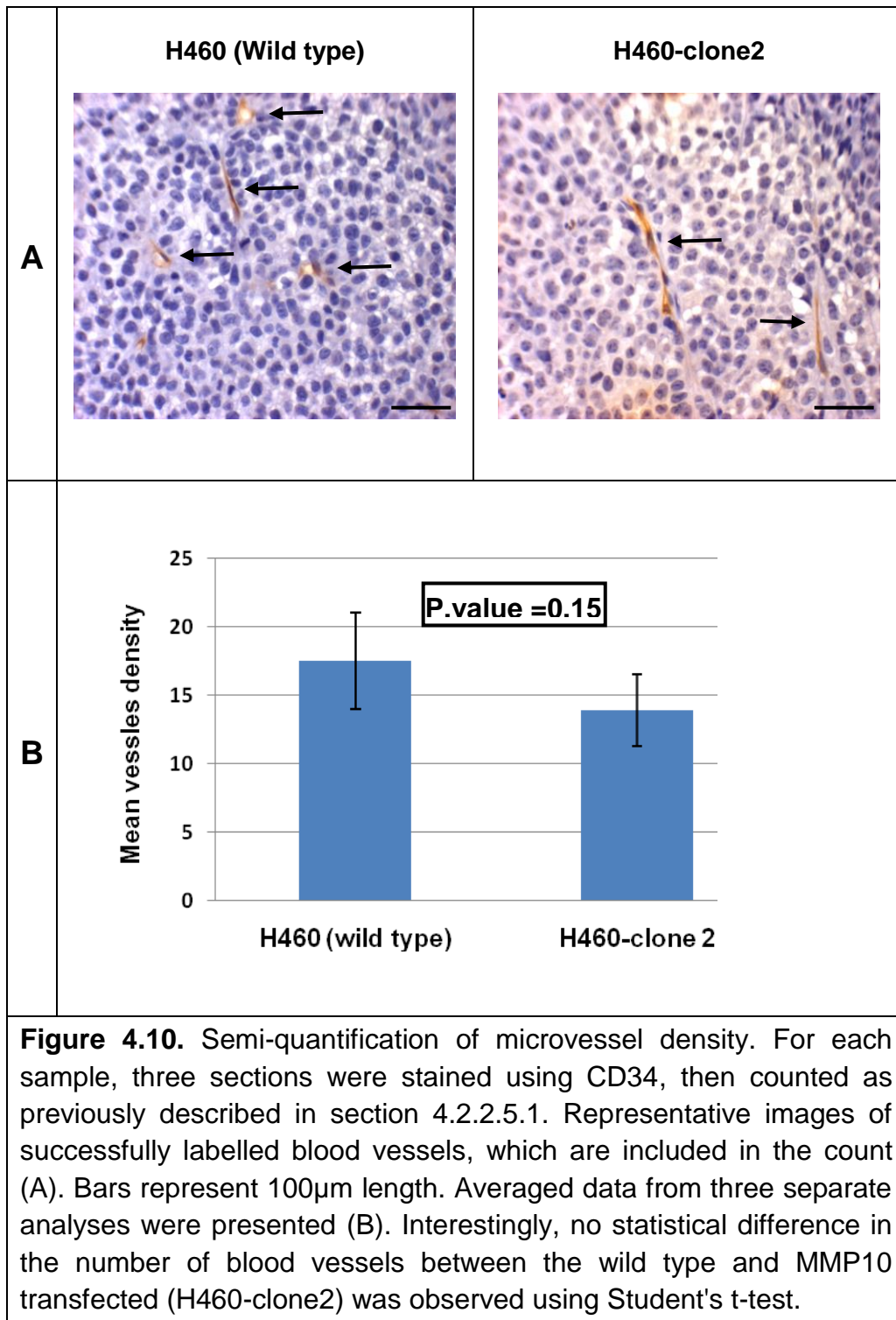
4.3.4 Confirmation of the Lack of Functional Activity of the H460-clone2 MMP10

To see if growing the cells in a more supportive environment *in vivo* would enhance MMP10 activity in the H460-clone2 cells, sections of tumour taken

from a previous *in vivo* study conducted to assess the consequence of MMP10 overexpression on tumour growth were evaluated for evidence of angiogenesis.

Although the semi-quantitative analysis of CD34 immunolabelling demonstrated a slight reduction in the vascular density of H460-clone2 xenografts compared to the wild type, there was statistically no significant difference between the two types of tumours (Figure 4.10). This provides further evidence that the elevated MMP10 levels seen in the H460-clone2 cells were non-functional. At this stage, it was decided not to make further use of the H460-clone 2 as an MMP10 overexpressing model.





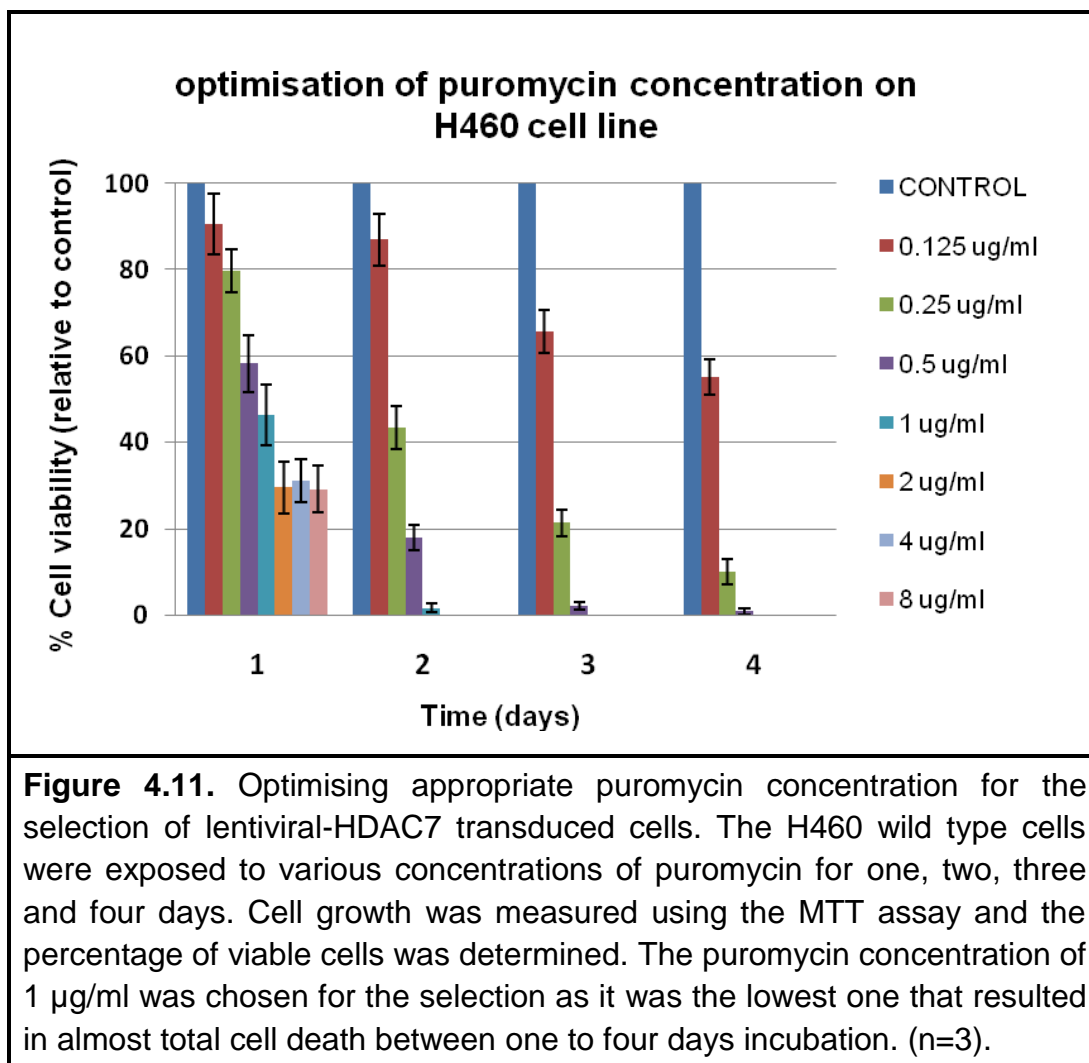
4.3.5 Lentiviral Transduction Mediates Stable HDAC7 in H460 Cells

Due to the failure of the direct transfection of MMP10 to generate a functionally overexpressing MMP10 preclinical model, another approach was tried. From the literature, it is known that HDAC7 silencing increases MMP10 expression in endothelial cells (Chang et al., 2006). To investigate whether this correlation also occurred in the NSCLC cells, HDAC7 was silenced permanently in the H460 cells by transcriptional stable gene silencing using the shRNA lentiviral transduction system as described in section 4.2.2.4.2.

4.3.5.1. Optimisation of puromycin concentration for H460-shHDAC7 cell selection.

To ensure that only stable transfectants were used for analysis, H460-shHDAC7 cells were selected using puromycin antibiotic. The ideal concentration to use for the selection was determined using a growth inhibition assay for the H460 cell line as described in section 4.2.2.4.3.

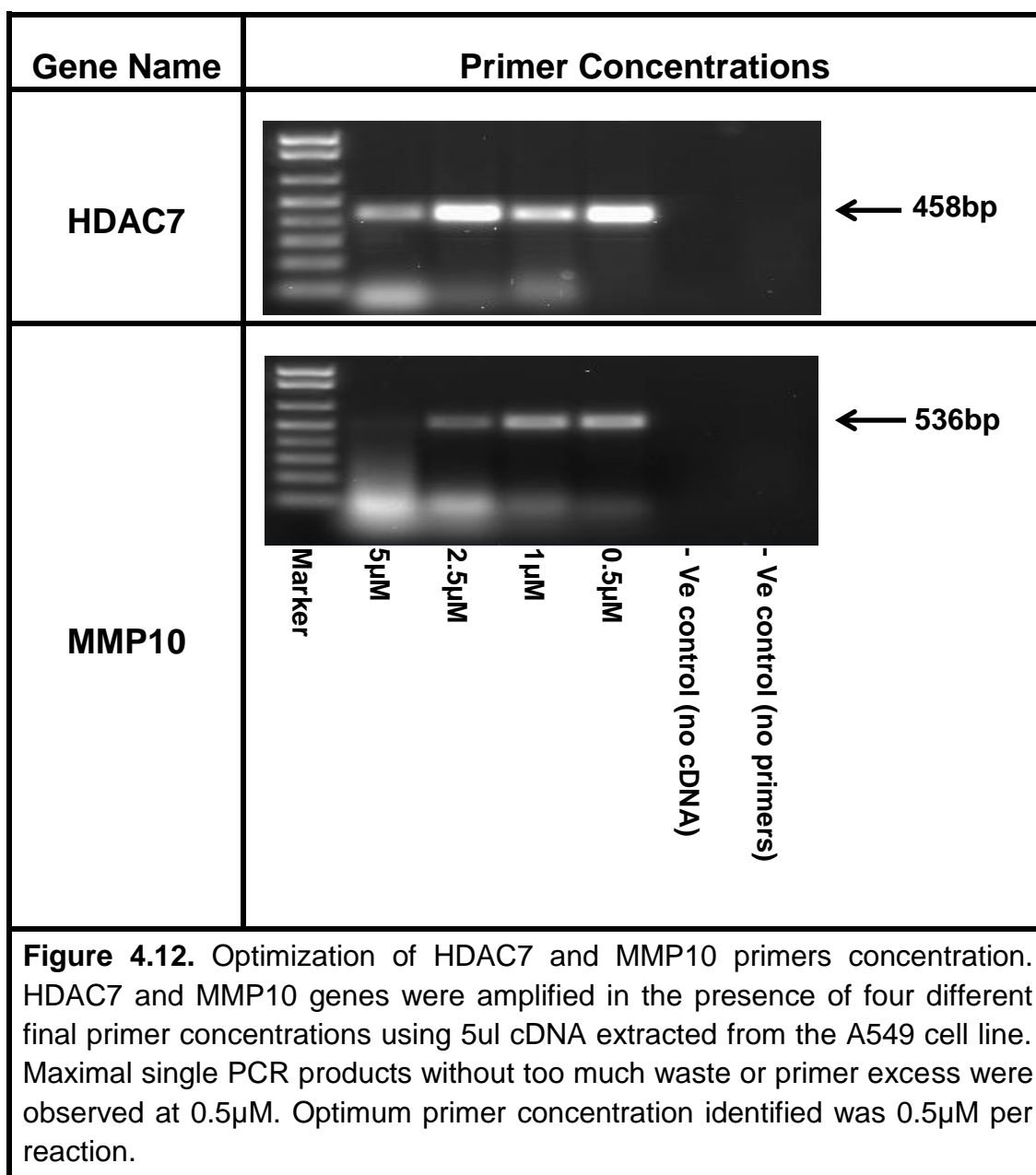
From the results shown in Figure 4.11, the minimum concentration of puromycin required to kill 100% of the H460 wild type cells within one to four days was 1ug/ml. This was chosen as the optimum concentration of puromycin for selection.



4.3.5.2 Optimisation of HDAC7 and MMP10 primers for RT-PCR analysis.

In terms of investigating the possible relationship between HDAC7 and MMP10 at the genetic level, primer concentration for both genes was optimised to ensure maximum accuracy and efficiency. A range of primer

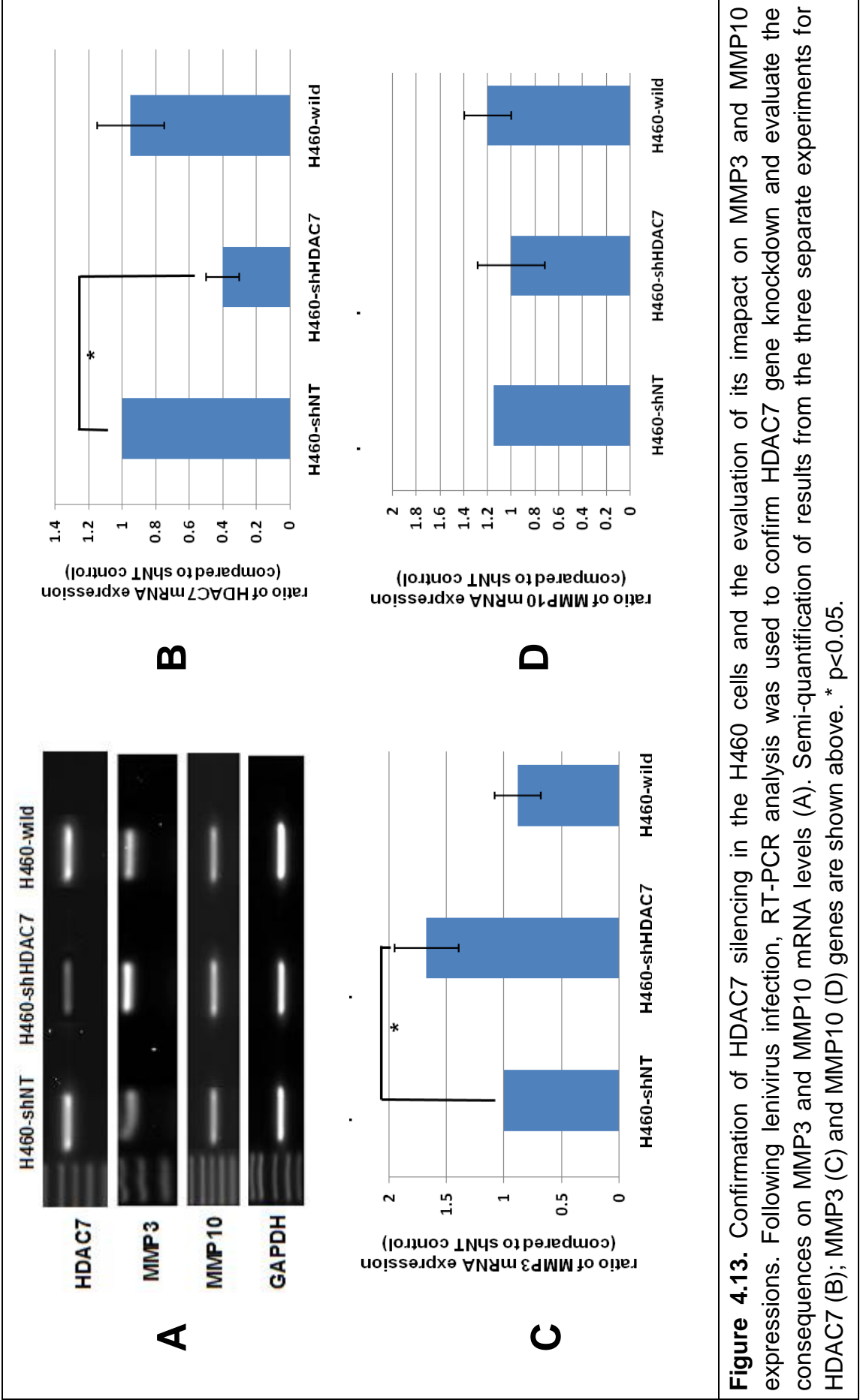
concentrations (0.5 μ M- 5 μ M) for HDAC7 and MMP10 was tested using the A549 cDNA as template. As the lowest primer concentration that produced the maximal single PCR product without excess primer was 0.5 μ M per 20 μ l reaction, it was chosen as the optimum primer concentration for the future PCR for HDAC7 and MMP10 genes (Figure 4.12).



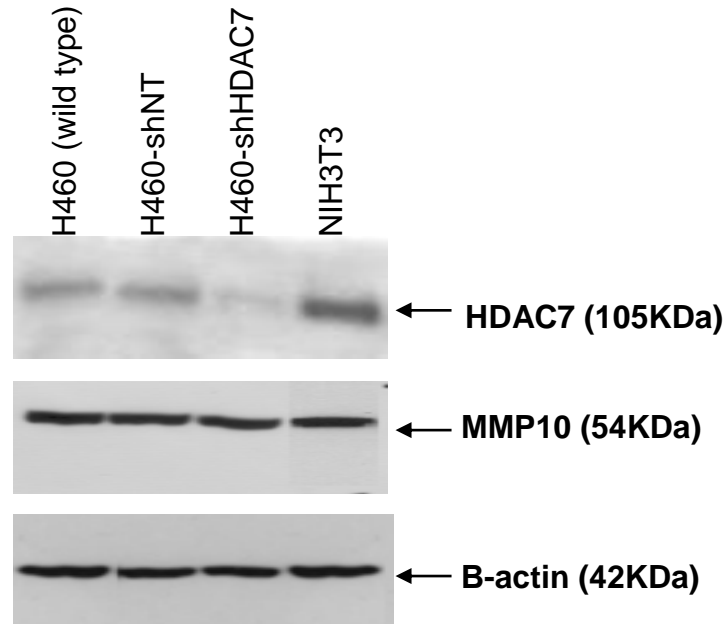
4.3.5.3 Impact of stable HDAC7 silencing on MMP3 and MMP10 expression in the H460 cells.

Following lentivirus infection, cells were verified at the transcriptional level for the expression of HDAC7 to ensure successful silencing. RT-PCR analysis demonstrated a significant HDAC7 gene knockdown in H460-shHDAC7 compared to the H460-shNT cells (Figure 4.13, A and B). Further evaluation of the long term impact of this knockdown on MMP expression was performed. Interestingly, HDAC7 silencing resulted in no change on MMP10 expression in H460 cells as shown in Figure 4.13, A and D. In addition, a significant elevation of MMP3 expression was observed as a result of HDAC7 down-regulation in these cells (Figure 4.13, A and C).

The effect of HDAC7 silencing on MMP3 and MMP10 observed at the transcriptional level should also be confirmed at protein level. However, an MMP3 antibody that does not cross-react with the closely-structured MMP10 protein could not be identified (See 3.4.5.1). As a consequence, protein analysis was limited to MMP10 only using the validated MMP10 antibody as confirmed in section 3.4.5.1. Similar to mRNA levels, marked HDAC7 protein silencing was achieved, but did not cause any change to the MMP10 protein levels (Figure 4.14). Although the long-term investigation did not reveal an MMP10 expression model, it demonstrated for the first time potential negative correlations at the transcriptional level between HDAC7 and MMP3 in the H460 cell line.



(A)



(B)

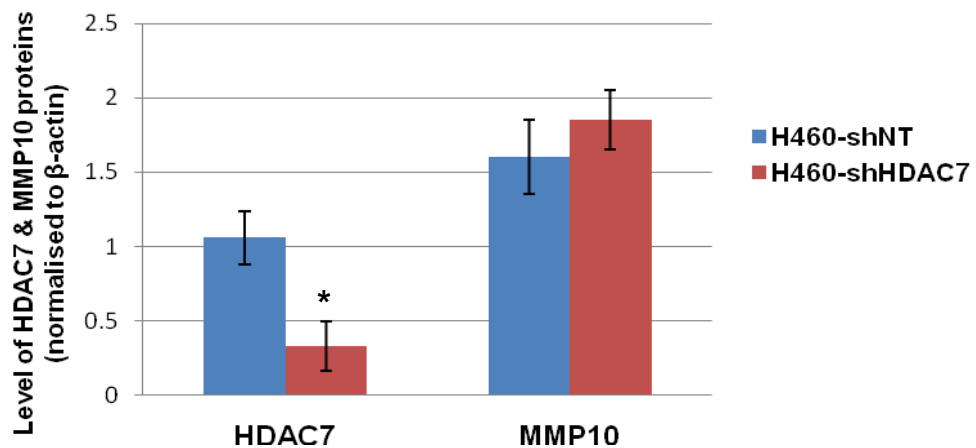


Figure 4.14. Verification of HDAC7 silencing at protein level and the evaluation of its impact on MMP10. Although a marked HDAC7 knockdown was achieved, no marked change in MMP10 expression was detected using Western blotting. Immunoblot images were shown in (A) and semi-quantification of results for H460-shNT and H460-shHDAC7 was presented in (B). A positive control (NIH3T3 whole cell lysate) for HDAC7 was used in compliance with the antibody supplier recommendations. β -actin was used as loading control. Data shown represents means \pm SD of three different experiments.* $p < 0.05$. For HDAC7 blot full image, see appendix 6.

4.3.6 Transient Transfection Studies

Since no stable MMP10 overexpressing model was identified, the next step was to try and develop a transient MMP10 model to be used for insight investigations. Transient gene impact studies based on RNA transfection have several advantages over the long term studies. Most importantly, there will be no risk of integration into the host genome, thereby causing relatively minimal cell stress (Kim and Eberwine, 2010; Yamamoto et al., 2009).

4.3.6.1 Optimising of siRNA knockdown conditions using HDAC7 siRNA.

Low transfection efficiency is the most common cause of unsuccessful siRNA gene knockdown experiments. To ensure high levels of transfection efficiency with minimal impact on cell viability, protocol optimisation was performed to choose the appropriate concentrations of siRNA and the transfection reagent to be used in the transfection procedure. The post transfection period was also optimised to ensure high-throughput gene silencing.

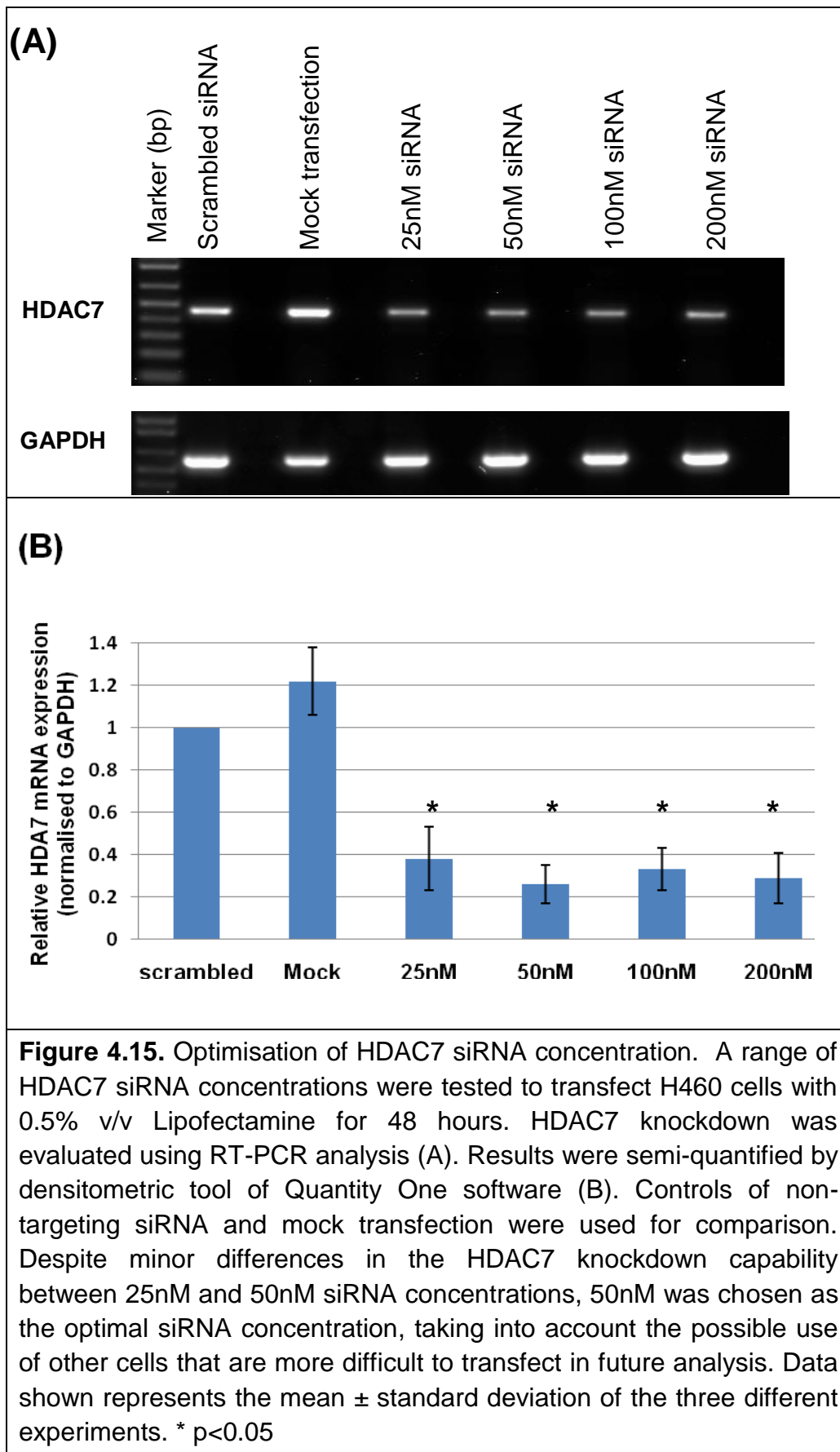
4.3.6.2 Optimising appropriate siRNA concentration for the transfection of the H460 cell line.

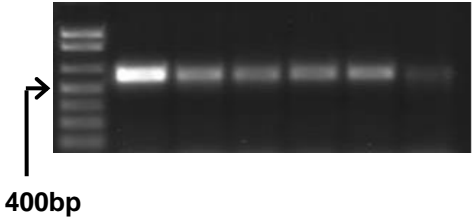
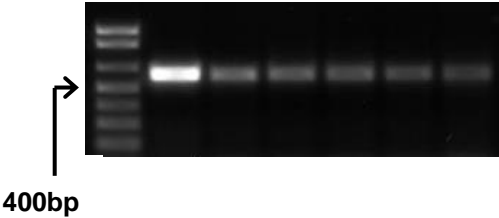
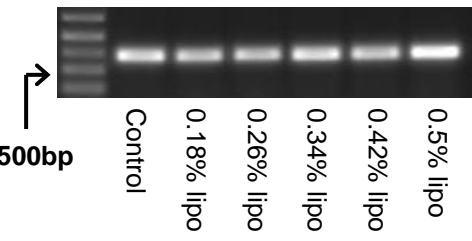
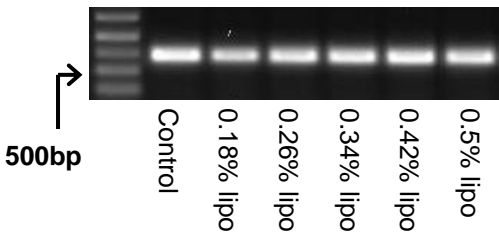
Optimisation of siRNA concentration on the H460 cells was performed using several concentrations of HDAC7-siRNA as described in section 4.2.2.7.2. A marked HDAC7 knockdown was achieved from as low as 25nM siRNA. Increasing the siRNA concentration from 25nM to 200nM did not improve the HDAC7 knockdown. Despite minor differences in HDAC7 knockdown capability

between 25nM and 50nM siRNA concentrations, 50nM was chosen as the optimal siRNA concentration, taking into consideration that results of this optimisation may be applied to other cells that are more difficult to transfect in future analysis (Figure 4.15).

4.3.6.3 Optimisation of a Lipofectamine RNAiMAX concentration for H460 transfection.

Optimising the concentration of the transfection reagent (Lipofectamine) is important for a successful siRNA delivery into cells. An ideal concentration of the transfection reagent is one that can yield a marked target gene silencing without significant cell mortality. To achieve this, the optimal concentration of 50nM HDAC7 siRNA and a range of Lipofectamine RNAiMAX concentrations (0.18, 0.26, 0.34, 0.42 and 0.5% v/v) were tested for H460 cell transfection at two time points. Lipofectamine RNAiMAX concentration of 0.5% v/v shows the highest transfection efficiency achieved with approximately 90% and 75% gene silencing for 24 and 48 hours post-transfection periods respectively (Figure 4.16).



	24 hours	48 hours
HDAC7		
GAPDH		

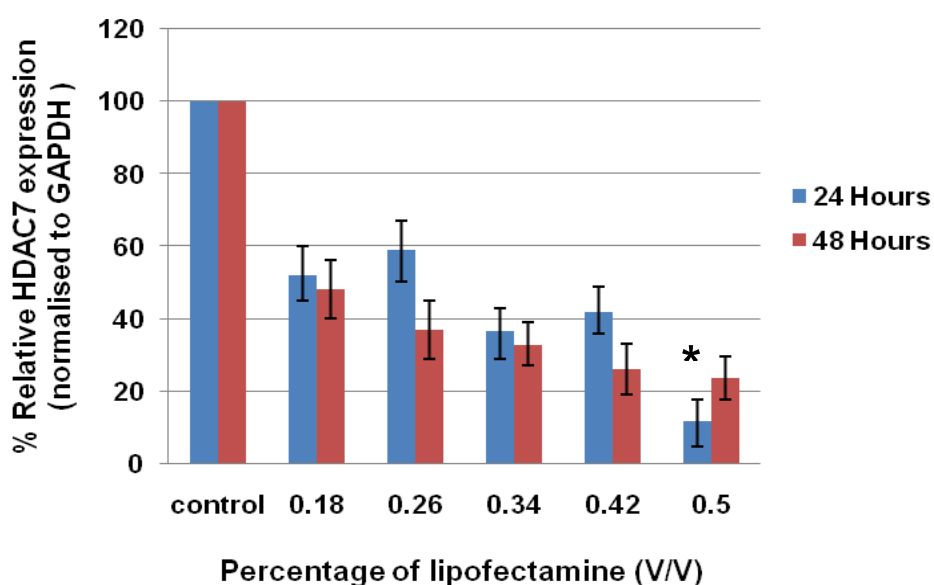


Figure 4.16. Identification of optimal Lipofectamine concentration for H460 cells transfection. Among the concentrations tested, the use of 0.5% v/v Lipofectamine RNAiMAX concentration results in the highest transfection efficiency achieved for both 24 and 48 hours. As such, this was chosen as the optimal concentration. The RT-PCR was performed for HDAC7 and GAPDH genes, followed by semi-quantification of the results by densitometry. Data shown represents the mean \pm standard deviation of the three different experiments. * $p < 0.05$.

4.3.6.3.1 Evaluation of Lipofectamine toxicity on H460 cells.

To evaluate whether the identified optimal concentration of Lipofectamine RNAiMAX has an impact on cell health, toxicity on the H460 cells was measured by MTT assay as described in section 4.2.2.3.3. Despite a minor reduction in cell viability observed in 0.58% v/v concentration, this analysis generally revealed no marked differences in viability between treated and non-treated cells as shown in Figure 4.17. As it demonstrates no considerable increase in toxicity, Lipofectamine concentration of 0.5% v/v was chosen as optimal for future experiments.

4.3.6.4 Duration of transient HDAC7 knockdown by siRNA transfection.

H460 cells were transfected in a six-well plate using the optimal transfection conditions identified (50nM HDAC7-siRNA and 0.5% v/v lipofectamine/well) for three post-transfection periods (24, 48, and 72 hours). Histone deacetylase 7 silencing was induced at as little as 24 hours post-transfection and continued over the next 48 hours (Figure 4.18). Results of the semi-quantification revealed that there was no marked difference in the gene silencing for the three time points tested, suggesting a constant inhibitory effect. Based on this, it was decided to choose 48 and 72 hours as the optimal post transfection periods for the analysis of the HDAC7 gene silencing effects.

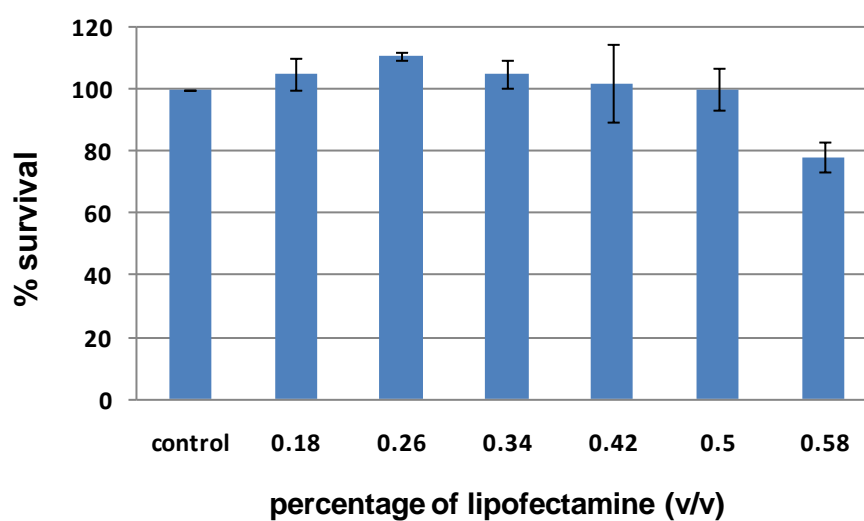
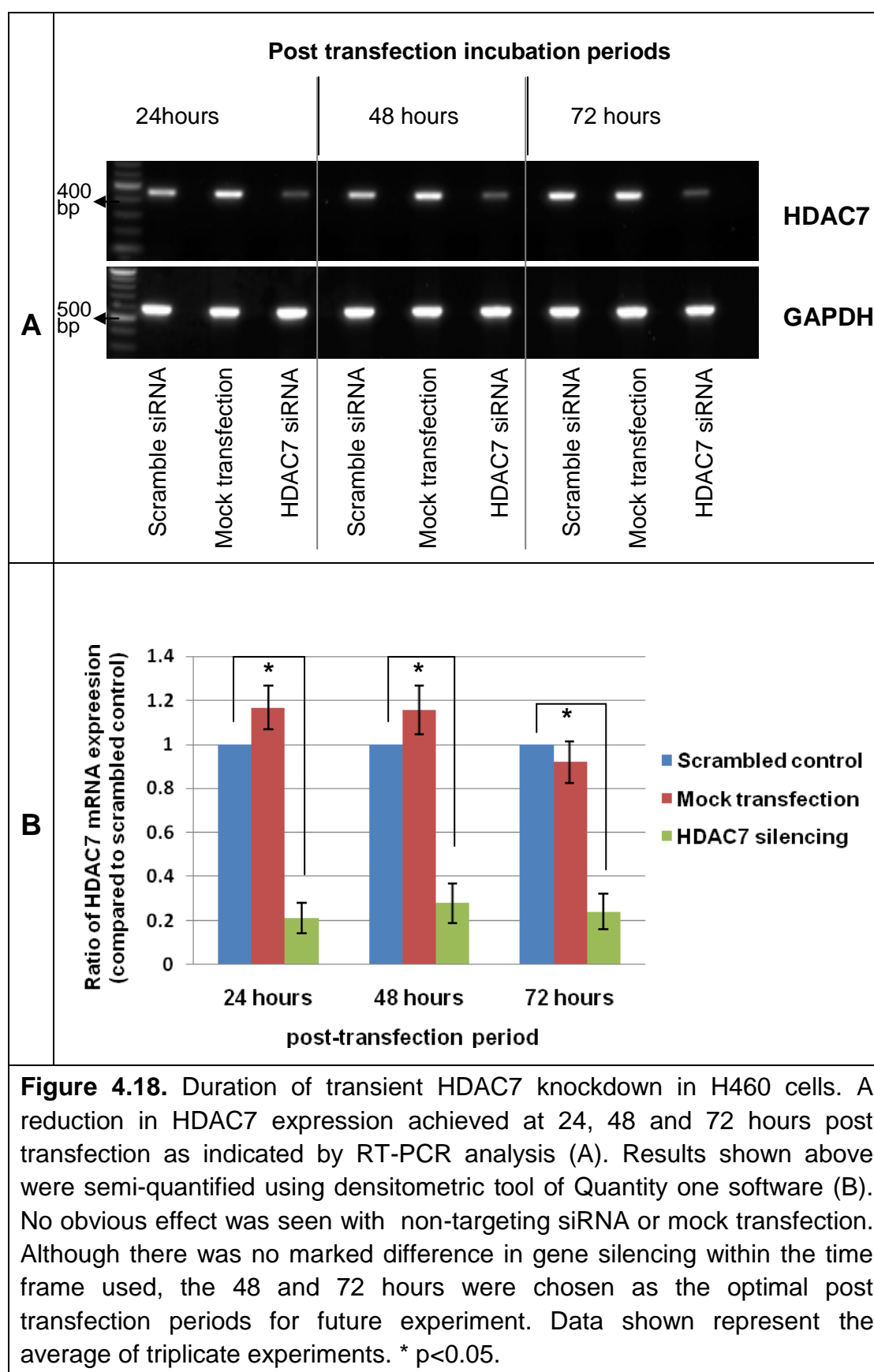


Figure 4.17. Evaluation of Lipofectamine toxicity on H460 cells using growth inhibition-based MTT assay. By following the procedure described in section 4.2.2.7.3.1, no marked reduction in cell viability was observed with Lipofectamine concentrations from 0.18 to 0.5% v/v. As it shows no considerable increase in toxicity, Lipofectamine concentration of 0.5% v/v was chosen as the optimal Lipofectamine concentration for future experiments. Data shown represents the means \pm SD of the three different experiments.



4.3.7 siRNA Mediates Silencing of HDAC7 in H460 Cells

Following the optimisation of the transfection conditions (50nM siRNA-HDAC7 and 0.5% v/v lipofectamine), a significant transient HDAC7 knockdown was achieved, and these cells were used for the study of the short term impact of HDAC7 silencing.

4.3.7.1 Impact of HDAC7 silencing on MMPs in H460 cells

While it has been demonstrated in other cell types that transient HDAC7 knockdown leads to the modulation of not only MMP10, but other endoproteases, such as MMP14 and MMP13 (Ha et al., 2008; Higashiyama et al., 2010) as well, this has not been reported for NSCLC cell lines. Therefore, this was evaluated here by assessing the mRNA levels of 22 MMPs in transiently HDAC7-silenced H460 cells.

Among the evaluated MMPs, results in Figure 4.19 show that HDAC7 silencing resulted in a marked induction of MMP3 mRNA expression, confirming that a negative correlation exists between HDAC7 and MMP3 in the H460 cell line. A slight decrease of MMP15 expression caused by this silencing was also observed. Matrix metalloproteinase 14 mRNA expression was below the detection level of this analysis. Similar to the long term impact studies, no effect on MMP10 mRNA expression was detected due to HDAC7 silencing. This suggests that the relationship between MMP10 and HDAC7, as seen in other studies, might be cell type specific.

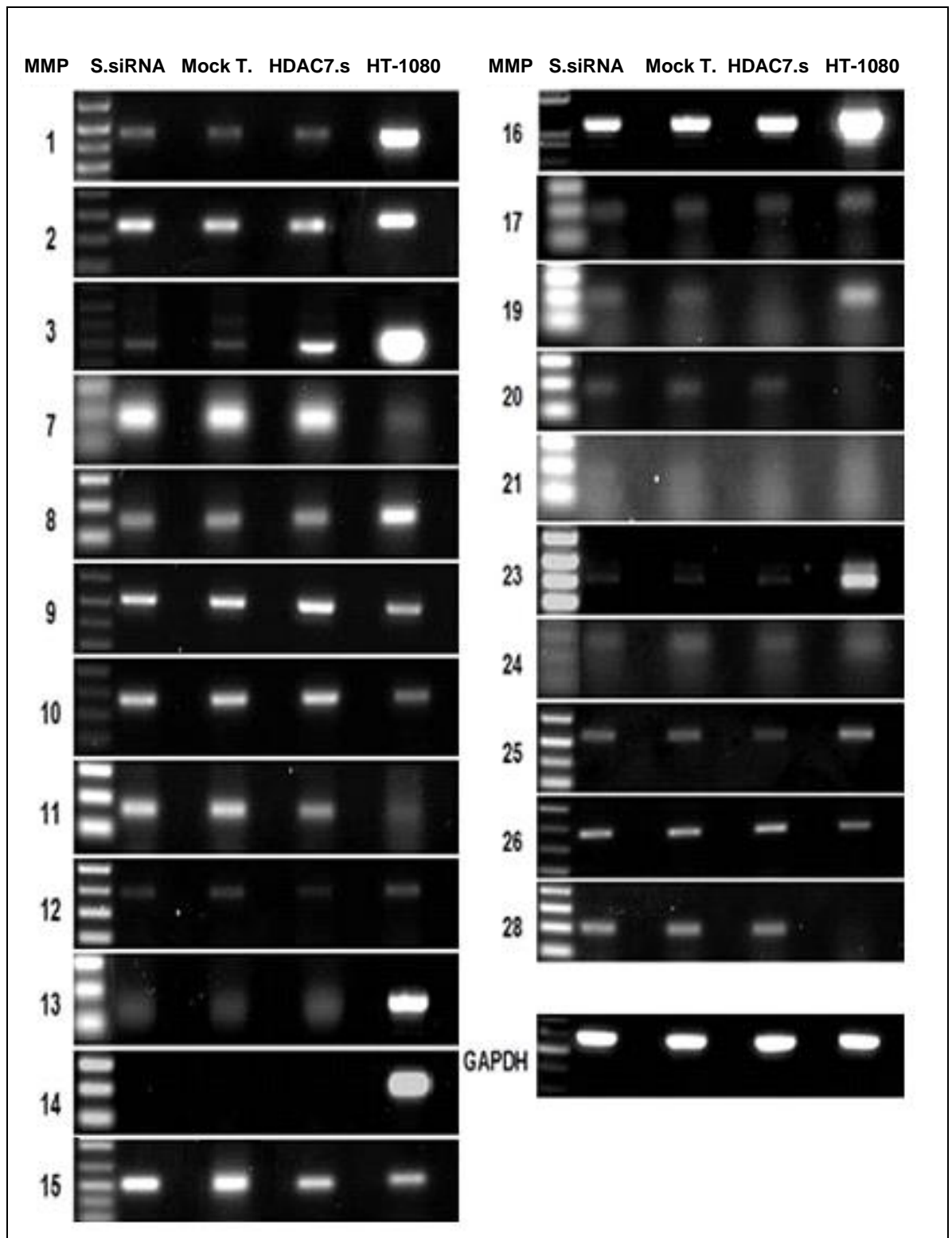
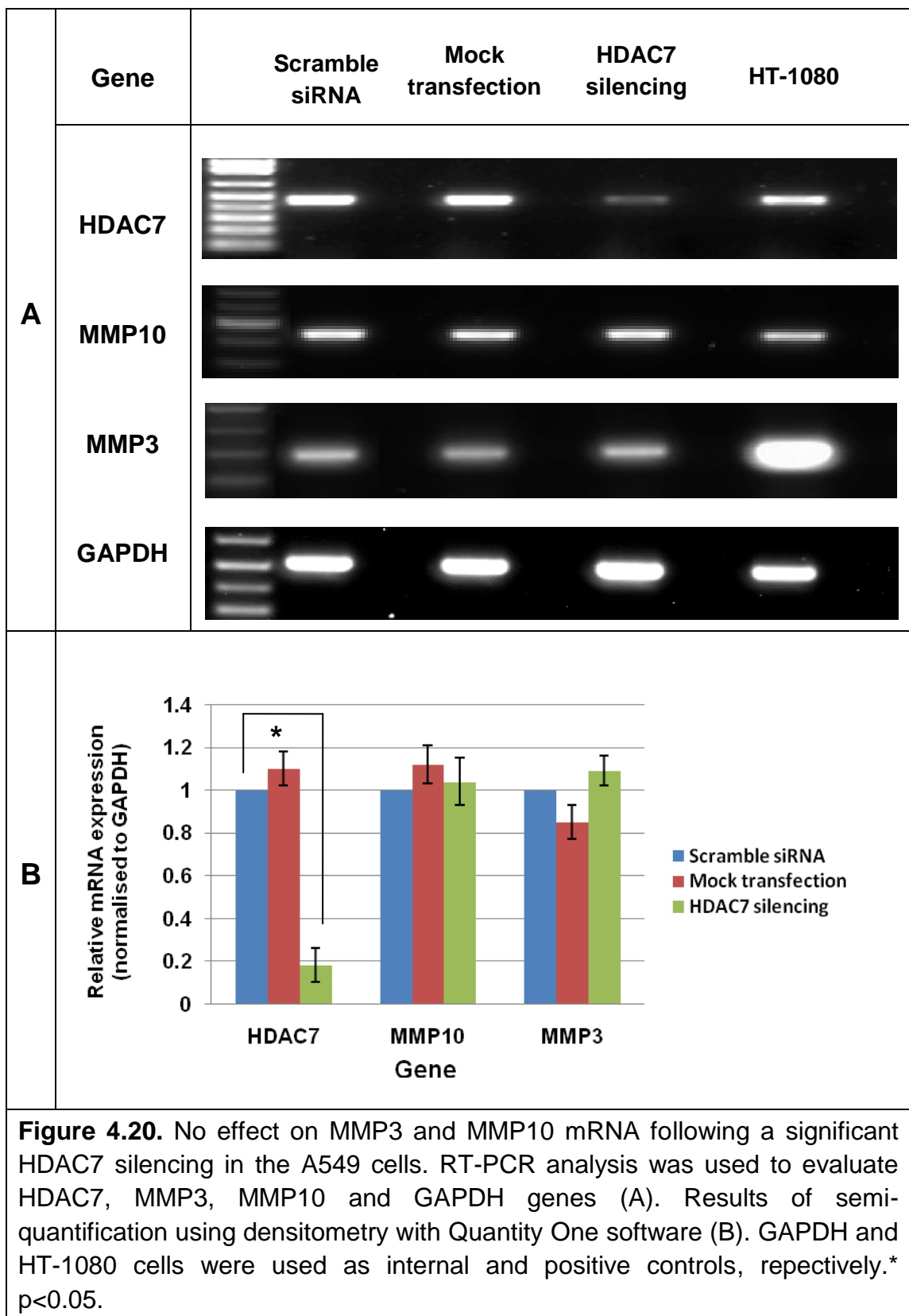


Figure 4.19. Impact of HDAC7 transfection on 22 MMPs mRNA expression using RT-PCR analysis. The HDAC7 silencing in the H460 cells results in a marked increase of MMP3 expression. Since most MMPs are mainly expressed in the HT-1080 cell line, it was used as a positive control. GAPDH was also used as a loading control. S.siRNA: scrambled siRNA; mock.T: mock transfection; HDAC7.s: HDAC7-siRNA

4.3.7.2 Lack of effects of HDAC7 silencing on MMP3 and MMP10 induction in A549 cells.

To address whether the reverse correlation observed for HDAC7 and MMP3 in the H460 cells is cell type specific, transient HDAC7 silencing in the A549 cells was performed. Although significant HDAC7 silencing was achieved in the A549 cells following the transfection procedure, no marked MMP3 induction was observed (Figure 4.20) unlike for the H460 cells. Thus, the relationship observed between HDAC7 and MMP3 might be cell type specific.

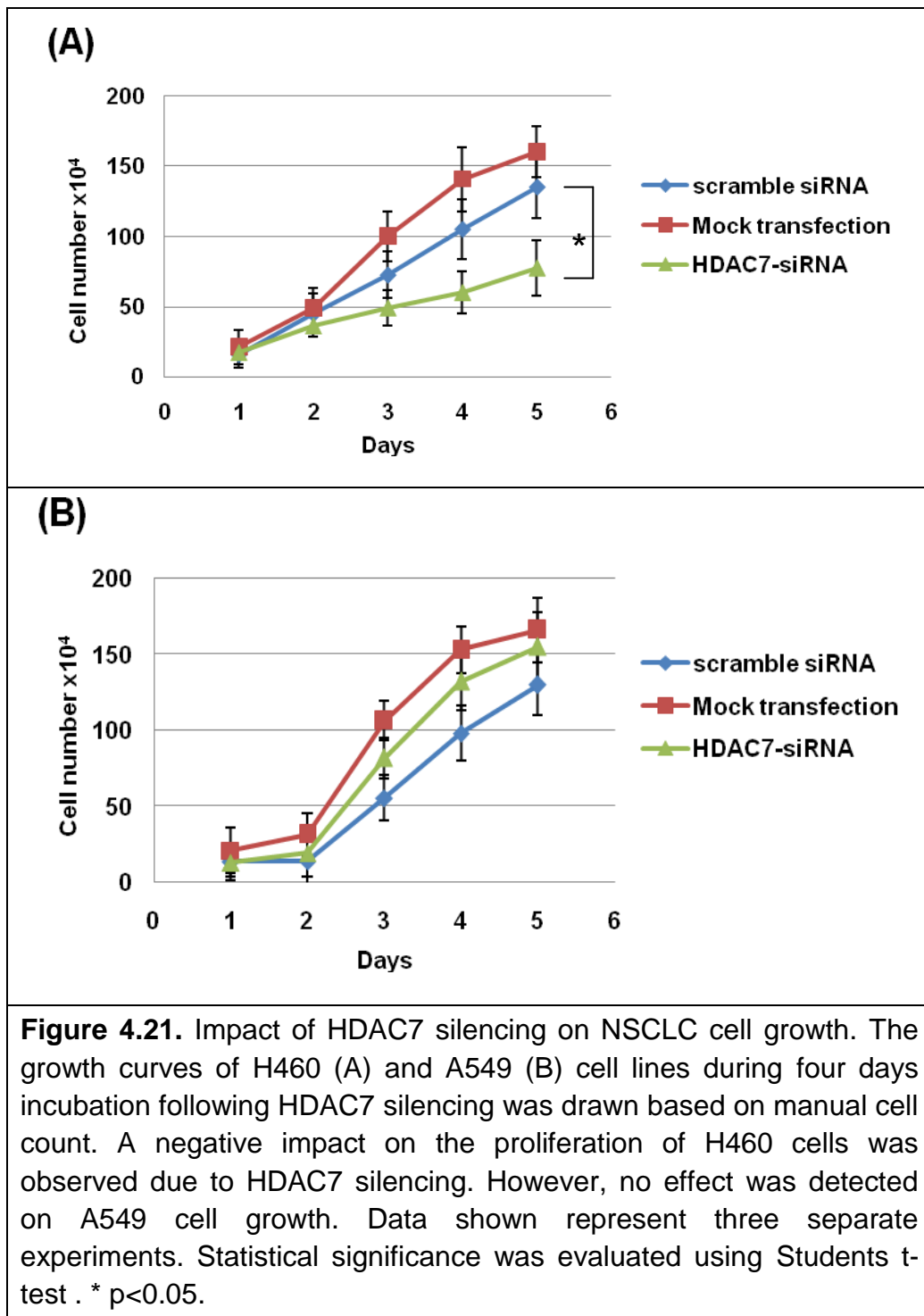
To confirm the absence of a relationship between HDAC7 and MMP10 in NSCLC, the impact of HDAC7 down-regulation on MMP10 expression in the A549 cells was also evaluated. Similar to H460 cells, no effect on MMP10 mRNA expression was observed due to HDAC7 silencing (Figure 4.20), suggesting no relationship between HDAC7 and MMP10 in terms of NSCLC.



4.3.7.3 Impact of HDAC7 silencing on NSCLC cell growth.

To evaluate the influence of HDAC7 knockdown on the growth of NSCLC cells, a comparison in proliferation rate was made between the HDAC7 transfected cells (A549-siRNA and H460-siRNA) and their corresponding controls. Following the optimal transfection procedure, HDAC7 silencing was verified by RT-PCR analysis and cells were counted throughout the next five days.

As has been shown, a marked HDAC7 silencing was successfully achieved in both the A549 and H460 cells as suggested by the RT-PCR. However, HDAC7 silencing results in a marked reduction of the H460 cell numbers (Figure 4.21a), while no effect was observed in the case of A549 (Figure 4.21 b). This suggests that a diversity between A549 and H460 in terms of HDAC7 function might exist.



4.4 Discussion

Overexpressing models are important in elucidating the function of specific proteins. Several MMP overexpressing preclinical models have been useful in assessing their roles in tumour progression. An MMP12 overexpressing model has shown MMP12 to play a key role in myelopoiesis modulation, immune suppression and lung tumourigenesis (Qu et al., 2011). Similarly, an MMP14 overexpressing model has shown MMP14 to be important in cell migration, this being via EGFR transactivation (Langlois et al., 2007). In human glioma, using an overexpressing model, MMP26 has been shown to promote cell invasion both *in vitro* and *in vivo* (Deng et al., 2010). As such, developing an MMP10 overexpressing preclinical model for NSCLC is important to elucidate the functions of MMP10 in this cancer.

Since the H460-clone2 cell line was previously engineered in this laboratory to overexpress MMP10, it was decided to confirm MMP10 levels in this model initially. The relative resistance to the selection marker (G418) observed in the H460-clone2 over the wild type is an early evidence of the presence and functionality of the MMP10 vector used. At the verification of the H460-clone2 by RT-PCR, a band at ≈ 700 bp was linked to mouse MMP10 mRNA. However, it has to be considered that the lack of band in the corresponding control (H460-wild type) could be due to the use of mouse primers on human cells. Initially, this vector was designed based on the findings described by (Madlener and Werner, 1997), and the right size for the mouse mRNA was calculated using their reported sequence in a blast search. Although the main focus of the present study is human MMP10, the use of a vector encoding mouse MMP10

should not compromise the results, as most MMP members, including MMP10, share the same sequence among the majority of vertebrates (Jackson et al., 2010).

The induction of angiogenesis was used as an indication for secreted MMP10 functionality in the present study. H460-clone2 did not cause any increase in both the tube formation capacity of HUVEC-Cs *in vitro* and the tumour microvessels density *in vivo*, indicating a lack of functional MMP10 in these cells. While the *in vitro* angiogenesis assay was validated to assess MMP10 functionality using recombinant MMP10 protein, the conditioned media from cells contain not only MMP10 but thousands of proteins that can influence the tube formation of HUVEC-Cs. To ensure the effect seen in this study on HUVEC-Cs, angiogenesis capacity was MMP-related, cells treated with the broad spectrum metalloprotease inhibitor (GM6001) was used as negative control. GM6001 has been shown to markedly decrease *in vitro* angiogenesis in several studies (Galardy et al., 1994; Koike et al., 2003; Witte et al., 1998). In accordance, the angiogenesis capacity was reduced when the HUVEC-Cs were exposed to the recommended concentration of GM6001 in the current study, indicating that the effects seen were related to MMP. As no specific MMP10 inhibitor is currently available and no MMP10-negative cell line was identified in this study, the use of a broad spectrum MMP inhibitor was the only option. Despite this, the lack of angiogenesis potential of H460 clone 2 could be due to the influence of the vector cloning on other angiogenic factors, thereby affecting the tube formation results. In addition, suitable control with non-targeting vector (empty vector) was not included to exclude the influence of transfection process on the cell behaviour which could be the case here. A better methodology would

be to set a comparison between the H460-clone2 and a proper empty-vector control, as well as including a confirmed specific MMP10 inhibitor, if this becomes available in the future. Overall, taking all these factors into consideration, caution was considered when interpreting the results of the angiogenesis assay regarding the H460-clone2. The results observed in the H460-clone2 cells of low angiogenesis potential *in vitro* and the absence of microvessels density induction *in vivo* indicated that the elevated MMP10 in these cells was not functional. Thus, they were not used for further analysis and another approach was taken to generate MMP10 overexpressing cells.

It has been reported that class II HDAC, HDAC7, represses MMP10 in the developing vasculature *in vivo*, suggesting a relationship between HDAC7 and MMP10 in endothelial cells (Chang et al., 2006). Such a relationship was observed in another study, confirming that the repression of MMP10 expression is dependent on HDAC7 activity or expression (Ha et al., 2008). Therefore, HDAC7 was silenced in the H460 cells in the current study to generate a functionally overexpressing MMP10 NSCLC preclinical model. While a significant HDAC7 knockdown (60%) was better achieved in the H460-shHDAC7 cells compared to control, more efficient HDAC7 gene silencing was expected (not less than 80%) as a lentiviral transduction system was used (Karnabi et al., 2009; Karra and Dahm, 2010; Yu et al., 2013). Several factors related to the gene of interest or the lentivirus itself could be the reasoning for this observation. For example, it was found that the virus integration site in the genome is critical for controlling the transcription of the gene of interest (Park, 2007). As a consequence, little gene silencing or gene expressing might be due to the viral integration into inactive heterochromatin. Another example is the

involvement of histone deacetylation process in the lentiviral transgene capability, which was reported in embryonic stem cells (Ma et al., 2003), and this could be evidenced here. Further studies reveal that determining the integration site of lentivirus on the DNA is based on histone function (Wang et al., 2007). As such, silencing HDAC7 might result in low histone deacetylation, thereby influencing the efficiency of lentiviral transduction.

In contrast to the reported relationship between HDAC7 and MMP10, the HDAC7 knockdown did not induce MMP10 mRNA expression in the NSCLC cell lines (A549 and H460) in this study. Inconsistent with this finding, HDAC7 silencing in human HepG2 hepatocellular carcinoma cell line reportedly induces the down-regulation of MMP10 expression (Zhang and Wang, 2010). While these data reinforce that the modulation of MMP10 by HDAC7 silencing may be cell type specific, further work is required to confirm this finding.

It is important also to remember that silencing HDAC7 was reported to not only affect MMP10 but also to modulate other several genes in the endothelial cells, such as platelet-derived growth factor- β (PDGF- β), its receptor (PDGFR- β) (Mottet et al., 2007), MMP13 (Higashiyama et al., 2010), FGF1, retinoic acid receptor, gamma (RAR- γ) and TIMP1 (Chang et al., 2006; Mottet et al., 2007). Owing to the observations that HDAC7 is a major gene transcriptional regulator, the impact of transient HDAC7 silencing on the expression of other MMP-family members in the H460 cells was also evaluated. Out of all the MMPs tested, a significant induction in expression was observed for MMP3, suggesting a correlation between HDAC7 and MMP3 in these cells. The current study seems to be the first to report such a correlation at the genetic level between HDAC7

and MMP3 in the context of NSCLC. Confirming the potential of this relationship at the translational level was required, but was unachievable in this study because a specific MMP3 antibody could not be identified. Given further time, an appropriate antibody may be identified, which may make this achievable. Nonetheless, this still remains as a hypothesis that needs to be further investigated.

To ascertain whether the effects of HDAC7 silencing on MMP3 mRNA expression was specific to the H460 cell line, the impact of transient HDAC7 knockdown on MMP3 mRNA expression in the A549 cells was evaluated. No marked induction in MMP3 expression was seen with the A549 in contrast to the H460 cells, supporting the hypothesis that the HDAC7-MMP3 relationship might be cell type specific. Indeed, it was reported that the effects of the HDAC down-regulation on MMP expression might be cell type specific. Evidence of this is in the observation that trichostatin A, a class I and II HDAC inhibitor, suppressed MMP2 expression in mouse 3T3 fibroblasts, but not in human HT-1080 fibrosarcoma cells (Ailenberg and Silverman, 2002; Ailenberg and Silverman, 2003).

In explaining the relation between HDAC7 and MMP3 observed in this study, *c-Myc*, a key regulatory gene that encodes the transcriptional factor *c-Myc*, which is implicated in many cancer types, appears to be key. *c-Myc* silencing has been shown to result in a reduction in both MMP1 and MMP3 expression, thus importantly, *c-Myc* expression induces MMP3 expression (Pap et al., 2004). Although HDAC7 activity has been reported as dependent on its interaction with class I HDAC3 (Fischle et al., 2001), HDAC3 silencing with or without HDAC7

silencing has been shown to have no influence on *c-Myc* expression. This would suggest that the relationship observed in this study between HDAC7 and MMP3 is most likely occurring due to the dependent signalling events of *c-Myc*, without the involvement of HDAC3.

While assessing the impact of transient HDAC7 silencing on the growth of NSCLC cells, a reduction in the cell viability of H460, but not A549, was observed, supporting a diversity between these cell lines in terms of HDAC7 function. The lack of effect seen with the A549 cells is different from findings of another study where HDAC7 knockdown resulted in cell cycle arrest in HCT116, MCF-7 and HH cancer cell lines, supporting HDAC7 silencing-induced cell cycle arrest as a common feature in several cancer cells (Chen et al., 2009; Zhu et al., 2011). While several pathways might be involved due to the roles of HDAC7 in cancer cellular proliferation (Clocchiatti et al., 2011), the growth reduction seen here can be attributed to the resulting MMP3 overexpression or the reduction in MMP15 expression in response to the HDAC7 silencing. Since these gene results were based on semi-quantitative PCR, further validation using quantitative PCR is required. In the meantime, a possible mechanism for the growth inhibitory effect is the stimulation of cell apoptosis caused by MMP15 reduction, with strong evidence regarding MMP-15 as an anti-apoptotic factor in HeLa cells (Abraham et al., 2005). Another mechanism could be due to the stimulation of cell apoptosis caused by MMP3 expression, with close correlation reported between MMP3 and cell apoptosis (Liu et al., 2013). In addition, it has been reported that HDAC7 silencing resulted in a decrease in the growth of HeLa cells and this effect was due to a mechanism involving *c-Myc* protein (Zhu et al., 2011). Collectively, these data support the growth regulatory function of

HDAC7, probably through MMP15 anti-apoptotic activity or a mechanism involving the *c-Myc* and MMP3, a relationship evidenced earlier in this research.

Recombinant MMP10 protein increased the tube formation capacity of HUVEC-Cs in a dose dependent manner, supporting the proangiogenic role of MMP10. Likewise, MMP10 in the A549 and H460 cells induced the *in vitro* tube formation, indicating an induction in angiogenesis in NSCLC tumours caused in part by MMP10. These findings are extensively discussed in the general discussion section of this research.

In conclusion, MMP10 in the established H460-clone2 was not functional, highlighting the importance of assessing the enzyme functionality in preclinical models before conducting MMP-related studies. In terms of the relationship between HDAC7 and MMP10, HDAC7 silencing did not increase MMP10 expression, but it did increase MMP3 expression at the gene level in the H460 cell line.

While a preclinical model with high and functional MMP10 could not be identified, the involvement of MMP10 to induce angiogenesis *in vitro* was observed to be significant. Overall, the induction of angiogenesis due to strong MMP10 expression in NSCLC cells seen herein, coupled with the expression and activity of MMP10 in the NSCLC clinical samples reported in the literature, support the potential of MMP10 as a target for therapeutic intervention in NSCLC.

Chapter 5: Identification of MMP Substrates and MMP-Activated Prodrugs Specifically Cleaved by MMP10

5.1 Introduction

In the development of MMP-targeted TAPs, therapeutic drugs ('effector') are attached to an MMP substrate peptide ('trigger') to control the selectivity and specificity of the effector (Vartak and Gemeinhart, 2007). Ideally, the peptide should only be cleaved by a specific MMP, resulting in the activation of the drug. The cleavage of the peptide by other enzymes (either proteases or other MMP) can lead to premature activation and systemic side effects of the prodrugs (Chau et al., 2006a; Chau et al., 2006b). Since the substrate peptide is the key for TAP specificity, enzyme-substrate cleavage studies should be conducted to ensure the high specificity of MMP towards the selected peptides.

Based on the findings of several studies focusing on MMP substrate specificities (Deng et al., 2000; Nagase and Fields, 1996; Netzel-Arnett et al., 1991; Turk et al., 2001), several MMP- targeted TAP were rationally designed in the last decade. For example, two doxorubicin prodrugs have been reported to demonstrate promising efficacy after selective activation by MMP2, 9, and 14 (Albright et al., 2005; Lee et al., 2006). Another TAP, the colchicine derivative ICT2588, has been designed and proven to be selectively activated by MMP14 (Atkinson et al., 2010).

In terms of MMP10, there is no specific MMP10 TAP that has been developed to date in spite of its expression and activity in several cancers, including

NSCLC. One reason is the incomplete data about MMP10 synthetic substrate specificity, which is in part due to the high similarity between MMP3 and MMP10.

At protein level, the resemblance between stromelysins (MMP3, MMP10 and MMP11) has become a major issue for studies focusing on an enzyme member of this MMP subgroup. Despite the similar domain structure of MMP11 to other stromelysins, it is readily distinguished due to the differences in enzymatic activity, size and amino acid sequence (Barrett et al., 2004). Matrix metalloproteinase 3 and MMP10 are, however, similar in nearly every aspect, including the primary domain structure. They have 78% identical overall amino acid sequence and 86% similarity in terms of catalytic domain. They both have no affinity for interstitial collagen and they cleave the same extracellular matrix molecules. They also both contribute in the activation of other pro MMPs (Bertini et al., 2004; Kucukguven and Khalil, 2013). In contrast, the most obvious differences that have so far been observed between MMP3 and MMP10 are in their differential pH optimum activity against synthetic substrates and their patterns of expression in tissues (Barrett et al., 2004). For maximum activity, optimum pH for MMP3 was 5.5–6.0 while it was 7.5–8.0 for MMP10 (Gunja-Smith et al., 1989; Harrison et al., 1992). Although traditional Western blotting can be used to distinguish between MMP3 and MMP10, it highly depends on selective antibody reactivity and does not measure protein activity. Thus, there is still a need for further studies on structure activity relationship for complete discrimination between MMP3 and MMP10 proteins.

5.1.1 Aims and Objectives

The main aim of this chapter is to identify MMP10-specific cleavable sequences that could be incorporated into an MMP10-targeted TAP.

The objectives are:

- To evaluate through *in vitro* cleavage studies, if commercially available, known MMP substrates can be used to differentiate between MMP10 and MMP3 cleavage using a mass spectrometry approach.
- In addition, MMP activated TAP candidates designed in-house will be assessed for their ability to be cleaved specifically by MMP10 and MMP3, again using a mass spectrometry approach.

This approach should result in the identification of a potential candidate sequence that could be utilised in a TAP.

5.2 Materials and Methods

5.2.1 Materials

Analytical grade chemicals for activity buffer, including APMA, Tris, NaCl, CaCl₂ and Brij 35, were bought from Sigma-Aldrich (Gillingham, UK). As, were formic acid (FA) and polypropylene auto sampler vials. HPLC grade methanol and triple distilled water were obtained from Fisher Scientific (Loughborough, UK). All novel compound used were provided in-house by the chemistry department at the Institute of Cancer Therapeutics (Bradford, UK). Full recombinant human MMP10 and MMP3 catalytic domain proteins were purchased from R and D systems (Abingdon, UK) and Calbiochem (Nottingham, UK), respectively. A panel of commercially available MMP substrates, cat. Number 444215, 444220, 444228, 444230, 444258 and 444259, were obtained from Calbiochem (Nottingham, UK). The sequence of these substrates is listed in Table 5.1. The MMP3 substrate (cat. number M-2105) and MMPs substrate (cat. number M-1895) were purchased from Bachem (Bubendorf, Switzerland). Commercially unavailable peptides were custom-made at Peptide Protein Research Ltd (Hampshire, UK).

5.2.2 Methods

5.2.2.1 Enzyme activation

Matrix metalloproteinase 10 recombinant pro enzyme was pre-activated with freshly made 1mM APMA prior to being used for any activity studies. An appropriate amount of APMA was dissolved in dimethyl sulfoxide to give 100mM concentration. The APMA solution was further diluted to 1mM using an

activity buffer that contains 50mM Tris; 0.15M NaCl; 5.0mM CaCl₂; 0.05% Brij 35 and a pH adjusted to 7.5. For activation, four parts of this 1mM APMA was then mixed with one part of MMP10 pro-enzyme and incubated at 37°C for three hours. Successful activation was confirmed by SDS-PAGE with a band corresponding to 44 KDa (Figure 5.1).

5.2.2.2 Liquid chromatography (LC)

5.2.2.2.1 High performance liquid chromatography coupled with mass spectrometry (LC-MS)

Sample analysis was carried out using high performance liquid chromatography (HPLC) reverse-phase separation and MS detection system. Drugs and metabolites were separated on a C18 HIRPB Hichrom column with 5µm silica particle size and 250mm x 4.6mm inner diameter. Subsequently, a waters 2695 autosampler, waters 2996 photodiode array detector and Micromass ZMD single quadrupole electrospray with Masslynx software (Waters) was used for spectral and mass to charge the analysis of the peaks of interests.

5.2.2.2.2 HPLC running conditions

To ensure maximum resolution, mobile phase A (MPA) (90% HPLC grade water, 10% MeOH and 0.1% formic acid) and mobile phase B (MPB) (10% HPLC grade water, 90% MeOH and 0.1% formic acid) were used in an optimal gradient manner. An initial ratio of 90% MPA and 10% MPB was changed to 100% MPB over 18 minutes. The later ratio was held for seven minutes until minute 25. Then, the ratio was changed again to 90% MPA and 10% MPB and kept constant until the end of the running time. All mobile phase solvents were

degassed before pumping onto the system using vacuum filtration through a 0.45µm pore nylon filter membrane. During the running time, the mobile phase was delivered at a flow-rate of 1 mL/min. The scanning range of photodiode array detector was set between 200-400nm. The volume of injected sample was 10µL and total running time for each was 40 minutes.

5.2.2.3 In vitro MMPs-substrate cleavage study

Active MMP10 and MMP3 were tested to determine their ability to cleave commercially available MMP substrates. A list of these substrates with their sequence, molecular weight and catalogue number are in Table 5.1.

For analysis, 200ng active recombinant MMP3 or MMP10 proteins were incubated with 50µM of each substrate in the activity buffer at 37°C for 18 hours. For special circumstances where cleavage rate is evaluated, several time points at zero, 30, 60, 120 and 240 minutes were used. Once incubation was completed, sample reactions were terminated by the addition of 100% Methanol in a ratio of 1:4. In parallel, substrates in the activity buffer were incubated for the same corresponding time point to serve as a negative control.

5.2.2.3.1 HPLC analysis of substrate cleavage

The same method was used as in section 5.2.2.2.

5.2.2.3.2 LC-MS analysis for MMPs-substrate cleavage study

Mass spectrometry was used in a positive mode under optimum conditions. These include desolvation gas flow 650l/hr, cone gas flow 30l/hr, desolvation temperature 200°C, source block temperature 100°C, sample cone 30V, RF

lens 0.20V, extraction cone 5V and capillary 3.00kV. A full spectrum scan ranging from 300-900m/z was used to detect parent substrates and their metabolite as either singularly or double positive charged ions. Selected ion recording (SIR) for substrates and their possible metabolites were also used for maximum possible sensitivity.

Table 5.1. MMP Substrates Used with Full Details of Sequence. Dpa: N3-(2,4-dinitrophenyl)-L-2,3-diaminopropionyl; Bz: Benzyl; DNP: 2,4-Dinitrophenol ; MCA: (7-methoxycoumarin-4-yl)acetyl; DANSYL: 5-dimethylamino-1-naphthalenesulfonyl; p-OMeBz: S-para-methoxybenzyl

Trade Name	Catalogue Number	Substrate Sequence	Molar Mass	Supplier
MMP-2/ MMP-9 Substrate I	444215	DNP-Pro-Leu-Gly-Met-Trp-Ser-Arg-OH	1012.1	Calibochem (UK)
MMP-3 Substrate I, Fluorogenic	444220	DNP-Pro-Tyr-Ala-Tyr-Trp-Met-Arg-OH	1152.3	
MMP-7 Substrate I, Fluorogenic	444228	DNP-Arg-Pro-Leu-Ala-Leu-Trp-Arg-Ser-OH	1164.3	
MMP-8 Substrate I, Fluorogenic	444230	DNP-Pro-Leu-Ala-Tyr-Trp-Ala-Arg-OH	1042.1	
MMP-14 Substrate I, Fluorogenic	444258	MCA-Pro-Leu-Ala-Cys(p-OMeBz)-Trp-Ala-Arg(Dpa)-NH ₂	1403.5	
MMP-14 Substrate II, Fluorogenic	444259	DANSYL-Pro-Leu-Ala-Cys(p-OMeBz)-Trp-Ala-Arg-NH ₂	1168.4	
MMP-3 substrate	M-2105	Mca-Arg-Pro-Lys-Pro-Tyr-Ala-Nva-Trp-Met-Lys(Dnp)-NH ₂	1656.8	Bachem (Switzerland)
Trifluoroacetate salt	M-1895	Mca-Pro-Leu-Gly-Leu-Dap(Dnp)-Ala-Arg-NH ₂	1093.1	
Part of Proteoglycan protein (ABD1)	Designed according to (Nguyen et al., 1993)	His-Asp-Arg-Ala-Ile-His-Ile-Gln-Ala-Glu-Asn-Gly-Pro-His-Leu-Leu-Val-Glu-Ala-Glu	2249.4	Synthesised by Peptide Protein Research Ltd (UK)

5.2.2.4 Activation of MMP Targeted TAPs by MMP10 and MMP3

5.2.2.4.1 MMPs targeted TAPs

A panel of MMP-targeted TAPs developed in-house at the ICT—ICT2588 (Atkinson et al., 2010), ICT3019, ICT3120, ICT3115, ICT3198 and ICT3146—were used to evaluate the ability and selectivity of MMP3 and MMP10 to activate these prodrugs *in vitro*. The sequence of these prodrugs is listed in Table 5.2.

5.2.2.4.2 MMP-targeted compounds activation study

For analysis, 200ng of active recombinant MMP3 or MMP10 protein were incubated with 50μM of each compound in the activity buffer at 37°C for 18 hours. The long incubation time was to ensure maximum accumulation of reaction products. Once completed, sample reactions were terminated by the addition of 100% MeOH in a ratio of 1:4. In parallel, compounds alone in the activity buffer were incubated for the same time point to serve as a negative control. In addition, MMP3 and MMP10 enzymes were incubated with MMPs substrate (444228), known to be cleaved by both to serve as enzyme positive control.

Table 5.2. Illustration of MMPs Targeted TAPs Used with Their Sequence. MB2 refers to amino colchicine. FITC: Flouoroisothiocyanate; ph: 2-methoxy-6-nitrophenyl	
Prodrug	Conjugate Sequence
ICT2588	FITC- β Ala-Arg-Ser-Cit-Gly-Hof-Tyr-Leu-Tyr-MB2
ICT3120	ph- β Ala-Leu-Tyr-Hof-Gly-Cit-Ser-Arg-Tyr-MB2
ICT3146	ph- β Ala-Leu-Ala-Hof-Gly-Arg-Ser-Arg-Tyr-MB2
ICT3115	FITC- β Ala-Arg-Ser-Cit-Gly-Hof- β Ala-Leu-Tyr-MB2
ICT3019	FITC- β Ala-Arg-Ser-Arg-Gly-Hof-Tyr-Leu-Tyr-MB2
ICT3198	Sugar- β Ala-Arg-Ser-Cit-Gly-Hof-Tyr-Leu-Tyr-MB2

5.2.2.4.3 HPLC analysis

The same method was described in section 5.2.2.2

5.2.2.4.4 LC-MS analysis for the activation of MMPs-targeted compounds by MMP3 and MMP10

Mass spectrometry was set at the same parameters previously described in section 5.2.2.3.2. However, following a full scan ranging from 400-1000m/z, selected ion recording (SIR) was used for compounds of interest and their possible metabolites as illustrated in Table 5.3.

Table 5.3. SIR for Compounds and Their Possible Metabolites Used in Mass Spectrometry

Compound Name	Molecular Weight	SIR (m/z)
ICT2588	1901.7	952.8 - 639.9 - 824.5
ICT3146	1613.7	842.49 - 808.8 - 791.45
ICT3198	1804.8	999.4 - 904.4 - 824.4 - 501.2
ICT3120	1706.7	855.3 - 590 - 548 - 791
ICT3115	1809.75	906.8 - 661.32 - 732.5-893.4
ICT3019	1900.79	952.3 - 662.3 - 985.4- 548.6

5.3 Results

5.3.1 Differentiation between MMP3 and MMP10

5.3.1.1 Full length versus activated MMP10

In this research, catalytically active MMP3 enzyme was compared to the MMP10 enzyme. According to the manufacturer (R and D Systems), recombinant MMP10 was supplied as pro (52 KDa) and active (43 KDa) forms. To confirm this, 150ng of the product was subjected to Western blotting using the monoclonal MMP10 antibody. The results show that the recombinant protein contains mainly pro MMP10 with a clear band at 52 KDa (Figure 5.1). In terms of enzyme activity, a comparison of cleavage efficiency was made between pre-activated and non-activated recombinant MMP10 product using the 444228 MMP substrate (Figure 5.2). No marked difference in cleavage efficiency should be detected if the activation of the recombinant protein is not necessary. However, the cleavage of the pre-activated MMP10 was more efficient than the non-activated with 46.5% of the parent remaining after 18 hours of incubation, supporting the earlier Western blot results. Therefore, MMP10 enzyme activation of this product was carried out for future cleavage studies.

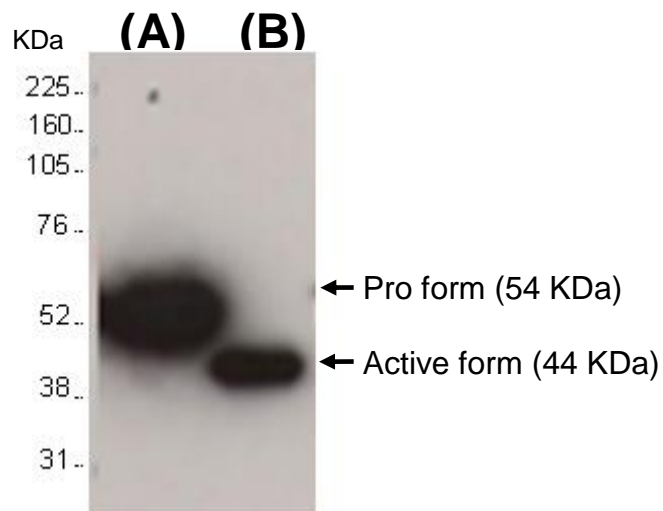
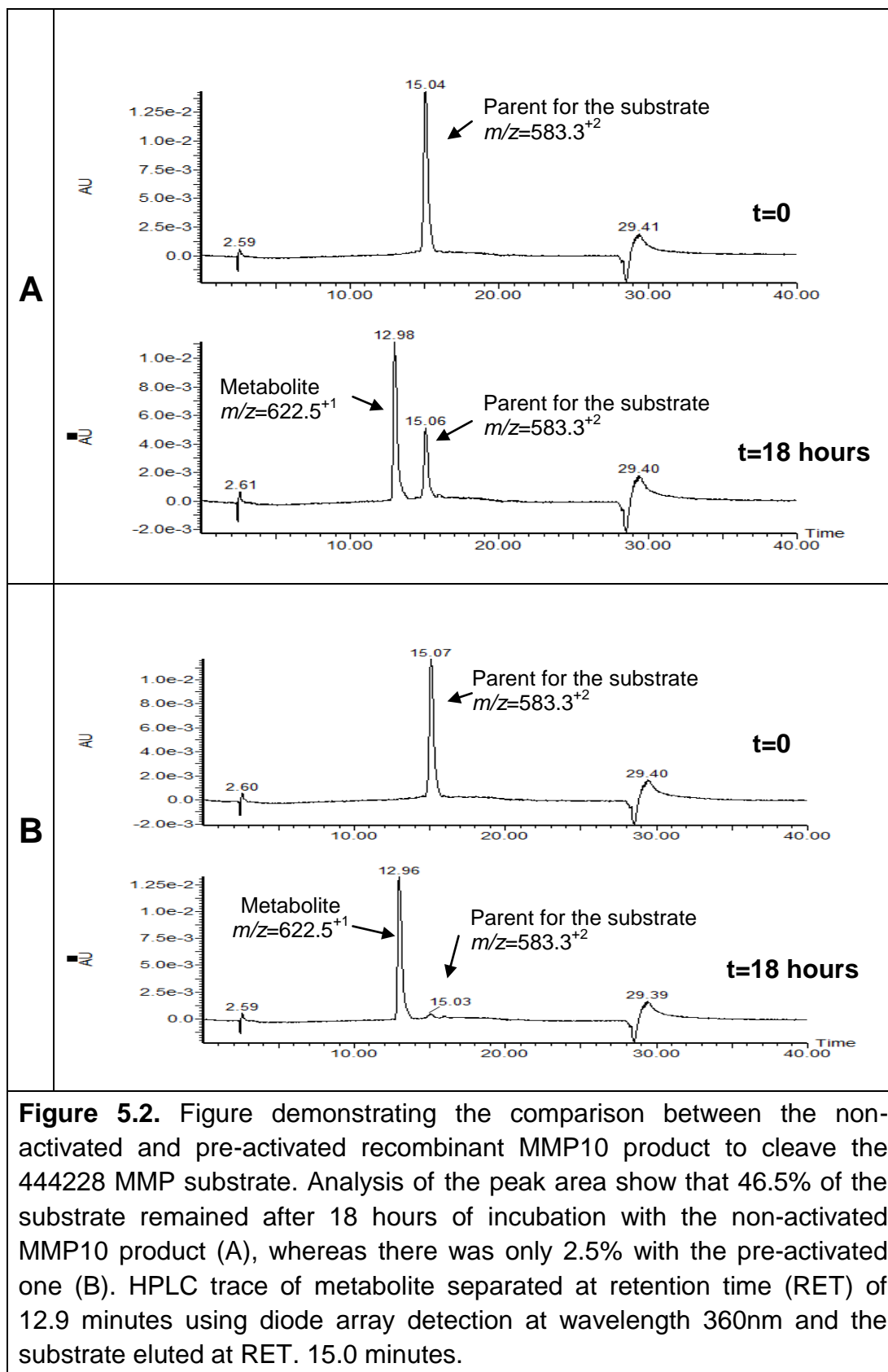


Figure 5.1. Validation of recombinant MMP10 using Western blotting. 120ng of the product produced a large band that correspond to the size of pro MMP10 (inactive form) (A). Activated product was run in parallel to locate the active form band (B). The recombinant MMP10 tested was supplied as a mixture of pro and active forms. These data suggest that the product contains mainly pro MMP10 and that pre-activation is necessary for activity studies.



5.3.1.2 MMPs-substrate cleavage study for peptides selectively cleaved by MMP10

To build the foundations for a rationally designed MMP10-activated TAP, a peptide sequence that is specifically cleaved by MMP10 needs to be identified. A major problem occurring in the exploitation of MMP10 in therapy is the existence of the closely structured MMP3. To identify peptide sequences that can distinguish between these two closely structured enzymes, substrate cleavage studies were carried out. A panel of MMP substrates was tested against MMP3 and MMP10 using a mass spectrometry approach. These substrates are illustrated in Table 5.1.

No cleavage was detected by both enzymes with substrate M-1895 under the experimental condition described in section 5.2.2.3. However, substrates 444215, 444220, 444228, 444230, 444258, 444259 and ABD1 were all cleaved by both enzymes in the same position following 18 hours of incubation at 37°C as shown in Figures 5.3–5.11. Results summarised in Table 5.4 show the difficulty of differentiating between these two enzymes. Despite this, such information is valuable to provide the structural basis for future rational drug design.

The initial aim of this chapter was to find a unique substrate that can distinguish between MMP3 and MMP10. Substrates 444258 (Figure 5.4) and 444259 (Figure 5.11) showed different cleavage capacities by MMP3 despite their similarity, providing a basis for the further investigation of these particular substrates.

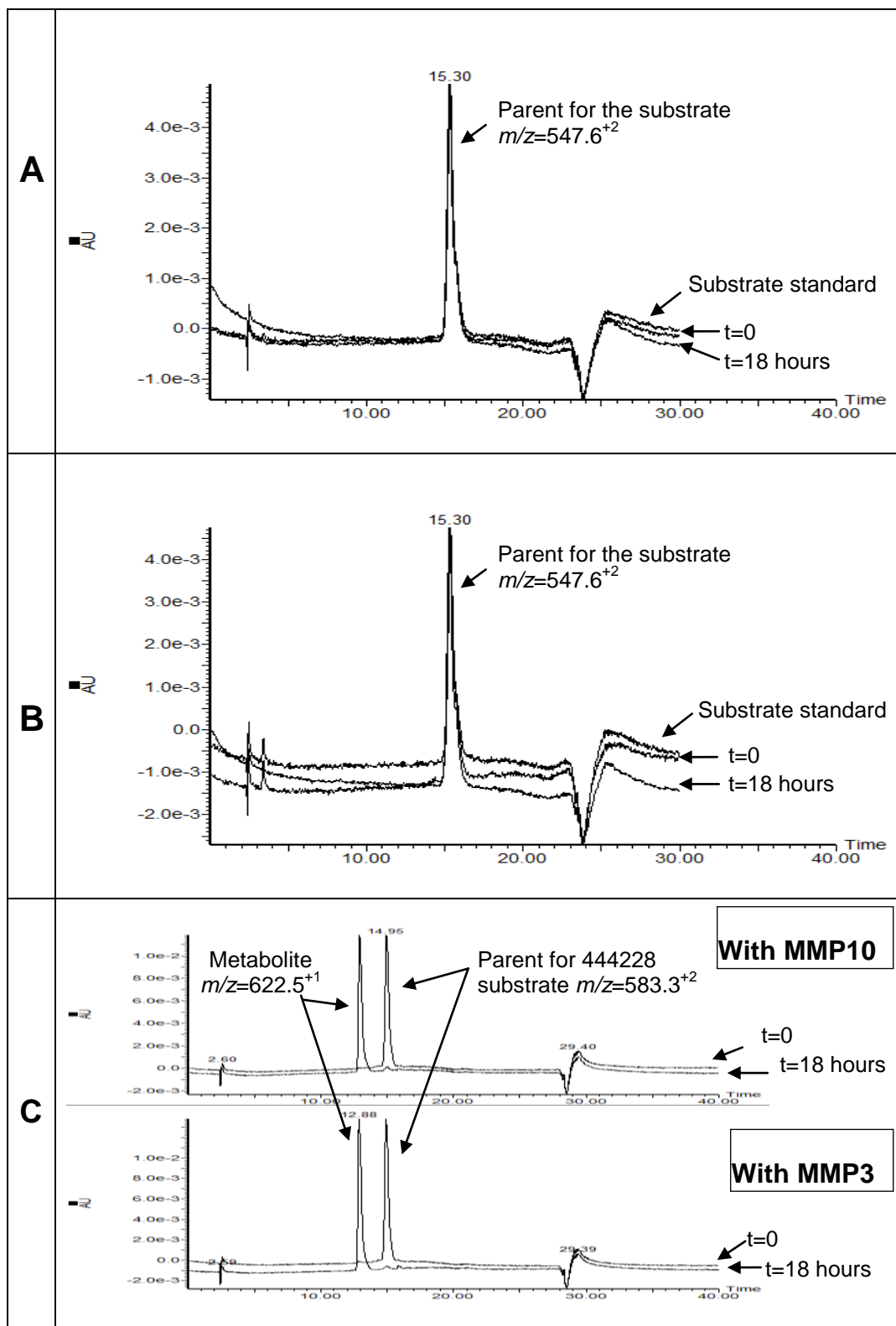
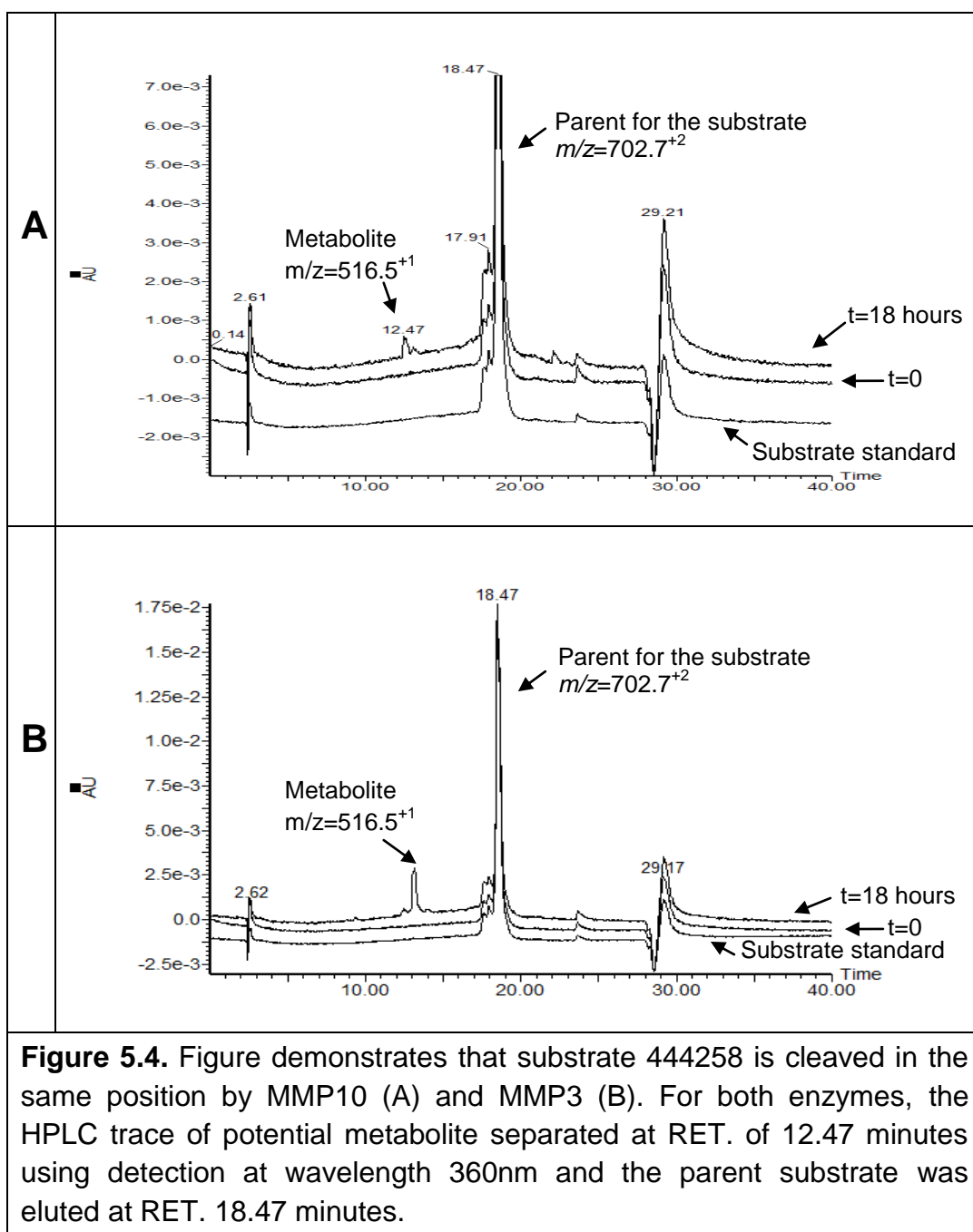
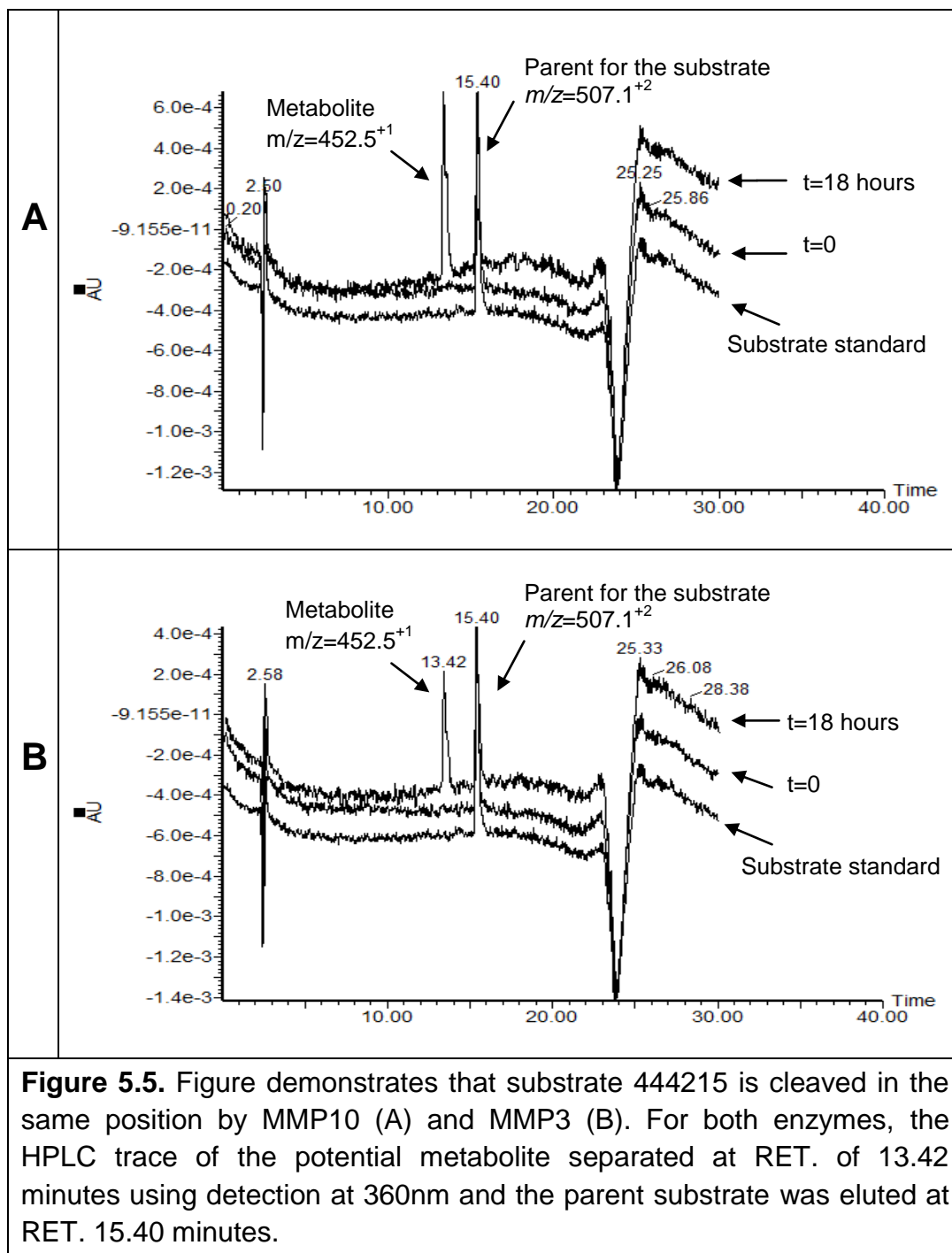
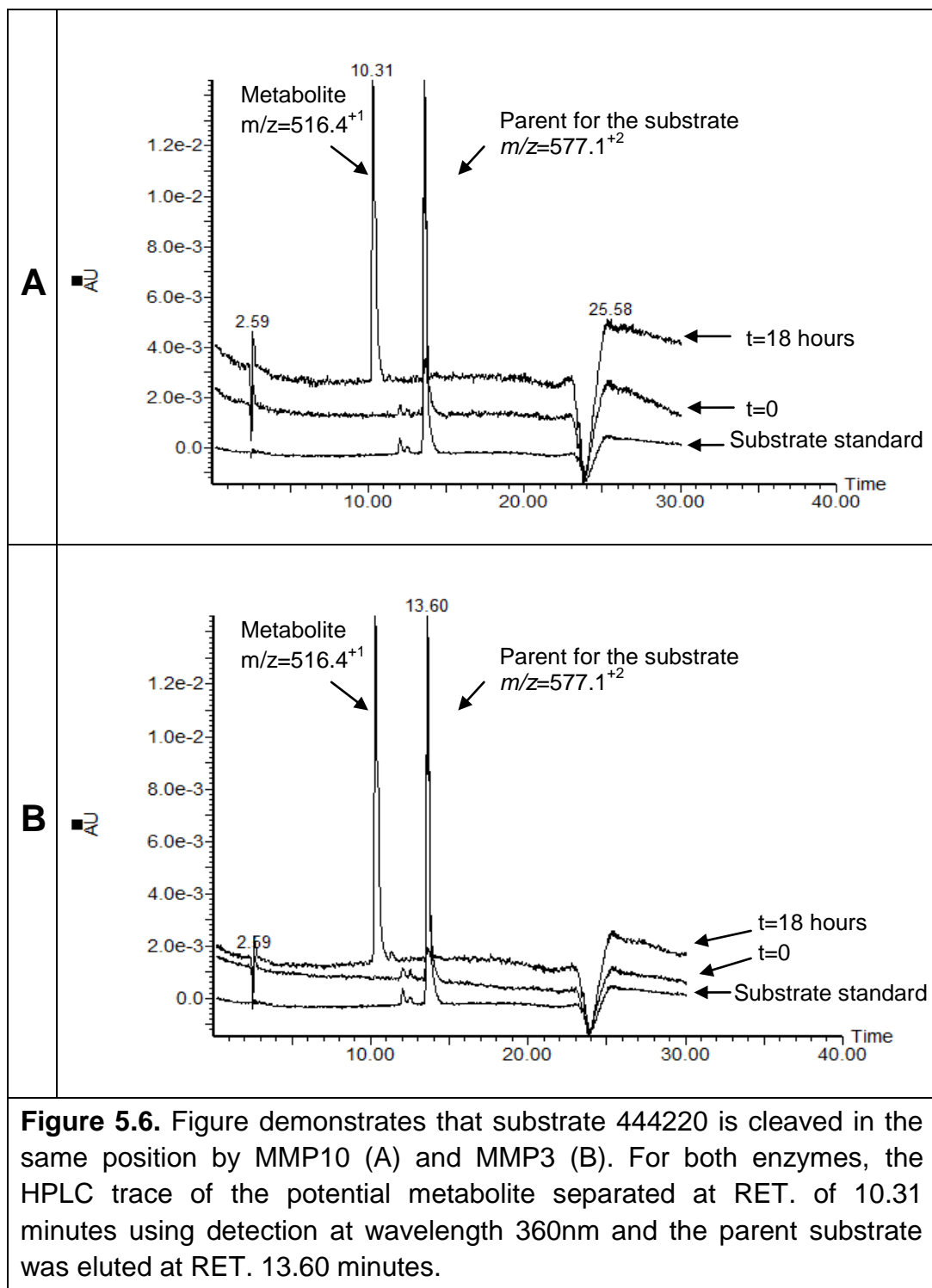
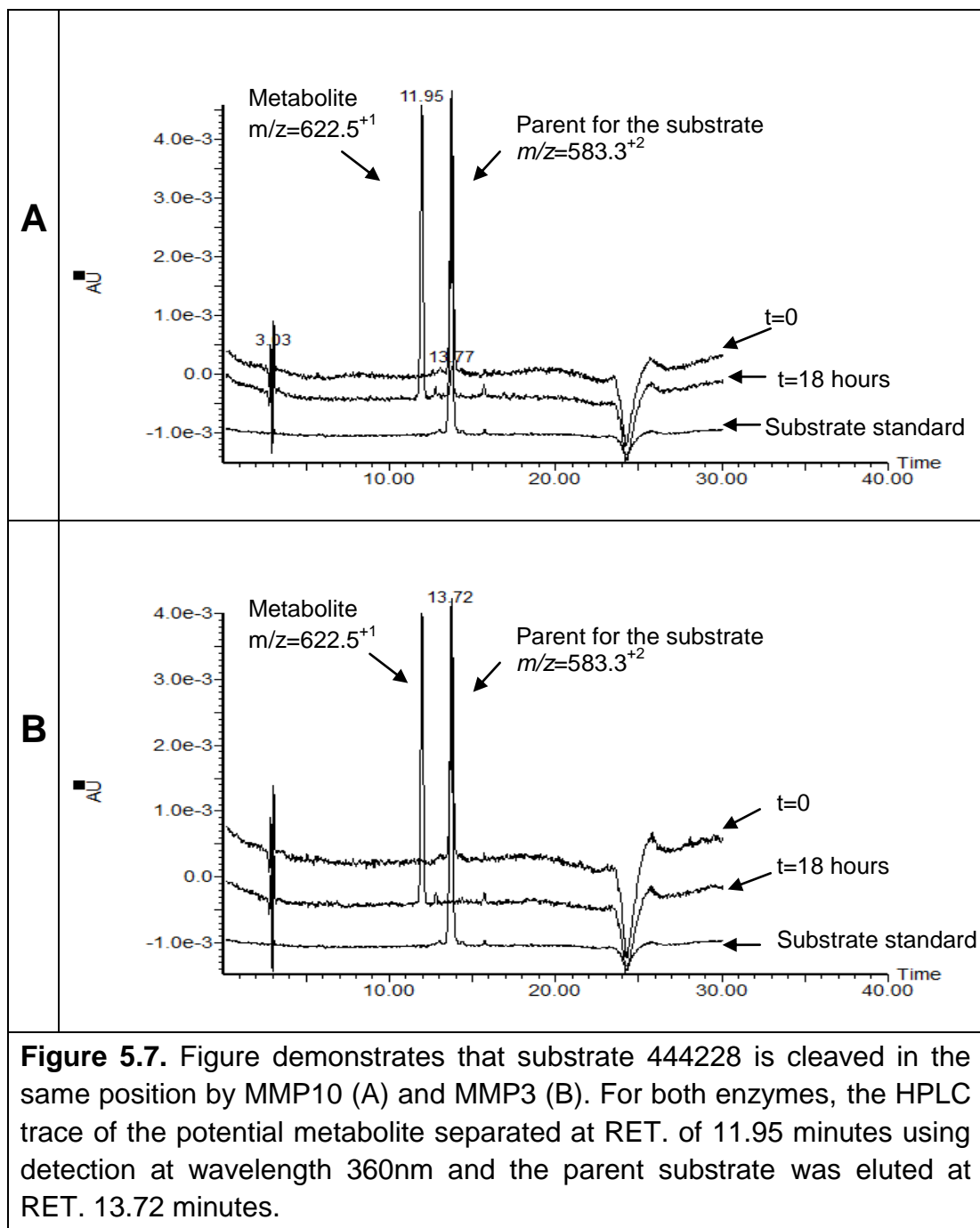


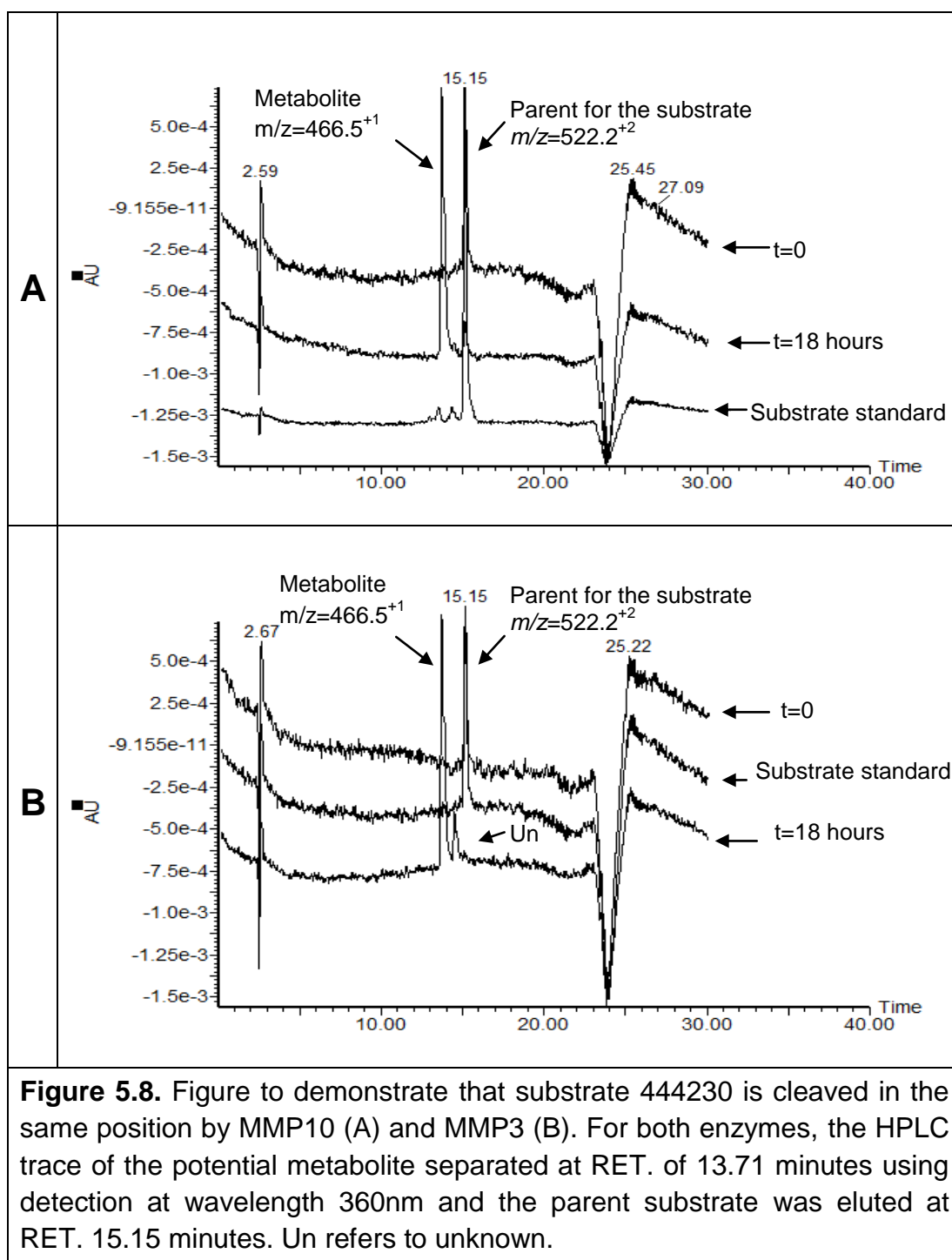
Figure 5.3. Figure to demonstrate that no metabolite was detected after 18 hours of incubation of the substrate (1895) with MMP10 (A) or MMP3 (B). For both enzymes, HPLC trace of the substrate (1895) eluted at RET. 15.30 minutes and was detected at a wavelength of 360nm. The 444228 substrate was used as +ve control to show activity in both enzymes (C).

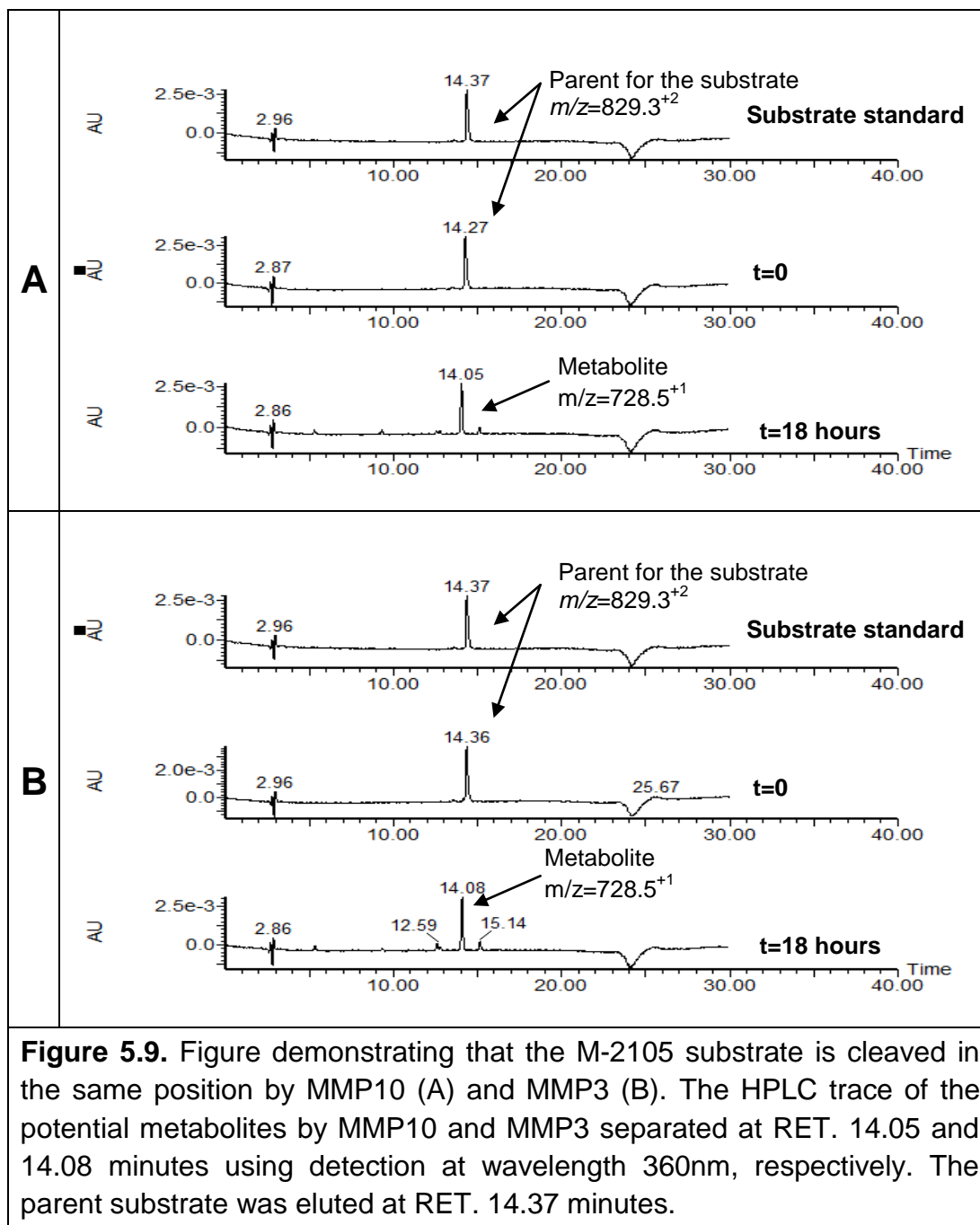












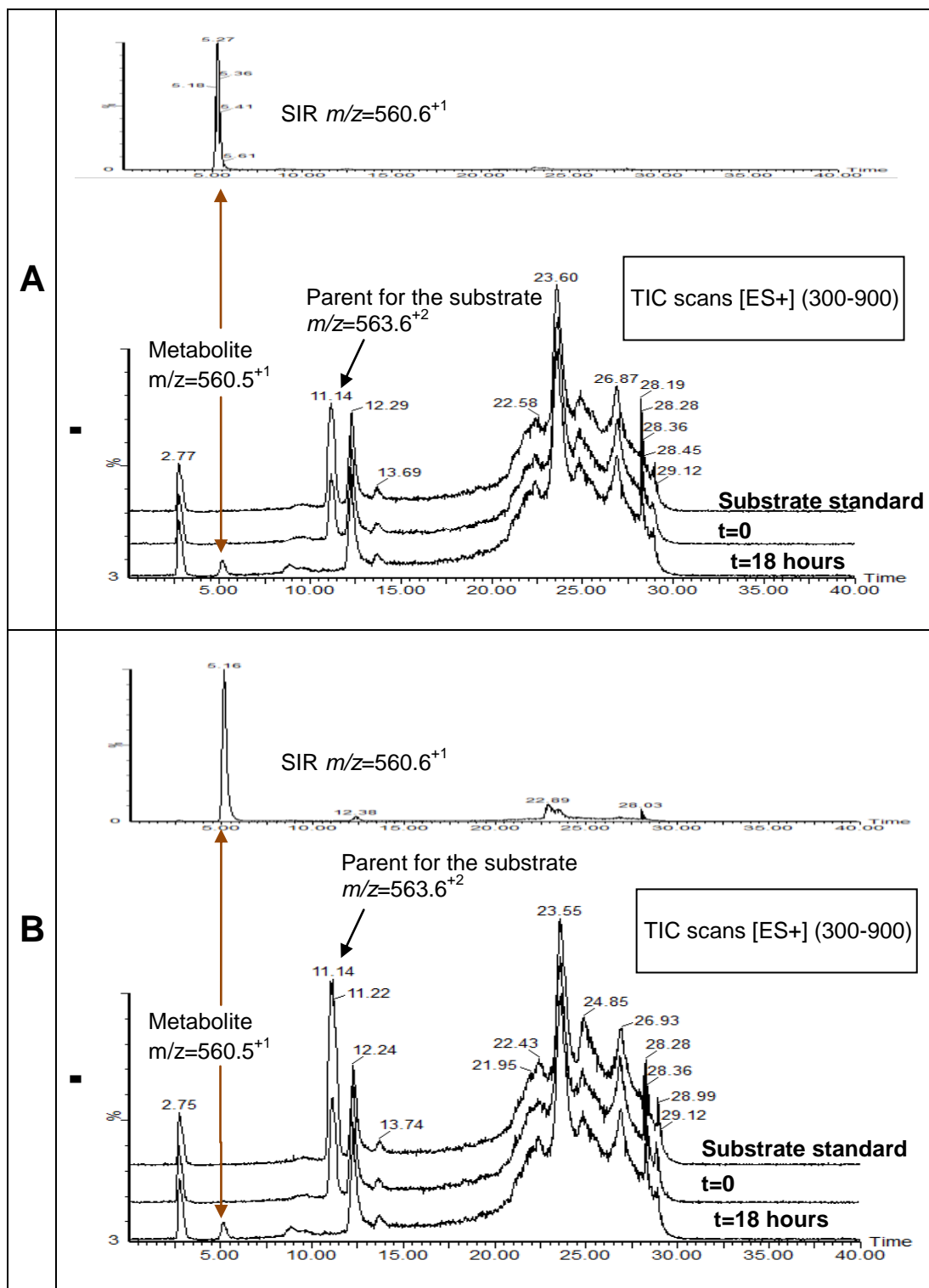


Figure 5.10. Figure demonstrates that ABD1 substrate is cleaved in the same position by MMP10 (A) and MMP3 (B). For both enzymes evaluated, total ion chromatogram (TIC) scanning following reverse phase LC separation shows metabolite at RET. 5.16 minutes and this was identified at $m/z=560.5$ using as SIR in specific [ES+1]. The parent substrate was eluted at RET. 11.14 minutes.

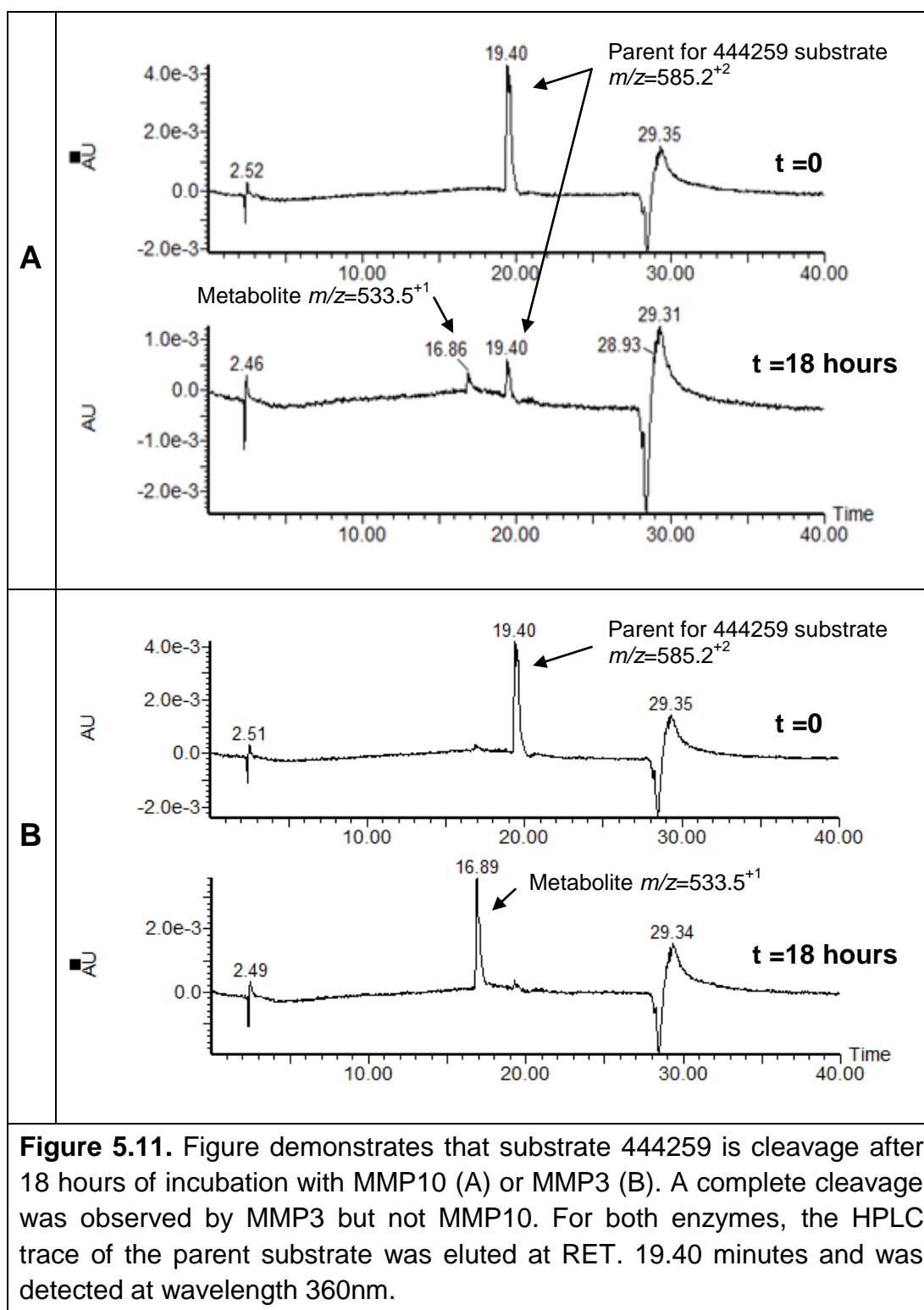
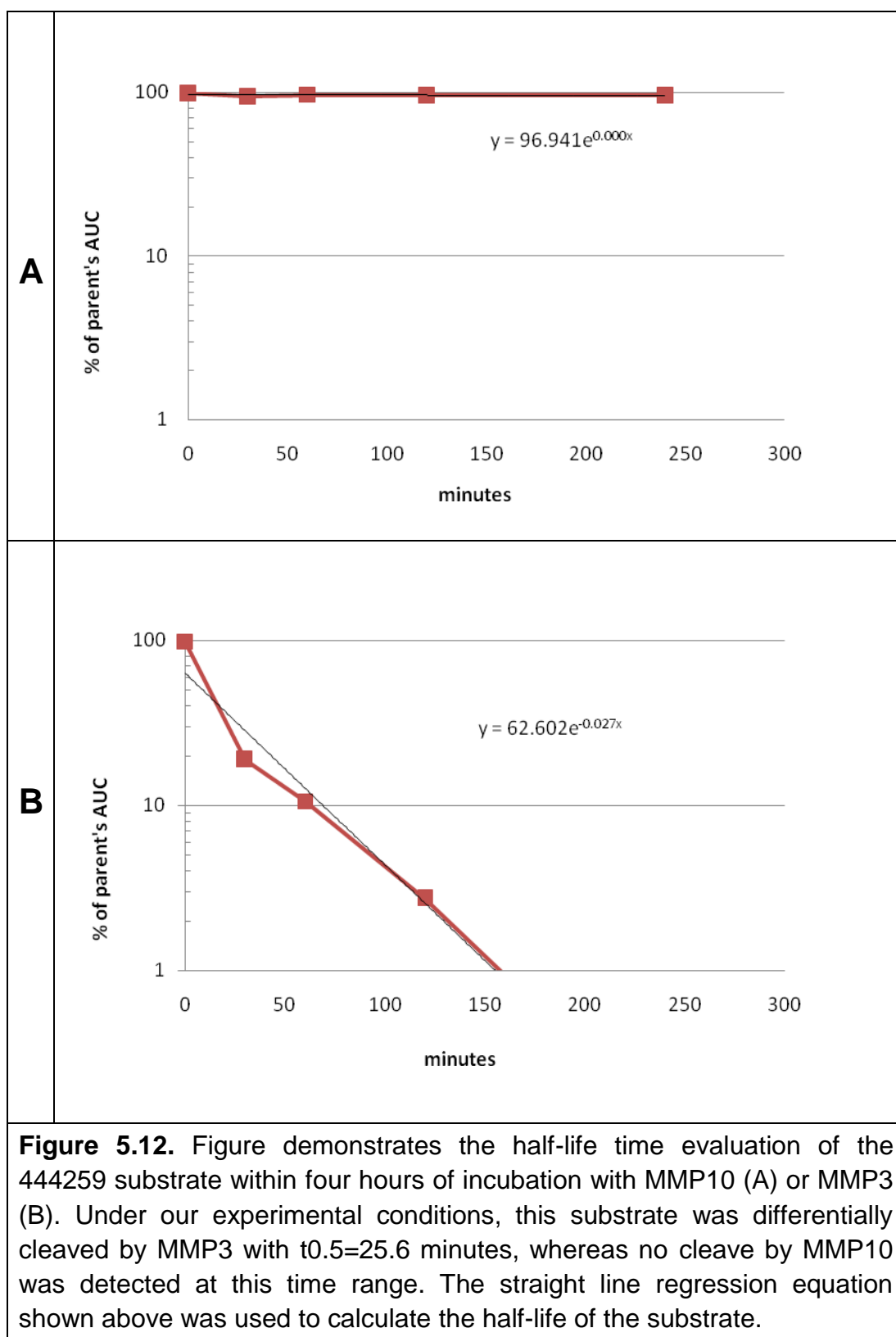


Table 5.4. Illustration of MMP-Substrate in *In Vitro* Cleavage Studies. Red lightning points to the cleavage position by both MMP3 and MMP10.

Trade Name	Catalogue Number	Peptide Sequence
Trifluoroacetate salt	M-1895	Mca-Pro-Leu-Gly-Leu-Dap(Dnp)-Ala-Arg-NH ₂
MMP-2/MMP-9 Substrate I	444215	DNP-Pro-Leu-Gly--Met-Trp-Ser-Arg-OH
MMP-3 Substrate I, Fluorogenic	444220	DNP-Pro-Tyr-Ala--Tyr-Trp-Met-Arg-OH
MMP-7 Substrate I, Fluorogenic	444228	DNP-Arg-Pro-Leu-Ala--Leu-Trp-Arg-Ser-OH
MMP-8 Substrate I, Fluorogenic	444230	DNP-Pro-Leu-Ala---Tyr-Trp-Ala-Arg-OH
MMP-14 Substrate I, Fluorogenic	444258	MCA-Pro-Leu-Ala-Cys--(p-OMeBz)-Trp-Ala-Arg(Dpa)-NH ₂
MMP-14 Substrate II, Fluorogenic	444259	DANSYL-Pro-Leu-Ala-Cys --(p-OMeBz)-Trp-Ala-Arg-NH ₂
MMP-3 substrate	M-2105	Mca-Arg-Pro-Lys-Pro-Tyr-Ala--Nva-Trp-Met-Lys(Dnp)-NH ₂
Part of Proteoglycan protein	ABD1	His-Asp-Arg-Ala-Ile-His-Ile-Gln-Ala-Glu-Asn-Gly-Pro-His-Leu--Leu-Val-Glu-Ala-Glu

5.3.1.3 Structure Activity Relationship Study of 444258 and 444259 Substrates

The 444258 substrate has almost the same structure as the 444259 substrate; however, these differ due to slight modifications, such as the replacement of the MCA and Dpa groups at the peptide terminals with a DANSYL group and hydrogen atom, respectively. These minor changes unpredictably made the substrate more susceptible to cleavage by MMPs. For the 444258 substrate, a partial cleavage was detected after incubation with MMP3 or MMP10 for 18 hours at 37°C, indicating a slow cleavage rate (Figure 5.4). In contrast, a complete cleavage was observed in the case of MMP3 with 444259 substrate under the same experimental conditions (Figure 5.11). For further insight, a half-life evaluation study of 444259 substrate after incubation with MMP3 and MMP10 enzymes was carried out. The half-life of the 444259 substrate after being incubated with MMP3 was 25.6 minutes (Figure 5.12), with initial cleavage detected as soon as 10 minutes. In contrast, the same substrate with MMP10 was very stable under the same experimental conditions. This peptide sequence represents a validated tool to differentiate *in vitro* between MMP3 and MMP10 activity as long as incubation time is less than four hours, paving the way for rational drug design.



5.3.2 Activation of MMP-Targeted Compounds by MMP10 and MMP3

To build the basis for the studies evaluating MMP10 as a prodrug activator and ensure high selectivity, a panel of novel MMP-targeted TAPs developed in-house at the ICT, ICT2588, ICT3019, ICT3120, ICT3115, ICT3198 and ICT3146, were incubated with pure MMP3 or MMP10 as described in section 5.2.2.4.2. These compounds were chosen with respect to their similarity to the reference compound ICT2588 to guide this primary structure activity relationship (SAR) study. MMP-substrate 444228, known to be cleaved by both enzymes, was used in parallel in each experiment to ensure enzyme functionality. Results from this are presented in Figures 5.13-5.18 and summarized in Table 5.5. The numbers in bold below refers to a prodrug result that is listed in the table.

The initial SAR began with ICT2588, which was cleaved by MMP3 but not MMP10 at the Hof-Tyr bond (**1**). Completely reversing the peptide sequence (ICT3120) causes no effect on enzymes selectivity with cleavage at Arg-Tyr bond by MMP3 only (**2**). Keeping this sequence constant and replacing cytosine with arginine and the tyrosine with alanine in the side chain of the amino acid residues (ICT3146) resulted in same selectivity and the cleavage shifted to Arg-Ser bond, indicating that the above positions are not crucial for guiding enzymes selectivity (**3**).

Further SAR efforts based on ICT2588 involves replacing tyrosine with B-alanine in the amino acid side chain (ICT3115), which resulted in the prevention of the compound being activated by both MMP3 and MMP10, suggesting a vital

site for both enzymes activity (4). In the same context, the replacement of cytosine in ICT2588 with arginine at the amino acids chain (ICT3019) results in selectivity identical to the ICT2588 and the cleavage shifted toward the carboxylic end at the Tyr-Leu bond, indicating important position in terms of specificity but not the selectivity (5). Most of these tested compounds were capped at the N-termini with FITC or Ph moieties to avoid pre-activation or aminopeptidase degradation. To evaluate whether the N-terminal capping type can affect the behaviour of the tested enzymes and whether this position can serve as a starting point for further modifications, the FITC end cap of the ICT2588 was replaced with a simple sugar end cap to give the ICT3198 compound. This surprisingly resulted in a decrease in selectivity as the compound was cleaved by both MMP3 and MMP10 at the same bond, Gly-Hof (6). These valuable findings represent a foundation for further studies to exploit MMP10 or MMP3's tremendous proteolytic activity as prodrug activators.

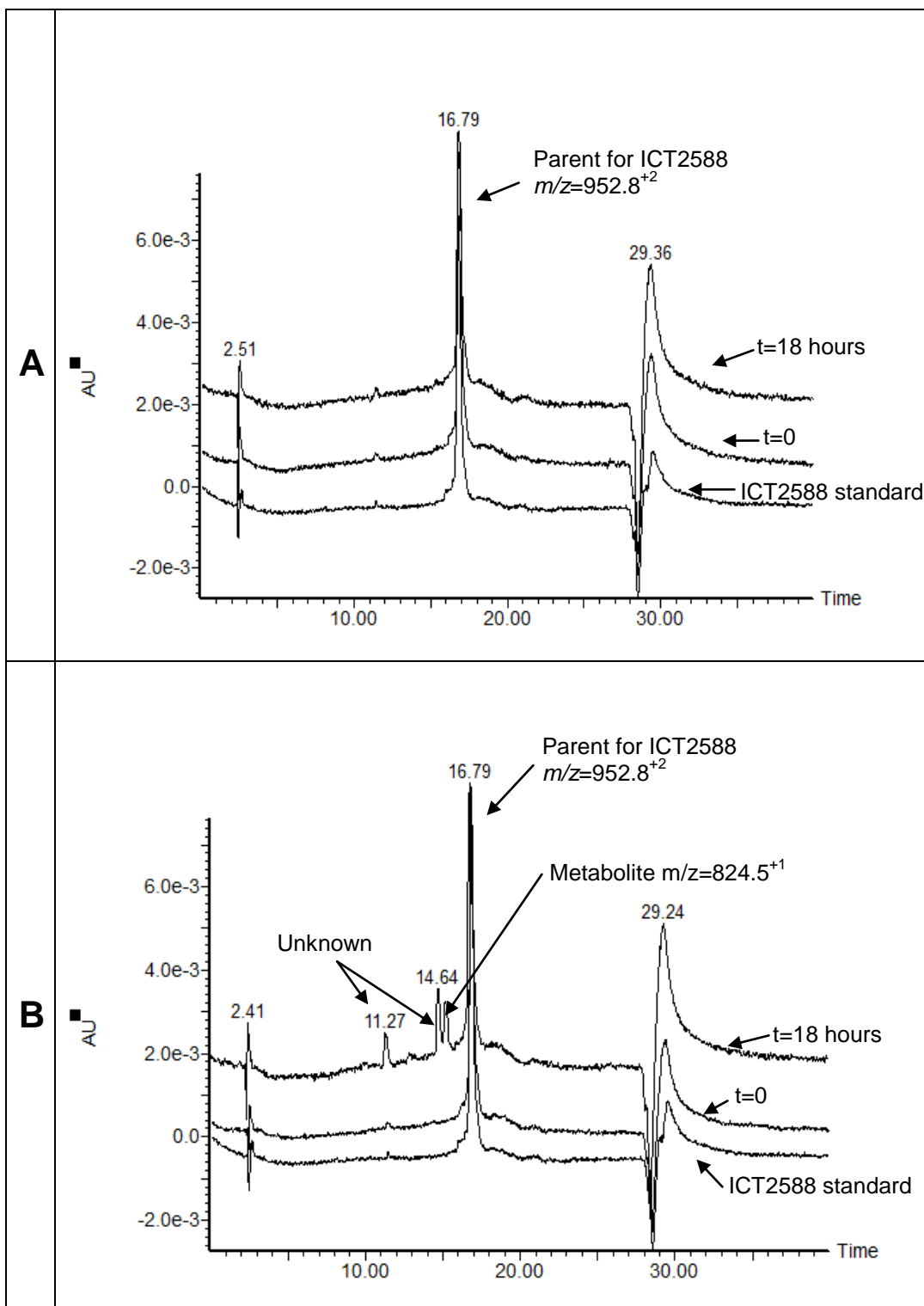


Figure 5.13. Figure demonstrating the comparison between MMP10 (A) and MMP3 (B) to activate the ICT2588 prodrug. Using detection at wavelength 360nm, no HPLC trace of potential metabolite was detected with MMP10, whereas metabolite separated at RET. of 15.00 minutes was detected in the case of MMP3. The prodrug was eluted at RET. of 16.79 minutes. Refer to Figure 5.19 for the positive controls of both enzymes.

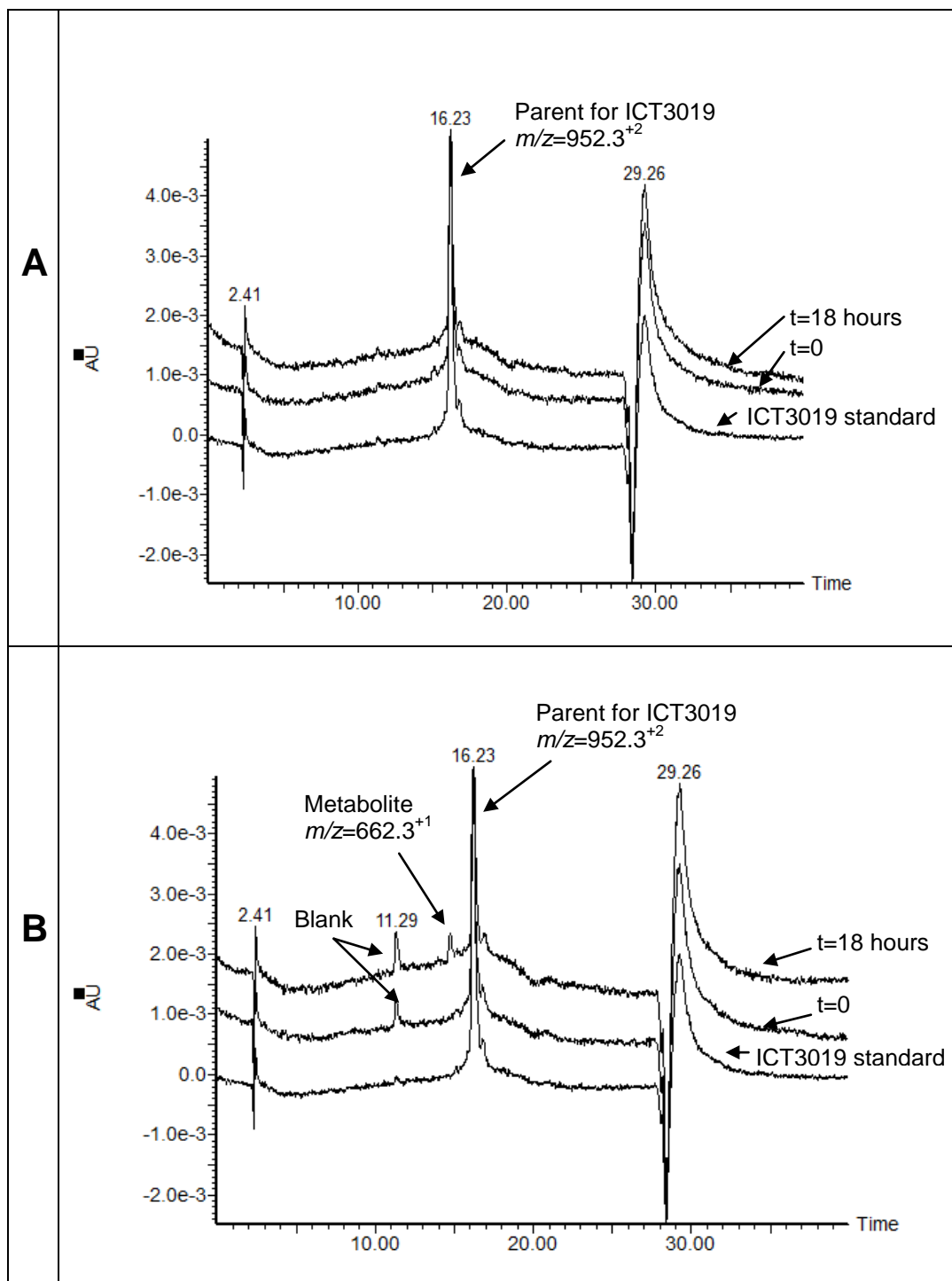
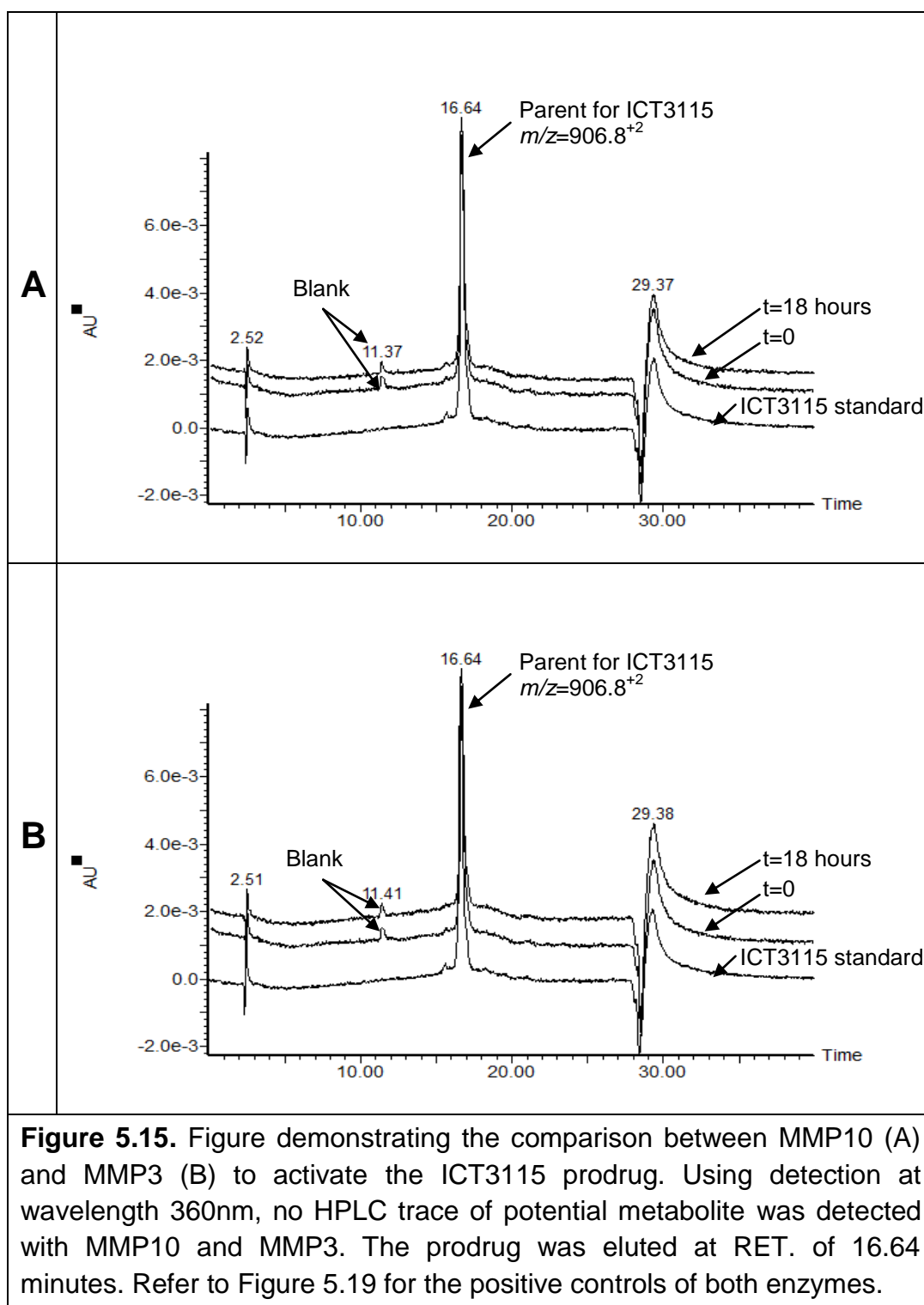


Figure 5.14. Figure demonstrating the comparison between MMP10 (A) and MMP3 (B) to activate the ICT3019 prodrug. Using detection at wavelength 360nm, no HPLC trace of the potential metabolite was detected with MMP10, whereas metabolite separated at RET. of 14.80 minutes was detected in the case of MMP3. The prodrug was eluted at RET. of 16.23 minutes. Refer to Figure 5.19 for the positive controls of both enzymes.



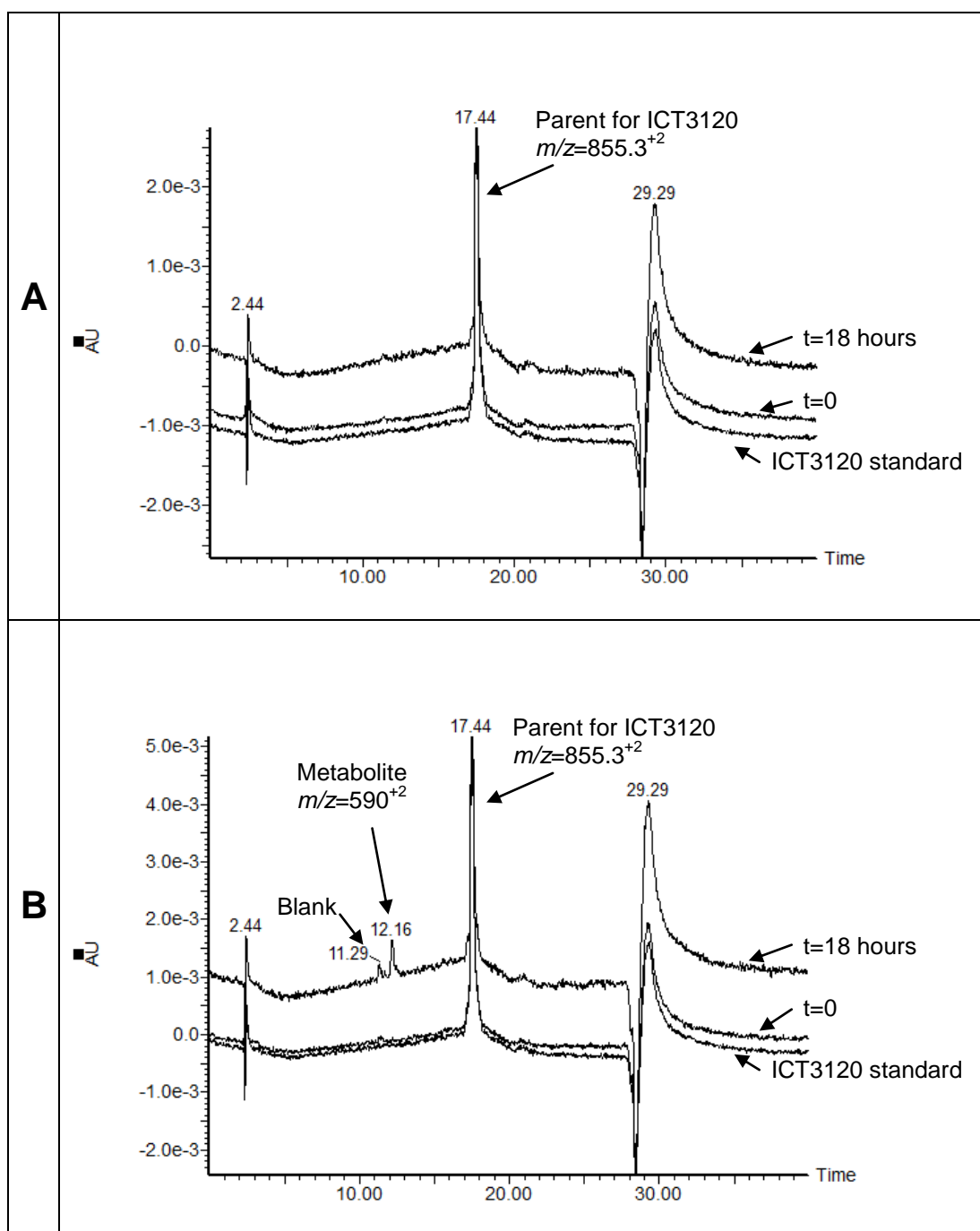


Figure 5.16. Figure demonstrating the comparison between MMP10 (A) and MMP3 (B) to activate the ICT3120 prodrug. Using detection at wavelength 360nm, no HPLC trace of potential metabolite was detected with MMP10, whereas metabolite separated at RET. of 12.16 minutes was detected in the case of MMP3. The prodrug was eluted at RET. of 17.44 minutes. Refer to Figure 5.19 for the positive controls of both enzymes.

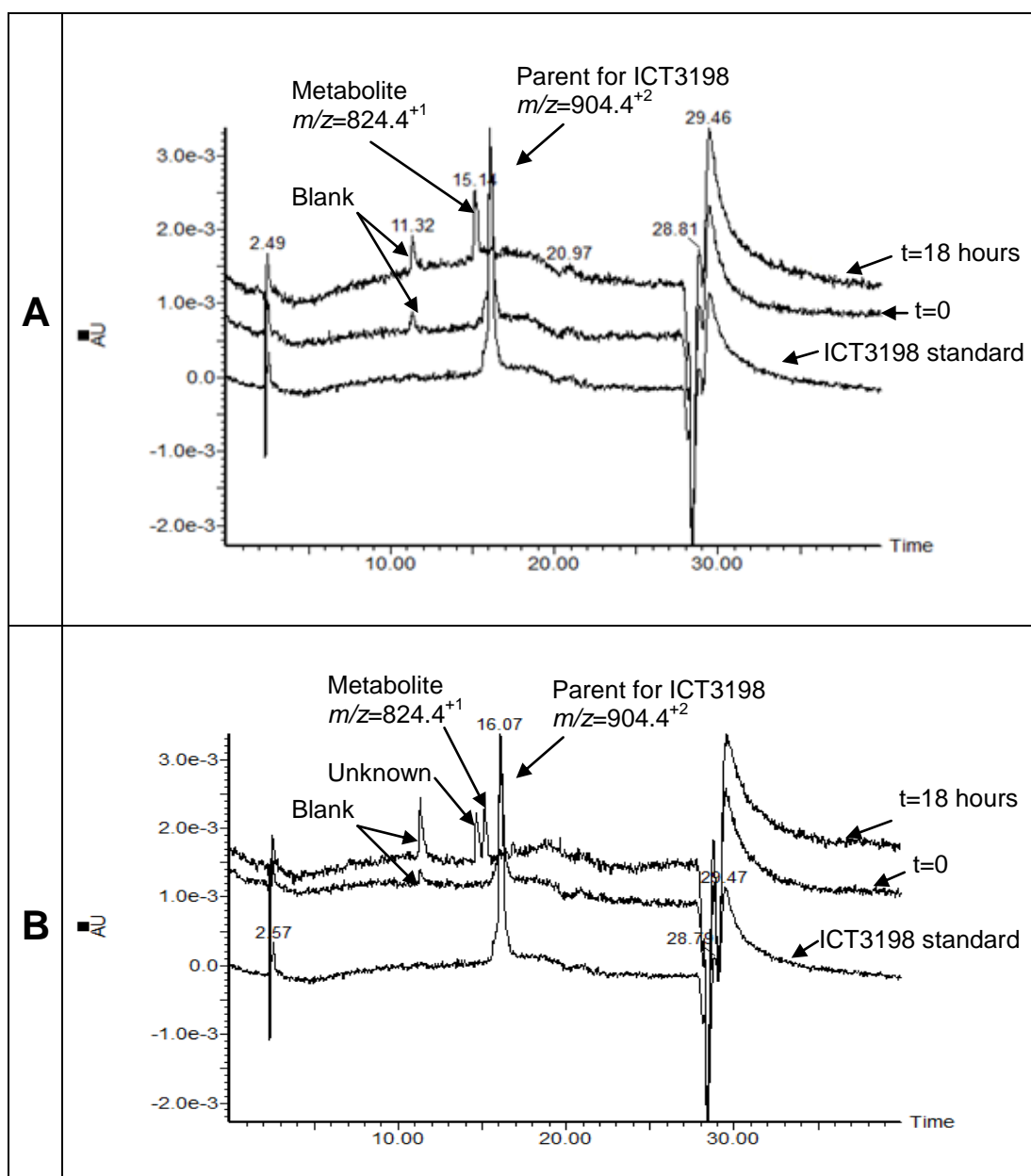
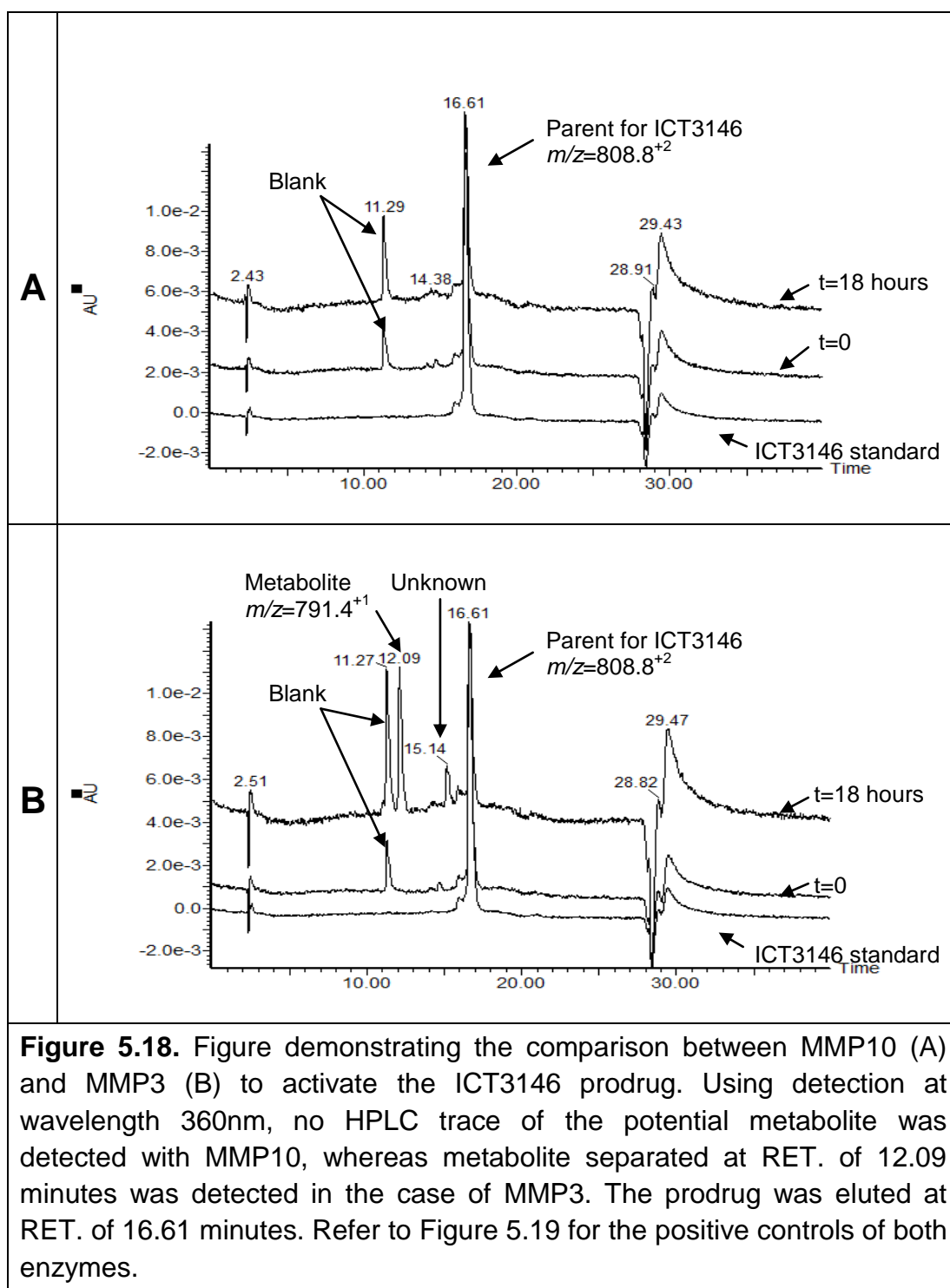


Figure 5.17. Figure demonstrating the comparison between MMP10 (A) and MMP3 (B) to activate the ICT3198 prodrug. Using diode array detection at wavelength 360nm, the HPLC trace of the potential metabolite by both enzymes separated at RET. of 15.14 minutes was detected. The prodrug was eluted at RET. of 16.07 minutes. Refer to Figure 5.19 for the positive controls of both enzymes.



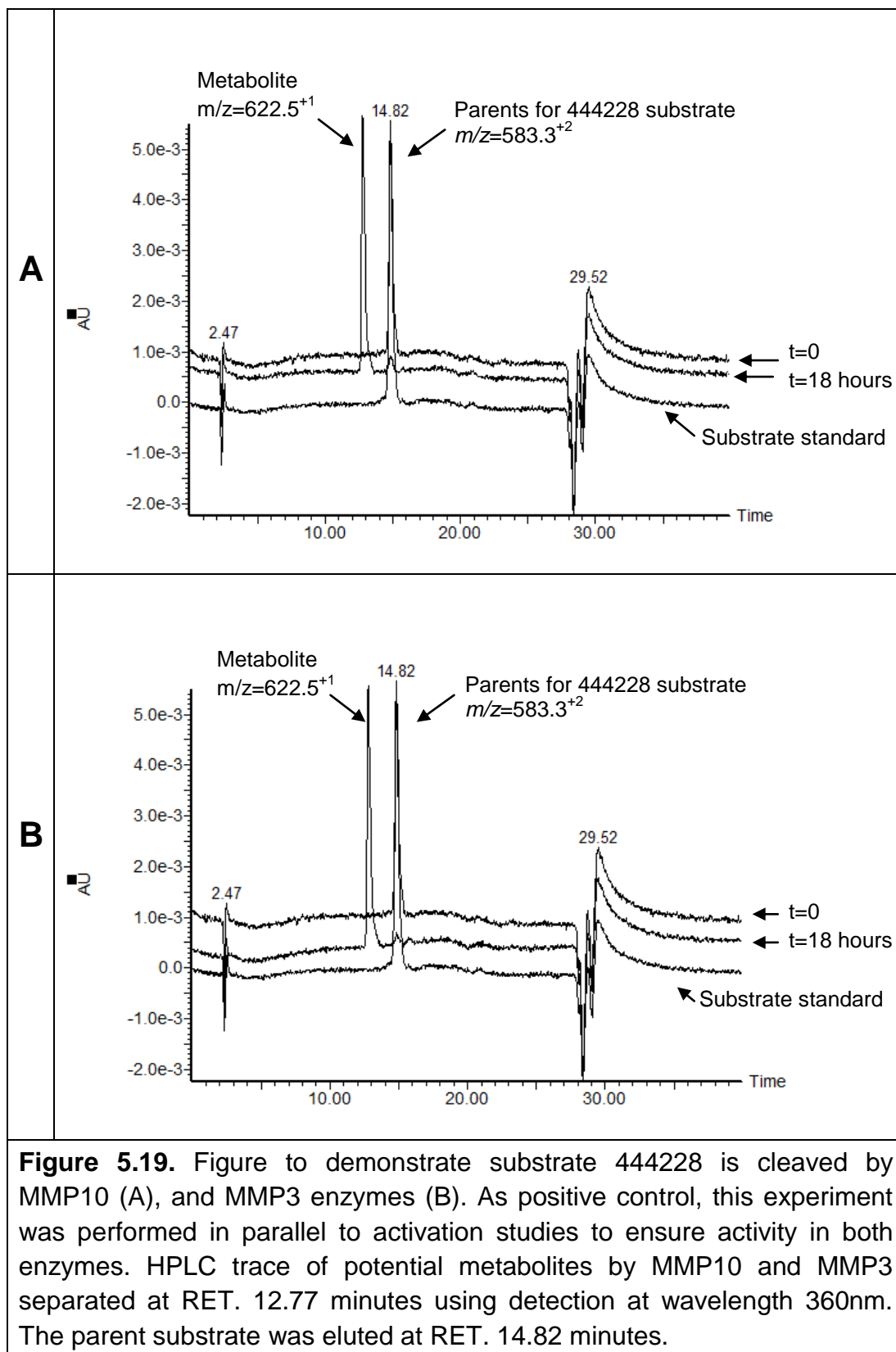


Table 5.5. Summary of the *in vitro* cleavage profile of peptide-colchicine conjugates by MMP3 and MMP10. MB2 refers to amino colchicine. Red colour indicates site of modification, whereas the blue thunder sign indicates potential cleavage site.

NO	Prodrug	Conjugate Sequence	Cleave by:	
			MMP 3	MMP 10
1	ICT2588	FITC-βAla-Arg-Ser-Cit-Gly-Hof-Tyr-Leu-Tyr-MB2	✓	✗
2	ICT3120	ph-βAla-Leu-Tyr-Hof-Gly-Cit-Ser-Arg-Tyr-MB2	✓	✗
3	ICT3146	ph-βAla-Leu-Ala-Hof-Gly-Arg-Ser-Arg-Tyr-MB2	✓	✗
4	ICT3115	FITC-βAla-Arg-Ser-Cit-Gly-Hof-βAla-Leu-Tyr-MB2	✗	✗
5	ICT3019	FITC-βAla-Arg-Ser-Arg-Gly-Hof-Tyr-Leu-Tyr-MB2	✓	✗
6	ICT3198	Sugar-βAla-Arg-Ser-Cit-Gly-Hof-Tyr-Leu-Tyr-MB2	✓	✓

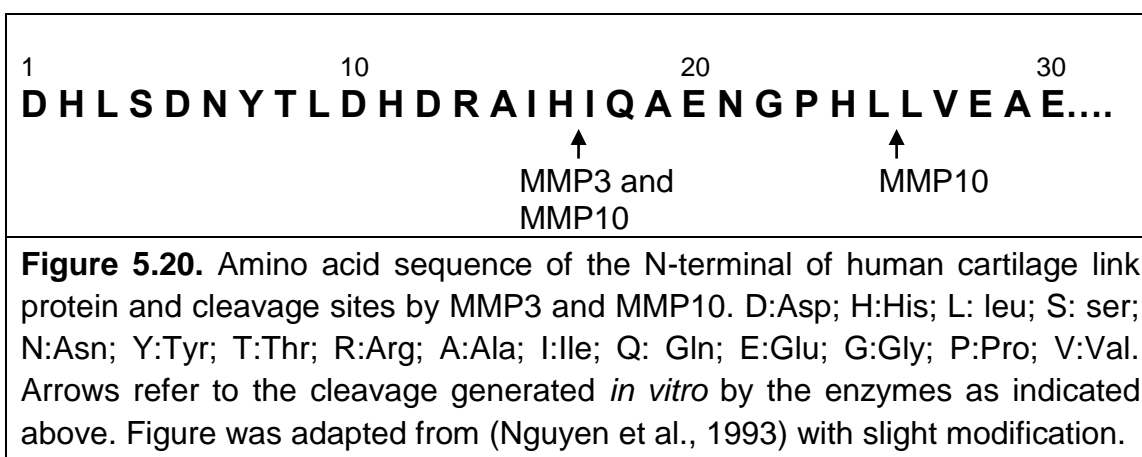
5.4 Discussion

In the development of MMP-targeted TAPs, a fundamental step is incorporating a substrate peptide ('trigger') to derive the specificity of the prodrugs (Atkinson et al., 2008). Therefore, the identification of a specific peptide sequence for MMP activation is critical, as it could determine the future prospects of MMP-activated TAPs. In the literature, there is currently a lack of data about MMP substrate specificities for several MMPs, including MMP10, the main focus of this research. The aim of the work in this chapter is to identify an MMP10-specific cleavable sequence to incorporate into an MMP10-targeted TAP. A major obstacle for targeting MMP10 is the presence of the highly similar MMP3. To improve specificity in targeting MMP10, the selected peptide should have a high affinity to MMP10 as compared to MMP3.

The activity of the enzyme needs to be addressed prior to performing the enzyme-substrate cleavage studies. While the precise enzymatic activity for MMP3 and MMP10 recombinant proteins could not be measured within the constraints of the current project, it was sufficient at this stage using the 444228 substrate, which is known to be cleaved by both enzymes, as a marker for their activity to be qualitatively evaluated. This assay was unexpectedly able to provide an idea about the cleavage efficiency of MMP10. The recombinant MMP10 was supplied as a mixture of both the pro and active forms. The comparison in the cleavage efficiency of recombinant MMP10 between the non-activated and the APMA pre-activated version using the 444228 substrate has revealed a higher efficiency (a faster cleavage rate) of the fully activated than the non-activated MMP10 protein. This indicates that the 444228 substrate-

enzyme cleavage assay successfully provided an accurate and a semi-quantitative evaluation for the MMP10 enzymatic activity.

Only one study in the literature has offered a peptide that could distinguish between MMP3 and MMP10 (Nguyen et al., 1993). In the reported study, human cartilage link protein with amino acid sequence, shown in Figure 5.20, was cleaved by MMP10 in two different sites compared to MMP3. The MMP3 and MMP10 cleaved between His'6 and Ile"7 and MMP10 specifically cleaved between Leu25 and Leu26. The part of the cartilage protein that exhibited resistance to the cleaving by the MMP3 has brought the attention of this research. It could provide a key for amino acid sequences to distinguish between the two closely structured MMP3 and MMP10. Based on this, a peptide of similar amino acid sequence was synthesised and tested with MMP3 and MMP10 in this research. Interestingly, the synthetic substrate was cleaved in the same position by both enzymes, indicating a lack of specificity. This discrepancy between the results may be attributed to the differences in assay conditions and tools of study. For example, the incubation time, concentrations, buffers and recombinant MMP enzyme sensitivity of the detection system used can greatly influence the results.



As the only MMP10 specific substrate sequence reported in the literature was found to be unreliable in terms of absolute specificity, a panel of synthetic MMP-sensitive substrates were screened in this research. The screening of synthetic substrates against enzymes, such as MMP10, can provide insight into the enzyme's behaviour and specificity toward different substrates, resulting in the identification of a unique substrate for the enzyme. As previously discussed (section 1.8.2.1), SAR studies have been conducted on several MMPs, leading to the identification of structural features within the substrates that are either necessary for cleavage by all MMPs or relatively specific for a few MMP members (Deng et al., 2000; Nagase and Fields, 1996; Netzel-Arnett et al., 1991; Turk et al., 2001; Vartak and Gemeinhart, 2007). For example, if the sequence analogue of the substrate is defined as “--A3--A2--A1=A1'--A2'--A3'--”, where A is any specific amino acid and = is the cleavage site (Vartak and Gemeinhart, 2007), an MMP substrate should typically have small amino acids at (A1), hydrophobic amino acids at (A1' and A2), proline at (A3) and hydrophobic or basic amino acids at (A2'). Special substrate features identified to date for MMPs, including MMP1, MMP2 and MMP9, require small residues at (A3'); MMP3, 7 and 14 prefer methionine at the same position; MMP2, MMP3 and MMP7 favour glutamic acid at A1. It is worth noticing that MMPs have a diverse tolerance for both aromatic amino acids at (A1) and the hydrophobic amino acid residues at (A2) (Vartak and Gemeinhart, 2007). The data from this chapter suggests that the substrate structural features for MMP3 and MMP10 are consistent with the general criteria for MMP substrates, except that hydrophobic amino acids at (A1') were not found to be essential for selectivity as demonstrated in the insertion of a polar tyrosine residue at (A1') in the

444220 and 444230 substrates. Although the intention was to develop an MMP10 substrate, the detailed amino acid sequence was not identified, due probably to the small scale screening of MMP substrates and the high resemblance between MMP3 and MMP10. Results of this study provide the foundation for future studies necessary to create a profile of the MMP10 substrate specificity. This will, in the future, result in the identification of MMP10-specific cleavable peptide sequences.

The *in vitro* cleavage studies for MMP substrates are a valuable tool to measure the affinity of individual MMPs to the selected linker peptides. It is desirable that the linker is rapidly cleaved once it encounters the specific MMP (Vartak and Gemeinhart, 2007). Data in the present study showed that MMP3 has higher affinity to the 444259 substrate *in vitro* than MMP10, supporting the 444259 substrate as a validated tool for differentiating *in vitro* the MMP3 and MMP10 activity. However, the behaviour of enzymes toward a substrate during the *in vitro* experiments can differ significantly in the more complex *in vivo* environment, where proteins and mediators are present at relevant concentrations (Overall and Blobel, 2007). Although in this research, MMP3 cleaved the 444259 substrate *in vitro* at a faster rate than the MMP10 and no other substrate showed the potential to distinguish between the two enzymes, it remains difficult to know whether the same happens *in vivo*. Therefore, a careful consideration is necessary when interpreting the *in vitro* experiment results and further confirmation in an *in vivo* setting is required.

The MMP-activatable prodrug ICT2588 has demonstrated great promise as an antitumour therapy, with a marked capacity to reduce HT-1080 fibrosarcoma

tumour xenografts with a low systemic toxicity. It involves the peptide conjugate (β Ala-Arg-Ser-Cit-Gly-Hof-Tyr-Leu-Tyr) linked to azademethylcolchicine. It was initially introduced as being selectively activated by MT-MMPs (Atkinson et al., 2010). This claim was supported by extensive enzyme-cleavage *in vitro* studies using recombinant proteins for all the MT-MMPs and for MMP1, 2, 10, 12, and 13. With the MMP3 enzyme not included in their evaluation, data of the present study unpredictably demonstrated cleavage of the ICT2588 prodrug by MMP3. Such finding probably allows the questioning of the selectivity of the ICT2588 prodrug, especially with evidence of it being slightly cleaved by MMP2 as well (Atkinson et al., 2010). In this regard, it has become increasingly acceptable that most peptide substrates in general are cleaved at certain conditions by various MMPs with only two to ten fold selectivity (Vartak and Gemeinhart, 2007), which could be the same case with the ICT2588. Thus, the design of the optimal peptide sequences to exhibit selective cleavage by specific MMPs has been proven difficult.

Continuing to identify the key structural features of the substrates that would allow the targeting of MMP10 specifically, SAR studies based on the ICT2588 prodrug and using MMP3 and MMP10 enzymes were also conducted in this research. If the sequence analogue of the ICT2588 is defined as 'FITC-P1-P2-P3-P4-P5-P6-P7-P8-P9-amino colchicine', where P is any specific amino acid, the addition of arginine at P4 (ICT3019) resulted in no effect on both enzymes' specificity. In addition, the use of β -alanine at the P7 site (ICT3115) led to the inhibition of the activation by MMP3, indicating a vital site for MMP3 specificity. Interestingly, the replacement of FITC at the N-terminal with a sugar residue as end-cap surprisingly allows the activation by MMP10, as

demonstrated with ICT3198. This sudden change in affinity of the MMP10 enzyme to the peptide substrate in ICT3198 might be due to the removal of the influence of the FITC residue, which has been reported to often compete with the substrate on the enzyme active site under certain conditions (Yang et al., 2000).

In conclusion, proper validation of commercial enzymes is critical prior to the conduction of the *in vitro* substrate-enzyme cleavage studies, as exemplified here with the recombinant MMP10. This should improve confidence and enhance the reliability of results. Cleavage studies *in vitro* reveal that the differentiation between closely related MMP3 and MMP10 can be successfully detected if cleavage rates are carefully monitored with the 444259 substrate using specific reaction conditions described in this study (Section 5.2.2.3). While a peptide sequence specific to MMP3 was uncovered, sequences specific to MMP10 to incorporate into a TAP were more elusive. The data provided herein is essential for building the foundation to achieve this goal. Developing a substrate specific to MMP10 (as with other MMPs) still remains a challenge.

Chapter 6: General Discussion

As previously described, MMPs are heavily implicated in the tumourigenicity of most cancers, in part through ECM degradation, which directly facilitates tumour invasion and metastasis or through their involvement in the release of several bioactive molecules that are known to contribute to the phenotypic evolution of cancer (Overall and Dean, 2006). Since MMPs are key players in cancer development, the evaluation of their expression, activity and localisation in human cancers is essential in terms of diagnosis, prognosis and therapy.

In NSCLC, there is still a need to identify new molecular targets that can be either targeted for novel therapeutics or exploited to improve the tumour-delivery of the current chemotherapeutics, thereby minimising systemic toxicity. Among MMPs, MMP10 has the most potential to be a good candidate as a target, given its expression, activity and its correlation to poor clinical outcome in NSCLC (Frederick et al., 2008). The main aims of this project were to investigate the role of MMP10 in the tumour microenvironment of NSCLC and to contribute to the evaluation of MMP10 as a target for therapeutic intervention.

It is worth noticing that the heterogeneous tumour microenvironment might contain other sources of MMP10 as well as tumour cells, such as tumour-associated epithelial, stromal and immune cells (Justilien et al., 2012). In fact, MMP10 has also been detected in normal cells such as bone marrow-derived macrophages as evidenced in a recent study (Murray et al., 2013). However, the rate of secreting MMP10 between stromal and tumour cells is different. Low levels of MMP10 in the lung epithelium have been reported *in vivo* compared to

those when oncogenic Kras is activated in tumour cells (Regala et al., 2009). Hence, tumour cells are the main source of MMP10 in tumour tissue, despite potential other sources.

In the literature, numerous studies have reported elevated expression of MMP10 in a wide range of tumour types (Gill et al., 2004; Mathew et al., 2002; Miyata et al., 2007; Rodriguez et al., 2008). Matrix metalloproteinase 10 expression has been linked to the progression of several cancers, including lymphoma, lung and head and neck cancers (Deraz et al., 2011; Frederick et al., 2008; Van Themsche et al., 2004). In NSCLC, MMP10 demonstrates elevated expression in both primary and secondary tumours, an observation that is independent of tumour status (Cho et al., 2003; Gill et al., 2004; Muller et al., 1991). In relation to this, MMP10 is also expressed in the early stages of NSCLC tumour development, rather than just tumour invasion and metastasis (Frederick et al., 2008; Justilien et al., 2012). In accordance with most studies concerning MMP10 expression in NSCLC, generally high MMP10 expression at the gene and protein levels were observed in the two NSCLC cell lines, A549 and H460. Owing to this, these cell lines were selected for use in the present study to evaluate the role of MMP10 in NSCLC. While the intention was to engineer the above cell lines to overexpress MMP10 to the expression levels observed clinically, this goal could not be achieved within the time scale of this project. Thus, the development of functional MMP10 overexpressing models *in vitro* as a future work of this project is a priority as it can provide insight regarding the roles of MMP10 in NSCLC tumour development and progression.

The results of the mRNA expression analysis in the above NSCLC cell lines showed high expression for MMP10. An identical observation was seen for the structurally similar MMP3 in these cell lines, suggesting the importance of these enzymes in these cells. Despite their structural similarity (Bertini et al., 2004; Kucukguven and Khalil, 2013), a study reveals that the use of recombinant active MMP10 but not MMP3 improves the transformation of NSCLC cells (Frederick et al., 2008), suggesting that MMP3 and MMP10 have different non-overlapping functions in NSCLC development. This difference in functions between these enzymes may be applicable to the regulatory mechanisms of their expression. An induction in the mRNA levels of MMP3 but not MMP10 was shown in this study to be due to HDAC7 silencing in the H460 cells. Confirmation of this finding at the translational level is required but was not attempted in this study due to the unavailability of any MMP3 specific antibody. Experience showed that several commercially available MMP 'specific' antibodies actually cross-reacted between these MMPs, requiring extreme caution when selecting an antibody for the studies. Future work in this research will involve further screening of other MMP3 antibodies to identify one that could distinguish between MMP3 and MMP10. Although it has been reported that immunolocalisation can be used to distinguish between these enzymes based on their differences in cellular synthesis and localisation (Bord et al., 1998; Saghizadeh et al., 2001), this has to be questioned since this technique still relies on antibody specificity.

At the protein level, the elevated expression of MMP10 correlated with the angiogenic potential in the NSCLC cell lines, suggesting a strong relationship between MMP10 protein level and functional activity in NSCLC. A similar

correlation has also been seen between the immunohistochemical expression of MMP10 and the more aggressive human clinical bladder tumours (Zhang et al., 2014a). In relation to this but at the gene level, a significant correlation in the NSCLC clinical samples has been observed between the MMP10 gene expression and tumour progression, invasiveness and metastasis (Baty et al., 2010). With respect to the differences between gene expression and the corresponding protein expression, the studies reported here support an association between the functional activity and levels of MMP10 mRNA and protein in the NSCLC clinical specimens. Since there is a consistency in results between the reported clinical studies and the present study, this supports the findings of this *in vitro* study in terms of its relevance to the clinical situation. Although MMP10 enzymatic activity was not measured because no experimentally validated MMP10-specific fluorescent substrate is available to date, the angiogenesis assay was alternatively used as indicative for MMP10 functional activity in the present study, owing to the high involvement of MMP10 in angiogenesis (Zhang et al., 2014a). The suitability of the angiogenesis assay was demonstrated using purified MMP10. The relationship between the expression and activity of the MMP10 seen in the current study indicates an important role for this enzyme in the NSCLC angiogenesis and its association with tumour development. To address the exact role of MMP10 in angiogenesis of NSCLC tumour, an *in vivo* model where MMP10 is silenced is needed to study the impact on the progression of tumour vasculature using a validated immunostaining technique for visualisation of blood vessels. Such an *in vivo* model could even be used to address the role of MMP10 in other phenotypic evolutions of cancer such as invasion. A link between MMP10 and invasion has

already been reported for macrophages (Deraz et al., 2011; Murray et al., 2013).

To assess the impact of the tumour microenvironment on MMP10 expression, a comparison of MMP10 mRNA levels between 2D monolayer culture and tumour xenografts was made in this study. Tumours are dependent on the microenvironment-generated growth factors and cytokines that are known to transcriptionally up-regulate MMPs (Stamenkovic, 2000). However, the elevated MMP10 expression patterns in the NSCLC tumour xenografts *in vivo* were consistent with those seen in the monolayer culture *in vitro*, indicating a minor influence of the tumour microenvironment on MMP10 mRNA expression. While a solid tumour is a heterogeneous mixture of tumour and 'normal' stromal and endothelial cells, taking into account post-translational modifications, these results indicate that the MMP10 secretion observed originated directly from the tumour cells. This idea has been reported in several previous studies for MMP10 (Impola et al., 2004; Muller et al., 1991; Nakamura et al., 1998), and it might explain why MMP10 protein in the NSCLC tissues were found to be highly expressed independently of tumour grade, stage, histological type, or lymph node status (Gill et al., 2004). Although data of the current study provide a clear evidence of MMP10 expression mainly in tumour cells, there might be certain levels of MMP10 coming from stromal cells, therefore caution should be considered when interpreting these data.

While the tumour microenvironment had little influence on MMP10 mRNA expression as shown by similar mRNA expression in cells and xenograft tissues, in contrast, a higher expression level of pro- and active-MMP10

proteins were observed in the tissue xenografts compared to cells. This pattern of MMP10 protein expression is consistent with a previous observation (Mishra et al., 2012), which showed that very low levels of MMP10 protein were detected in the cells grown in 2D culture, but significantly higher levels when the same cells were xenografted. Taken together, these findings suggest that the tumour microenvironment has a minor influence on MMP10 mRNA, but can markedly increase the MMP10 protein level through indirect mechanisms that could be related to the post-translational modifications. This also highlights that studies evaluating the levels and functions of MMP10 protein should be focussed on *in vivo* systems, which would take into account many other stimuli unavailable in the current *in vitro* system.

While MMP10 expression has been widely reported to be linked to invasion and the metastatic potential of cancer cells, its role in angiogenesis is not fully understood (Deraz et al., 2011; Justilien et al., 2012; Zhang et al., 2014b). Vascular integrity is currently recognised to be maintained by tight junctions between adjacent endothelial and smooth muscle cells, as well as pericytes that possess a crucial role in stabilisation of the vessel wall (Ribatti et al., 2011). It is also recognised that the upregulation of MMPs presumably degrades these junctional complexes, facilitating the detachment and migration of endothelial cells into the surrounding tissues (Rundhaug, 2005; Saunders et al., 2005), a process that involve MMP10. However, once endothelial cells reach their destination, MMPs, including MMP10 are down-regulated to allow for the formation of the junctional complex and consequently blood vessel formation (Chang et al., 2006; Rundhaug, 2005; Yoon et al., 2003). There are several studies supporting the involvement of MMP10 in angiogenesis (Chang et al.,

2006; Ha et al., 2008; Heo et al., 2010). One of these studies has reported an angiogenic role of MMP10 in the context of tumour progression (Zhang et al., 2014a). In this current study, an induction of angiogenesis due to secreted MMP10 was observed in two NSCLC cell lines (A549 and H460), indicating that MMP10 could facilitate angiogenesis in the NSCLC tumours. However, this induction of angiogenesis may not be directly due to the cleavage activity of MMP10. It could be the consequence of the downstream effects of MMP10 on the MMP signalling cascade, leading to the secretion and activation of several angiogenic proteins, and thereby facilitating angiogenesis. In this context, it has been reported that MMP10 expression can up-regulate many key angiogenic proteins in tumour cells, indirectly facilitating angiogenesis. For example, MMP9 and hypoxia-inducible factor 1- α proteins confirmed to be expressed in response to MMP10 overexpression in engineered HeLa cells, are implicated in angiogenesis (Zhang et al., 2014a). Furthermore, the down-regulation of MMP10 in HUVEC-Cs results in the reduction of VEGF-induced vessel formation *in vivo* and capillary tube formation *in vitro*, suggesting a link between MMP10 and VEGF expression (Heo et al., 2010). Thus, the MMP10 induced angiogenesis seen in the current study may not be exclusively due to MMP10-ECM degradation, but to the up-regulation of other key angiogenic stimulators as a result of MMP10 expression.

For further understanding and to underlie the mechanism by which MMP10 expression facilitates the angiogenesis, it is important to identify all potential matrix substrates or molecules that are cleaved by MMP10 when it is activated. In this regard, immunoprecipitation and Western blotting could be utilised to determine the complexes formed with MMP10 when in its active state, as this

may delineate specific pathways for MMP10-related tumour progression. Another approach has recently been proven to be powerful procedure in the identification of the substrates of proteases with broad or unknown specificity, is terminal amine isotopic labeling of substrates (TAILS) (Kleifeld et al., 2010). The success of this tandem mass spectrometry based approach is exemplified with the discovery that galectin-1 is cleaved by MMP-11 in human breast cancer cells (Kleifeld et al., 2010). Another interesting example was when this strategy helped in identifying that a disintegrin and metalloproteinase with thrombospondin motifs ADAMTS-like protein 1 (ADAMTSL1) is a direct MMP10 substrate (Schlage et al., 2014). As such, this strategy could be used in the future of this project to address the role of MMP10 in several hallmarks of NSCLC tumour development such as angiogenesis, migration and invasion.

In contrast to the majority of studies (including this research) suggesting MMP10 as a facilitator of angiogenesis, a few key studies in this field have shown MMP10 up-regulation in HUVEC-Cs to be associated with both the inhibition of the tube formation capacity and capillary tube regression (Chang et al., 2006; Saunders et al., 2005). The apparent contradiction regarding the role of MMP10 in angiogenesis might have arisen from the differences in study design. Most studies did not take into account the fact that MMP10 can lead to the modulation of several endoproteases that could be pro- and anti-angiogenic. Another reason is that the function of MMP10 and other proteases in vascular development is believed to be temporal (Stetler-Stevenson, 1999). In addition, it has been demonstrated that both the absence or excess of proteolytic activity can negatively impact angiogenesis (Devy et al., 2002). Consequently, to exhibit the angiogenic phenotype, MMP10 activity towards endothelial cells

needs to be at the right time and right place. Therefore, to understand the exact role of MMP10 in angiogenesis, studies should first elucidate where, when and how MMP10 is involved, as well as reveal potential relationships between MMP10 and all other MMPs. Such goals cannot be achieved using the transient or stable gene expression systems used in the current study. Future work on this project should involve inducible transgenic systems, such as a tetracycline transactivator (tTA) or 'Tet- Off' and reverse tetracycline transactivator (rtTA) or 'Tet-On], that would be used to produce a temporal control of MMP10 expression to mimic its activity during angiogenesis in NSCLC.

It is known that nearly all MMPs are synthesised as zymogens and secreted instantly, either extracellularly or to the cell membrane. An exception is MMP8 and MMP9, which are synthesised and stored in cytoplasmic granules of neutrophils prior to secretion when neutrophils are activated (Jackson et al., 2010; Sternlicht and Werb, 2001). In solid tumours, MMP10 has been reported to be secreted mainly by the tumour cells following synthesis (Impola et al., 2004; Muller et al., 1991; Nakamura et al., 1998). In the present study, levels of MMP10 in the conditioned media from the NSCLC cell lines were consistent with those in the whole cell lysates, suggesting a similarity between intracellular and extracellular MMP10 levels. This finding supports a scenario similar to that of MMP8 and MMP9 but within tumour cells. As such, it is conceivable to assume that in tumour cells, MMP10 might be stored in granules in the cell cytoplasm prior to their secretion when required. This assumption is supported by the immunohistochemical observations of low levels of extracellular MMP10 protein compared to cytoplasmic MMP10 in NSCLC clinical tissues (Gill et al., 2004). Further support of this was reported in another study where MMP10 was

mainly detected in the cancer cell cytoplasm in prostate clinical tissues (Maruta et al., 2010). However, there are currently no studies specifically comparing the intracellular and extracellular levels of MMP10; therefore, this observation needs further investigation. Since confirming this observation might further support MMP10 as a target for therapeutic intervention, future work on this project would involve immunohistochemistry studies utilising a tumour cell-specific membrane marker, as well as MMP10 antibody. This will allow differentiation between intracellular and extracellular MMP10 protein levels, making it possible to evaluate where MMP10 is mainly localised in the tumour microenvironment.

A major aim of this research is to evaluate MMP10 as a target for therapeutic intervention in NSCLC. The observation that it could be a major contributor in tumour development due to several factors: expression in the NSCLC cell lines; the existence of a relationship between the expression and the activity of MMP10; secretion mainly by tumour cells; and its involvement in facilitating angiogenesis, all support the idea that MMP10 could offer a novel therapeutic target for intervention in NSCLC. In support of this, evidence shows that silencing MMP10 expression suppresses the enhanced self-renewal and tumourigenic properties of lung cancer cells (with stem cell-like characteristics) (Batra et al., 2012; Justilien et al., 2012). Moreover, genetic loss of MMP10 has been shown to suppress tumourigenesis and tumour growth in the mouse models of oncogenic Kras-mediated lung adenocarcinoma (Batra et al., 2012; Regala et al., 2011). Taken together with the reported findings that MMP10 is highly expressed in the majority of the NSCLC clinical specimens (Gill et al., 2004) and its expression being associated with poor prognosis (Frederick et al.,

2008), this further supports MMP10 as a potential target for therapeutic intervention in this disease.

Targeting MMP with non-selective inhibitors has not been successful (Choi et al., 2012; Coussens et al., 2002). However, identifying specific MMP10-inhibitors may be a better approach for the future if the physiological roles of MMP10 are fully revealed. An alternative strategy for the use of elevated MMP10 expression and proteolytic activity in the NSCLC tumours is to use this to improve drug delivery at the tumour sites, an approach called tumour-activated prodrugs (TAP). Tumour-activated prodrugs that utilise MMP10 would restrict the pharmacological effect to the tumour tissue, thereby lowering systemic toxicity and allowing for a wider therapeutic margin (Albright et al., 2005; Atkinson et al., 2008). The key to the robustness of this approach is to completely rely on the enzyme activity, which can be inhibited due to the influence of the natural regulators of the MMP function, the TIMPs (Ikenaka et al., 2003). Four homologous mammalian TIMPs have been identified (Brew et al., 2000; Curran et al., 2001; Gomez et al., 1997), with evidence of overlapping inhibitory specificity among them (Nagase and Brew, 2002). However, only TIMP1 was reported to inhibit MMP10 in a stoichiometric manner (Nicholson et al., 1989; Windsor et al., 1993). Since TIMPs were not included in this study, there was no way to assess their influence on MMP10 in the context of NSCLC. Nonetheless, it remains a place of further investigation to ensure that levels of TIMPs, especially TIMP1 in the NSCLC tumours, does not negatively impact the potential to use the endopeptidase activity of MMP10 in the development of TAPs.

The ultimate goal of cancer chemotherapeutic development is to increase drug targeting to the tumour with consequential diminution of systemic toxicities. The TAP approach has the potential to achieve this goal by selectively delivering chemotherapeutics to the tumour tissue (Atkinson et al., 2010) through the exploitation of the difference in the expression of selected MMPs between the tumour and normal tissues. The use of selected MMPs as prodrug activating enzymes has resulted in promising selectivity and anti-tumour efficacy, as exemplified with ICT2588 using MMP14 (Atkinson et al., 2010). As such, MMP10, in particular, might be a good candidate as a prodrug activator in NSCLC, given its selective high expression and activity in tumours and its ability to endopeptidase-cleave short peptide sequences.

A primary step for targeting individual MMPs to improve drug delivery is the identification of a unique peptide (trigger) that is specific for the enzyme of interest. One way to achieve this goal is to fully elucidate the physiological MMP substrates that would provide the amino acid sequence essential for developing a peptide conjugate specific for that MMP. However, such a strategy has been proven to be quite challenging due to the significant overlap in the MMP substrate's specificity in natural physiological substrates, a very few examples of which are listed in Table 6.1. Due to the MMP activity on a wide range of substrates, identifying unique, MMP-specific peptide conjugates for each MMP is challenging, thereby restraining the development of MMP-targeted prodrugs.

Table 6.1. Examples of Significant Overlap in MMP Substrate Specificity. Most natural MMP substrates are cleaved by numerous MMPs. Consequently, identifying a specific peptide sequence for individual MMP has become a challenge.

MMP	Natural MMP Substrate
MMP1, 2, 8 and 13	collagen I (degradation) (Vartak and Gemeinhart, 2007).
MMP2, 3, 7, 10 and 11	Fibronectin (degradation) (Vartak and Gemeinhart, 2007).
MMP14 and 16	proMMP-2 (activation) (Nagase and Fields, 1996).
MMP2 and 9	TGF β 1 and TGF β 2 (Activation) (McCawley and Matrisian, 2001).
MMP1, 3 and 7	Tumour necrosis factor alpha (release of the cell surface) (Stamenkovic, 2003).

In addition to the general overlap in specificity between MMPs, a particular obstacle in targeting MMP10 is the presence of the closely structured MMP3. In this context, there is a lack of data in the literature regarding MMP10 substrate specificities. In an attempt to identify peptide sequences that can distinguish between these two closely structured enzymes, MMP-substrate cleavage studies were carried out in this study. The data showed that MMP3 has higher affinity to the synthetic substrate 444259 than MMP10, representing a validated tool to differentiate *in vitro* between MMP3 and MMP10 activity. It is important to evaluate whether this is mirrored *in vivo*, given the enormous number of endo- and exopeptidases present in the living tissues relative to *in vitro* systems. The sequence of this peptide can also provide a source of insight regarding the structural relationship of peptide/protein selectivity between MMP3 and MMP10. Substrate 444259 therefore should be used as a starting point for further SAR studies to create a profile regarding MMP10-substrate specificity to identify an

MMP10-specific cleavable peptide sequence. Identification of such a specific peptide sequence for MMP10 is critical as it will determine the future prospects of MMP10 as a prodrug activator. Such an approach has led to the identification of a specific peptide sequence incorporated into the ICT2588, an MMP14 selective TAP poised to enter clinical trials in 2015 (Loadman, Falconer and Patterson, personal communication).

6.1 Overall Summary

The main aim of this project is to evaluate the potential of MMP10 as a target for therapeutic intervention. In a series of preclinical experiments, MMP10 was shown to be highly expressed in the NSCLC cell lines and that high levels of MMP10 contribute to tumour development, in part by the induction of angiogenesis. Together, these findings, with the expression and activity of MMP10 in the NSCLC clinical samples that were reported in the literature, support MMP10 as a target candidate for therapeutic intervention in NSCLC. While specific targeting of MMP10 with an inhibitor might be elusive at the moment due to the un-elucidated physiological functions of MMP10, as well as the unavailability of MMP10 specific inhibitors, the selective high MMP10 expression and proteolytic activity in tumours could be harnessed to activate antitumour prodrugs in NSCLC. The current research is the first to attempt to develop specific MMP10 activatable prodrugs. The data generated herein will provide the foundations necessary to successfully achieve such a goal in the future. This project has also highlighted the importance of assessing enzyme functionality in preclinical models before conducting MMP-related studies.

References

- Abraham, R., Schäfer, J., Rothe, M., Bange, J., Knyazev, P., and Ullrich, A. (2005). Identification of MMP-15 as an anti-apoptotic factor in cancer cells. *Journal of Biological Chemistry* 280, 34123-34132.
- Acuff, H. B., Sinnamon, M., Fingleton, B., Boone, B., Levy, S. E., Chen, X., Pozzi, A., Carbone, D. P., Schwartz, D. R., and Moin, K. (2006). Analysis of Host-and Tumor-Derived Proteinases Using a Custom Dual Species Microarray Reveals a Protective Role for Stromal Matrix Metalloproteinase-12 in Non-Small Cell Lung Cancer. *Cancer research* 66, 7968.
- Ailenberg, M., and Silverman, M. (2002). Trichostatin A—histone deacetylase inhibitor with clinical therapeutic potential—is also a selective and potent inhibitor of gelatinase A expression. *Biochemical and Biophysical Research Communications* 298, 110-115.
- Ailenberg, M., and Silverman, M. (2003). Differential effects of trichostatin A on gelatinase A expression in 3T3 fibroblasts and HT-1080 fibrosarcoma cells: implications for use of TSA in cancer therapy. *Biochemical and Biophysical Research Communications* 302, 181-185.
- Albert, A. (1958). Chemical aspects of selective toxicity. *Nature* 182, 421.
- Albertella, M. R., Loadman, P. M., Jones, P. H., Phillips, R. M., Rampling, R., Burnet, N., Alcock, C., Anthoney, A., Vjaters, E., and Dunk, C. R. (2008). Hypoxia-selective targeting by the bioreductive prodrug AQ4N in patients with solid tumors: results of a phase I study. *Clinical Cancer Research* 14, 1096-1104.
- Albright, C. F., Graciani, N., Han, W., Yue, E., Stein, R., Lai, Z., Diamond, M., Dowling, R., Grimminger, L., and Zhang, S.-Y. (2005). Matrix metalloproteinase-activated doxorubicin prodrugs inhibit HT1080 xenograft growth better than doxorubicin with less toxicity. *Molecular cancer therapeutics* 4, 751-760.
- Algire, G. H., Chalkley, H. W., Legallais, F. Y., and Park, H. D. (1945). Vascular reactions of normal and malignant tissues in vivo. I. Vascular reactions of mice to wounds and to normal and neoplastic transplants. *J Natl Cancer Inst* 6, 42.
- Ambudkar, S. V., Dey, S., Hrycyna, C. A., Ramachandra, M., Pastan, I., and Gottesman, M. M. (1999). Biochemical, cellular, and pharmacological aspects of the multidrug transporter 1. *Annual review of pharmacology and toxicology* 39, 361-398.
- Atkinson, J., Siller, C., and Gill, J. (2008). Tumour endoproteases: the cutting edge of cancer drug delivery? *British journal of pharmacology* 153, 1344-1352.

Atkinson, J. M., Falconer, R. A., Edwards, D. R., Pennington, C. J., Siller, C. S., Shnyder, S. D., Bibby, M. C., Patterson, L. H., Loadman, P. M., and Gill, J. H. (2010). Development of a novel tumor-targeted vascular disrupting agent activated by membrane-type matrix metalloproteinases. *Cancer research* 70, 6902-6912.

Atkinson, J. M., Pennington, C., Martin, S., Anikin, V., Mearns, A., Loadman, P., Edwards, D., and Gill, J. (2007). Membrane type matrix metalloproteinases (MMPs) show differential expression in non-small cell lung cancer (NSCLC) compared to normal lung: Correlation of MMP-14 mRNA expression and proteolytic activity. *European Journal of Cancer* 43, 1764-1771.

Banks-Schlegel, S. P., Gazdar, A. F., and Harris, C. C. (1985). Intermediate filament and cross-linked envelope expression in human lung tumor cell lines. *Cancer research* 45, 1187-1197.

Baricos, W. H., Murphy, G., Zhou, Y., Nguyen, H. H., and Shah, S. V. (1988). Degradation of glomerular basement membrane by purified mammalian metalloproteinases. *Biochem J* 254, 609-612.

Barrett, A. J., Woessner, J. F., and Rawlings, N. D. (2004). *Handbook of proteolytic enzymes*, Vol 1: Elsevier).

Batra, J., Robinson, J., Soares, A. S., Fields, A. P., Radisky, D. C., and Radisky, E. S. (2012). Matrix Metalloproteinase-10 (MMP-10) Interaction with Tissue Inhibitors of Metalloproteinases TIMP-1 and TIMP-2 BINDING STUDIES AND CRYSTAL STRUCTURE. *Journal of Biological Chemistry* 287, 15935-15946.

Baty, F., Facompré, M., Kaiser, S., Schumacher, M., Pless, M., Bubendorf, L., Savic, S., Marrer, E., Budach, W., and Buess, M. (2010). Gene profiling of clinical routine biopsies and prediction of survival in non-small cell lung cancer. *American journal of respiratory and critical care medicine* 181, 181-188.

Bejarano, P. A., Noelken, M. E., Suzuki, K., Hudson, B., and Nagase, H. (1988). Degradation of basement membranes by human matrix metalloproteinase 3 (stromelysin). *Biochem J* 256, 413-419.

Benjamin, L. E., Golijanin, D., Itin, A., Pode, D., and Keshet, E. (1999). Selective ablation of immature blood vessels in established human tumors follows vascular endothelial growth factor withdrawal. *The Journal of clinical investigation* 103, 159-165.

Bergers, G., Brekken, R., McMahon, G., Vu, T. H., Itoh, T., Tamaki, K., Tanzawa, K., Thorpe, P., Itohara, S., Werb, Z., and Hanahan, D. (2000). Matrix metalloproteinase-9 triggers the angiogenic switch during carcinogenesis. *Nat Cell Biol* 2, 737-744.

Bertini, I., Calderone, V., Fragai, M., Luchinat, C., Mangani, S., and Terni, B. (2004). Crystal structure of the catalytic domain of human matrix metalloproteinase 10. *Journal of Molecular Biology* 336, 707-716.

- Bissett, D., O'Byrne, K. J., Von Pawel, J., Gatzemeier, U., Price, A., Nicolson, M., Mercier, R., Mazabel, E., Penning, C., and Zhang, M. H. (2005). Phase III study of matrix metalloproteinase inhibitor prinomastat in non-small-cell lung cancer. *Journal of clinical oncology* 23, 842-849.
- Blobel, C. P. (2005). ADAMs: key components in EGFR signalling and development. *Nature Reviews Molecular Cell Biology* 6, 32-43.
- Bodey, B., Bodey Jr, B., Gröger, A., Siegel, S., and Kaiser, H. (2000). Invasion and metastasis: the expression and significance of matrix metalloproteinases in carcinomas of the lung. *In vivo (Athens, Greece)* 15, 175-180.
- Bogdanov, B., and Smith, R. D. (2005). Proteomics by FTICR mass spectrometry: top down and bottom up. *Mass Spectrometry Reviews* 24, 168-200.
- Boisen, L., Drasbek, K. R., Pedersen, A. S., and Kristensen, P. (2010). Evaluation of endothelial cell culture as a model system of vascular ageing. *Experimental gerontology* 45, 779-787.
- Bord, S., Horner, A., Hembry, R., and Compston, J. (1998). Stromelysin-1 (MMP-3) and stromelysin-2 (MMP-10) expression in developing human bone: potential roles in skeletal development. *Bone* 23, 7-12.
- Bourboulia, D., and Stetler-Stevenson, W. G. (2010). Matrix metalloproteinases (MMPs) and tissue inhibitors of metalloproteinases (TIMPs): positive and negative regulators in tumor cell adhesion. (Elsevier).
- Brabender, J., Danenberg, K. D., Metzger, R., Schneider, P. M., Park, J., Salonga, D., Hölscher, A. H., and Danenberg, P. V. (2001). Epidermal growth factor receptor and HER2-neu mRNA expression in non-small cell lung cancer is correlated with survival. *Clinical Cancer Research* 7, 1850-1855.
- Breuker, K., Jin, M., Han, X., Jiang, H., and McLafferty, F. W. (2008). Top-down identification and characterization of biomolecules by mass spectrometry. *Journal of the American Society for Mass Spectrometry* 19, 1045-1053.
- Brew, K., Dinakarbandian, D., and Nagase, H. (2000). Tissue inhibitors of metalloproteinases: evolution, structure and function. *Biochim Biophys Acta* 1477, 267-283.
- Brinckerhoff, C. E., Rutter, J. L., and Benbow, U. (2000). Interstitial collagenases as markers of tumor progression. *Clinical Cancer Research* 6, 4823-4830.
- Brown, J. M., and Giaccia, A. J. (1998). The unique physiology of solid tumors: opportunities (and problems) for cancer therapy. *Cancer research* 58, 1408-1416.
- Butler, G. S., Dean, R. A., Morrison, C. J., and Overall, C. M. (2010). Identification of cellular MMP substrates using quantitative proteomics: isotope-coded affinity tags (ICAT) and isobaric tags for relative and absolute

quantification (iTRAQ). In *Matrix Metalloproteinase Protocols*, (Springer), pp. 451-470.

Camidge, D. R., Bang, Y.-J., Kwak, E. L., Iafrate, A. J., Varella-Garcia, M., Fox, S. B., Riely, G. J., Solomon, B., Ou, S.-H. I., and Kim, D.-W. (2012). Activity and safety of crizotinib in patients with *ALK*-positive non-small-cell lung cancer: updated results from a phase 1 study. *The lancet oncology* 13, 1011-1019.

Carmeliet, P. (2003). Angiogenesis in health and disease. *Nature medicine* 9, 653-660.

Catelinois, O., Rogel, A., Laurier, D., Billon, S., Hemon, D., Verger, P., and Tirmarche, M. (2006). Lung cancer attributable to indoor radon exposure in france: impact of the risk models and uncertainty analysis. *Environmental health perspectives* 114, 1361.

Chandramouli, K., and Qian, P.-Y. (2009). Proteomics: challenges, techniques and possibilities to overcome biological sample complexity. *Human Genomics and Proteomics* 1, 239204.

Chang, J.-H., Javier, J. A. D., Chang, G.-Y., Oliveira, H. B., and Azar, D. T. (2005). Functional characterization of neostatins, the MMP-derived, enzymatic cleavage products of type XVIII collagen. *FEBS Letters* 579, 3601-3606.

Chang, S., Young, B. D., Li, S., Qi, X., Richardson, J. A., and Olson, E. N. (2006). Histone deacetylase 7 maintains vascular integrity by repressing matrix metalloproteinase 10. *Cell* 126, 321-334.

Chaplin, D., Pettit, G., Parkins, C., and Hill, S. (1996). Antivascular approaches to solid tumour therapy: evaluation of tubulin binding agents. *The British journal of cancer Supplement* 27, S86.

Chau, Y., Dang, N. M., Tan, F. E., and Langer, R. (2006a). Investigation of targeting mechanism of new dextran-peptide-methotrexate conjugates using biodistribution study in matrix-metalloproteinase-overexpressing tumor xenograft model. *Journal of pharmaceutical sciences* 95, 542-551.

Chau, Y., Padera, R. F., Dang, N. M., and Langer, R. (2006b). Antitumor efficacy of a novel polymer-peptide-drug conjugate in human tumor xenograft models. *International journal of cancer* 118, 1519-1526.

Chen, J., Fiskus, W., Eaton, K., Fernandez, P., Wang, Y., Rao, R., Lee, P., Joshi, R., Yang, Y., and Kolhe, R. (2009). Cotreatment with BCL-2 antagonist sensitizes cutaneous T-cell lymphoma to lethal action of HDAC7-Nur77-based mechanism. *Blood* 113, 4038-4048.

Cho, N. H., Hong, K. P., Hong, S. H., Kang, S., Chung, K. Y., and Cho, S. H. (2003). MMP expression profiling in recurred stage IB lung cancer. *Oncogene* 23, 845-851.

Choi, K. Y., Swierczewska, M., Lee, S., and Chen, X. (2012). Protease-activated drug development. *Theranostics* 2, 156.

Clark, I. M., Swingler, T. E., Sampieri, C. L., and Edwards, D. R. (2008). The regulation of matrix metalloproteinases and their inhibitors. *The international journal of biochemistry & cell biology* 40, 1362-1378.

Clocchiatti, A., Florean, C., and Brancolini, C. (2011). Class IIa HDACs: from important roles in differentiation to possible implications in tumourigenesis. *Journal of cellular and molecular medicine* 15, 1833-1846.

Corthals, G. L., Wasinger, V. C., Hochstrasser, D. F., and Sanchez, J. C. (2000). The dynamic range of protein expression: a challenge for proteomic research. *Electrophoresis* 21, 1104-1115.

Coussens, L. M., Fingleton, B., and Matrisian, L. M. (2002). Matrix metalloproteinase inhibitors and cancer—trials and tribulations. *Science* 295, 2387.

Crinò, L., and Metro, G. (2014). Therapeutic options targeting angiogenesis in nonsmall cell lung cancer. *European Respiratory Review* 23, 79-91.

CRUK (2014a). All cancers combined key facts 2014.

CRUK (2014b). Worldwide cancer mortality statistics.

Curran, J. A., Lavery, F. S., Campbell, D., Macdiarmid, J., and Wilson, J. B. (2001). Epstein-Barr virus encoded latent membrane protein-1 induces epithelial cell proliferation and sensitizes transgenic mice to chemical carcinogenesis. *Cancer Res* 61, 6730-6738.

Curran, S., and Murray, G. (2000). Matrix metalloproteinases:: molecular aspects of their roles in tumour invasion and metastasis. *European Journal of Cancer* 36, 1621-1630.

Daja, M., Niu, X., Zhao, Z., Brown, J., and Russell, P. (2003). Characterization of expression of matrix metalloproteinases and tissue inhibitors of metalloproteinases in prostate cancer cell lines. *Prostate cancer and prostatic diseases* 6, 15-26.

De Bock, K., Mazzone, M., and Carmeliet, P. (2011). Antiangiogenic therapy, hypoxia, and metastasis: risky liaisons, or not? *Nature Reviews Clinical Oncology* 8, 393-404.

de Sousa Abreu, R., Penalva, L. O., Marcotte, E. M., and Vogel, C. (2009). Global signatures of protein and mRNA expression levels. *Molecular Biosystems* 5, 1512-1526.

Deng, S.-J., Bickett, D. M., Mitchell, J. L., Lambert, M. H., Blackburn, R. K., Carter, H. L., Neugebauer, J., Pahel, G., Weiner, M. P., and Moss, M. L. (2000). Substrate specificity of human collagenase 3 assessed using a phage-displayed peptide library. *Journal of Biological Chemistry* 275, 31422-31427.

Deng, Y., Li, W., Li, Y., Yang, H., Xu, H., Liang, S., Zhang, L., and Li, Y. (2010). Expression of matrix metalloproteinase-26 promotes human glioma U251 cell invasion in vitro and in vivo. *Oncology reports* 23, 69-78.

Denny, W. A. (2001). Prodrug strategies in cancer therapy. *European journal of medicinal chemistry* 36, 577-595.

Deraz, E. M., Kudo, Y., Yoshida, M., Obayashi, M., Tsunematsu, T., Tani, H., Siriwardena, S. B., Kiekhäe, M. R., Qi, G., and Iizuka, S. (2011). MMP-10/stromelysin-2 promotes invasion of head and neck cancer. *PLoS One* 6, e25438.

Devy, L., Blacher, S., Grignet-Debrus, C., Bajou, K., Masson, V., Gerard, R. D., Gils, A., Carmeliet, G., Carmeliet, P., and Declerck, P. J. (2002). The pro-or antiangiogenic effect of plasminogen activator inhibitor 1 is dose dependent. *The FASEB journal* 16, 147-154.

Du, R., Lu, K. V., Petritsch, C., Liu, P., Ganss, R., Passequé, E., Song, H., VandenBerg, S., Johnson, R. S., Werb, Z., and Bergers, G. (2008). HIF1 α Induces the Recruitment of Bone Marrow-Derived Vascular Modulatory Cells to Regulate Tumor Angiogenesis and Invasion. *Cancer Cell* 13, 206-220.

Duan, J.-X., Jiao, H., Kaizerman, J., Stanton, T., Evans, J. W., Lan, L., Lorente, G., Banica, M., Jung, D., and Wang, J. (2008). Potent and highly selective hypoxia-activated achiral phosphoramidate mustards as anticancer drugs. *Journal of medicinal chemistry* 51, 2412-2420.

Duffy, M. J., Maguire, T. M., Hill, A., McDermott, E., and O'Higgins, N. (2000). Metalloproteinases: role in breast carcinogenesis, invasion and metastasis. *Breast Cancer Research* 2, 252.

Duffy, M. J., McKiernan, E., O'Donovan, N., and McGowan, P. M. (2009a). Role of ADAMs in cancer formation and progression. *Clinical Cancer Research* 15, 1140-1144.

Duffy, M. J., McKiernan, E., O'Donovan, N., and McGowan, P. M. (2009b). The role of ADAMs in disease pathophysiology. *Clinica Chimica Acta* 403, 31-36.

Duffy, M. J., Mullooly, M., O'Donovan, N., Sukor, S., Crown, J., Pierce, A., and McGowan, P. M. (2011). The ADAMs family of proteases: new biomarkers and therapeutic targets for cancer. *Clin Proteomics* 8, 9.

Eastman, A., and Schulte, N. (1988). Enhanced DNA repair as a mechanism of resistance to cis-diamminedichloroplatinum (II). *Biochemistry* 27, 4730-4734.

Eccles, K. A., Sowden, H., Porter, K. E., Parkin, S. M., Homer-Vanniasinkam, S., and Graham, A. M. (2008). Simvastatin alters human endothelial cell adhesion molecule expression and inhibits leukocyte adhesion under flow. *Atherosclerosis* 200, 69-79.

Egeblad, M., and Werb, Z. (2002). New functions for the matrix metalloproteinases in cancer progression. *Nature Reviews Cancer* 2, 163-176.

- Eming, S. A., Krieg, T., and Davidson, J. M. (2007). Inflammation in wound repair: molecular and cellular mechanisms. *Journal of Investigative Dermatology* 127, 514-525.
- Epstein, F. H., and Luster, A. D. (1998). Chemokines—chemotactic cytokines that mediate inflammation. *New England Journal of Medicine* 338, 436-445.
- Fanjul-Fernández, M., Folgueras, A. R., Cabrera, S., and López-Otín, C. (2010). Matrix metalloproteinases: evolution, gene regulation and functional analysis in mouse models. *Biochimica et Biophysica Acta (BBA)-Molecular Cell Research* 1803, 3-19.
- Feng, Z. (2010). p53 regulation of the IGF-1/AKT/mTOR pathways and the endosomal compartment. *Cold Spring Harbor perspectives in biology* 2, a001057.
- Ferrara, N. (2000). Vascular endothelial growth factor and the regulation of angiogenesis. *Recent progress in hormone research* 55, 15.
- Ferrara, N., Gerber, H. P., and LeCouter, J. (2003). The biology of VEGF and its receptors. *Nature medicine* 9, 669-676.
- Ferrara, N., and Kerbel, R. S. (2005). Angiogenesis as a therapeutic target. *Nature* 438, 967-974.
- Fina, L., Molgaard, H. V., Robertson, D., Bradley, N. J., Monaghan, P., Delia, D., Sutherland, D. R., Baker, M. A., and Greaves, M. F. (1990). Expression of the CD34 gene in vascular endothelial cells. *Blood* 75, 2417-2426.
- Fingleton, B. (2003). Matrix metalloproteinase inhibitors for cancer therapy: the current situation and future prospects. *Expert opinion on therapeutic targets* 7, 385-397.
- Fischle, W., Dequiedt, F., Fillion, M., Hendzel, M. J., Voelter, W., and Verdin, E. (2001). Human HDAC7 Histone Deacetylase Activity Is Associated with HDAC3in Vivo. *Journal of Biological Chemistry* 276, 35826-35835.
- Foda, H. D., and Zucker, S. (2001). Matrix metalloproteinases in cancer invasion, metastasis and angiogenesis. *Drug discovery today* 6, 478-482.
- Folgueras, A. R., Pendas, A. M., Sánchez, L. M., and López-Otín, C. (2004). Matrix metalloproteinases in cancer: from new functions to improved inhibition strategies. *International Journal of Developmental Biology* 48, 411-424.
- Folkman, J. (1990). What Is the Evidence That Tumors Are Angiogenesis Dependent? *Journal of the National Cancer Institute* 82, 4-7.
- Folkman, J. (1995). Angiogenesis in cancer, vascular, rheumatoid and other disease. *Nature medicine* 1, 27-30.

Forsberg, E. C., and Bresnick, E. H. (2001). Histone acetylation beyond promoters: long-range acetylation patterns in the chromatin world. *Bioessays* 23, 820-830.

Frederick, L., Matthews, J., Jamieson, L., Justilien, V., Thompson, E., Radisky, D., and Fields, A. (2008). Matrix metalloproteinase-10 is a critical effector of protein kinase C α -mediated lung cancer. *Oncogene* 27, 4841-4853.

Fu, N., Drinnenberg, I., Kelso, J., Wu, J. R., Pääbo, S., Zeng, R., and Khaitovich, P. (2007). Comparison of protein and mRNA expression evolution in humans and chimpanzees. *PLoS One* 2, e216.

Fukuoka, M., Wu, Y.-L., Thongprasert, S., Sunpaweravong, P., Leong, S.-S., Sriuranpong, V., Chao, T.-Y., Nakagawa, K., Chu, D.-T., and Saijo, N. (2011). Biomarker analyses and final overall survival results from a phase III, randomized, open-label, first-line study of gefitinib versus carboplatin/paclitaxel in clinically selected patients with advanced non-small-cell lung cancer in Asia (IPASS). *Journal of clinical oncology* 29, 2866-2874.

Galaray, R. E., Grobelny, D., Foellmer, H. G., and Fernandez, L. A. (1994). Inhibition of angiogenesis by the matrix metalloprotease inhibitor N-[2R-2-(hydroxamidocarbonylmethyl)-4-methylpentanoyl]-L-tryptophan methylamide. *Cancer research* 54, 4715-4718.

Gaya, A., and Rustin, G. (2005). Vascular disrupting agents: a new class of drug in cancer therapy. *Clinical Oncology* 17, 277-290.

Gialeli, C., Theocharis, A. D., and Karamanos, N. K. (2011). Roles of matrix metalloproteinases in cancer progression and their pharmacological targeting. *FEBS Journal* 278, 16-27.

Giard, D. J., Aaronson, S. A., Todaro, G. J., Arnstein, P., Kersey, J. H., Dosik, H., and Parks, W. P. (1973). In vitro cultivation of human tumors: establishment of cell lines derived from a series of solid tumors. *Journal of the National Cancer Institute* 51, 1417-1423.

Gill, J. H., Kirwan, I. G., Seargent, J. M., Martin, S. W., Tijani, S., Anikin, V. A., Mearns, A. J., Bibby, M. C., Anthoney, A., and Loadman, P. M. (2004). MMP-10 is overexpressed, proteolytically active, and a potential target for therapeutic intervention in human lung carcinomas. *Neoplasia (New York, NY)* 6, 777.

Gomez, D. E., Alonso, D. F., Yoshiji, H., and Thorgeirsson, U. P. (1997). Tissue inhibitors of metalloproteinases: structure, regulation and biological functions. *Eur J Cell Biol* 74, 111-122.

Gorman, J. L., Ispanovic, E., and Haas, T. L. (2011). Regulation of matrix metalloproteinase expression. *Drug Discovery Today: Disease Models* 8, 5-11.

Grasso, G., Fragai, M., Rizzarelli, E., Spoto, G., and Yeo, K. J. (2006). In Situ AP/MALDI-MS characterization of anchored matrix metalloproteinases. *Journal of mass spectrometry* 41, 1561-1569.

Group, N.-S. C. L. C. C. (2010). Chemotherapy and supportive care versus supportive care alone for advanced non-small cell lung cancer. *Cochrane Database Syst Rev* 5.

Grunt, T., Lametschwandtner, A., and Staindl, O. (1985). The vascular pattern of basal cell tumors: light microscopy and scanning electron microscopic study on vascular corrosion casts. *Microvascular research* 29, 371-386.

Gunja-Smith, Z., Nagase, H., and Woessner, J. (1989). Purification of the neutral proteoglycan-degrading metalloproteinase from human articular cartilage tissue and its identification as stromelysin matrix metalloproteinase-3. *Biochem J* 258, 115-119.

Ha, C. H., Jhun, B. S., Kao, H. Y., and Jin, Z. G. (2008). VEGF stimulates HDAC7 phosphorylation and cytoplasmic accumulation modulating matrix metalloproteinase expression and angiogenesis. *Arteriosclerosis, thrombosis, and vascular biology* 28, 1782-1788.

Hagemann, C., Anacker, J., Haas, S., Riesner, D., Schömig, B., Ernestus, R. I., and Vince, G. H. (2010). Comparative expression pattern of Matrix-Metalloproteinases in human glioblastoma cell-lines and primary cultures. *BMC Research Notes* 3, 293.

Han, H., Silverman, J. F., Santucci, T. S., Macherey, R. S., Tung, M. Y., Weyant, R. J., and Landreneau, R. J. (2001). Vascular endothelial growth factor expression in stage I non-small cell lung cancer correlates with neoangiogenesis and a poor prognosis. *Annals of surgical oncology* 8, 72-79.

Hanahan, D., and Folkman, J. (1996a). Patterns and emerging mechanisms of the angiogenic switch during tumorigenesis. *Cell* 86, 353.

Hanahan, D., and Folkman, J. (1996b). Patterns and emerging mechanisms of the angiogenic switch during tumorigenesis. *Cell* 86, 353-364.

Hanahan, D., and Weinberg, R. A. (2011). Hallmarks of cancer: the next generation. *Cell* 144, 646-674.

Harms, K. L., and Chen, X. (2007). Histone deacetylase 2 modulates p53 transcriptional activities through regulation of p53-DNA binding activity. *Cancer research* 67, 3145.

Harris, A. (2003). Angiogenesis as a new target for cancer control. *European Journal of Cancer Supplements* 1, 1-12.

Harrison, R. K., Chang, B., Niedzwiecki, L., and Stein, R. L. (1992). Mechanistic studies on the human matrix metalloproteinase stromelysin. *Biochemistry* 31, 10757-10762.

Heljasvaara, R., Nyberg, P., Luostarinen, J., Parikka, M., Heikkilä, P., Rehn, M., Sorsa, T., Salo, T., and Pihlajaniemi, T. (2005). Generation of biologically active endostatin fragments from human collagen XVIII by distinct matrix metalloproteases. *Experimental Cell Research* 307, 292-304.

Heo, S. H., Choi, Y. J., Ryoo, H. M., and Cho, J. Y. (2010). Expression profiling of ETS and MMP factors in VEGF-activated endothelial cells: Role of MMP-10 in VEGF-induced angiogenesis. *Journal of Cellular Physiology* 224, 734-742.

Higashiyama, R., Miyaki, S., Yamashita, S., Yoshitaka, T., Lindman, G., Ito, Y., Sasho, T., Takahashi, K., Lotz, M., and Asahara, H. (2010). Correlation between MMP-13 and HDAC7 expression in human knee osteoarthritis. *Modern rheumatology* 20, 11-17.

Hoekstra, R., Eskens, F., and Verweij, J. (2001). Matrix metalloproteinase inhibitors: current developments and future perspectives. *The Oncologist* 6, 415-427.

Hoshi, H., and Mckeehan, W. L. (1984). Brain-and liver cell-derived factors are required for growth of human endothelial cells in serum-free culture. *Proceedings of the National Academy of Sciences* 81, 6413-6417.

Huang, P. S., and Oliff, A. (2001). Drug-targeting strategies in cancer therapy. *Current opinion in genetics & development* 11, 104-110.

Huttunen, K. M., Raunio, H., and Rautio, J. (2011). Prodrugs—from serendipity to rational design. *Pharmacological reviews* 63, 750-771.

Ikenaka, Y., Yoshiji, H., Kuriyama, S., Yoshii, J., Noguchi, R., Tsujinoue, H., Yanase, K., Namisaki, T., Imazu, H., and Masaki, T. (2003). Tissue inhibitor of metalloproteinases-1 (TIMP-1) inhibits tumor growth and angiogenesis in the TIMP-1 transgenic mouse model. *International journal of cancer* 105, 340-346.

Impola, U., Uitto, V. J., Hietanen, J., Hakkinen, L., Zhang, L., Larjava, H., Isaka, K., and Saarialho-Kere, U. (2004). Differential expression of matrilysin-1 (MMP-7), 92 kD gelatinase (MMP-9), and metalloelastase (MMP-12) in oral verrucous and squamous cell cancer. *The Journal of Pathology* 202, 14-22.

Iozzo, R. V., Zoeller, J. J., and Nyström, A. (2009). Basement membrane proteoglycans: modulators Par Excellence of cancer growth and angiogenesis. *Molecules and cells* 27, 503-513.

Ishikawa, F., Miyoshi, H., Nose, K., and Shibamura, M. (2009). Transcriptional induction of MMP-10 by TGF- β , mediated by activation of MEF2A and downregulation of class IIa HDACs. *Oncogene* 29, 909-919.

Ito, K., Barnes, P. J., and Adcock, I. M. (2000). Glucocorticoid receptor recruitment of histone deacetylase 2 inhibits interleukin-1 β -induced histone H4 acetylation on lysines 8 and 12. *Molecular and cellular biology* 20, 6891.

Jackson, B. C., Nebert, D. W., and Vasiliou, V. (2010). Update of human and mouse matrix metalloproteinase families. *Human genomics* 4, 194.

Jaffe, E. A., Nachman, R. L., Becker, C. G., and Minick, C. R. (1973). Culture of human endothelial cells derived from umbilical veins. Identification by morphologic and immunologic criteria. *Journal of Clinical Investigation* 52, 2745.

Jassem, J., Langer, C., Karp, D., Mok, T., Benner, R., Green, S., Park, K., Novello, S., Strausz, J., and Gualberto, A. (2010). Randomized, open label, phase III trial of figitumumab in combination with paclitaxel and carboplatin versus paclitaxel and carboplatin in patients with non-small cell lung cancer (NSCLC). *J Clin Oncol* 28, 7500.

Jemal, A., Bray, F., Center, M. M., Ferlay, J., Ward, E., and Forman, D. (2011). Global cancer statistics. *CA: a cancer journal for clinicians*.

John, A., and Tuszynski, G. (2001). The role of matrix metalloproteinases in tumor angiogenesis and tumor metastasis. *Pathology & Oncology Research* 7, 14-23.

Johnson, J. L., Pillai, S., Pernazza, D., Sebti, S. M., Lawrence, N. J., and Chellappan, S. P. (2012). Regulation of matrix metalloproteinase genes by E2F transcription factors: Rb–Raf-1 interaction as a novel target for metastatic disease. *Cancer research* 72, 516-526.

Joyce, J. A., and Pollard, J. W. (2008). Microenvironmental regulation of metastasis. *Nature Reviews Cancer* 9, 239-252.

Jumper, C., Cobos, E., and Lox, C. (2004). Determination of the serum matrix metalloproteinase-9 (MMP-9) and tissue inhibitor of matrix metalloproteinase-1 (TIMP-1) in patients with either advanced small-cell lung cancer or non-small-cell lung cancer prior to treatment. *Respiratory Medicine* 98, 173-177.

Junttila, M. R., and de Sauvage, F. J. (2013). Influence of tumour micro-environment heterogeneity on therapeutic response. *Nature* 501, 346-354.

Justilien, V., Regala, R. P., Tseng, I.-C., Walsh, M. P., Batra, J., Radisky, E. S., Murray, N. R., and Fields, A. P. (2012). Matrix metalloproteinase-10 is required for lung cancer stem cell maintenance, tumor initiation and metastatic potential. *PLoS One* 7, e35040.

Kabir, Z., Bennett, K., and Clancy, L. (2007). Lung cancer and urban air-pollution in Dublin: a temporal association? *Ir Med J* 100, 367-369.

Kalluri, R., and Zeisberg, M. (2006). Fibroblasts in cancer. *Nature Reviews Cancer* 6, 392-401.

Kamat, A. A., Fletcher, M., Gruman, L. M., Mueller, P., Lopez, A., Landen, C. N., Han, L., Gershenson, D. M., and Sood, A. K. (2006). The clinical relevance of stromal matrix metalloproteinase expression in ovarian cancer. *Clinical Cancer Research* 12, 1707-1714.

Kamio, K., Liu, X., Sugiura, H., Togo, S., Kawasaki, S., Wang, X., Ahn, Y., Hogaboam, C., and Rennard, S. (2010). Statins inhibit matrix metalloproteinase release from human lung fibroblasts. *European Respiratory Journal* 35, 637-646.

Kao, H.-Y., Verdel, A., Tsai, C.-C., Simon, C., Juguilon, H., and Khochbin, S. (2001). Mechanism for nucleocytoplasmic shuttling of histone deacetylase 7. *Journal of Biological Chemistry* 276, 47496-47507.

Karnabi, E., Qu, Y., Mancarella, S., Yue, Y., Wadgaonkar, R., and Boutjdir, M. (2009). Silencing of Cav1. 2 gene in neonatal cardiomyocytes by lentiviral delivered shRNA. *Biochemical and Biophysical Research Communications* 384, 409-414.

Karra, D., and Dahm, R. (2010). Transfection techniques for neuronal cells. *The Journal of Neuroscience* 30, 6171-6177.

Kavallaris, M., Kuo, D., Burkhart, C. A., Regl, D. L., Norris, M. D., Haber, M., and Horwitz, S. B. (1997). Taxol-resistant epithelial ovarian tumors are associated with altered expression of specific beta-tubulin isotypes. *Journal of Clinical Investigation* 100, 1282.

Kerbel, R., and Folkman, J. (2002). Clinical translation of angiogenesis inhibitors. *Nature Reviews Cancer* 2, 727-739.

Kerkela, E., Ala-aho, R., Lohi, J., Grenman, R., V, M. K., and Saarialho-Kere, U. (2001). Differential patterns of stromelysin-2 (MMP-10) and MT1-MMP (MMP-14) expression in epithelial skin cancers. *Br J Cancer* 84, 659-669.

Kerkelä, E., and Saarialho-Kere, U. (2003). Matrix metalloproteinases in tumor progression: focus on basal and squamous cell skin cancer. *Experimental dermatology* 12, 109-125.

Kessenbrock, K., Plaks, V., and Werb, Z. (2010). Matrix metalloproteinases: regulators of the tumor microenvironment. *Cell* 141, 52-67.

Khuri, F., Herbst, R., and Fossella, F. (2001). Emerging therapies in non-small-cell lung cancer. *Annals of oncology* 12, 739-744.

Kim, S. H., Jeong, J. W., Park, J. A., Lee, J. W., Seo, J. H., Jung, B. K., Bae, M. K., and Kim, K. W. (2007). Regulation of the HIF-1alpha stability by histone deacetylases. *Oncol Rep* 17, 647-651.

Kim, T. K., and Eberwine, J. H. (2010). Mammalian cell transfection: the present and the future. *Analytical and bioanalytical chemistry* 397, 3173-3178.

Kleifeld, O., Doucet, A., auf dem Keller, U., Prudova, A., Schilling, O., Kainthan, R. K., Starr, A. E., Foster, L. J., Kizhakkedathu, J. N., and Overall, C. M. (2010). Isotopic labeling of terminal amines in complex samples identifies protein N-termini and protease cleavage products. *Nature biotechnology* 28, 281-288.

Köhrmann, A., Kammerer, U., Kapp, M., Dietl, J., and Anacker, J. (2009). Expression of matrix metalloproteinases (MMPs) in primary human breast cancer and breast cancer cell lines: New findings and review of the literature. *BMC cancer* 9, 188.

Koike, T., Vernon, R. B., Gooden, M. D., Sadoun, E., and Reed, M. J. (2003). Inhibited angiogenesis in aging: a role for TIMP-2. *The Journals of Gerontology Series A: Biological Sciences and Medical Sciences* 58, B798-B805.

Konttinen, Y. T., Ainola, M., Valleala, H., Ma, J., Ida, H., Mandelin, J., Kinne, R. W., Santavirta, S., Sorsa, T., and López-Otín, C. (1999). Analysis of 16 different matrix metalloproteinases (MMP-1 to MMP-20) in the synovial membrane: different profiles in trauma and rheumatoid arthritis. *Annals of the rheumatic diseases* 58, 691-697.

Kucukguven, A., and Khalil, R. A. (2013). Matrix metalloproteinases as potential targets in the venous dilation associated with varicose veins. *Current drug targets* 14, 287.

Lagger, G., O'Carroll, D., Rembold, M., Khier, H., Tischler, J., Weitzer, G., Schuettengruber, B., Hauser, C., Brunmeir, R., and Jenuwein, T. (2002). Essential function of histone deacetylase 1 in proliferation control and CDK inhibitor repression. *The EMBO journal* 21, 2672-2681.

Langer, C. J., Besse, B., Gualberto, A., Brambilla, E., and Soria, J.-C. (2010). The evolving role of histology in the management of advanced non-small-cell lung cancer. *Journal of clinical oncology* 28, 5311-5320.

Langlois, S., Nyalendo, C., Di Tomasso, G., Labrecque, L., Roghi, C., Murphy, G., Gingras, D., and Béliveau, R. (2007). Membrane-type 1 matrix metalloproteinase stimulates cell migration through epidermal growth factor receptor transactivation. *Molecular cancer research* 5, 569-583.

Latchman, D. S. (1997). Transcription factors: An overview. *The International Journal of Biochemistry & Cell Biology* 29, 1305-1312.

Lee, G. Y., Song, J. h., Kim, S. Y., Park, K., and Byun, Y. (2006). Peptide-doxorubicin conjugates specifically degraded by matrix metalloproteinases expressed from tumor. *Drug development research* 67, 438-447.

Lee, M., Fridman, R., and Mobashery, S. (2004). Extracellular proteases as targets for treatment of cancer metastases. *Chemical Society Reviews* 33, 401-409.

Lichtinghagen, R., Musholt, P. B., Lein, M., Römer, A., Rudolph, B., Kristiansen, G., Hauptmann, S., Schnorr, D., Loening, S. A., and Jung, K. (2002). Different mRNA and protein expression of matrix metalloproteinases 2 and 9 and tissue inhibitor of metalloproteinases 1 in benign and malignant prostate tissue. *European urology* 42, 398-406.

Liddiard, K., Rosas, M., Davies, L. C., Jones, S. A., and Taylor, P. R. (2011). Macrophage heterogeneity and acute inflammation. *European journal of immunology* 41, 2503-2508.

Lim, M. D., and Craik, C. S. (2009). Using specificity to strategically target proteases. *Bioorganic & medicinal chemistry* 17, 1094-1100.

- Liu, D., Nakano, J., Ishikawa, S., Yokomise, H., Ueno, M., Kadota, K., Urushihara, M., and Huang, C.-I. (2007). Overexpression of matrix metalloproteinase-7 (MMP-7) correlates with tumor proliferation, and a poor prognosis in non-small cell lung cancer. *Lung Cancer* 58, 384-391.
- Liu, M., Wilson, N. O., Hibbert, J. M., and Stiles, J. K. (2013). Stat3 regulates MMP3 in heme-induced endothelial cell apoptosis. *PLoS One* 8, e71366.
- Liu, W.-T., Kersten, R. D., Yang, Y.-L., Moore, B. S., and Dorrestein, P. C. (2011). Imaging mass spectrometry and genome mining via short sequence tagging identified the anti-infective agent arylomycin in *Streptomyces roseosporus*. *Journal of the American Chemical Society* 133, 18010-18013.
- Lockhart, A. C., Braun, R. D., Yu, D., Ross, J. R., Dewhirst, M. W., Humphrey, J. S., Thompson, S., Williams, K. M., Klitzman, B., and Yuan, F. (2003). Reduction of wound angiogenesis in patients treated with BMS-275291, a broad spectrum matrix metalloproteinase inhibitor. *Clinical Cancer Research* 9, 586-593.
- Löffek, S., Schilling, O., and Franzke, C.-W. (2011). Biological role of matrix metalloproteinases: a critical balance. *European Respiratory Journal* 38, 191-208.
- López-Otín, C., and Overall, C. M. (2002). Protease degradomics: a new challenge for proteomics. *Nature Reviews Molecular Cell Biology* 3, 509-519.
- Ludovini, V., Bellezza, G., Pistola, L., Bianconi, F., Di Carlo, L., Sidoni, A., Semeraro, A., Del Sordo, R., Tofanetti, F., and Mameli, M. (2009). High coexpression of both insulin-like growth factor receptor-1 (IGFR-1) and epidermal growth factor receptor (EGFR) is associated with shorter disease-free survival in resected non-small-cell lung cancer patients. *Annals of oncology* 20, 842-849.
- Ma, Y., Ramezani, A., Lewis, R., Hawley, R. G., and Thomson, J. A. (2003). High-level sustained transgene expression in human embryonic stem cells using lentiviral vectors. *Stem cells* 21, 111-117.
- Madlener, M., and Werner, S. (1997). cDNA cloning and expression of the gene encoding murine stromelysin-2 (MMP-10). *Gene* 202, 75-81.
- Mann, M. (2008). Can proteomics retire the western blot? *J Proteome Res* 7, 3065-3065.
- Mao, L., Lee, J. S., Kurie, J. M., Fan, Y. H., Lippman, S. M., Broxson, A., Khuri, F. R., Hong, W. K., Lee, J. J., and Yu, R. (1997). Clonal genetic alterations in the lungs of current and former smokers. *Journal of the National Cancer Institute* 89, 857-862.
- Margariti, A., Zampetaki, A., Xiao, Q., Zhou, B., Karamariti, E., Martin, D., Yin, X., Mayr, M., Li, H., and Zhang, Z. (2010). Histone deacetylase 7 controls endothelial cell growth through modulation of β -catenin. *Circulation research* 106, 1202-1211.

Maruta, S., Miyata, Y., Sagara, Y., Kanda, S., Iwata, T., Watanabe, S.-i., Sakai, H., Hayashi, T., and Kanetake, H. (2010). Expression of matrix metalloproteinase-10 in non-metastatic prostate cancer: Correlation with an imbalance in cell proliferation and apoptosis. *Oncology letters* 1, 417-421.

Marx, V. (2013). Finding the right antibody for the job. *Nat Methods* 10, 703-707.

Mathew, R., Khanna, R., Kumar, R., Mathur, M., Shukla, N. K., and Ralhan, R. (2002). Stromelysin-2 overexpression in human esophageal squamous cell carcinoma: potential clinical implications. *Cancer detection and prevention* 26, 222-228.

McCawley, L. J., Crawford, H. C., King, L. E., Mudgett, J., and Matrisian, L. M. (2004). A protective role for matrix metalloproteinase-3 in squamous cell carcinoma. *Cancer research* 64, 6965.

McCawley, L. J., and Matrisian, L. M. (2001). Matrix metalloproteinases: they're not just for matrix anymore! *Current opinion in cell biology* 13, 534-540.

Meng, F., Evans, J. W., Bhupathi, D., Banica, M., Lan, L., Lorente, G., Duan, J.-X., Cai, X., Mowday, A. M., and Guise, C. P. (2012). Molecular and cellular pharmacology of the hypoxia-activated prodrug TH-302. *Molecular cancer therapeutics* 11, 740-751.

Minna, J. D., Roth, J. A., and Gazdar, A. F. (2002). Focus on lung cancer. *Cancer Cell* 1, 49-52.

Mishra, D. K., Sakamoto, J. H., Thrall, M. J., Baird, B. N., Blackmon, S. H., Ferrari, M., Kurie, J. M., and Kim, M. P. (2012). Human lung cancer cells grown in an ex vivo 3D lung model produce matrix metalloproteinases not produced in 2D culture. *PLoS One* 7, e45308.

Miyata, Y., Iwata, T., Maruta, S., Kanda, S., Nishikido, M., Koga, S., and Kanetake, H. (2007). Expression of matrix metalloproteinase-10 in renal cell carcinoma and its prognostic role. *European urology* 52, 791-797.

Mosmann, T. (1983). Rapid colorimetric assay for cellular growth and survival: application to proliferation and cytotoxicity assays. *Journal of Immunological Methods* 65, 55-63.

Motrescu, E. R., Blaise, S., Etique, N., Messaddeq, N., Chenard, M.-P., Stoll, I., Tomasetto, C., and Rio, M.-C. (2008). Matrix metalloproteinase-11/stromelysin-3 exhibits collagenolytic function against collagen VI under normal and malignant conditions. *Oncogene* 27, 6347-6355.

Mottet, D., Bellahcene, A., Pirotte, S., Waltregny, D., Deroanne, C., Lamour, V., Lidereau, R., and Castronovo, V. (2007). Histone deacetylase 7 silencing alters endothelial cell migration, a key step in angiogenesis. *Circulation research* 101, 1237.

Muller, D., Breathnach, R., Engelmann, A., Millon, R., Bronner, G., Flesch, H., Dumont, P., Eber, M., and Abecassis, J. (1991). Expression of collagenase-related metalloproteinase genes in human lung or head and neck tumours. *Int J Cancer* 48, 550-556.

Murphy, G., Cockett, M. I., Ward, R., and Docherty, A. (1991). Matrix metalloproteinase degradation of elastin, type IV collagen and proteoglycan. A quantitative comparison of the activities of 95 kDa and 72 kDa gelatinases, stromelysins-1 and-2 and punctuated metalloproteinase (PUMP). *Biochem J* 277, 277-279.

Murphy, G., and Nagase, H. (2008). Progress in matrix metalloproteinase research. *Molecular aspects of medicine* 29, 290-308.

Murray, M. Y., Birkland, T. P., Howe, J. D., Rowan, A. D., Fidock, M., Parks, W. C., and Gavrilovic, J. (2013). Macrophage migration and invasion is regulated by MMP10 expression. *PLoS One* 8, e63555.

Nagase, H., and Brew, K. (2002). Engineering of tissue inhibitor of metalloproteinases mutants as potential therapeutics. *Arthritis Res* 4, S51-61.

Nagase, H., and Fields, G. B. (1996). Human matrix metalloproteinase specificity studies using collagen sequence-based synthetic peptides. *Peptide Science* 40, 399-416.

Nagase, H., Visse, R., and Murphy, G. (2006). Structure and function of matrix metalloproteinases and TIMPs. *Cardiovascular research* 69, 562.

Nagase, H., and Woessner, J. F. (1999). Matrix metalloproteinases. *Journal of Biological Chemistry* 274, 21491-21494.

Nakamura, H., Fujii, Y., Ohuchi, E., Yamamoto, E., and Okada, Y. (1998). Activation of the precursor of human stromelysin 2 and its interactions with other matrix metalloproteinases. *European Journal of Biochemistry* 253, 67-75.

Nemunaitis, J., Poole, C., Primrose, J., Rosemurgy, A., Malfetano, J., Brown, P., Berrington, A., Cornish, A., Lynch, K., Rasmussen, H., *et al.* (1998). Combined analysis of studies of the effects of the matrix metalloproteinase inhibitor marimastat on serum tumor markers in advanced cancer: selection of a biologically active and tolerable dose for longer-term studies. *Clin Cancer Res* 4, 1101-1109.

Netzel-Arnett, S., Fields, G., Birkedal-Hansen, H., Van Wart, H., and Fields, G. (1991). Sequence specificities of human fibroblast and neutrophil collagenases. *Journal of Biological Chemistry* 266, 6747-6755.

Ngoka, L. (2008). Sample prep for proteomics of breast cancer: proteomics and gene ontology reveal dramatic differences in protein solubilization preferences of radioimmunoprecipitation assay and urea lysis buffers. *Proteome Sci* 6, 30.

- Nguyen, Q., Murphy, G., Hughes, C., Mort, J., and Roughley, P. (1993). Matrix metalloproteinases cleave at two distinct sites on human cartilage link protein. *Biochem J* 295, 595-598.
- Nicholson, R., Murphy, G., and Breathnach, R. (1989). Human and rat malignant-tumor-associated mRNAs encode stromelysin-like metalloproteinases. *Biochemistry* 28, 5195-5203.
- Nishida, N., Yano, H., Nishida, T., Kamura, T., and Kojiro, M. (2006). Angiogenesis in cancer. *Vascular health and risk management* 2, 213.
- Nishio, K., Nakamura, T., Koh, Y., Suzuki, T., Fukumoto, H., and Saijo, N. (1999). Drug resistance in lung cancer. *Current opinion in oncology* 11, 109.
- Noël, A., Jost, M., and Maquoi, E. (2008). Matrix metalloproteinases at cancer tumor–host interface. Paper presented at: Seminars in cell & developmental biology (Elsevier).
- Nyberg, P., Xie, L., and Kalluri, R. (2005). Endogenous inhibitors of angiogenesis. *Cancer research* 65, 3967.
- O'Reilly, K. M., McLaughlin, A. M., Beckett, W. S., and Sime, P. J. (2007). Asbestos-related lung disease. *Am Fam Physician* 75, 683-688.
- O'Reilly, M. S., Wiederschain, D., Stetler-Stevenson, W. G., Folkman, J., and Moses, M. A. (1999). Regulation of angiostatin production by matrix metalloproteinase-2 in a model of concomitant resistance. *J Biol Chem* 274, 29568-29571.
- Oh, J., Takahashi, R., Kondo, S., Mizoguchi, A., Adachi, E., Sasahara, R. M., Nishimura, S., Imamura, Y., Kitayama, H., Alexander, D. B., *et al.* (2001). The Membrane-Anchored MMP Inhibitor RECK Is a Key Regulator of Extracellular Matrix Integrity and Angiogenesis. *Cell* 107, 789-800.
- Overall, C., and Kleifeld, O. (2006). Towards third generation matrix metalloproteinase inhibitors for cancer therapy. *British journal of cancer* 94, 941-946.
- Overall, C. M., and Blobel, C. P. (2007). In search of partners: linking extracellular proteases to substrates. *Nature Reviews Molecular Cell Biology* 8, 245-257.
- Overall, C. M., and Dean, R. A. (2006). Degradomics: systems biology of the protease web. Pleiotropic roles of MMPs in cancer. *Cancer and Metastasis Reviews* 25, 69-75.
- Overall, C. M., and López-Otín, C. (2002). Strategies for MMP inhibition in cancer: innovations for the post-trial era. *Nature Reviews Cancer* 2, 657-672.
- Palermo, C., and Joyce, J. A. (2008). Cysteine cathepsin proteases as pharmacological targets in cancer. *Trends in pharmacological sciences* 29, 22-28.

- Pap, T., Nawrath, M., Heinrich, J., Bosse, M., Baier, A., Hummel, K. M., Petrow, P., Kuchen, S., Michel, B. A., and Gay, R. E. (2004). Cooperation of Ras-and c-Myc-dependent pathways in regulating the growth and invasiveness of synovial fibroblasts in rheumatoid arthritis. *Arthritis & Rheumatism* 50, 2794-2802.
- Park, F. (2007). Lentiviral vectors: are they the future of animal transgenesis? *Physiological genomics* 31, 159-173.
- Patterson, L., and McKeown, S. (2000). AQ4N: a new approach to hypoxia-activated cancer chemotherapy. *British journal of cancer* 83, 1589.
- Patterson, L. H. (2002). Bioeductively activated antitumor N-oxides: the case of AQ4N, a unique approach to hypoxia-activated cancer chemotherapy. *Drug metabolism reviews* 34, 581-592.
- Pavlaki, M., and Zucker, S. (2003). Matrix metalloproteinase inhibitors (MMPis): the beginning of phase I or the termination of phase III clinical trials. *Cancer and Metastasis Reviews* 22, 177-203.
- Paz-Ares, L., Ross, H., O'brien, M., Riviere, A., Gatzemeier, U., Von Pawel, J., Kaukel, E., Freitag, L., Digel, W., and Bischoff, H. (2008). Phase III trial comparing paclitaxel poliglumex vs docetaxel in the second-line treatment of non-small-cell lung cancer. *British journal of cancer* 98, 1608-1613.
- Paz-Ares, L. G., Biesma, B., Heigener, D., von Pawel, J., Eisen, T., Bennouna, J., Zhang, L., Liao, M., Sun, Y., and Gans, S. (2012). Phase III, randomized, double-blind, placebo-controlled trial of gemcitabine/cisplatin alone or with sorafenib for the first-line treatment of advanced, nonsquamous non-small-cell lung cancer. *Journal of clinical oncology* 30, 3084-3092.
- Pesta, M., Kulda, V., Kucera, R., Pesek, M., Vrzalova, J., Liska, V., Pecen, L., Treska, V., Safranek, J., and Prazakova, M. (2011). Prognostic significance of TIMP-1 in non-small cell lung cancer. *Anticancer research* 31, 4031-4038.
- Peters, S., Adjei, A., Gridelli, C., Reck, M., Kerr, K., and Felip, E. (2012). Metastatic non-small-cell lung cancer (NSCLC): ESMO Clinical Practice Guidelines for diagnosis, treatment and follow-up. *Annals of oncology* 23, vii56-vii64.
- Pirker, R., Pereira, J. R., Szczesna, A., Von Pawel, J., Krzakowski, M., Ramlau, R., Vynnychenko, I., Park, K., Yu, C.-T., and Ganul, V. (2009). Cetuximab plus chemotherapy in patients with advanced non-small-cell lung cancer (FLEX): an open-label randomised phase III trial. *The Lancet* 373, 1525-1531.
- Podlaha, O., Riester, M., De, S., and Michor, F. (2012). Evolution of the cancer genome. *Trends in Genetics*.
- Prieels, J.-P., POORTMANS, J., and DOLMANS, M. (2006). nci series of cell lines: an historical perspective. *Journal of Cellular Biochemistry*.

Puente, X. S., Sánchez, L. M., Overall, C. M., and López-Otín, C. (2003). Human and mouse proteases: a comparative genomic approach. *Nature Reviews Genetics* 4, 544-558.

Qu, P., Yan, C., and Du, H. (2011). Matrix metalloproteinase 12 overexpression in myeloid lineage cells plays a key role in modulating myelopoiesis, immune suppression, and lung tumorigenesis. *Blood* 117, 4476-4489.

Radisky, E. S., and Radisky, D. C. (2010). Matrix metalloproteinase-induced epithelial-mesenchymal transition in breast cancer. *Journal of mammary gland biology and neoplasia* 15, 201-212.

Ramos-DeSimone, N., Hahn-Dantona, E., Siple, J., Nagase, H., French, D. L., and Quigley, J. P. (1999). Activation of matrix metalloproteinase-9 (MMP-9) via a converging plasmin/stromelysin-1 cascade enhances tumor cell invasion. *Journal of Biological Chemistry* 274, 13066-13076.

Rasheed, S., Nelson-Rees, W. A., Toth, E. M., Arnstein, P., and Gardner, M. B. (1974). Characterization of a newly derived human sarcoma cell line (HT-1080). *Cancer* 33, 1027-1033.

Rautio, J., Kumpulainen, H., Heimbach, T., Oliyai, R., Oh, D., Järvinen, T., and Savolainen, J. (2008). Prodrugs: design and clinical applications. *Nature Reviews Drug Discovery* 7, 255-270.

Regala, R. P., Davis, R. K., Kunz, A., Khor, A., Leitges, M., and Fields, A. P. (2009). Atypical protein kinase C α is required for bronchioalveolar stem cell expansion and lung tumorigenesis. *Cancer research* 69, 7603-7611.

Regala, R. P., Justilien, V., Walsh, M. P., Weems, C., Khor, A., Murray, N. R., and Fields, A. P. (2011). Matrix metalloproteinase-10 promotes Kras-mediated bronchio-alveolar stem cell expansion and lung cancer formation. *PLoS One* 6, e26439.

Reikvam, H., Nepstad, I., Bruserud, Ø., and Hatfield, K. J. (2013). Pharmacological targeting of the PI3K/mTOR pathway alters the release of angioregulatory mediators both from primary human acute myeloid leukemia cells and their neighboring stromal cells. *Oncotarget* 4, 830.

Reungwetwattana, T., and Dy, G. K. (2013). Targeted therapies in development for non-small cell lung cancer. *Journal of carcinogenesis* 12, 22.

Rhys-Evans, P. H., and Eccles, S. A. (2001). Expression of matrix metalloproteinases and their inhibitors correlates with invasion and metastasis in squamous cell carcinoma of the head and neck. *Archives of Otolaryngology-Head and Neck Surgery* 127, 813.

Ribatti, D., Nico, B., and Crivellato, E. (2011). The role of pericytes in angiogenesis. *International Journal of Developmental Biology* 55, 261.

Ries, C., Pitsch, T., Mentele, R., Zahler, S., Egea, V., Nagase, H., and Jochum, M. (2007). Identification of a novel 82 kDa proMMP-9 species associated with

the surface of leukaemic cells:(auto-) catalytic activation and resistance to inhibition by TIMP-1. *Biochem J* 405, 547-558.

Rio, M. (2005). From a unique cell to metastasis is a long way to go: clues to stromelysin-3 participation. *Biochimie* 87, 299-306.

Rodriguez, J. A., Orbe, J., Martinez, L. S., Calvayrac, O., Rodriguez, C., Martinez-Gonzalez, J., and Paramo, J. A. (2008). Metalloproteinases and atherothrombosis: MMP-10 mediates vascular remodeling promoted by inflammatory stimuli. *Frontiers in bioscience: a journal and virtual library* 13, 2916.

Rossi, M., Rooprai, H., Maidment, S., Rucklidge, G., and Pilkington, G. (1995). The influence of sequential, in vitro passage on secretion of matrix metalloproteinases by human brain tumour cells. *Anticancer research* 16, 121-128.

Roy, R., Yang, J., and Moses, M. A. (2009). Matrix metalloproteinases as novel biomarkers and potential therapeutic targets in human cancer. *Journal of clinical oncology* 27, 5287-5297.

Rundhaug, J. E. (2003). Matrix metalloproteinases, angiogenesis, and cancer. *Clinical Cancer Research* 9, 551-554.

Rundhaug, J. E. (2005). Matrix metalloproteinases and angiogenesis. *Journal of cellular and molecular medicine* 9, 267-285.

Safranek, J., Pesta, M., Holubec, L., Kulda, V., Dreslerova, J., Vrzalova, J., Topolcan, O., Pesek, M., Finek, J., and Treska, V. (2009). Expression of MMP-7, MMP-9, TIMP-1 and TIMP-2 mRNA in lung tissue of patients with non-small cell lung cancer (NSCLC) and benign pulmonary disease. *Anticancer research* 29, 2513-2517.

Saghizadeh, M., Brown, D. J., Castellon, R., Chwa, M., Huang, G. H., Ljubimova, J. Y., Rosenberg, S., Spirin, K. S., Stolitenko, R. B., and Adachi, W. (2001). Overexpression of matrix metalloproteinase-10 and matrix metalloproteinase-3 in human diabetic corneas: a possible mechanism of basement membrane and integrin alterations. *The American journal of pathology* 158, 723-734.

Sandler, A., Gray, R., Perry, M. C., Brahmer, J., Schiller, J. H., Dowlati, A., Lilenbaum, R., and Johnson, D. H. (2006). Paclitaxel-carboplatin alone or with bevacizumab for non-small-cell lung cancer. *New England Journal of Medicine* 355, 2542-2550.

Saunders, W. B., Bayless, K. J., and Davis, G. E. (2005). MMP-1 activation by serine proteases and MMP-10 induces human capillary tubular network collapse and regression in 3D collagen matrices. *J Cell Sci* 118, 2325-2340.

Scagliotti, G., Novello, S., von Pawel, J., Reck, M., Pereira, J. R., Thomas, M., Miziara, J. E. A., Balint, B., De Marinis, F., and Keller, A. (2010). Phase III study

of carboplatin and paclitaxel alone or with sorafenib in advanced non–small-cell lung cancer. *Journal of clinical oncology* 28, 1835-1842.

Schiller, J. H., Harrington, D., Belani, C. P., Langer, C., Sandler, A., Krook, J., Zhu, J., and Johnson, D. H. (2002). Comparison of Four Chemotherapy Regimens for Advanced Non–Small-Cell Lung Cancer. *New England Journal of Medicine* 346, 92-98.

Schlage, P., Egli, F. E., Nanni, P., Wang, L. W., Kizhakkedathu, J. N., Apte, S. S., and auf dem Keller, U. (2014). Time-resolved analysis of the matrix metalloproteinase 10 substrate degradome. *Molecular & Cellular Proteomics* 13, 580-593.

Schlondorff, J., and Blobel, C. P. (1999). Metalloprotease-disintegrins: modular proteins capable of promoting cell-cell interactions and triggering signals by protein-ectodomain shedding. *Journal of cell science* 112, 3603-3617.

Schütz, A., Schneidenbach, D., Aust, G., Tannapfel, A., Steinert, M., and Wittekind, C. (2002). Differential expression and activity status of MMP-1, MMP-2 and MMP-9 in tumor and stromal cells of squamous cell carcinomas of the lung. *Tumor biology* 23, 179-184.

Seargent, J. M., Loadman, P. M., Martin, S. W., Naylor, B., Bibby, M. C., and Gill, J. H. (2005). Expression of matrix metalloproteinase-10 in human bladder transitional cell carcinoma. *Urology* 65, 815-820.

Sechler, M., Cizmic, A. D., Avasarala, S., Van Scoyk, M., Brzezinski, C., Kelley, N., Bikkavilli, R. K., and Winn, R. A. (2013). Non-small-cell lung cancer: molecular targeted therapy and personalized medicine—drug resistance, mechanisms, and strategies. *Pharmacogenomics and personalized medicine* 6, 25.

Semple, T. U., Quinn, L. A., Woods, L. K., and Moore, G. E. (1978). Tumor and lymphoid cell lines from a patient with carcinoma of the colon for a cytotoxicity model. *Cancer research* 38, 1345-1355.

Sengupta, N., and Seto, E. (2004). Regulation of histone deacetylase activities. *Journal of Cellular Biochemistry* 93, 57-67.

Senter, P. D. (2009). Potent antibody drug conjugates for cancer therapy. *Current opinion in chemical biology* 13, 235-244.

Sequist, L. V., Yang, J. C.-H., Yamamoto, N., O'Byrne, K., Hirsh, V., Mok, T., Geater, S. L., Orlov, S., Tsai, C.-M., and Boyer, M. (2013). Phase III study of afatinib or cisplatin plus pemetrexed in patients with metastatic lung adenocarcinoma with EGFR mutations. *Journal of clinical oncology* 31, 3327-3334.

Sethi, T., Rintoul, R. C., Moore, S. M., MacKinnon, A. C., Salter, D., Choo, C., Chilvers, E. R., Dransfield, I., Donnelly, S. C., and Strieter, R. (1999). Extracellular matrix proteins protect small cell lung cancer cells against

apoptosis: a mechanism for small cell lung cancer growth and drug resistance in vivo. *Nature medicine* 5, 662-668.

Seymour, L. W., Ferry, D. R., Kerr, D. J., Rea, D., Whitlock, M., Poyner, R., Boivin, C., Hesslewood, S., Twelves, C., and Blackie, R. (2009). Phase II studies of polymer-doxorubicin (PK1, FCE28068) in the treatment of breast, lung and colorectal cancer. *International journal of oncology* 34, 1629.

Sherwood, L. M., Parris, E. E., and Folkman, J. (1971). Tumor angiogenesis: therapeutic implications. *New England Journal of Medicine* 285, 1182-1186.

Shevchenko, A., Wilm, M., Vorm, O., and Mann, M. (1996). Mass spectrometric sequencing of proteins from silver-stained polyacrylamide gels. *Analytical chemistry* 68, 850-858.

Shuo, T., Koshikawa, N., Hoshino, D., Minegishi, T., Ao-Kondo, H., Oyama, M., Sekiya, S., Iwamoto, S., Tanaka, K., and Seiki, M. (2012). Detection of the heterogeneous O-glycosylation profile of MT1-MMP expressed in cancer cells by a simple MALDI-MS method. *PLoS One* 7, e43751.

Sorsa, T., Tjäderhane, L., and Salo, T. (2004). Matrix metalloproteinases (MMPs) in oral diseases. *Oral diseases* 10, 311-318.

Sottrup-Jensen, L. (1989). Alpha-macroglobulins: structure, shape, and mechanism of proteinase complex formation. *J Biol Chem* 264, 11539-11542.

Sounni, N. E., Janssen, M., Foidart, J. M., and Noël, A. (2003). Membrane type-1 matrix metalloproteinase and TIMP-2 in tumor angiogenesis. *Matrix biology* 22, 55-61.

Sparano, J. A., Bernardo, P., Stephenson, P., Gradishar, W. J., Ingle, J. N., Zucker, S., and Davidson, N. E. (2004). Randomized phase III trial of marimastat versus placebo in patients with metastatic breast cancer who have responding or stable disease after first-line chemotherapy: Eastern Cooperative Oncology Group trial E2196. *Journal of clinical oncology* 22, 4683-4690.

Spinale, F. G. (2007). Myocardial matrix remodeling and the matrix metalloproteinases: influence on cardiac form and function. *Physiological reviews* 87, 1285-1342.

Spira, A., Beane, J., Shah, V., Liu, G., Schembri, F., Yang, X., Palma, J., and Brody, J. S. (2004). Effects of cigarette smoke on the human airway epithelial cell transcriptome. *Proceedings of the National Academy of Sciences of the United States of America* 101, 10143-10148.

Stamenkovic, I. (2000). *Matrix metalloproteinases in tumor invasion and metastasis.* (Elsevier).

Stamenkovic, I. (2003). Extracellular matrix remodelling: the role of matrix metalloproteinases. *The Journal of Pathology* 200, 448-464.

Stanton, R. A., Gernert, K. M., Nettles, J. H., and Aneja, R. (2011). Drugs that target dynamic microtubules: a new molecular perspective. *Medicinal research reviews* 31, 443-481.

Starr, A. E., Bellac, C. L., Dufour, A., Goebeler, V., and Overall, C. M. (2012). Biochemical Characterization and N-terminomics Analysis of Leukolysin, the Membrane-type 6 Matrix Metalloprotease (MMP25) CHEMOKINE AND VIMENTIN CLEAVAGES ENHANCE CELL MIGRATION AND MACROPHAGE PHAGOCYTIC ACTIVITIES. *Journal of Biological Chemistry* 287, 13382-13395.

Staton, C. A., Reed, M. W., and Brown, N. J. (2009). A critical analysis of current in vitro and in vivo angiogenesis assays. *International journal of experimental pathology* 90, 195-221.

Stefanou, D., Batistatou, A., Arkoumani, E., Ntzani, E., and Agnantis, N. (2004). Expression of vascular endothelial growth factor (VEGF) and association with microvessel density in small-cell and non-small-cell lung carcinomas.

Sternlicht, M. D., and Werb, Z. (2001). How matrix metalloproteinases regulate cell behavior. *Annual review of cell and developmental biology* 17, 463.

Stetler-Stevenson, W. G. (1999). Matrix metalloproteinases in angiogenesis: a moving target for therapeutic intervention. *The Journal of clinical investigation* 103, 1237-1241.

Stuschke, M., Sak, A., Wurm, R., Sinn, B., Wolf, G., Stüben, G., and Budach, V. (2002). Radiation-induced apoptosis in human non-small-cell lung cancer cell lines is secondary to cell-cycle progression beyond the G2-phase checkpoint. *International journal of radiation biology* 78, 807-819.

Su, L., Zhou, W., Park, S., Wain, J. C., Lynch, T. J., Liu, G., and Christiani, D. C. (2005). Matrix metalloproteinase-1 promoter polymorphism and lung cancer risk. *Cancer Epidemiology Biomarkers & Prevention* 14, 567-570.

Sugiura, Y., Shimada, H., Seeger, R. C., Laug, W. E., and DeClerck, Y. A. (1998). Matrix metalloproteinases-2 and-9 are expressed in human neuroblastoma: contribution of stromal cells to their production and correlation with metastasis. *Cancer research* 58, 2209-2216.

Szarvas, T., vom Dorp, F., Ergün, S., and Rübber, H. (2011). Matrix metalloproteinases and their clinical relevance in urinary bladder cancer. *Nature Reviews Urology* 8, 241-254.

Theocharis, A. D., Skandalis, S. S., Tzanakakis, G. N., and Karamanos, N. K. (2010). Proteoglycans in health and disease: novel roles for proteoglycans in malignancy and their pharmacological targeting. *FEBS Journal* 277, 3904-3923.

Thun, M. J., Hannan, L. M., Adams-Campbell, L. L., Boffetta, P., Buring, J. E., Feskanich, D., Flanders, W. D., Jee, S. H., Katanoda, K., Kolonel, L. N., *et al.* (2008). Lung Cancer Occurrence in Never-Smokers: An Analysis of 13 Cohorts and 22 Cancer Registry Studies. *PLoS Med* 5, e185.

Townsend, D. M., and Tew, K. D. (2003). The role of glutathione-S-transferase in anti-cancer drug resistance. *Oncogene* 22, 7369-7375.

Trédan, O., Galmarini, C. M., Patel, K., and Tannock, I. F. (2007). Drug resistance and the solid tumor microenvironment. *Journal of the National Cancer Institute* 99, 1441-1454.

Trog, D., Yeghiazaryan, K., Fountoulakis, M., Friedlein, A., Moenkemann, H., Haertel, N., Schueller, H., Breipohl, W., Schild, H., and Leppert, D. (2006). Pro-invasive gene regulating effect of irradiation and combined temozolomide-radiation treatment on surviving human malignant glioma cells. *European journal of pharmacology* 542, 8-15.

Turk, B. E., Huang, L. L., Piro, E. T., and Cantley, L. C. (2001). Determination of protease cleavage site motifs using mixture-based oriented peptide libraries. *Nature biotechnology* 19, 661-667.

Ullmann, R., Morbini, P., Halbwedl, I., Bongiovanni, M., Gogg-Kammerer, M., Papotti, M., Gabor, S., Renner, H., and Popper, H. H. (2004). Protein expression profiles in adenocarcinomas and squamous cell carcinomas of the lung generated using tissue microarrays. *The Journal of Pathology* 203, 798-807.

Upadhyay, J., Shekariz, B., Nemeth, J. A., Dong, Z., Cummings, G. D., Fridman, R., Sakr, W., Grignon, D. J., and Cher, M. L. (1999). Membrane type 1-matrix metalloproteinase (MT1-MMP) and MMP-2 immunolocalization in human prostate: change in cellular localization associated with high-grade prostatic intraepithelial neoplasia. *Clinical Cancer Research* 5, 4105-4110.

Vaisar, T., Kassim, S. Y., Gomez, I. G., Green, P. S., Hargarten, S., Gough, P. J., Parks, W. C., Wilson, C. L., Raines, E. W., and Heinecke, J. W. (2009). MMP-9 sheds the β 2 integrin subunit (CD18) from macrophages. *Molecular & Cellular Proteomics* 8, 1044-1060.

Van Themsche, C., Alain, T., Kossakowska, A. E., Urbanski, S., Potworowski, É. F., and St-Pierre, Y. (2004). Stromelysin-2 (matrix metalloproteinase 10) is inducible in lymphoma cells and accelerates the growth of lymphoid tumors in vivo. *The Journal of Immunology* 173, 3605-3611.

Vartak, D. G., and Gemeinhart, R. A. (2007). Matrix metalloproteases: underutilized targets for drug delivery. *Journal of drug targeting* 15, 1-20.

Vaupel, P., Kallinowski, F., and Okunieff, P. (1989). Blood flow, oxygen and nutrient supply, and metabolic microenvironment of human tumors: a review. *Cancer research* 49, 6449-6465.

Verdin, E., Dequiedt, F., and Kasler, H. G. (2003). Class II histone deacetylases: versatile regulators. *Trends in Genetics* 19, 286-293.

Verma, R. P., and Hansch, C. (2007). Matrix metalloproteinases (MMPs): chemical-biological functions and (Q) SARs. *Bioorganic & medicinal chemistry* 15, 2223-2268.

Verweij, J., and de Jonge, M. J. A. Achievements and future of chemotherapy. *European Journal of Cancer* 36, 1479-1487.

Vihinen, P., and Kähäri, V. M. (2002). Matrix metalloproteinases in cancer: prognostic markers and therapeutic targets. *International journal of cancer* 99, 157-166.

Visvader, J. E., and Lindeman, G. J. (2008). Cancer stem cells in solid tumours: accumulating evidence and unresolved questions. *Nature Reviews Cancer* 8, 755-768.

Vizoso, F., Gonzalez, L., Corte, M., Rodriguez, J., Vazquez, J., Lamelas, M., Junquera, S., Merino, A., and Garcia-Muniz, J. (2007). Study of matrix metalloproteinases and their inhibitors in breast cancer. *British journal of cancer* 96, 903-911.

Wade, P. A. (2001). Transcriptional control at regulatory checkpoints by histone deacetylases: molecular connections between cancer and chromatin. *Human molecular genetics* 10, 693.

Wang, G. P., Ciuffi, A., Leipzig, J., Berry, C. C., and Bushman, F. D. (2007). HIV integration site selection: analysis by massively parallel pyrosequencing reveals association with epigenetic modifications. *Genome research* 17, 1186-1194.

Wehr, T. (2006). Top-down versus bottom-up approaches in proteomics.

Wells, A. (1999). EGF receptor. *The international journal of biochemistry & cell biology* 31, 637-643.

Windsor, L. J., Grenett, H., Birkedal-Hansen, B., Bodden, M., Engler, J., and Birkedal-Hansen, H. (1993). Cell type-specific regulation of SL-1 and SL-2 genes. Induction of the SL-2 gene but not the SL-1 gene by human keratinocytes in response to cytokines and phorbol esters. *Journal of Biological Chemistry* 268, 17341-17347.

Wistuba, I. I., Berry, J., Behrens, C., Maitra, A., Shivapurkar, N., Milchgrub, S., Mackay, B., Minna, J. D., and Gazdar, A. F. (2000). Molecular changes in the bronchial epithelium of patients with small cell lung cancer. *Clinical Cancer Research* 6, 2604-2610.

Wistuba, I. I., Bryant, D., Behrens, C., Milchgrub, S., Virmani, A. K., Ashfaq, R., Minna, J. D., and Gazdar, A. F. (1999). Comparison of features of human lung cancer cell lines and their corresponding tumors. *Clinical Cancer Research* 5, 991-1000.

Witte, M. B., Thornton, F. J., Kiyama, T., Efron, D. T., Schulz, G. S., Moldawer, L. L., and Barbul, A. (1998). Metalloproteinase inhibitors and wound healing: a novel enhancer of wound strength. *Surgery* 124, 464-470.

Woessner, J. F. (1991). Matrix metalloproteinases and their inhibitors in connective tissue remodeling. *The FASEB journal* 5, 2145.

- Wood, S. L., Pernemalm, M., Crosbie, P. A., and Whetton, A. D. (2014). The role of the tumor-microenvironment in lung cancer-metastasis and its relationship to potential therapeutic targets. *Cancer treatment reviews* 40, 558-566.
- Workman, P., Aboagye, E., Balkwill, F., Balmain, A., Bruder, G., Chaplin, D., Double, J., Everitt, J., Farningham, D., and Glennie, M. (2010). Guidelines for the welfare and use of animals in cancer research. *British journal of cancer* 102, 1555-1577.
- Wu, L., Chien, W.-M., Hartman, M. E., Moussavi-Harami, F., Liu, Y., and Chin, M. T. (2011). Regulation of MMP10 expression by the transcription factor CHF1/Hey2 is mediated by multiple E boxes. *Biochemical and Biophysical Research Communications* 415, 662-668.
- Yamamoto, A., Kormann, M., Rosenecker, J., and Rudolph, C. (2009). Current prospects for mRNA gene delivery. *European Journal of Pharmaceutics and Biopharmaceutics* 71, 484-489.
- Yan, C., and Boyd, D. D. (2007). Regulation of matrix metalloproteinase gene expression. *Journal of Cellular Physiology* 211, 19-26.
- Yang, S. J., Jiang, S. S., Van, R. C., Hsiao, Y. Y., and Pan, R.-L. (2000). A lysine residue involved in the inhibition of vacuolar H⁺-pyrophosphatase by fluorescein 5'-isothiocyanate. *Biochimica et Biophysica Acta (BBA)-Bioenergetics* 1460, 375-383.
- Yao, J., Xiong, S., Klos, K., Nguyen, N., Grijalva, R., Li, P., and Yu, D. (2001). Multiple signaling pathways involved in activation of matrix metalloproteinase-9 (MMP-9) by heregulin-beta1 in human breast cancer cells. *Oncogene* 20, 8066-8074.
- Yoon, S. O., Park, S. J., Yun, C. H., and Chung, A. S. (2003). Roles of matrix metalloproteinases in tumor metastasis and angiogenesis. *Journal of biochemistry and molecular biology* 36, 128-137.
- Yu, L.-L., Chang, K., Lu, L.-S., Zhao, D., Han, J., Zheng, Y.-R., Yan, Y.-H., Yi, P., Guo, J.-X., and Zhou, Y.-G. (2013). Lentivirus-mediated RNA interference targeting the H19 gene inhibits cell proliferation and apoptosis in human choriocarcinoma cell line JAR. *BMC cell biology* 14, 26.
- Zhang, G., Miyake, M., Lawton, A., Goodison, S., and Rosser, C. J. (2014a). Matrix metalloproteinase-10 promotes tumor progression through regulation of angiogenic and apoptotic pathways in cervical tumors. *BMC cancer* 14, 310.
- Zhang, G., and Wang, Z. (2010). [RNA interference of HDAC7 expression in hepatocellular carcinoma]. *Zhong Nan Da Xue Xue Bao Yi Xue Ban* 35, 718-724.
- Zhang, J.-J., Zhu, Y., Xie, K.-L., Peng, Y.-P., Tao, J.-Q., Tang, J., Li, Z., Xu, Z.-K., Dai, C.-C., and Qian, Z.-Y. (2014b). Yin Yang-1 suppresses invasion and

metastasis of pancreatic ductal adenocarcinoma by downregulating MMP10 in a MUC4/ErbB2/p38/MEF2C-dependent mechanism. *Molecular cancer* 13, 130.

Zhang, X., Yin, P., Di, D., Luo, G., Zheng, L., Wei, J., Zhang, J., Shi, Y., Zhang, J., and Xu, N. (2009). IL-6 regulates MMP-10 expression via JAK2/STAT3 signaling pathway in a human lung adenocarcinoma cell line. *Anticancer research* 29, 4497-4501.

Zhang, X., Zhu, S., Luo, G., Zheng, L., Wei, J., Zhu, J., Mu, Q., and Xu, N. (2007). Expression of MMP-10 in lung cancer. *Anticancer research* 27, 2791-2795.

Zhong, J. L., Poghosyan, Z., Pennington, C. J., Scott, X., Handsley, M. M., Warn, A., Gavrilovic, J., Honert, K., Krüger, A., and Span, P. N. (2008). Distinct functions of natural ADAM-15 cytoplasmic domain variants in human mammary carcinoma. *Molecular cancer research* 6, 383-394.

Zhu, C., Chen, Q., Xie, Z., Ai, J., Tong, L., Ding, J., and Geng, M. (2011). The role of histone deacetylase 7 (HDAC7) in cancer cell proliferation: regulation on c-Myc. *Journal of Molecular Medicine* 89, 279-289.

Zucker, S., and Cao, J. (2009). Selective matrix metalloproteinase (MMP) inhibitors in cancer therapy. *Cancer biology & therapy* 8, 2371-2373.

Zucker, S., Cao, J., and Chen, W.-T. (2000). Critical appraisal of the use of matrix metalloproteinase inhibitors in cancer treatment. *Oncogene* 19, 6642-6650.

Appendices

Appendix 1. TAE Buffer (10X) Recipe

Components	
Tris-base (pH 7.6)	242g
Glacial acetic acid	57.1ml
0.5M sodium EDTA	100ml
Distilled water	Up to 1 litre

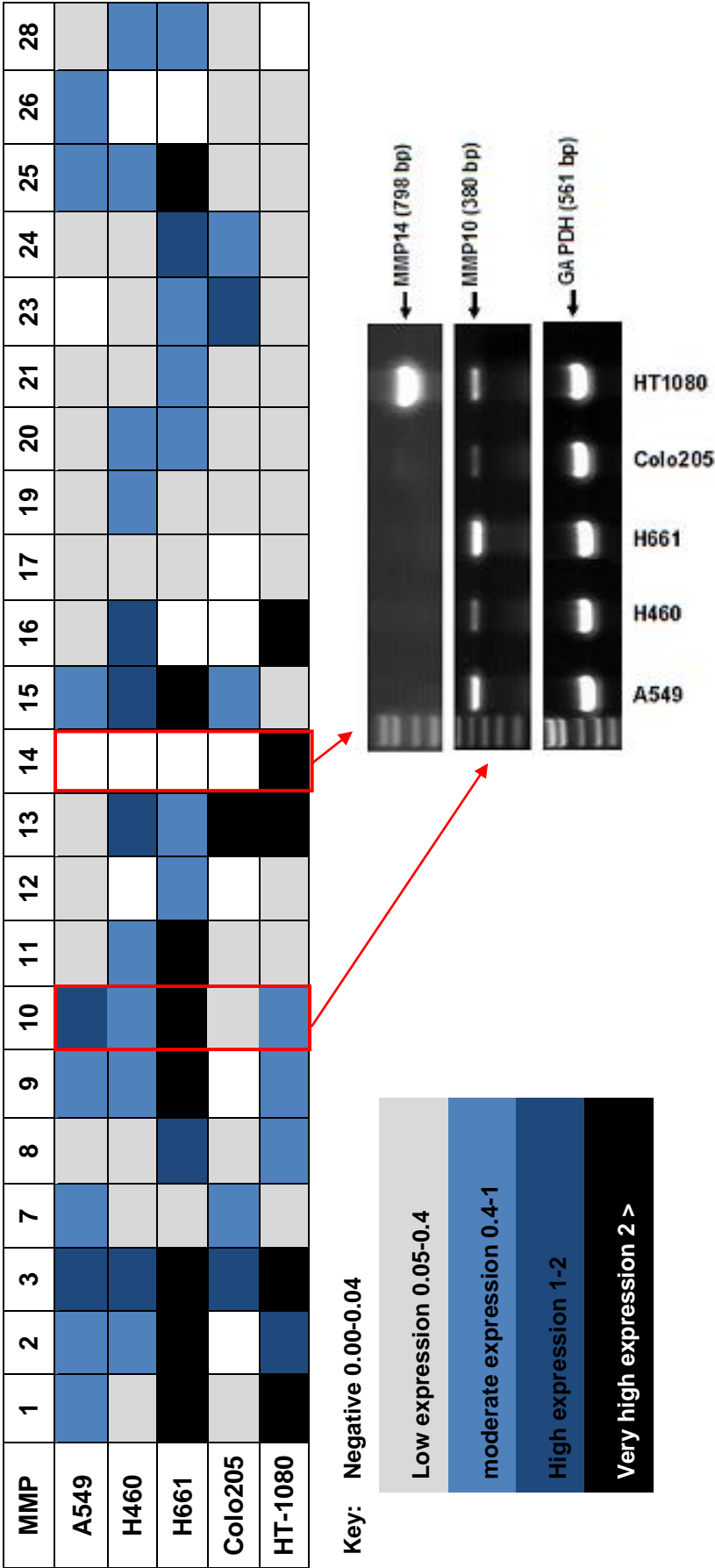
Appendix 2. Preparation of 10% Separating and 5% Stacking Gels

Appendix 2. Recipe for 10% Separating and 5% Stacking Gels							
	30% acrylamide/ Bisacrylamide mix solution	1.5M Tris (pH 8.8)	1M Tris (pH 6.8)	10% SDS	distilled H ₂ O	10% AP	TEMED
10% separating gel (10ml)	3.3ml	2.5ml	0	100ul	4ml	100ul	4ul
5% stacking gel (3ml)	0.5ml	0	0.38ml	30ul	2.1ml	30ul	3ul
AP: Ammonium Persulfate TEMED: Tetramethylethylenediamine							

Appendix 3. Illustration of the Contents of Peptide Calibration Standard Mixture for MALDI/MS

Appendix 3. Illustration of the Contents of Peptide Calibration Standard Mixture for MALDI/MS	
Peptide standard	Mass to mono charge ratio (m/z)
Angiotensin II	1046.5418
Angiotensin I	1296.6848
Substance P	1347.7354
Bombesin	1619.8223
ACTH clip 1-17	2093.0862
ACTH clip 18-39	2465.1983
Somatostatin 28	3147.4710

Appendix 4. MMP expression in selected NSCLC cell lines



Appendix 4. MMP10 mRNA expression is elevated in human NSCLC preclinical tumour models as measured by semi-quantitative RT-PCR. The HT-1080 and Colo205 cell lines were used as positive and negative controls, respectively. The gel images of MMP10 and MMP14 were shown as a representative of the actual data obtained. Expression values were measured after normalisation to GAPDH. Classification of expression levels was determined based on band intensity as stated in the key for colour scheme.

Appendix 5. Supplementary Data for MALDI-MS Analysis

A	Row	User File	OK	Accession	Protein	MW (kDa)	pI	#Alt. Prote In	Score	#Peptide	EC (%)	RM 880 (ppm)	Rank
	1		true	PCXL_HUMAN	Pecanolic	288.5	6.8	1	254 (M:25)	1	0.9	8879	1
	2		true	ANGL4_HUMAN	Angiopoietin	45.2	10	1	172 (M:17)	1	4.7	8339	2
	3		true	DPYD_HUMAN	Dihydropyrimidinase	61.9	6	1	164 (M:16)	1	3.9	7543	3
	4		true	NOX4_HUMAN	Non-phosphorylated	54.2	9.6	1	156 (M:15)	1	4.7	8458	4
	5		true	CD37_HUMAN	Leukocyte	31.7	9.5	1	146 (M:14)	1	8.9	3889	5
	6		true	NAT5_HUMAN	N-acetyltransferase	31.4	9.2	1	139 (M:13)	1	6.3	3168	6
	7		true	TTN_HUMAN	Titin	3813.7	6	1	139 (M:13)	1	0.1	9983	7
	8		true	DOCK1_HUMAN	Dedicator of cytokinesis	237.5	8.6	1	126 (M:12)	1	1	43	8
	9		true	DOCK8_HUMAN	Dedicator of cytokinesis	67	9.5	1	126 (M:12)	1	3.4	9175	9
	10		true	NALP3_HUMAN	NACHT, domain containing	118.1	6.2	1	124 (M:12)	1	0.8	6179	10
	11		true	OSCR5_HUMAN	Olfactory receptor	46.3	9.4	1	122 (M:12)	1	5	8341	11
	12		true	TR19L_HUMAN	Tumor necrosis factor receptor	46.1	10.2	1	122 (M:12)	1	4.2	8384	12
	13		true	OLIGO3_HUMAN	Oligodendrocyte	47.3	9.5	1	118 (M:11)	1	5.1	7114	13
	14		true	GP173_HUMAN	Probable G-protein-coupled receptor	41.5	10.4	1	116 (M:11)	1	6.4	3238	14
	15		true	IPIL1_HUMAN	Inositol 1-phosphatase	63.4	6	1	114 (M:11)	1	4.1	9171	15
	16		true	MAST1_HUMAN	Microtubule-associated	170.6	9.4	1	107 (M:10)	1	1.5	9865	16
	17		true	TBC19_HUMAN	TBC1 domain containing	80.2	5.6	1	103 (M:10)	1	3.6	7896	17
	18		true	RUSC1_HUMAN	RUN and DNA binding	96.4	5.9	1	101 (M:10)	1	2.4	94.4	18
B	MMP10												
	10	20	30	40	50	60							
	MMHIAFLVLL	CLPVC SAYPL	SGAAKEEDSN	KDLAQQYLEK	YYNLEKDVKQ	FRRKDSNLIV							
	70	80	90	100	110	120							
	KKIQGMQKFL	GLEVTGKLDI	DTLEVMRKPR	CGVPDVGHS	SFPGMPKWRK	THLTIRIVNY							
	130	140	150	160	170	180							
	TPDLPRDAVD	SAIEKALKWV	EEVTPLTFSR	LYEGEADIMI	SFAVKEHGDF	YSFDGPGHSL							
	190	200	210	220	230	240							
	AHAYPPGPGL	YGDIFDDE	KWTEDASGTN	LFLVAAHEL	GSLGLFHSAN	TEAMYPYLYN							
	250	260	270	280	290	300							
	SFTELAQFRL	SQDDVNGIQS	LYGPPPASTE	EPLVPTKSP	SGSEMPAKCD	PALSFDAIST							
	310	320	330	340	350	360							
	LRGEYLFFKD	RYFWRRSHWN	PEPEFHLISA	FWPSLPSYLD	AAYEVNSRDT	VFIKQNEFW							
	370	380	390	400	410	420							
	AIRQNEVQAG	YPRGIHTLGF	PPTIRKIDAA	VSDKEKKKTY	FFAADKYWRF	DENSQSMEQG							
	430	440	450	460	470								
	FPRIIADDFP	GVEPKVDAVL	QAFGFFYFFS	GSSQFEFDPN	ARMVTHILKS	NSWLHC							

MMP3					
10	20	30	40	50	60
MKSLPILLLL	CVAVCSAYPL	DGAARGEDTS	MNLVQKYLEN	YYDLKKDVKQ	FVRRKDSGPV
70	80	90	100	110	120
VKKIREMQKF	LGLEVTGKLD	SDTLEVMRKP	RCGVDPVGHF	RTFPGIPKWR	KTHLTYSRIVN
130	140	150	160	170	180
YTPDLPKDAV	DSAVEKALKV	WEEVTPLTFS	RLYEGEADIM	ISFAVREHGD	FYPFDGPGNV
190	200	210	220	230	240
LAHAYAPGPG	INGDAHFDDE	EQWTKDTTGT	NLFLVAAHEI	GHSGLGLFHS	NTEALMYPLY
250	260	270	280	290	300
HSLTDLTRFR	LSQDDINGIQ	SLYGPPPDSP	ETPLVPTPEV	PPEPGTPANC	DPALSFDAVS
310	320	330	340	350	360
TLRGEILIFK	DRHFWRKSLR	KLEPELHLIS	SFWPSLPSGV	DAAYEVTSKD	LVFIFKGNQF
370	380	390	400	410	420
WAIRGNEVRA	GYPRGIHTLG	FPPTVRKIDA	AISDKEKNKT	YFFVEDKYWR	FDEKRNSMEP
430	440	450	460	470	
GFPRQIAEDF	PGIDSKIDAV	FEEFGFFYFF	TGSSQLEFDP	NAKKVTHTLK	SNSWLNC

Appendix 5. Supplementary Data for MALDI-MS Analysis. (A) List of proteins identified in samples analysed by LC MALDI. (B) The location and sequence ID of the dominant peptide signals detected. Selective MMP10 peptide is in red and the one found in both MMP3 and10 is in blue.

Appendix 6. HDAC7 detection by Western blotting

Appendix 6. HDAC7 detection by Western blotting in H460 cells. NIH3T3 cell line was used as a positive control.

